ЖУРНАЛ
ПРИКЛАДНОЙ ХИМИИ

Volume 32, No. 8
August 1959

JOURNAL OF
APPLIED CHEMISTRY
OF THE USSR

(ZHURNAL PRIKLADNOI KHIMII)

IN ENGLISH TRANSLATION

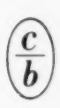

CONSULTANTS BUREAU, INC.

Volume 32, No. 8
August 1959

JOURNAL OF
APPLIED CHEMISTRY
OF THE USSR

(ZHURNAL PRIKLADNOI KHIMII)

A publication of the Academy of Sciences of the USSR

IN ENGLISH TRANSLATION

Year and issue of first translation:
Vol. 23, No. 1 January 1950

	U. S. and Canada	*Foreign*
Annual subscription	*$60.00*	*$65.00*
Annual subscription for libraries of nonprofit academic institutions	*20.00*	*25.00*
Single issue	*7.50*	*7.50*

Printed in the United States of America

JOURNAL OF APPLIED CHEMISTRY OF THE USSR

Volume 32, Number 8 August 1959

CONTENTS

CONTENTS (continued)

CONTENTS (continued)

PRESENT STATE AND FUTURE DEVELOPMENT PROSPECTS FOR THE PRODUCTION AND USE OF LIQUID FERTILIZERS

V. A. Klevke and Ya. I. Kil'man

Liquid fertilizers occupy a prominent position in the range of mineral fertilizers used in foreigh countries, especially in the United States. Until the Second World War liquid fertilizers (liquefied anhydrous ammonia, aqueous ammonia solutions, and ammoniates) were used only on a very limited scale for direct introduction into the soil.

Interest in this type of fertilizers increased when the agricultural effects of their use became apparent. Nitrogenous fertilizers are the most widely used of the liquid fertilizers. The question of using liquid ammonia or aqueous ammonia, introduced directly into the soil without costly conversion into the usual solid fertilizers, arose quite a long time ago. The work of a number of scientists, and especially of Academician D. N. Pryanishnikov, laid the foundation for a successful solution of this problem. He brilliantly demonstrated the important fact that nitrates are not essential as a nitrogen source of plant food, and that ammonium salts can be used as a direct source of nitrogen even without conversion into nitrates, because they are even closer than nitrates to the physiological nature of plants. These researches provided the theoretical basis for development of the modern nitrogen industry, which depends mainly on the production of ammonium salts from synthetic ammonia [1].

In soils with pH of 5 or less, where the rate of nitrification is low, free ammonia is a good nitrogen source. Where the nitrification of ammonia is weak, it is retained unchanged by the soil until spring; where nitrification is extensive (at pH = 5.5 or over) a considerable part of the ammonia is converted into nitrate, which is subject to leaching [2].

Agronomical research into the use of liquid ammonia and ammoniates for direct introduction into the soil was carried out in our country, for the first time in world agricultural practice, by the staff of the Scientific Research Institute of Fertilizers and Insectofungicides (NIUIF) in 1932-1935 [3, 4]. During this period, cultivation experiments and field trials were carried out in order to study the comparative effects of liquid nitrogenous fertilizers. In accordance with theory, these experiments showed that if all losses of bound nitrogen are eliminated during introduction of liquid ammonia or ammoniates into the soil, these fertilizers are assimilated by plants and have the same effects on the yield as the usual solid nitrogenous fertilizers – ammonium nitrate (Table 1).

The results of field trials on the use of ammoniates, both by deep implantation into the soil and by introduction with water under irrigation conditions, are presented in Table 2, which shows that the yield increase is virtually the same as that produced by introduction of "dry" ammonium nitrate.

In surface application of liquid ammonia or ammoniates the losses of combined nitrogen are considerable even at high dilutions with water.

Special experiments showed that the surface application of 1% ammonia solution the loss reaches about 4-5% on chernozems, and 13-17% on sierozems. It follows that in nonirrigated cultivation the use of liquid nitrogenous fertilizers can be highly effective only if they are introduced deep into the soil.

Despite the obvious advantages of liquid nitrogenous fertilizers, for a number of reasons they could not be adopted in our country at that time. In the United States ammonia was being used to some extent even in the 1920's, small amounts (about 2%) being added to superphosphate.

TABLE 1

Results of NIUIF Cultivation Experiments on Different Soils

Fertilizer type	Yield (g)				
	podzolic loam		chernozem		sierozem
	oats				corn
	grain	total	grain	total	total
Without nitrogen	4.1	10.2	4.0	9.5	8.4
Ammonia	10.0	26.9	10.3	24.7	33.3
Ammoniate	10.8	26.0	10.4	23.7	32.8
Ammonium nitrate	9.5	23.6	9.4	22.7	33.2
Urea	13.0	30.2	—	—	34.9

TABLE 2

Results of Field Trials

Nitrogeneous fertilizers	Yield (centners per hectare)		
	cotton*	potatoes**	potatoes ***
Without nitrogen	24.2	194.5	138.0
Ammonium nitrate			
dry	30.1	279.5	150.0
solution	26.9	275.5	149.0
Ammoniates	30.1	271.7	150.0

* Ammoniates introduced with irrigation water before cotton sowing.

** Trials on podzolic soils at the Lyubertsy experimental field.

*** Dolgoprudnaya Experimental Agrochemical Station.

Experiments performed in NIUIF showed that in ammoniation of superphosphate by means of ammoniates (in the proportion of 1 mole of NH_3 per mole of P_2O_5) rather than ammonia a product containing 13-14% P_2O_5 and 7-8% combined nitrogen is obtained. This fertilizer has good nutrient and physical properties.

The effectiveness of superphosphates ammoniated by the action of ammoniates is illustrated by the data in Table 3.

The production of ammoniated superphosphate of this composition (Table 3) is especially desirable for regions where sugar beet is grown, as it would be an excellent source of combined nitrogen and phosphorus.

According to published data, from about 1953-1954 the production and use of liquid nitrogenous fertilizers has tended to increase. This type of fertilizer is becoming increasingly used both for direct application to the soil and for ammoniation of superphosphates and mixed fertilizers. Ammoniates are being used with success for the latter purpose, instead of ammonia as formerly, so that the nitrogen content of ammoniated superphosphate can be raised to 6-7% without a decrease of the available P_2O_5 content and without the use of high-pressure equipment.

According to several American sources, the amounts of nitrogenous fertilizers, calculated as nitrogen, introduced into the soil in liquid form (as ammonia, aqua ammonia, and ammoniacal salt solutions) in the United States were:

Years	Amounts of nitrogenous fertilizers (1000's of tons)
1951-1952	154
1952-1953	225
1953-1954	292
1954-1955	373

According to Nosden [5], a 19% increase in the production and use of liquid nitrogenous fertilizers was planned for 1955-1956. Later data [6] from the U. S. Department of Agriculture indicate that, of the simple fertilizers, the one most used in the 1957 agricultural year was liquid ammonia (334, 500 tons), an increase of 7.9% over the 1956 consumption. The use of aqua ammonia also increased to 69,165 tons (calculated as nitrogen), which is an increase of 22.9% over the 1956 figure. The consumption of other nitrogenous solutions was 67,716 tons, an increase of 118% over 1956.

TABLE 3

Data on the Effect of Superphosphates Ammoniated by Means of Ammoniates

Fertilizer	Composition (%)			Yield of oats (g)	
	P_2O_5	N_{total}	N_{amm}	grain	total
Without P_2O_5	—	—	—	7.5	16.3
	12.85	6.54	2.82	9.9	24.2
Ammoniated superphosphate	13.92	6.77	2.93	10.5	24.2
	13.00	8.00	3.47	10.5	25.1
	11.70	14.8	6.45	8.7	21.5
Superphosphate	18.2	—	—	11.0	27.2
Phosphorite	22.0	—	—	7.7	16.2
$Ca_3(PO_4)_2$	45.0	—	—	8.0	16.8

These data are indicative of the continously increasing consumption of liquid nitrogenous fertilizers, and especially of anhydrous ammonia, as fertilizers for direct application to the soil.

Liquid fertilizers are used in the United States over an area exceeding 7,000,000 hectares [5-10].

The scale of production and utilization of liquid fertilizers is also increasing in a number of other Western capitalist countries: Italy, England, France, Norway, Holland, and other countries of Western Europe, and in the Peoples' Democracies: Poland and Czechoslovakia. Aqua ammonia was first used in Poland in 1952, when 837 tons (as N_2) was introduced into the soil. By 1956 the use of aqua ammonia rose to 6610 tons (as N_2). The consumption of 20,000 tons of nitrogen in the form of liquid fertilizers is planned for 1960. New transportation equipment and a variety of plants are to be built in the agricultural system. The Ministry of Chemical Industry, jointly with the Ministry of the Food Industry, have decided that aqua ammonia is to be used in the operating regions of sugar and nitrogen factories; the necessary containers are to be built for the purpose and technical assistance in introduction of liquid fertilizers into the soil is to be given. After the urea plant has come into operation it is proposed to carry out large-scale trials on the use of concentrated solutions of urea in aqua ammonia [11].

In Czechoslovakia, experiments on the use of liquid fertilizers, especially liquid ammonia, commenced around 1949-1950 [11]. In 1955, 15 tons of ammonia was used, in 1956, 45 tons, and in 1957, up to 2000 tons. In 1955 the first large series of machines for introduction of liquid ammonia into the soil was constructed; some of these machines were supplied to the Soviet Union for trial.

In addition to anhydrous ammonia, aqua ammonia, and ammoniates, in recent years complete (mixed) liquid fertilizers, containing 2 or 3 nutrient elements ($N-P_2O_5$ or $N-P_2O_5-K_2O$) have come into use in foreign countries. These fertilizers may also contain trace elements, herbicides, insectidides, and growth substances (α-naphthylacetic and indolebutyric acids, etc.)

Complete (mixed) liquid fertilizers are preferable to single fertilizers because their use eliminates the difficulties associated with separate addition of liquid (nitrogenous) and solid (phosphorus and potash) fertilizers to the soil. Therefore, production and use of complete fertilizers in solution form, containing phosphorus and potash in addition to nitrogen, with the nutrient elements in various proportions, is more advantageous for agricultural practice [12, 13].

According to publications in the foreign journals [14], there is a trend toward an increase in the production and consumption of the so-called ammonia-free fertilizer solutions – complete liquid fertilizers [14].

Mixed fertilizers comprise 66% of the total fertilizer consumption in the United States (22,700,000 tons) since 1955-1956. This total included more than 1536 varieties of mixed liquid fertilizers, not less than 3000 tons of each.

The proportions of the nutrient elements in complete (mixed) liquid fertilizers are: $N : P_2O_5 : K_2O =$ $= 1:1:1, 1:2:1, 1:2:2, 2:1:2, 1:3:1, 1:3:3, 1:4:4$ [15].

Slack [16] reports that about 147 companies in the United States are producing various brands of fertilizer solutions, differing in their contents and relative proportions of nitrogen, phosphorus, and potash. Of the total number of liquid fertilizers produced, 54 brands are complete nitrogen-phosphorus-potash fertilizers, 7 contain phosphorus and potash, and 38 contain nitrogen and phosphorus; of the latter the 17-7-0, 10-20-0, 12-15-0 and 8-24-0 grades are the most common (the last grade is most widely used in California).

A complete liquid fertilizer with 1 : 1 : 1 nutrient ratio is now being increasingly used [15]. This form of liquid fertilizer is used mainly for orchards and vegetable crops, and also for pasture lands, forests (sprayed from airplanes), and water reservoirs for increasing vegetation used as food by fish. For forest cultivation mixed liquid fertilizers of 12-12-12 composition are recommended; they increase tree growth by 40-65%. Fertilizers of 8 : 8 : 2, 10-10-5 or 12-12-4 composition are put into reservoirs. This measure increases the fish weight 4-fold; if pasture lands are fertilized it is possible to increase the number of head of cattle per unit pasture area (the grass is ready for mowing 1.5-2 months earlier) [17]. The raw materials used in the production of complete liquid fertilizers are generally phosphoric acid (furnace or wet-process), liquid ammonia, and potassium chloride. Superphosphoric acid, produced from elemental phosphorus made in the electric furnace, is also used. This acid contains about 76% P_2O_5, about one half of which is present in the ortho form, and the rest mainly in the pyro form (ordinary phosphoric acid contains about 54% P_2O_5 in the ortho form).

In the production of complete liquid fertilizers the starting materials may be, in addition to superphosphoric acid, ammonium phosphate, potassium nitrate, caustic potash or potassium chloride, ammonium nitrate, urea, etc.

The production of a complete liquid fertilizer consists of two stages: 1) production of ammonium phosphate by neutralization of phosphoric acid with ammonia; 2) additions of the amounts of the other ingredients to give the required proportions of nutrients.

Apart from gaseous ammonia, anhydrous or aqueous ammonia, ammoniated solutions of ammonium nitrate, solutions of ammonia with urea, etc., can be used for neutralization of phosphoric acid.

If the proportions of nitrogen, phosphorus, and potash present in the original components are chosen correctly, it is possible to obtain a complete liquid fertilizer with the same amounts of nutrients, and in the same proportions, as solid mixed fertilizers [18-21]. The total concentration of nutrients in complete liquid fertilizers is 26% and over. With the use of urea as the nitrogenous component the total nutrient concentration can be raised to 30%.

An important factor in regard to homogeneity of the solution is its crystallization temperature; according to the data of certain American authors, this varies from −29 to +11°.

One of the most important factors influencing salt crystallization is the degree of neutralization of the phosphoric acid. In the solubility relationships of the system $NH_3-P_2O_5-KCl-H_2O$ there is a relatively narrow range of concentrations and $NH_3 : P_2O_5$ ratios in which all the salts can be kept in solution.

According to Langguth et al. [22], the amount of nitrogen present as free ammonia in ammoniated solutions should have the following values (as % of total nitrogen) for neutral solutions of different compositions:

$N : P_2O_5$ ratio	1 : 3	1 : 2	2 : 3	1 : 1	2 : 1	3 : 1
Nitrogen present as free ammonia, as % of total nitrogen	100	66.7	50.0	33.3	16.7	11.1

To ensure that salts are not precipitated, the concentration of the nutrient elements is usually lowered to 9 : 9 : 9 or 8 : 8 : 8 ratios, so that the total nutrient concentration is from 30 to 24%.

The production of complete liquid fertilizers in the United States has been much assisted by the experience gained in the use of liquid nitrogenous fertilizers, and by the availability of equipment for application of liquid fertilizers, but so far this production has not been extensive. According to recent data, the sales of complete liquid fertilizers amounted to 27,500 tons in 1954; of this, 20,500 tons went to California and only 7,000 tons to the other states [23]. Scholl et al. [24] report a certain decrease in the production of mixed fertilizers recently.

The production of mixed fertilizers involves certain complications and difficulties. The pH of liquid fertilizers should be between 6.5 and 7.0. As soon as the pH exceeds 7, which is usually accociated with the appearance of free ammonia, phosphate solubility decreases and salt precipitation begins. Decrease of pH below 6.5 results in increased corrosion of iron storage tanks and the equipment used for these solutions.

To avoid these disadvantages in the use of liquid fertilizers, the Flo-Mix Fertilizer Corporation [25] has produced equipment for simultaneous application of three individual liquid fertilizers (nitrogen, phosphate, potash) in any desired proportions. The equipment comprises two trailers carrying three tanks, one for each type of fertilizer, and an air compressor driven by the road wheels. The potash and phosphate fertilizers are fed through the same pipe by means of compressed air, while liquid ammonia is fed through another pipe under its own pressure.

Cultivation experiments and field trials with complete mixed liquid fertilizers have shown that the P_2O_5 present in them is not inferior to the phosphate in solid fertilizers in regard to fertilizing properties.

Results of Experimental Work Carried Out on Liquid Nitrogenous Fertilizers in the USSR

The extensive use of liquid nitrogenous fertilizers began in the USSR in 1956 [26-33]. Extensive production trials were conducted over large areas in different parts of the country in order to elucidate the technical and economic advantages of the production and use of liquid fertilizers, to gain experience in their application, and to improve further the machine design and agricultural techniques. For example, in the summer of 1956 trials of liquid nitrogenous fertilizers were conducted over an area of 4,500 hectares in the Uzbek SSR, and 6,800 hectares in the Ukraine [26].

During the period of these trials alone, up to 1000 tons of liquid fertilizers was applied, mainly for cotton and sugar beet. The liquid nitrogenous fertilizers were applied both as liquid ammonia and aqua ammonia, and as ammoniates made from ammonium nitrate and mixtures of the latter with calcium nitrate. The yields showed that in many cases the liquid nitrogenous fertilizers were even more effective than the usual fertilizers, and their application involved much less labor. Liquid fertilizers often proved more effective when applied to non-irrigated sowings of sugar beet. Whereas in 1956 liquid nitrogenous fertilizers were applied over an area of 12,000 hectares (of which an area of 50 hectares was treated with aqua ammonia), in 1957 the area had already risen to 58,500 hectares, and aqua ammonia was applied to an area of 44,300 hectares; this confirms that under certain conditions aqua ammonia has advantages over other liquid nitrogenous fertilizers [31].

These advantages are seen particularly clearly in the results for the Irkutsk province, where aqua ammonia was applied over an area of 32,000 hectares. Application of aqua ammonia over such a large area was possible owing to the initiative displayed by the Irkutsk specialists, collective farmers, and State farm workers.

In the plan for 1958, of the 255,000 hectares to be treated with liquid nitrogenous fertilizers, 244,500 hectares, or 96% of the total area, was to receive aqua ammonia. Of this, 200,000 hectares is in the Irkutsk province.

Production trials in 1957 again confirmed the effectiveness of liquid nitrogenous fertilizers in increasing yields of all the agricultural crops studied (corn, cotton, summer wheat, potatoes, vegetables, sugar beet, etc.). The yield increase was about 10-12% more than that produced by ordinary fertilizers [1]. Protasov et al. [30] state that the cost of applying 1 ton of pure nitrogen in the form of solid ammonium nitrate is 3590 rubles, whereas the cost of applying 1 ton of pure N_2 in the form of aqua ammonia is 2783 rubles. The corresponding numbers of working days required are 23.2 and 12.1.

In trials with cotton, it was found fertilizers are much more effective if applied before irrigation, while the irrigation trenches are being cut, than after irrigation. A considerable proportion (30%) of the annual quota of fertilizer can be applied before sowing; this gives a greater increase (by 2-3 centners) in the yield of raw cotton than is given by the procedure now used, with all the annual quota of nitrogen applied exclusively during the growth period. This is a very important result, because it reduces the very expensive storage capacity needed for liquid fertilizers, which are to be used on an especially large scale in the cotton-growing republics of Central Asia.

Since aqua ammonia will become the principal, if not the only, liquid nitrogenous fertilizer, results of trials with it are of particular interest [1, 31].

Extensive production experience gained over a period of more than 3 years in the use of liquid fertilizers has confirmed that they are assimilated by plants better than solid fertilizers, especially under conditions of inadequate soil humidity. Liquid fertilizers have a more lasting action in the soil, nitrification is accelerated, to say nothing of the convenience of their application [27]. The main advantage of liquid fertilizers is the low cost of their constituent nutrients. For example, the cost per unit weight of fixed nitrogen is approximately 30% lower in anhydrous ammonia than in ammonium nitrate, and 45% lower than in calcium nitrate.

With the use of liquid nitrogenous fertilizers all unloading, loading, and application operations can be fully mechanized. The fertilizers are distributed more uniformly over the application area.

If liquid nitrogenous fertilizers (ammonia and aqua ammonia) are to be produced, nitrogen factories can be built more rapidly by the "short plan," without equipment for conversion of ammonia into nitric acid and ammonium nitrate. This reduces the amount of building work for power, transport, and storage, auxiliary services, and dwelling houses. As a result, in the construction of a nitrogen factory with an annual capacity of 100,000 tons of ammonia, the saving in capital and working costs if aqua ammonia is produced rather than ammonium nitrate may reach 90,000,000 rubles, and the saving in metal, 7,000 tons.

The cost of fixed nitrogen in ammonium nitrate has been estimated at 930 rubles per ton, whereas in aqua ammonia it is 662 rubles per ton [32].

Since the cost of unit weight of nitrogen in ammonia is about 35% lower than in ammonium nitrate, operational costs are reduced considerably and the fertilizers are therefore cheaper.

The total annual decrease in manufacturing costs (in a factory producing 100,000 tons of NH_3 per year) would be between 20 and 25 millions of rubles. The number of plant personnel is reduced by 500. No paper bags are required.

The vast demands made by the agriculture of our country for nitrogenous fertilizers, and the present deficit of these fertilizers, made it necessary to build new factories are rapidly as possible and to expand production at existing factories.

Since production of liquid nitrogenous fertilizers can be organized more rapidly, and requires considerably lower capital outlay per unit weight of nitrogen produced, extensive utilization of these types of fertilizers under our agricultural conditions is very desirable.

From the economic and organizational point of view the advantage of liquid fertilizers is that all stages of operation with these fertilizers are fully mechanized; this is very convenient, especially for application over large areas, and results in considerable savings of labor costs in the use of fertilizers.

The proportion of liquid nitrogenous fertilizers (liquid ammonia and aqua ammonia) in the total amount of nitrogenous fertilizers consumed during the next seven-year period may be not less than 15%. However, it is known that the main difficulties in the use of liquid fertilizers, especially liquid ammonia, arise in storage, transport, and application rather than in production. Storage and transport of liquid fertilizers involves the construction of special containers, means of transportation, and machines for application; this involves the use of considerable amounts of metal and capital outlay.

In some factories it would be advisable to provide for the production of some types of ammoniates, which are more highly concentrated liquid nitrogenous fertilizers than aqua ammonia, and are especially useful for ammoniation of superphosphate and mixed fertilizers in order to improve their physical properties and effectiveness as fertilizers. Such ammoniates include products based on ammonium nitrate and urea, of the following compositions [28] (Table 4).

TABLE 4

Composition of Ammoniates Based on Ammonium Nitrate and Urea

Ammoniate no.	Chemical composition (%)				Contents (%)		Temperature of solid-phase deposition (°C)
	NH_4NO_3	$CO(NH_2)_2$	NH_3	H_2O	total nitrogen	organic nitrate	
1	45.1	15.2	20.1	19.6	39.4	7.1	—32.1
2	40.1	15.1	22.6	22.2	39.68	7.04	—36.2
3	40.3	20.0	20.1	19.6	40.0	9.3	—29.6
4	50.0	10.0	20.1	20.0	38.7	4.7	—28.3

Future Tasks in the Fields of Production and Application of Liquid Fertilizers

The data in this article on the present state of production and application of liquid nitrogenous fertilizers, and the results of large-scale agricultural trials carried out in our country, demonstrate the undoubted economic advantages of this form of fertilizer. Of the known liquid nitrogenous fertilizers, anhydrous ammonia is unquestionably the most advantageous with regard to capital outlay and production costs. However, preliminary technical and economic studies show that the use of liquid ammonia in agriculture is costly because thick-walled steel vessels which can withstand high pressures (about 20 atmos) are required for its transportation and storage. The weight of the tank cars used for transport of anhydrous ammonia is therefore very considerable, and this makes it less convenient to transport. Therefore, during the first stages of introduction of liquid nitrogenous fertilizers into agricultural practice, the most convenient form would be 25% aqueous ammonia solution (20% N). According to data supplied by agricultural chemists, aqueous ammonia is as effective as anhydrous ammonia for a number of agricultural crops, and with a fixed-nitrogen content of about 20% it is no less transportable than ammonium sulfate. The production and application of aqua ammonia is easy; since the vapor pressure of ammonia is low, ordinary thin-walled tank cars and containers (used for tractor fuel) can be used for storage and transport; it is safe in use; therefore, despite the lower content of fixed nitrogen, this is a liquid fertilizer of primary importance.

Thus, with regard to the amount of metal required for tank care and storage containers, the use of aqua ammonia is less complicated and more economical then the use of anhydrous ammonia. The use of aqua ammonia as fertilizer becomes economically inexpedient if the railroad transportation radius is greater than 400-500 kilometers, and the subsequent transportation by road involves distances greater than 30-40 kilometers. It must be remembered that aqua ammonia retains its advantages if transported by rail and road over shorter distances (of the order of 160-200 km).

One of the important tasks in the extensive adoption of the use of liquid nitrogenous fertilizers in our country is to produce as soon as possible all the machinery required for application of the fertilizers to the

soil and to set up intermediate bases (distribution points). In the opinion of some workers of the agricultural organization of the Union Republics, distribution points for storage and supply of liquid fertilizers should be set up at points where interregional bases of the Main Administration for Marketing of the Products of the Chemical Industry are available or else built to the pattern of oil storage bases at railroad stations.

In connection with reorganization of machine and tractor service stations, we consider that machine repair stations should undertake organization of the supply and application of liquid fertilizers. Liquid fertilizers should be supplied by rail to bases at stations, and transported from there in tank trucks over relatively short distances.

Tasks relating to the future development of liquid fertilizers in our country also include work on different types of complete (mixed) liquid fertilizers, with the most suitable proportions of nutrients (N : P_2O_5 : K_2O).

LITERATURE CITED

[1] P. A. Baranov, "The use of aqua ammonia as a fertilizer for agricultural crops," Proceedings of Conference of the Ministry of Agriculture RSFSR [in Russian] (Irkutsk, 1958).

[2] Chem. Eng. 1 (1948).

[3] K. L. Zeidenber et al., Chemization of Socialist Agriculture (November, 1935).

[4] K. I. Zeidenber et al., Symposium: Nitrogen in the Soviet (1935)[in Russian].

[5] J. Agric. Food Chem. 6, 2 (1958).

[6] R. Bateman, Oil and Gas J. 56, 35 (1958).

[7] Agric. Chem. 5 (1957).

[8] R. Messing and S. Perkins, Petrol. Pr. 12, 9 (1957).

[9] Ch. Eng. News, 35, 32 (1957).

[10] Ch. Eng. News, 35, 29 (1957).

[11] The Mineral Fertilizer Industry [in Russian] (State Sci.-Tech. Press Chem. Lit., 1958).

[12] W. R. Bone, J. Agric. Food Chem. 3, No. 8, 663 (1955).

[13] H. Bowen, J. Ferguson, and W. Pierce, J. Agric. Food Chem. 4, No. 4, 316 (1956).

[14] R. Jacob and W. Scholl, Comm. Fertilizer 91, 3A (1955); Referat. Zhur. Khim. 15 (1956).

[15] J. Agric. Food Chem. 6, No. 1 (1958).

[16] A. Slack, J. Agric. Food Chem. 3, No. 7, 569 (1955).

[17] Chem. Eng. News, 34, 41 (1956).

[18] E. F. Linnik, Fertilizer and Harvest, 11 (1958).

[19] R. Langguth, J. Payne, et al., J. Agric. Food Chem. 3, 8 (1955).

[20] V. Klevke, The Mineral Fertilizer Industry [in Russian] (State Chem. Press, 1958).

[21] Vierling and E. Donald, U. S. Patent 2,770,540 (1956).

[22] R. Langguth, J. Payne, et al., Agric. Food Chem. 3, 8 (1955).

[23] J. Agric. Food Chem. 3, No. 7, 569 (1955).

[24] W. Scholl and M. Davis, J. Agric. Food Chem. 7, No. 2, 77 (1959).

[25] Rice J. 5 (1955).

[26] I. Burlachenko, A. Kulik, T. Poznyakova, and A. Ilyasov, Chem. Ind. 8 (1958).

[27] Ya. Kil'man, V. Klevke, and D. Gambur, J. Chem. Ind. 3 (1957).

[28] V. Klevke, Ya. Kil'man, and A. Kantor, Trans. State Inst. Nitrogen Ind. 9, (1958).

[29] I. Modraimov, Socialist Agriculture of Uzbekistan 6 (1957).

[30] P. Protasov and G. Yarovenko, Fertilizer and Harvest 3, (1958).

[31] P. A. Baranov, Fertilizer and Harvest 8 (1958).

[32] A. Zotov, Lowering of Capital Investment in the Construction of Mineral Fertilizer Factories [in Russian] (Moscow, 1958).

[33] Ya. Kil'man and V. A. Klevke, Bull. Tech. and Econ. Inf. 9 (1959).

Received May 4, 1959

INDUSTRIAL PRODUCTION OF NATURAL SODA

G. S. Sedel'nikov

The N. S. Kurnakov Institute of General and Inorganic Chemistry,
Academy of Sciences, USSR

Natural soda represents about 5% of the total soda production in our country. Since natural soda is important for Siberia and other regions where there are no synthetic soda factories, it would evidently be wrong not to use this source.

Promising regions for soda prospecting might be the Yakut Autonomous SSR, which has soda lakes, the Onon-Borzinskii region of the Chita Province, and several others.

Large deposits of soda are relatively rare, but some of the known deposits in Africa and North America have soda reserves estimated at tens and hundreds of millions of tons.

Soda is found naturally in solution (brines, soil solutions, alkaline rock waters, and mineral springs), and as solid deposits in the form of crystalline $Na_2CO_3 \cdot 10H_2O$ or trona, $Na_2CO_3 \cdot NaHCO_3 \cdot 2H_2O$. Soda layers, like deposits of other salts, are found at various depths in accordance with their age and formation conditions.

During oil-drilling operations at Verkhnii Chusovsk in the Perm' province in 1940, a soda layer 1.2 meter thick was traversed. The rock samples taken were recorded as marl. It was not until 4 years later, in the course of a study of the rocks from one of the wells, that Aprodova [1] discovered soda in the deposits. However, it was later found that the depth of the seam could not be established. Chemical analysis of the soda samples, which had partially effloresced by that time, showed them to contain Na_2CO_3 (60.0%) and H_2O (36.0%).

A trona seam was found at a depth of 500 meters during oil-well drilling in Wyoming (United States of America).

It has been reported [2] that a factory with an output of 300,000 tons of soda ash per year was established there in 1953. The building costs per ton of soda were roughly one-tenth of the building cost of an ammonia – soda plant.

Soda is rarely found pure in nature; it is usually accompanied by sodium chloride and sulfate. In solid deposits, the amounts of sodium sulfate may be considerable. For example, soda from lake Shara-Burdyinnur in the Mongolian Peoples' Republic has the following composition (in %): Na_2CO_3 23.76, $NaHCO_3$ 17.57, Na_2SO_4 33.43, $CaCO_3$ 0.10, $MgCO_3$ 0.28, insoluble residue 13.18.

The predominant impurity in natural soda solution is NaCl. Soda solutions also often contain potassium and lithium salts, borax, and other minor impurities in variable amounts. The brine of lake Tanatar I of the Mikhailovka region in the Altai has the following composition in summer (in % by weight): Na_2CO_3 15.15, $NaHCO_3$ 2.13, NaCl 5.57, Na_2SO_4 3.35, $Na_2B_4O_7$ 0.153, KCl 0.097, NaBr 0.007; total salts 26.46%; density 1.2672; calcium and magnesium salts absent (sample taken July 19, 1957, analysis performed by E. P. Danilova).

At the present time, the main raw material used at the Mikhailovka Soda Works consists of soda ore and soda brines from the lakes Tanatar I, II, and III. The site covers an area of about 20 square km and consists of the system of Tanatar lakes I to VII and lake Kucherpak. Lenticular accumulations of crystalline soda in

a sand matrix are deposited at the bottom of these lakes. The Na_2CO_3 content of the rock varies over a very wide range, but ore containing not less than 9% Na_2CO_3 is worked.

The lake deposits are impregnated with saturated salt solutions to a depth of 7 meters; these solutions come to the surface and form surface brine. The concentration of salts in the brine falls in winter to 6-7%, while in summer it may reach 28% or as far as crystallization of solid phases. Concentration of the brine in summer is facilitated by the hot and dry climate and the large evaporation surface of the lakes. The concentrated brine is collected in a settler, where $Na_2CO_3 \cdot 10H_2O$, known as raw soda, crystallizes out on cooling. The raw soda is subsequently processed together with soda ore.

The flow sheet of the existing soda works is given below.

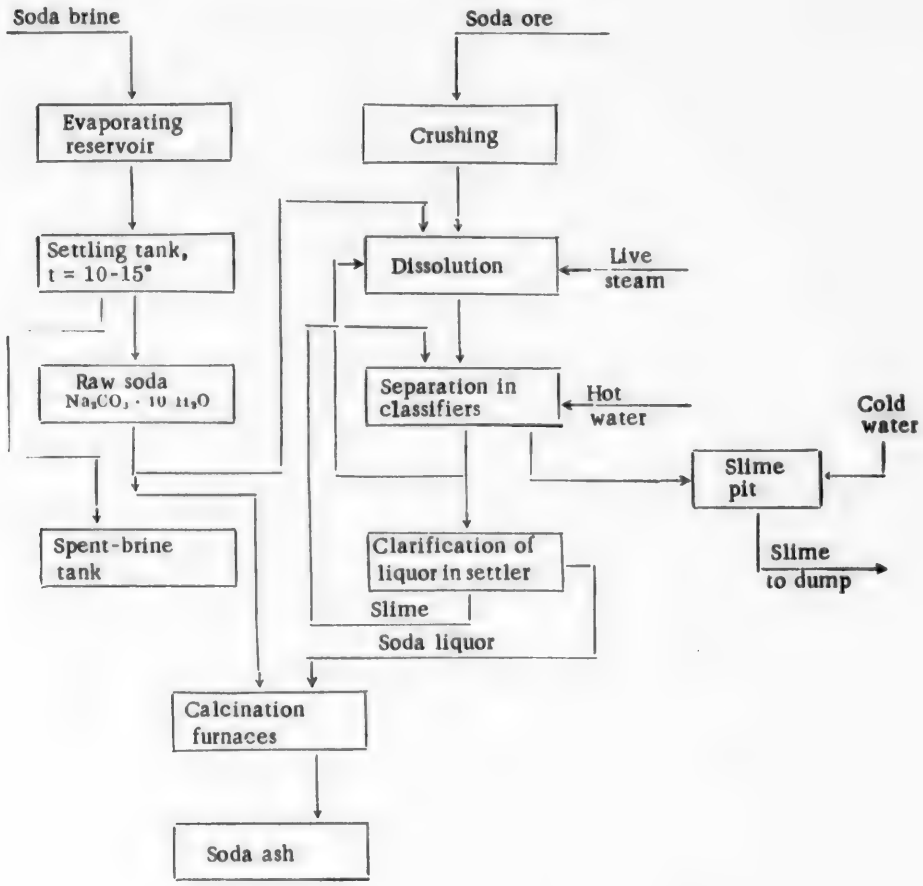

As the scheme does not require any special explanation, we shall not consider it in detail but shall merely draw attention to its main defects. The new Mikhailovka factory was built at high speed during the difficult years of the Great Patriotic War; this was reflected in the choice of the process and later in the quality of the product. The soda ash produced by this factory has an average content of about 80% Na_2CO_3 calculated on the dry substance.

An important disadvantage of this process for conversion of native soda is that the composition of the product depends entirely on the composition of the raw material, as the soda is not subjected to any chemical purification. In order to improve the quality of the soda ash, it is necessary to process the ore selectively and to use raw soda with a reduced sulfate content, which lowers the soda yield. The over-all utilization of soda for the whole site is only about 50% of the certified supply.

In the opinion of the author, who visited this factory in July, 1957, it is now time to revise the process and to change over from conversion of soda ore to conversion of the liquid raw material – soda brine. The results of hydrogeological surveys carried out by a geological prospecting expedition of the All-Union Scientific Research Institute of Halurgy [3] and results of trials of experimental reservoirs carried out at the factory on V. G. Ediger's suggestion, indicate that the restoration of the soda content of the brine by natural dissolution of crystalline soda can be brought up to a level ensuring raw material supplies to the factory throughout the year.

If the factory is converted to the use of liquid raw material, the mine, which at present takes up a great deal of the factory's resources, will become superfluous, as will the dissolution section.

The old process, based on mechanical conversion of the raw material, should be replaced by a new one, based on chemical methods for isolation of pure soda from solutions containing other salt components.

A process for production of soda, with intermediate formation of trona, by partial carbonation and subsequent evaporation of the brine [4] is shown schematically below (p. 1699).

In this process the starting material is natural brine. The brine concentration is artificially regulated, by concentration in tanks and by increase of concentration by dissolution of raw soda in the brine. This last step is absolutely essential in winter, when the salt concentration of the brine falls. The total salt concentration of the brine must not exceed 25%, as at higher concentrations trona starts to crystallize and clog the apparatus during carbonation of the brine in towers. The special features of this process are detailed below.

1. Carbonates are partially converted into bicarbonates by carbonation of the brine by means of flue gases. In accordance with the equilibrium conditions for the system, one-third of the soda must be converted into bicarbonate. The brine contains 10-12% of soda in bicarbonate form, and therefore about 25% must be carbonated artificially.

2. The solution is evaporated in vacuum pans until trona separates out, but crystallization of sulfate must be avoided; for this, it is necessary to bring the total Na_2CO_3 concentration in the mass to 25% (the total is taken as % Na_2CO_3 + % 0.63 $NaHCO_3$).

Pilot-plant trials show that the trona, filtered and washed in centrifuges, has the following composition (in %): Na_2CO_3 43.36, $NaHCO_3$ 34.01, Na_2SO_4 0.25 and H_2O 22.38. The total Na_2CO_3 content in the crude trona is 65%.

The degree of extraction of soda in the form of trona from the brine is 70% under plant conditions, while under laboratory conditions it reaches 80%.

The filtrate after separation of trona is again evaporated in order to precipitate the double salt $2Na_2SO_4 \cdot Na_2CO_3$. After separation of the double salt, the mother liquor has the following composition, according to laboratory data (in %): Na_2CO_3 12.69, NaCl 17.85, Na_2SO_4 1.95, $Na_2B_4O_7$ 0.564, KCl 0.347, total salts 33.40. It contains soda, which can be extracted further in the form of raw soda in the winter settling tank; the raw soda can then be used for trona production. The total yield of soda from the brine reaches 90÷95%, of which about 85% is trona. The spent brine should be treated with magnesium oxide in order to extract B_2O_3. Despite the fact that the boron concentration of the brine is low, if it is converted into a low-percentage boron-magnesium fertilizer the amounts are appreciable. The most vulnerable stage in this process is vacuum evaporation of the soda liquors, which takes a considerable amount of steam. The amount of water to be evaporated (in tons per ton of crude trona) is given by the following expression:

$$W = \frac{(25 - a)\,65}{a \cdot 0.7 \cdot 25}$$

where a is total Na_2CO_3 (in wt. %) in the original liquor, 0.7 is the degree of extraction of soda from liquor, 25 is the total Na_2CO_3 in the mass after evaporation, and 65 is the total Na_2CO_3 in the crude trona.

The physicochemical principles of the process may be briefly represented as follows. In the light of the phase rule the native soda system should be regarded, in the first approximation, as a five-component

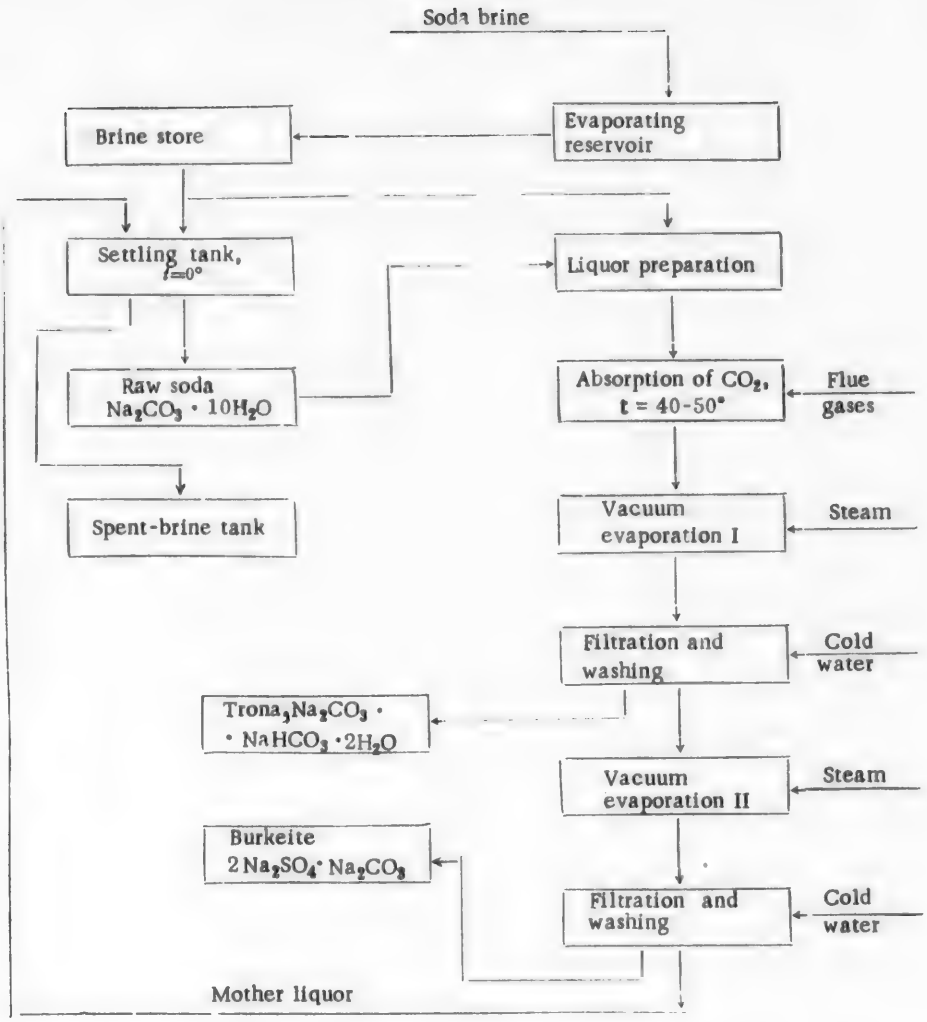

system: $Na_2CO_3 + NaHCO_3 + NaCl + Na_2SO_4 + H_2O$. Such systems can be represented at different temperatures and pressures in a multidimensional space. However, in this instance the diagram can be simplified and represented as a projection on a plane. Figures 1 and 2 are two triangular diagrams: the diagram in Fig. 1 represents crystallization of trona, while Fig. 2 represents the next stage, separation of burkeite. The process is carried out at constant temperatures: at 60° during crystallization of trona, and at 100° during separation of burkeite. The two systems also differ in degree of complexity: Fig. 1 represents four salts, two of which are situated at one corner of the triangle, and Fig. 2 represents three salts. To make the diagrams simpler and clearer [5], the salt concentrations are not indicated. A comparison reveals a qualitative difference between the systems, reflected in the diagrams in the form of crystallization fields of the different solid phases. Each diagram contains point 1, representing the salt composition of the original solution taken for carbonation and subsequent evaporation. In Fig. 1 this point lies in the crystallization field of trona, and,therefore, when the solution is evaporated trona is the first phase to crystallize out. However, as there is very little sodium bicarbonate in the original solution, the system soon passes into the simpler system represented in Fig. 2, and on further evaporation a mixture of burkeite and sodium carbonate monohydrate is deposited.

If point 3 is taken as the composition of the final solution, not yet saturated with sodium chloride, the corresponding salt mixture is represented by the point m. In this salt mixture the ratio of sodium carbonate to sodium sulfate is close to that found in the finished product from the Mikhailovka Soda Combine, and which is in general a characteristic value for this deposit. It is,therefore, evident that it is impossible to isolate soda

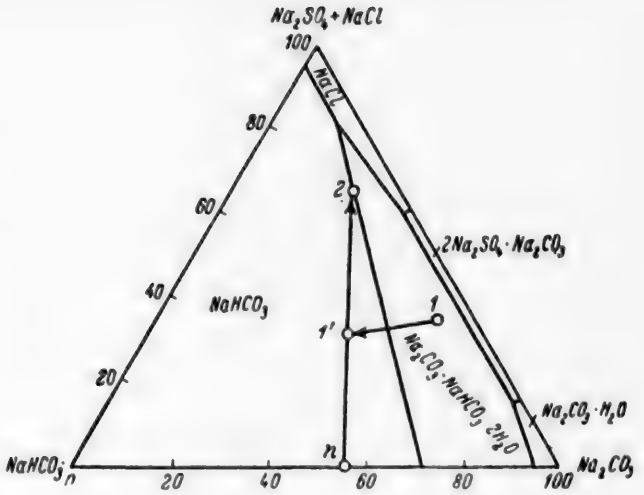

Fig. 1. 60° solubility isotherm for the system Na_2CO_3 + + $NaHCO_3$ + Na_2SO_4 + NaCl + H_2O (in wt. %), salt projection. Points: 1) composition of brine from lake Tanatar I; 1') the same, after partial carbonation; 2) composition of trona filtrate; n) composition of trona $Na_2CO_3 \cdot NaHCO_3 \cdot 2H_2O$.

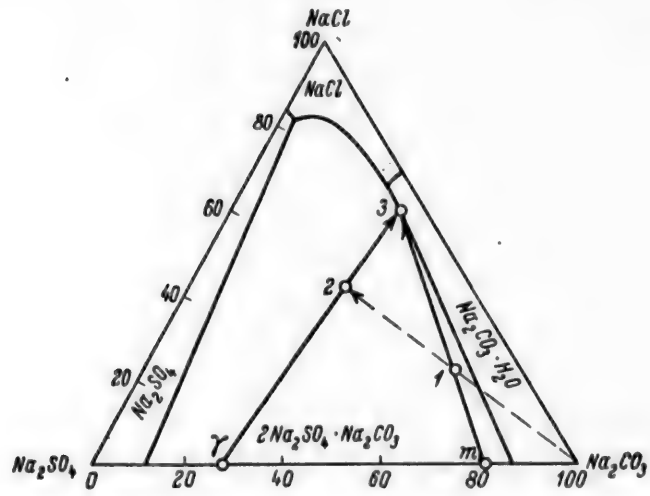

Fig. 2. 100° solubility isotherm for the system Na_2CO_3 + + Na_2SO_4 + NaCl + H_2O (in wt. %), salt projection. Points: 1) composition of brine from lake Tanatar I, 2) composition of trona filtrate, 3) composition of burkeite filtrate, γ) composition of burkeite, $2Na_2SO_4 \cdot Na_2CO_3$.

without an admixture of sulfate by simple evaporation of the native brine. The brine is, therefore, subjected to additional carbonation, after which trona is deposited from solution. This process is represented in Fig. 1. The point 1 shifts to 1', and lies on the trona crystallization path n-1-2. Despite the fact that the composition of the solution at the point 1' lies in the crystallization field of $NaHCO_3$, nevertheless, trona of the composition $Na_2CO_3 \cdot NaHCO_3 \cdot 2H_2O$ is precipitated during evaporation. This is because trona crystallizes from incongruently-saturated solutions, analogously to crystallization of carnallite from solutions containing excess magnesium chloride.

After separation of trona the mother liquor may be regarded as a solution of three salts, apart from bicarbonate, and therefore Fig. 2 is used for all subsequent constructions. The point 2 lies on the burkeite crystallization path $\gamma - 2 - 3$, and when the solution is evaporated the double salt (burkeite) of the composition $2Na_2SO_4 \cdot Na_2CO_3$ is precipitated. The carbonate–sulfate ratio in this compound is quite different from that in the original brine; whereas, in the brine it is close to 5, in burkeite it is 0.4. Thus, two-stage evaporation with preliminary partial carbonation solves the problem of production of pure soda, not inferior to Solvay soda in quality, directly from natural brines. This fact is of special significance for the halurgy industry. Until now this branch of chemical industry has been strongly influenced by the mining industry. This means that in some cases preference is given to conversion of solid salt deposits whereas it would be more advantageous to use solutions for the production of the same salts. Conversion of natural brines offers far more opportunities for complex processes, in which a number of other valuable substances present in natural brines can be obtained in addition to the main product. The process discussed above is an example. Other native soda solutions can be converted similarly. Such solutions are found not only in soda lakes but also at considerable depths in oil-bearing regions and as alkaline springs, mainly in mountainous regions. They can also be subjected to complex conversion from production of soda and other salts.

LITERATURE CITED

[1] A. A. Aprodova, Proc. Acad. Sci. USSR 48, 4, 293 (1945).

[2] Chem. Eng. 118 and 120 (May, 1953).

[3] E. S. Telentyuk, Trans. All-Union Sci. Res. Inst. Halurgy 24, 162 (1952).

[4] G. S. Sedel'nikov and A. I. Lazareva, Authors' Certif. 76241 (1948); Bull. Inventions 7 (1948).

[5] A. B. Zdanovskii, A. I. Lyakhovskaya, and R. E. Shleimovich, Solubilities of Salt Systems, II [in Russian] (Goskhimizdat, 1954) p. 693, 1082.

Received April 30, 1958

SALTING OUT OF THE DOUBLE SULFATE OF NIOBIUM AND AMMONIUM FROM SOLUTIONS IN SULFURIC ACID IN PRESENCE OF TANTALUM AND TITANIUM

Ya. G. Goroshchenko, M. I. Andreeva, and A. G. Babkin

Separation of niobium and tantalum is one of the very difficult problems of chemical technology. Separation of niobium from tantalum becomes even more difficult in presence of titanium. The method now used for separation of niobium and tantalum, which was first proposed by Marignac [1] as long ago as 1866 and which has been improved in recent years, gives satisfactory results in treatment of tantalates and niobates. However, this process is not suitable for treatment of intermediates obtained from titanium–niobium ores. Methods involving the use of sulfuric acid are promising for production of niobium and tantalum from such materials, and such processes should be developed. Separation of niobium and tantalum in sulfate media may be effected by means of two known double sulfates of niobium and ammonium. The double sulfate $NH_4NbO(SO_4)_2$ crystallizes from melts containing sulfuric acid and ammonium sulfate, together with a small admixture of tantalum. It can be used for freeing niobium from tantalum if the content of the latter does not exceed 20-30%. After crystallization, this salt can be used for preparation of niobium pentoxide containing 0.5-1.5% Ta_2O_5, in 70-80% yield. A disadvantage of this method is the necessity of removing titanium dioxide, which interferes with crystallization of the double sulfate, from the niobium–tantalum concentrates.

Another double sulfate of niobium and ammonium, in which the average valence of niobium is 3.67 and the composition of which may be represented by the formula $3(NH_4)_2SO_4 \cdot (NbO)_2(SO_4)_3 \cdot 2Nb_2(SO_4)_3$, is precipitated from sulfate solutions in presence of ammonium sulfate after reduction of niobium to the appropriate valence state.

Crystallization of niobium in the form of this compound, which we term the 3.67 salt, can be used for removal of tantalum and titanium from niobium. However, the methods presently available for reduction of niobium in 70% sulfuric acid with subsequent precipitation by ammonium sulfate as the 3.67 salt greatly complicate the process. For simplification of the technological process it is of interest to study the possible salting out of the 3.67 salt directly from sulfate solutions formed in the treatment of titanium–niobium concentrates after separation of titanium and earth metals, and containing 360-400 g/ liter H_2SO_4 and 180-200 g/ liter $(NH_4)_2SO_4$.

This paper contains the results of a study of the conditions of crystallization of 3.67 salt from sulfate solutions containing ammonium sulfate, and precipitation of this salt after reduction by zinc amalgam in presence of titanium.

EXPERIMENTAL

Solubility of 3.67 salt in aqueous solutions of sulfuric acid and ammonium sulfate. The solubility of 3.67 salt was studied in order to determine the concentration region in which it is stable, and to find favorable conditions for its precipitation.

Saturated solutions were prepared by dissolution of 3.67 salt crystals in mixtures of ammonium sulfate and sulfuric acid. The process was in glass vessels, immersed in a water thermostat, in a CO_2 atmosphere with continuous stirring during 30 minutes. The temperature in the thermostat was maintained at $25 \pm 0.2°$ by means

of a thermoregulator. Special experiments showed that after 30 minutes the solutions were in equilibrium with the solid phase. Samples of liquid phase were taken for analysis by means of a pipet, after filtration through a glass filter in a CO_2 atmosphere. The following were determined in the liquid phase: H_2SO_4 by titration with alkali, $(NH_4)_2O$ by distillation of ammonia and absorption in standard acid solution, total Nb_2O_5 by precipitation with ammonia, and Nb_2O_5 by titration of a sample with 0.1 N $KMnO_4$ solution in a CO_2 atmosphere. The composition of the solid phase was checked by examination of the crystals under the microscope. The stability of 3.67 salt in solution was judged by its color.

The 3.67 salt used in the experiments was prepared from niobium pentoxide of 97% purity. 1.5 g of vanadium pentoxide was dissolved in 100 g of sulfuric acid (oil of vitriol) with warming. The cooled solution was diluted with water to a concentration of 70% H_2SO_4. Niobium was reduced in an electrolytic cell with a mercury cathode [2], and ammonium sulfate was added in the proportion of 100 g per liter to precipitate 3.67 salt. The salt was kept together with the mother liquor in a jar filled with CO_2 and fitted with a ground-glass stopper. Before the start of a saturation experiment the 3.67 salt crystals were filtered off on a funnel with a porous plate (filled with CO_2), washed with solvent, and transferred to the dissolution vessel. The solvent was saturated with CO_2 before use in order to displace dissolved air.

The 3.67 salt is stable at H_2SO_4 concentrations above 150 g/ liter. At lower sulfuric acid concentrations 3.67 salt decomposes with formation of a dark green solution. This is evidently the result of dissociation of the complex ion containing 1 niobium atom in the quinquevalent form and 2 in the trivalent form, and formation of a complex ion in which there is 1 atom of quinquevalent niobium and 5 atoms of trivalent niobium, and which has a dark green color [2].

TABLE 1

Solubility of $3(NH_4)_2SO_4 \cdot (NbO)_2(SO_4)_3 \cdot 2Nb_2(SO_4)_3$ in Sulfuric Acid–Ammonium Sulfate Mixtures at 25°

Concentration (wt. %)					Concentration (g/ liter)		
total Nb_2O_5	Nb_2O_5 in trivalent form	$\frac{Nb^{+3}}{Nb^{+5}}$	SO_3	$(NH_4)_2O$	Nb_2O_5	H_2SO_4	$(NH_4)_2SO_4$
0.139	0.008	0.06	19.87	3.54	1.62	206	105
0.007	0.006	0.9	31.01	3.10	0.09	412	101
0.012	0.011	0.9	41.17	2.92	0.17	628	103
0.009	0.013	1.4	49.86	2.71	0.14	858	82
0.012	0.012	1.0	57.55	2.49	0.19	1064	102
0.090	0.053	0.6	61.81	2.47	1.54	1254	107
0.171	0.126	0.74	64.62	2.57	2.96	1288	113
0.590	0.350	0.59	66.82	2.47	10.4	1355	110
0.031	0.017	0.6	23.96	6.48	0.37	206	198
0.009	0.009	1.0	34.52	5.82	0.12	411	193
0.007	0.014	2.0	43.17	5.60	0.10	615	203
0.005	0.009	2.0	51.76	5.03	0.08	825	195
0.013	0.006	0.5	59.42	4.68	0.21	1051	195
0.084	0.042	0.5	64.83	3.82	1.45	1245	167
0.208	0.140	0.67	67.05	4.59	3.67	1297	205
0.96	0.60	0.63	68.35	4.56	17.0	1334	205
3.26	2.08	0.64	69.47	3.26	58.2	1409	148

The solubility minimum of 3.67 salt (Table 1) is found in the range of sulfuric acid concentrations from 200 to 1000 g H_2SO_4 per liter. The solubility of the salt is decreased in presence of ammonium sulfate. The concentrations of solutions obtained by treatment of titanium–niobium concentrates in which niobium is concentrated, lie in the region of minimum solubility of 3.67 salt.

Despite the measures taken to prevent oxidation of niobium, we did not succeed in obtaining solutions with a 2 : 1 ratio of trivalent to quinquevalent niobium, as in the original salt. Trivalent niobium is probably oxidized slowly in solution by water or sulfuric acid. Solutions saturated with 3.67 salt emit an odor of hydrogen sulfide after long standing.

Reduction of niobium, tantalum, and titanium by zinc amalgam in sulfuric acid solutions. In sulfuric acid solutions the electrochemical reduction of niobium, even on mercury or lead cathodes, proceeds at low current efficiencies [3]. According to our results, the current efficiency falls to 5-6% in presence of ammonium sulfate. Zinc amalgam is a more active reducing agent for niobium.

Reduction of niobium, tantalum, and titanium by zinc amalgam was studied in solutions containing 10-70% sulfuric acid and 100-200 g ammonium sulfate per liter, i.e., in the concentration region in which 3.67 salt may be precipitated. Oxide samples weighing 0.1-0.2 g were taken for the reduction, and fused with potassium pyrosulfate.

The oxides were prepared from the technical products, and were purified by recrystallization of the double salts.

The titanium dioxide contained not less than 99.9% TiO_2. Niobium pentoxide was contaminated with less than 0.2% of titanium (TiO_2) and less than 0.5% of tantalum (Ta_2O_5). Tantalum pentoxide contained less than 0.5% of niobium pentoxide. The oxides were taken to be 100% pure in the calculations.

The pyrosulfate melt was dissolved in 50-70 ml of solution with the required concentration of sulfuric acid. A few drops of perhydrol were added to prevent hydrolysis. The titanium and niobium solutions prepared as described were transparent in all experiments. Hydrolysis of tantalum sulfates could not be prevented. The tantalum solutions were usually turbid, owing to hydrolysis.

TABLE 2

Reduction of Niobium by Zinc Amalgam in Sulfuric Acid Solutions

Solution concentration (g/ liter)		Average valence of niobium after reduction	H_2SO_4 concentration (%)	Average valence of niobium after reduction
H_2SO_4	$(NH_4)_2SO_4$			
200	100	3.353	10	3.308
200	100	3.395	10	3.279
200	100	3.353	10	3.345
400	200	3.333	20	3.209
400	200	3.420	20	3.250
600	100	3.340	20	3.252
600	100	3.362	20	3.292
800	100	3.204	20	3.308
800	100	3.223	20	3.378
900	100	3.253	20	3.407
900	100	3.256	20	3.186
1000	100	3.235	40	3.311
1000	100	3.285	40	3.394
1100	100	3.362	40	3.310
1100	100	3.370	70	3.538
1200	100	3.496	70	3.597
1200	100	3.498	70	3.573

The reduction by means of zinc amalgam was effected in glass separatory funnels, shaken for 10 minutes in a CO_2 atmosphere. The degree of reduction was determined by titration of the solutions, after decantation from the zinc amalgam, by 0.1 N $KMnO_4$ solution. A correction determinated in a blank experiment was applied in calculations of the average valence. This correction was considerable only at sulfuric acid concentrations above 40%.

Zinc amalgam reduces niobium in sulfuric acid solutions to an average valence of 3.2-3.6 (Table 2). The reduction of niobium proceeds more easily in solutions containing 300-600 g H_2SO_4 per liter. The zinc consumption is then close to the theoretical. Increase of the sulfuric acid concentration favors liberation of hydrogen during reduction by zinc amalgam. In solutions containing 70% H_2SO_4, niobium is reduced to an average valence of 3.5-3.6.

The color of niobium solutions containing less than 40% H_2SO_4 changes from blue to dark green during reduction. Ions of quadrivalent niobium are blue [2], while dark green is the color of the complex ion of average valence 3.33. It follows that in these solutions the reduction of niobium does not halt at an average valence of 3.67. Solutions containing over 40% sulfuric acid become red-brown immediately on reduction, without an

TABLE 3

Reduction of Tantalum by Zinc Amalgam in Sulfuric Acid Solutions

Solution concentration (g / liter)		Average valence of tantalum after reduction	Conc. of H_2SO_4 solution (%)	Average valence of tantalum after reduction
H_2SO_4	$(NH_4)_2SO_4$			
200	100	5.00	20	4.374
200	100	5.00	20	4.698
200	100	5.00	20	4.403
400	200	4.441	40	4.606
400	200	4.709	40	4.967
600	100	4.812	70	4.939
600	100	4.851		
800	100	4.723		
800	100	4.594		
900	100	4.624		
900	100	4.616		
1000	100	4.786		
1000	100	4.841		
1100	100	4.935		
1100	100	4.890		
1200	100	4.935		
1200	100	4.948		

TABLE 4

Reduction of Titanium by Zinc Amalgam in Sulfuric Acid Solutions

Solution concentration (g/ liter)		Valence of titanium after reduction	Conc. of H_2SO_4 solution (%)	Valence of titanium after reduction
H_2SO_4	$(NH_4)_2SO_4$			
200	100	2.993	10	3.002
200	100	2.988	10	3.013
200	100	3.005	10	3.013
400	200	3.029	20	3.001
400	200	3.017	20	3.005
600	100	2.990	20	3.015
600	100	2.992	40	2.983
800	100	2.946	40	2.980
800	100	2.993	70	3.041
900	100	2.998	70	3.023
900	100	3.004		
1000	100	2.899		
1000	100	2.909		
1100	100	3.020		
1100	100	3.001		
1200	100	3.041		
1200	100	3.026		

intermediate stage of blue coloration. Increase of the sulfuric acid concentration favors the formation of complex ions of average valence 3.67. In solutions of sulfuric acid and ammonium sulfate, at a sulfuric acid concentration of 200 g/ liter, the color changes from blue through red-brown to dark green. At sulfuric acid concentration of 400 g per liter and over the solutions become red-brown in color during reduction of niobium by zinc amalgam; subsequently, the color changes to dark green. Thus, ammonium sulfate favors formation of 3.67 ions in solution, probably because of the lower solubility of the ammonium salt.

Tantalum is only partially reduced by zinc amalgam, to an average valence of 4.4 (Table 3). The solution remains colorless.

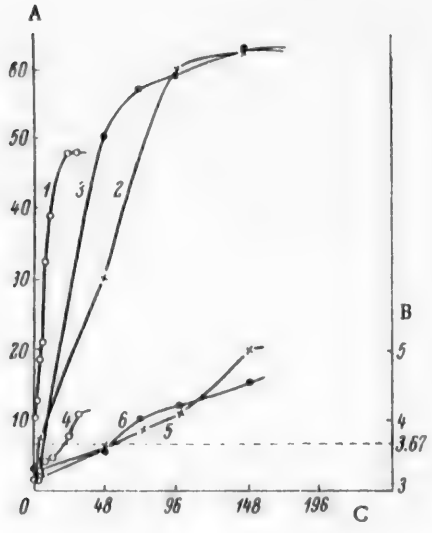

Precipitation of niobium as 3.67 salt in presence of titanium from a solution containing 400 g H_2SO_4 and 200 g $(NH_4)_2SO_4$ per liter, after reduction by zinc amalgam. A) Nb_2O_5 extracted (%), B) average valence of niobium, C) time (hours); TiO_2 contents (%): 1,4) 13.6; 2,5) 20; 3,6) 30. 1-3) Extraction of niobium; 4-6) variations of the average valence of niobium in solution.

Titanium in sulfuric acid solutions is reduced by zinc amalgam to an average valence of 3 (Table 4).

Salting out of niobium as the 3.67 salt from sulfuric acid solutions in presence of titanium. The presence of titanium has no influence on the reduction of niobium by zinc amalgam in sulfuric acid solutions, although titanium forms complex compounds with niobium in sulfuric acid solutions in presence of ammonium sulfate. However, titanium apparently retards polymerization of quinque- and trivalent niobium ions with formation of ions of average valence 3.67. Niobium sulfate solutions in mixtures of sulfuric acid and ammonium sulfate are dark blue or dark green in presence of titanium. The crystallization of 3.67 salt from them is slow.

In ammonium sulfate – sulfuric acid solutions containing niobium and titanium, two processes take place after reduction of the latter: precipitation of the 3.67 salt and oxidation of dissolved niobium. It was found experimentally that, if niobium is reduced to average valence 3.67, precipitation of the double salt lasts for 5-6 hours, after which it almost ceases. During this time about 40% of the niobium is precipitated as the 3.67 salt. Precipitation of 3.67 salt ceases owing to oxidation of niobium in solution. The niobium yield therefore depends on the relative rates of these two processes.

To determine the maximum yield of 3.67 salt obtainable in presence of titanium, a study was made of the kinetics of precipitation of this salt from solutions with different titanium contents, in which niobium had been reduced to a valence lower than 3.67. The solutions contained 400 g H_2SO_4 and 200 g $(NH_4)_2SO_4$ per liter. After reduction the solutions were kept in stoppered separatory funnels containing CO_2. Solution samples were taken at intervals, and the total Nb_2O_5 contents and trivalent niobium were determined.

Studies of the kinetics of precipitation of 3.67 salt from over-reduced solutions showed that after a single reduction by zinc amalgam the maximum amount of niobium which can be precipitated is about 60% (see figure). The maximum yield of 3.67 salt is independent of the amount of titanium, within the limits studied (from 15 to 30% on niobium pentoxide), but it does depend on the degree of initial reduction of the niobium. Precipitation of 3.67 salt terminates owing to autoxidation of niobium in solution. The yield of 3.67 salt can be raised by repeated reduction of niobium by zinc amalgam.

Separation of niobium and tantalum by precipitation of 3.67 salt. Data on separation of niobium and tantalum by precipitation of 3.67 salt after reduction of niobium by zinc amalgam are presented in Table 5. The solutions contained 400 g H_2SO_4 and 200 g $(NH_4)_2SO_4$ per liter; niobium was reduced by zinc amalgam to an average valence of about 3.67. The precipitated 3.67 salt was filtered off after 1-3 days and washed

with a solution containing 400 g of sulfuric acid and 200 g of ammonium sulfate per liter. The distribution of tantalum between the liquid phase and the precipitate was determined by means of radioactive Ta^{182} isotope.

TABLE 5

Separation of Niobium and Tantalum by Precipitation of $3(NH_4)_2SO_4 \cdot (NbO)_2(SO_4)_3 \cdot 2Nb_2(SO_4)_3$ from Solutions Containing 400 g H_2SO_4 and 200 g $(NH_4)_2SO_4$ per Liter

Conc. in original solution (g/ liter)			Extracted into precipitate (%)			Niobium pentoxide in precipitated 3.67 salt (%)		
Nb_2O_5	Ta_2O_5	TiO_2	Nb_2O_5	Ta_2O_5	TiO_2	Nb_2O_5	Ta_2O_5	TiO_2
13.11	0.83	2.90	41.6	1.43	1.73	98.87	0.22	0.91
12.68	0.87	3.25	24.8	0.50	0.48	99.36	0.14	0.50
9.42	4.06	1.96	39.8	1.13	0.68	98.45	1.20	0.35
3.73	8.70	1.88	28.9	0.48	0.49	95.46	3.72	0.82
4.05	12.05	1.64	7.3	0.16	0.18	93.16	5.92	0.92

Precipitation of 3.67 salt yielded niobium of 98-99% purity. The amount of tantalum pentoxide with the niobium pentoxide is reduced to 0.1-0.2%. The amount of tantalum can be decreased to a few hundredths of one per cent by means of reprecipitation. In presence of considerable amounts of tantalum the separation of niobium and tantalum is less efficient. The process is effective if the tantalum content relative to niobium does not exceed 40-50%.

SUMMARY

1. Reduction of niobium, tantalum, and titanium by zinc amalgam in sulfuric acid solutions in presence of ammonium sulfate was studied; it was found that niobium is reduced by zinc amalgam to an average valence of 3.2-3.6, titanium to an average valence of 3, and tantalum is reduced slightly to an average valence of 4.4

2. Reduction of niobium by zinc amalgam can be used for precipitation of niobium from sulfuric acid solutions in the form of the salt $3(NH_4)_2SO_4 \cdot (NbO)_2(SO_4)_3 \cdot 2Nb_2(SO_4)_3$ in presence of tantalum and titanium. Precipitation of niobium as this salt can be recommended as a method for production of niobium pentoxide of 98-99% purity from titanium–niobium concentrates and intermediate products obtained from them.

LITERATURE CITED

[1] J. Marignac, Ann. Chem. phys. 8, 5 (1866).

[2] E. W. Golibersuch and R. C. Young, J. Am. Chem. Soc. 71, 2402 (1949).

[3] E. I. Krylov and V. S. Kolevatova, J. Appl. Chem. 29, 1292 (1956).

Received May 30, 1958

STUDY OF THE HYDRATION OF MAGNESIUM CHLORIDE IN CONTACT WITH MOIST AIR

V. V. Sergeev and I. S. Kachanovskaya

The All-Union Aluminum and Magnesium Institute

The production of titanium by thermal reduction of its tetrachloride by fused magnesium, with removal of the reaction mass, is considerably complicated by the tendency of magnesium chloride to undergo hydration in contact with moist air.

The reaction mass obtained after the reduction process contains about 30% of magnesium chloride, and the spongy titanium after separation contains about 0.1%. Magnesium chloride is hydrated at room temperature to hydrates containing 1, 2, 4, and 6 water molecules. Part of the water of hydration can be removed in the apparatus used for vacuum distillation of the titanium sponge, by means of stepwise heating. In this procedure the reaction mass is held at a temperature of about 200° before distillation, while the reaction products are evacuated by means of a vacuum pump. In this process the higher hydrates are dehydrated virtually without hyfrolysis, whereas the monohydrate, according to Kelly [1], undergoes hydrolysis to the extent of 76 molar %, so that most of the oxygen of the monohydrate passes into the titanium sponge during separation [2]. In this connection the question of the degree of hydration of the hydrates formed during humidification is of great interest to technologists. The present communication deals with this problem.

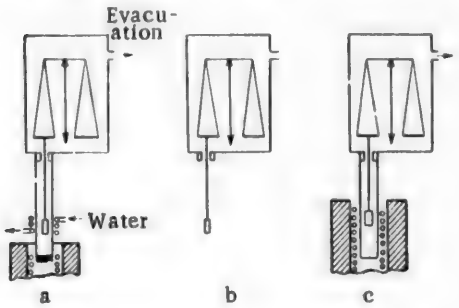

Fig. 1. Schematic diagram of apparatus: a) preparation of anhydrous magnesium chloride, b) hydration of magnesium chloride in air, c) thermal analysis of magnesium chloride.

METHOD OF INVESTIGATION

Preparation of anhydrous $MgCl_2$ and hydration of the product. The apparatus used is depicted schematically in Fig. 1. A quartz tube 13 mm in diameter and 90 mm long was suspended from a vacuum balance by means of a steel thread, and enclosed in a retort. The retort contained 40-50 g of previously remelted magnesium chloride. The whole system was evacuated for 2-3 hours down to 10^{-3} mm residual pressure. The degree of removal of adsorbed moisture from the retort walls was such that the weight increase of a sample of anhydrous magnesium chloride did not exceed 0.2% in 8 hours.

To prepare anhydrous magnesium chloride, the bottom of the retort was heated to 900°, and the retort walls in the region where the quartz tube was located were cooled by water. Magnesium chloride which evaporated from the bottom of the retort condensed on the walls and partially on the quartz tube. By this method 3-5 g of $MgCl_2$ was deposited on the tube in a layer 1-2 mm thick. The retort was then cooled on room temperature and opened, and the magnesium chloride deposited on the quartz tube was exposed to air containing 10-12 g of moisture per m^3 for periods of 15 minutes and 0.5, 1, 2, 3, and 5 hours. Upon longer humidification a saturated solution is formed on the salt surface. At the end of the necessary time the cleaned retort was again attached to the balance; the retort walls were heated in the region where the sample was suspended; the system was evacuated and thermal analysis was carried out.

Thermal analysis of magnesium chloride hydrates. The analysis was based on separation of the dehydration stages of magnesium chloride, i. e., on the creation of conditions under which each of the reactions:

$$MgCl_2 \cdot 6H_2O \rightarrow MgCl_2 \cdot 4H_2O + 2H_2O, \quad (1)$$

$$MgCl_2 \cdot 4H_2O \rightarrow MgCl_2 \cdot 2H_2O + 2H_2O, \quad (2)$$

$$MgCl_2 \cdot 2H_2O \rightarrow MgCl_2 \cdot H_2O + H_2O, \quad (3)$$

$$MgCl_2 \cdot H_2O \rightarrow \begin{matrix} MgOHCl + HCl \\ \searrow MgCl_2 + H_2O \end{matrix} \quad (4)$$

occurred only after removal of water by the preceding reaction was complete. This can be achieved in two ways: 1) by variation of the water-vapor pressure in the system in accordance with the water-vapor pressure for these reactions at a definite temperature, and 2) by variation of temperature at a definite water-vapor pressure in the system.

The second method was used – a weighed sample was heated in four stages, and held at each temperature to constant weight.

The water-vapor pressure in the system was maintained in the range of 60-200 μ and 1-2 mm by means of a vacuum pump.

The weight change at each temperature stage corresponded to removal of H_2O and HCl by one of the Reactions (1-4). The temperatures of the stages were so chosen that the vapor pressure for a given dehydration

TABLE 1

Vapor Pressures of H_2O and HCl over $MgCl_2$ Hydrates at Various Temperatures

Dehydration reactions	Vapor pressure (mm) at temperature				
	25°	80°	100°	127°	177°
$MgCl_2 \cdot 5H_2O \rightleftarrows MgCl_2 \cdot 4H_2O + 2H_2O$	0.76	24.5	72	—	—
$MgCl_2 \cdot 4H_2O \rightleftarrows MgCl_2 \cdot 2H_2O + 2H_2O$	0.05	2.65	12.3	—	—
$MgCl_2 \cdot 2H_2O \rightleftarrows MgCl_2 \cdot H_2O + H_2O$	0.01	0.74	5—6	15.1	156
$MgCl_2 \cdot H_2O$ ↙↗ $MgCl_2 + H_2O$	$4.3 \cdot 10^{-5}$	$6.3 \cdot 10^{-3}$	0.2	0.213	3.3
$MgCl_2 \cdot H_2O$ ↖↘ $MgOHCl + HCl$	$5.9 \cdot 10^{-4}$	0.05	0.1	1.13	13.3

TABLE 2

Stepwise- Dehydration Temperatures

Dehydration reactions	Temperature (°C) at 1-2 mm (60-200 μ) pressure in system	
$MgCl_2 \cdot 6H_2O \rightarrow MgCl_2 \cdot 4H_2O + 2H_2O$	70	35
$MgCl_2 \cdot 4H_2O \rightarrow MgCl_2 \cdot 2H_2O + 2H_2O$	110	80
$MgCl_2 \cdot 2H_2O \rightarrow MgCl_2 \cdot H_2O + H_2O$	200	100
$MgCl_2 \cdot H_2O \nearrow MgCl_2 + H_2O$ $\searrow MgOHCl + HCl$		200

reaction allowed rapid liberation of moisture. At the same time, in order to avoid occurrence of the next reaction, the chosen temperature must be low enough, so that the vapor pressure in the next reaction is less than or equal to the water-vapor pressure in the system. The temperatures of the dehydration stages were chosen with the aid of Kelly's data [1], presented in Table 1.

The chosen temperatures are given in Table 2.

RESULTS

The rate of hydration of magnesium chloride in air with a moisture content of 10-12 g / m^3 is represented by the curve in Fig. 2.

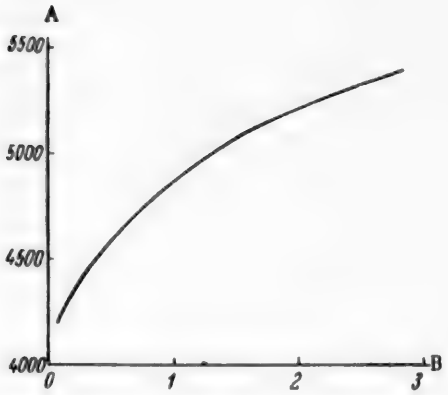

Fig. 2. Hydration of magnesium chloride: A) weight of $MgCl_2$ (mg), B) hydration of time (hours).

By four-stage heating of the hydrated product all 4 reactions of $MgCl_2 \cdot nH_2O$ dehydration could be carried out separately at a H_2O-vapor pressure of 60-200 μ. The results of these experiments are plotted in Fig. 3; at 30° water is removed by Reaction (2) $MgCl_2 \cdot 6H_2O = MgCl_2 \cdot 4H_2O + 2H_2O$; the tetrahydrate does not undergo dehydration to an appreciable extent, as the H_2O vapor pressure of $MgCl_2 \cdot 4H_2O$ at 30° is lower than that in the system. The amount of water removed converting $MgCl_2 \cdot 6H_2O$ into $MgCl_2 \cdot 4H_2O$ is represented by the intercept a in the graph.

At 80° the water-vapor pressure over $MgCl_2 \cdot 4H_2O$ is 2.65 mm, which is above the H_2O pressure in the system, and therefore the reaction $MgCl_2 \cdot 4H_2O \rightarrow MgCl_2 \cdot 2H_2O + 2H_2O$ not only becomes possible, but proceeds fairly rapidly. Removal of water by the reaction $MgCl_2 \cdot 2H_2O \rightarrow MgCl_2 \cdot H_2O + H_2O$ is, again, still impossible because $MgCl_2 \cdot 2H_2O$ does not have a high enough H_2O vapor pressure at 80°. At this stage magnesium chloride hexahydrate is no longer present in the sample because of its complete conversion into $MgCl_2 \cdot 4H_2O$, and therefore the weight change at 80° corresponds to the amount of water removed in the reac- $MgCl_2 \cdot 4H_2O \rightarrow MgCl_2 \cdot 2H_2O + 2H_2O$. This is represented by the intercept b on the graph.

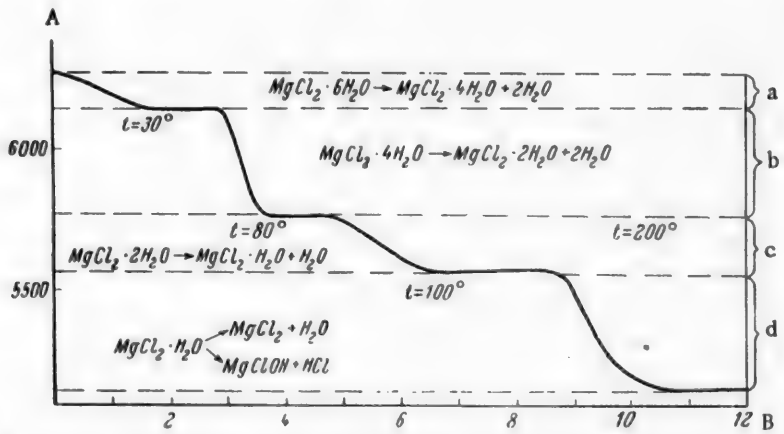

Fig. 3. Stepwise dehydration of hydrated magnesium chloride at 60-200 μ pressure in the system: A) weight (mg), B) time (hours).

The amount of water removed in the reaction $MgCl_2 \cdot 2H_2O \rightarrow MgCl_2 \cdot H_2O + H_2O$ at 100° is represented by the intercept c.

Intercept d represents the weight of H_2O and HCl liberated during dehydration of the monohydrate by the reactions:

$$MgCl_2 \cdot H_2O \begin{cases} \nearrow MgCl_2 + H_2O \\ \searrow MgClOH + HCl. \end{cases}$$

The results of thermal analysis of magnesium chloride exposed to humid air for different times are presented in Table 3.

TABLE 3.

Thermal Analysis of Magnesium Chloride after Different Times of Hydration

Hydration time (hours)	Amounts of H_2O and HCl removed, at temperatures								Amts. of moisture absorbed (in millimoles)
	35°	80°	100°	200°	35°	80°	100°	200°	
	in mg				in millimoles				
0.25	—	30	15	150	—	1.7	0.8	4.5	7
0.5	—	210	100	510	—	11.6	5.5	16	33.1
1	—	320	170	420	—	17.8	9.4	13.1	40.3
2	120	400	200	390	6.7	22.2	11.1	12.2	52.2
3.83	220	510	260	440	12.2	28.3	14.4	13.8	68.7
5	560	1000	500	870	31.1	55.5	27.7	28	142.3

The aggregate of H_2O and HCl (in millimoles) removed at the 200° temperature stage by the reactions

$$MgCl_2 \cdot H_2O \begin{cases} \nearrow MgCl_2 + H_2O, \\ \searrow MgOHCl + HCl \end{cases}$$

was calculated from the average molecular weight (M_{av}) of the gaseous mixture removed, on the assumption that, in accordance with Kelly's data, the degree of hydrolysis of the monohydrate at 200° is 76 molar %: $M_{av} = 0.76 \cdot 36.5 + 0.24 \cdot 18 = 31.9$; the number of millimoles is P/M_{av}.

TABLE 4

Results of Thermal Analysis, as Percentages of the Total Amount of Water of Crystallization

Hydration time (hours)	Molar % of the absorbed water, removed in the reactions			
	$MgCl_2 \cdot 6H_2O \rightarrow MgCl_2 \cdot 4H_2O + 2H_2O$	$MgCl_2 \cdot 4H_2O \rightarrow MgCl_2 \cdot 2H_2O + 2H_2O$	$MgCl_2 \cdot 2H_2O \rightarrow MgCl_2 \cdot H_2O + H_2O$	$MgCl_2 \cdot H_2O \rightarrow MgCl_2 + H_2O$ $MgOHCl + HCl$
0.25	—	24	12	64
0.5	—	35	17	48
1	—	44	23	33
2	11	44	22	23
3.83	18	41	21	20
5	22	39	19.5	19.5

The calculated results are given in Column 9 of Table 3; the total amount of water absorbed (in millimoles) was calculated as the molar total removed at all the dehydration stages, as hydrolysis and dehydration of 1 mole of $MgCl_2 \cdot H_2O$ leads to formation of 1 mole of gaseous HCl and H_2O mixture of molecular weight

31.9, and the number of moles removed at 200° is equal to the number of H_2O moles bound as $MgCl_2 \cdot H_2O$. However, the amount of absorbed moisture calculated in this way was 10% less than the weight increase recorded on the balance during all the hydration experiments.

This may be attributed to incomplete removal of moisture at 200° and to errors in the literature data on the degree of hydrolysis.

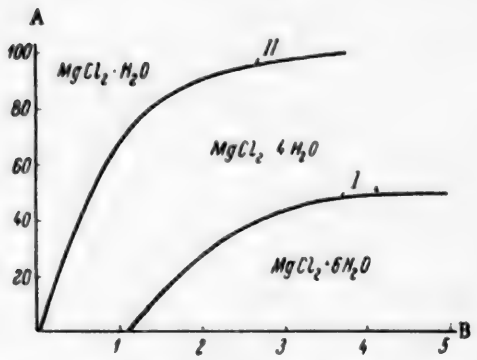

Fig. 4. Effect of hydration time on the composition of $MgCl_2$ hydrates: A) composition (molar % of the amount of hydrated $MgCl_2$), B) hydration time (hours).

The weights of the anhydrous magnesium chloride samples used in these experiments varied from 2.5 to 5.5 g. The area of magnesium chloride on the tube also varied, as it proved impossible to ensure absolutely identical conditions for deposition of magnesium chloride. It would, therefore, be erroneous to draw conclusions concerning the course of hydration of magnesium chloride in time from the absolute amounts of the hydrates formed, or even from the amounts expressed as percentages of the sample weight. Therefore, the experimental results are expressed as percentages of the total amount of water present in magnesium chloride in all the hydrate forms.

The condensate layer in all the experiments was thicker than the penetration depth of moisture into the magnesium chloride. This follows from the fact that after hydration only 20-50% of the total weight of the sample is combined with water in a particular hydrated form. Otherwise, if no anhydrous magnesium chloride was present in the samples, the formation of higher hydrates would lead to erroneous results.

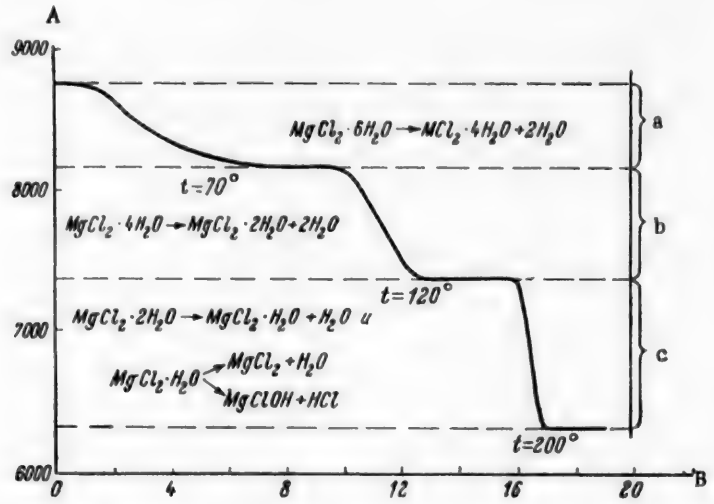

Fig. 5. Stepwise dehydration of hydrated magnesium chloride at 1-2 mm pressure in the system: A) weight (mg), B) time (hours).

The amounts of H_2O and HCl removed at each dehydration stage, expressed as molar percentages of the total, are given in Table 4.

Variations of the percentage composition of hydrated magnesium chloride with the time of exposure of $MgCl_2$ to moist air are plotted in Fig. 4. The amount of magnesium chloride combined with water in a particular hydrated form is taken as 100%. This value does not include anhydrous magnesium chloride. The ordinate intercepts from the abscissa axis to Curve I represent the molar percentage of $MgCl_2 \cdot 6H_2O$ in the composition

of the hydrated magnesium chloride. The ordinate intercepts between Curves I and II represent the amount of $MgCl_2 \cdot 4H_2O$ in the same quantities. The amounts of monohydrate are represented by the ordinate intercepts from Curve II to the abscissa for 100%.

Reactions (3) and (4) could not be separated when the water-vapor pressure in the system was 1-2 mm, as the temperature regulation needed was more accurate than could be achieved by means of the available equipment. Therefore, intercept c in Fig. 5 represents the aggregate weight change due to Reactions (3) and (4).

DISCUSSION OF RESULTS

Figure 2 shows that the curve for the rate of hydration of magnesium chloride is parabolic in character.

The rate of hydration diminishes as the surface becomes humidified. The nature of the hydration curve is consistent with Fig. 3 and 4, which show the same smooth increase in the contents of higher hydrates in humidified magnesium chloride. It is evident from these graphs that the initial instant of humidification of magnesium chloride involves formation of the monohydrate. As the time of hydration increases, the proportion of tetrahydrate in the hydrated magnesium chloride increases. The hexahydrate is formed only after nearly all the monohydrate has been converted to the tetrahydrate. Thus, after 15 minutes of hydration 80% of the hydrated magnesium chloride is present as $MgCl_2 \cdot H_2O$ and only 20% as $MgCl_2 \cdot 4H_2O$. If the product is heated to 200°, only 1/3 of the absorbed moisture is removed by dehydration of $HgCl_2 \cdot 4H_2O$ to the monohydrate, and 2/3 of the absorbed moisture would give up its oxygen to titanium almost completely during separation. On more prolonged contact of magnesium chloride with moist air the proportion of higher hydrates in the hydrated magnesium chloride increases. Thus, after 1 hour of hydration 70% $MgCl_2 \cdot 4H_2O$ and 30% $MgCl_2 \cdot H_2O$ is already formed. This corresponds to removal of 2/3 of the absorbed moisture by dehydration of $MgCl_2 \cdot 4H_2O$ to $MgCl_2 \cdot H_2O$; that is, the effectiveness of stepwise heating increases after more prolonged hydration. Magnesium chloride humidified for longer than 1 hour contains the hexahydrate. However, not all the tetrahydrate is converted into the hexahydrate even after prolonged humidification (5 hours), and despite the formation of magnesium chloride solution on the surface the proportion of hexahydrate in the hydrated magnesium chloride is only 50%. Not less than 20% of the absorbed moisture corresponds to the monohydrate formed by decomposition of $MgCl_2 \cdot 6H_2O$ and $MgCl_2 \cdot 4H_2O$.

For removal of water from the monohydrate with the minimum contamination of titanium by oxygen, the reaction mass should be heated up sharply, as the degree of hydrolysis during dehydration of the monohydrate decreases with increase of temperature. Therefore, a more correct regime of stepwise heating would be heating at a temperature at which the polyhydrates are decomposed down to the monohydrate, followed by a sharp rise of temperature to the separation temperature.

The results of thermal analysis indicate that with good evacuation of the apparatus down to a pressure of 60-200 μ the appropriate temperature is 100-110°. Reactions of dehydration of $MgCl_2 \cdot nH_2O$ to $MgCl_2 \cdot 2H_2O$ proceed fairly rapidly at that temperature. Dehydration of the dihydrate is not rapid, making determination of the end of the process difficult. This fact made 100° disadvantageous as the heating temperature. Thermal analysis of magnesium chloride exposed to moist air for different times did not reveal the dihydrate in the hydrated product. In fact, the amount of water removed at the 80° temperature stage was twice as much as the amount of water removed at the 100° stage, in all the experiments (within the limits of experimental error). This proportion corresponds to removal of two water molecules in the reaction $MgCl_2 \cdot 4H_2O \rightarrow MgCl_2 \cdot 2H_2O + 2H_2O$ and one water molecule at 100° in the reaction $MgCl_2 \cdot 2H_2O \rightarrow MgCl_2 \cdot H_2O + H_2O$; that is, water is removed only from the dihydrate formed by decomposition of higher hydrates. This indicates that hydration of magnesium chloride proceeds as follows:

$$MgCl_2 + H_2O \rightarrow MgCl_2 \cdot H_2O,$$

$$MgCl_2 \cdot H_2O + 3H_2O \rightarrow MgCl_2 \cdot 4H_2O,$$

$$MgCl_2 \cdot 4H_2O + 2H_2O \rightarrow MgCl_2 \cdot 6H_2O,$$

$$MgCl_2 \cdot 6H_2O + H_2O \rightarrow \text{Saturated solution.}$$

Hydration of magnesium chloride proceeds from the surface without touching the grain centers. Even after 5 hours of humidification of a sample with a condensate layer 1-2 mm thick, when formation of a surface solution became apparent, about 50% of the magnesium chloride was found to be anhydrous; this means that the penetration depth of moisture into the layer of condensed magnesium chloride does not exceed 1-2 mm.

SUMMARY

1. Magnesium chloride is hydrated from the surface only. The penetration depth of moisture into $MgCl_2$ condensed under our experimental conditions does not exceed 1-2 mm.

2. The monohydrate is formed mainly at the initial instant of hydration of magnesium chloride.

Longer exposure of magnesium chloride to moist air increases the content of $MgCl_2 \cdot 4H_2O$ in the hydrated product. The haxahydrate is formed only after nearly all the $MgCl_2 \cdot H_2O$ has been converted to $MgCl_2 \cdot 4H_2O$.

3. The hydration curve of magnesium chloride is parabolic in character. The rate of hydration diminishes as higher hydrates are formed on the surface.

4. Stepwise heating of the reaction mass before vacuum separation is ineffective after brief humidification. After 15 minutes of contact with moist air only 1/3 of the absorbed moisture can be removed. With longer humidification this measure becomes more effective, and 2/3 of the absorbed moisture can be removed after humidification lasting one hour. However, if stepwise heating is used, not less than 20% of the moisture reacts almost entirely with titanium in all cases.

LITERATURE CITED

[1] Kelly,* Quantity of Energy Expended and Equilibrium Conditions in Dehydration, Hydrolysis, and Decomposition of Magnesium Chloride (Washington, 1954).

[2] V. V. Sergeev and I. S. Kachanovskaya, Bull. Nonferrous Metallurgy TsIIN 4, 105 (1958).

[3] N. Ya. Orobei and V. M. Zhogina, Trans. All-Union Aluminum and Magnesium Inst. 11-12 (1935).

Received July 11, 1958

*Name not verified.

INVESTIGATION OF THE ELASTIC PROPERTIES OF CERTAIN CERAMIC COMPOSITIONS

V. Z. Petrova and A. I. Avgustinik

Investigations of the elastic properties of concretes, refractories, glass, and porcelain by sonic and ultrasonic methods [1-6] provide ways of determining the quality of the products without destruction.

The purpose of the present investigation was to determine the relationship between the elasticity modulus E, the compressive strength σ_{com}, and the bending strength σ_{bend} of porcelain containing different amounts of quartz of different particle sizes.

The determinations of E were performed by the resonance method with the IChMK-2 instrument constructed by the Laboratory of Radio-transmission Devices of the Lenin Institute of Electrical Engineering, Leningrad. The circuit and operation of the earlier model of the IChMK-2 instrument were described by Veselova [7]. The IChMK-2 instrument used in our experiments can be used for determinations of the shearing modulus G and the Poisson ratio μ, in addition to E; the frequency range of the new instrument has been extended to 12,000 cycles/second.

For determination of E, bending oscillations were induced in the specimen. At the instant of resonance between the generator frequency and the fundamental frequency of the specimen the indicator device shows a sharp increase of the oscillation amplitude. This method gives the fundamental vibration frequency of the specimen; if its weight and dimensions are known, E can be found from the appropriate formula, which is, for specimens of circular section:

$$E = 1.638N^2\left(\frac{l}{d}\right)^3\frac{P}{b}\quad 10^{-3}\ \text{kg/cm}^2,$$

and for specimens of rectangular section:

$$E = 0.9653N^2\left(\frac{l}{h}\right)^3\frac{P}{b}\quad 10^{-6}\ \text{kg/cm}^2,$$

where N is the fundamental frequency of the specimen, P is its weight (in kg), l is the length (in cm), b is the width (in cm), and h is the height (in cm) in the vibration plane.

The body composition of the porcelains used for the tests are given in Table 1, which also gives the duration and method of quartz grinding. The chemical composition of the raw materials is given in Table 2.

Samples of porcelain body from the "Proletarii" works, of the following composition (%): Prosyanaya kaolin 14, Kyshtym kaolin 14, Chasov Yar clay 17, quartz sand 13.5, pegmatite 36.5, grog 5, and from the Artem accessory and insulator plant were used.

The ground mixes were dehydrated in plaster beakers to a residual moisture content of about 23%. The particle-size composition of the ground sand was determined by the pipet method (Table 3). The specimens were fired in tunnel kilns of the "proletarii" and Artem works, in the scove kiln of the Artem works by the normal procedure, and in a Silit laboratory furnace at 1200 and 1320°.

TABLE 1

Composition of Porcelain Bodies and Grinding Methods

Material	Body No.												Grinding time (hours)	Grinding method
	1	2	3	4	5	6	7	8	9	10	11	12		
Kyshtym kaolin	50	50	50	50	50	50	50	50	50	50	50	50	Passed through sieve with 10,000 holes/ cm^2	
Feldspar	30	25	20	25	25	25	25	25	50	37.5	25	10		
Quartz sand	—	—	—	25	—	—	—	—	—	—	—	—	3	In vibratory mill
	—	—	—	—	25	—	—	—	—	—	—	—	6	
	—	—	—	—	—	25	—	—	—	—	—	—	8	
	20	25	30	—	—	—	—	—	—	—	—	—	70	In ball mill
	—	—	—	—	—	—	—	—	—	12.5	25	40	10	
Alumina	—	—	—	—	—	—	—	25	—	—	—	—	1.5	In vibratory mill
	—	—	—	—	—	—	25	—	—	—	—	—	4	

The specimens had the following dimensions: for the resonance tests, length 170 mm and diameter 25 mm; for the bending tests, length 70 mm and diameter 8 mm; for the compressive tests (the specimens were cut by a diamond saw), length 25 mm, diameter 25 mm. This method was taken from Veselova's paper [7].

TABLE 2

Chemical Composition of Raw Materials (%)

Material	SiO_2	Al_2O_3 + TiO_2	Fe_2O_3	CaO	MgO	K_2O	Na_2O	Calcination loss	Total	Hygroscopic moisture
Kyshtym kaolin	45.95	38.88	0.95	0.70	0.19	—	—	13.45	100.13	0.68
Feldspar	66.64	18.53	0.27	0.72	0.09	9.65	3.22	0.72	99.84	0.16
Luga quartz sand	97.48	1.16	0.32	0.20	0.17	—	—	0.56	99.89	0.12

The results of the compressive tests were very erratic, evidently owing to the stresses which arose when the specimens were sawn. Therefore, specimens for compressive tests should be made from the raw mass.

For specimens made from bodies No. 1-8, E was determined by the sonic method. In addition, to this method, the ultrasonic method was used for determinations of E for specimens made from bodies No. 9-12. The shearing modulus (G) and Poisson ratio (μ) were also determined for these last body numbers. It was found that E and G vary symbatically, both with changes of composition and with changes of firing temperature (Fig. 1; a,b,c,d); therefore, only one of these characteristics need be determined.

It is important to note that the bending strength and elasticity modulus of porcelain increased with increase of the quartz content up to 25% only (both with a grinding time of 10 hours for No. 10, 11, and 12,

and a time of 70 hours for No. 1, 2, and 3); these values decreased with further increase of quartz content, as is clear from Fig. 1. A high quartz content also has an adverse effect on the compressive strength of porcelain (Fig. 2).

TABLE 3

Particle-Size Composition of the Porcelain Bodies

Fraction No.	Particle diameter (mm)	Ball mill	Vibratory mill grinding time (hours)				
		70	3	6	8	1.5	4
		contents (%)					
		quartz			alumina		
1	<0.01	21.9	56.8	58.9	66.1	6.4	22.4
2	<0.005	11.1	31.8	37.3	42.9	1.25	15.35
3	<0.001	1.84	4.14	6.15	11.7	2.50	10.21

The explanation of the maxima on the E and G curves may be that with increase of the quartz content (up to about 25%) in the porcelain the silica content of the feldspar melt increases, so that the glass phase becomes more acid and stronger, while its relative proportion decreases owing to increase of the quartz content.

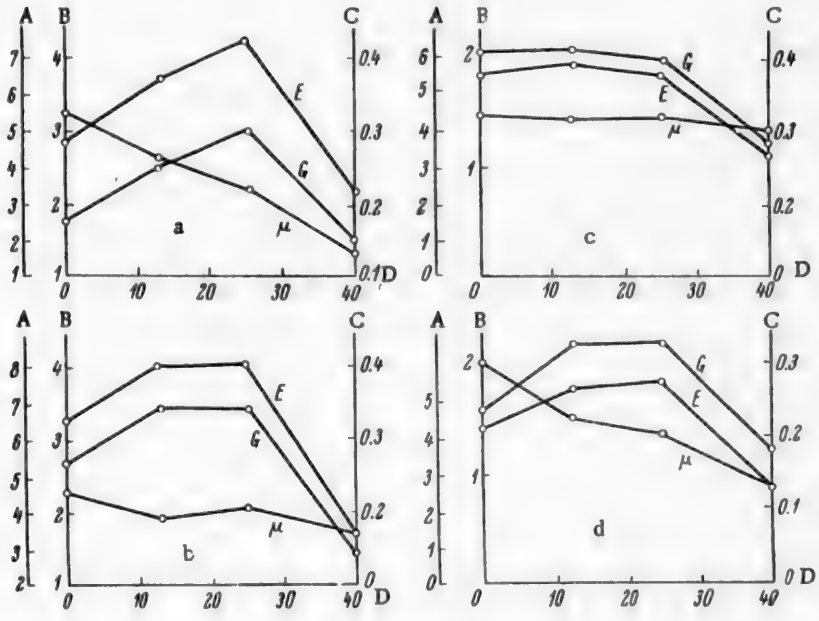

Fig. 1. Variations of E, G, and μ with quartz content: A) $E \cdot 10^{-5}$ (kg/ cm²), B) $G \cdot 10^{-5}$ (kg/ cm²), C) μ, D) quartz contents (%); firing temperature (°C) and time (hours) respectively: a) 1250, 2; b) 1250, 5; c) 1350, 6; d) 1350, 1.

Increase of the quartz content of the porcelain is accompanied by an increase of the number of regions in which thermal stresses can develop on cooling, because of the considerable difference between the expansion coefficients of quartz (α = 1.38% [6]) and the glass phase (α = 0.53 – 0.79% [6]). The greater contraction of the quartz grains than of the surrounding glass phase on cooling results in the appearance of stresses, mainly

of a tensile nature, in the grains and between the grains and the glass phase. These stresses weaken the porcelain, i.e., they oppose the increase in the porcelain strength caused by dissolution of quartz in the glass phase.

Increase of the heating time at a somewhat lower temperature (1250°) or increase of the heating temperature (1350°) apparently creates conditions for saturation of the glass phase with silica at a lower quartz content, and this retards the course of the E and G curves (causing flattened maxima). Further increase of the quartz content in the porcelain (above 25%) does not favor further dissolution of silica in the glass phase, but only increases the number of tensile-stress sites.

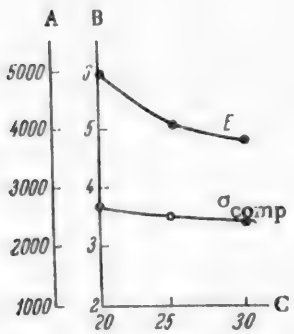

Fig. 2. Variations of E with body composition, for a firing temperature of 1200°. A) σ_{com} (kg /cm^2), B) E · $\cdot 10^{-5}$ (kg/ cm^2), C) quartz content (%).

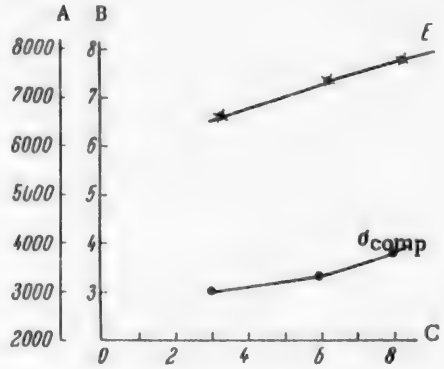

Fig. 3. Variations of E with degree of grinding, for a firing temperature of 1200°: A) σ_{com} (kg/ cm^2), B) E · 10^{-5} (kg/ cm^2), C) time of vibratory grinding (hours).

Having touched on the question of stresses in porcelain and having correlated the extent of their significance with the number of such sites, in which primary microstresses arise, we must draw attention to two opposing viewpoints on the nature of the stresses. Marzahl [5] considers that because of the difference between the expansion coefficients of the glass phase compressive stresses arise in the glass phase of porcelain, and this increases the strength of the porcelain. Genin [6] believes that radial tensile stresses arise in the quartz grains and in the glass phase, while compressive stresses appear at the quartz–glass phase boundary; a fault of Genin's paper is lack of experimental data [6]. both authors correlate the quantitative aspects of the microstresses with the quartz content and its particle size.

If compressive stresses arose in porcelain or cooling, increase of the quartz content should lead to an increase in the mechanical strength of the porcelain, and hence to an increase of E. However, our experimental data (Tables 4, 5 and Figs. 1-3) show that these values pass through maxima. Hence our data are more consistent with Genin's view.

We attribute the maxima on the E and G curves (Fig. 1) to increase of the mechanical strength of porcelain owing to dissolution of quartz in the glass phase. After the glass phase has become saturated with quartz, the mechanical strength falls with further increase of quartz content owing to increasing tensile stresses at the quartz–glass phase boundary.

If the grinding time of the quartz is increased, porcelain with high values of E and G is obtained; this may be attributed to better dissolution of silica in the glass phase, more uniform sintering, and consequent greater homogeneity of the porcelain. Examination of polished sections (microphotographs of these are not given in this paper) shows that the thickness of the glassy interlayers decreases from 10-8 to 5-2 μ with increasing fineness of the quartz and with increasing quartz content.

Our results are confirmed by the work of Keshishyan [8], carried out in order to determine the relationship between mechanical strength and crystallization of glasses; in the authors' opinion, the latter results in considerable tensile stresses owing to the density difference between the two phases.

TABLE 4

Elasticity Modulus and Technical Characteristics of Bodies Fired in the Laboratory Furnace (Firing temperature 1320°)

Body No.	Elasticity modulus $E \cdot 10^{-5}$ (kg/cm²)	Compressive (kg/cm²)	Bulk density (g/cc)
1	6.7920	2520	2.355
2	6.6740	2495	2.355
3	6.4630	2495	2.355
4	7.1430	2650	2.368
5	7.2960	2760	2.369
6	7.3640	3185	2.370
7	10.3350	3787	2.745
8	11.1750	4660	2.747

Note. The values of E were obtained from 5-6 determinations: the variation was 5-7%.

TABLE 5

Elasticity Modulus and Technical Characteristics of Bodies Fired in the Laboratory Furnace (Firing temperature 1200°)

Body No.	Elasticity modulus $E \cdot 10^{-5}$ (kg/cm²)	Compressive strength (kg/cm²)	Bulk density (g/cc)
1	5.9776	2660	2.33
2	5.0713	2565	2.42
3	4.8076	2510	2.108
4	6.5831	3025	2.366
5	7.3553	3270	2.388
6	7.8103	3765	2.416
7	7.1277	2690	2.486
8	8.9901	4010	2.562

TABLE 6

Variations of the Elasticity Modulus and Technical Characteristics with Heating Times and Final Temperatures

Firing	Firing temperature (°C)	Time (hours)	Elasticity modulus $E \cdot 10^{-5}$ (kg/cm²)	Water absorption (%)	Strength (kg/cm²)		Density (g/cc)
					compressive	bending	
$П_5$	1350	4	5.04	4.68	1876	445.5	2.488
$П_1$	1300	1	5.323	5.37	1505	477.0	2.462
$П_3$	1350	1	5 612	5.70	1655	480.6	2.459
$П_6$	1250	4	5.743	4.93	2073	501.0	2.474
$П_4$	1300	4	6.306	1.725	3005	602.4	2.500
$П_2$	1320	2	7.638	0.173	3010	672.7	2.522

The second (suspension) method for determination of E for rods was used in order to find E at different temperatures and to find the relationship between E and σ_{bend}. The results are presented in Fig. 4 and 5.

The variations of E and σ_{bend} are represented by almost parallel curves. The main advantage of this method is that a specimen can be used for determination of σ_{bend} after determination of E without the laborious cutting of the specimen by means of a diamond saw which is necessary to preparation in specimens for compressive-strength tests.

Procelain body from the "Proletarii" works was thoroughly studied. In order to find whether it is possible to test the quality of the product without destruction of the specimens and to determine the influence of the technological process on the elastic constants, 200 specimens were molded at "Proletarii" works and fired in the works tunnel kiln and in the laboratory furnace under various conditions.

In Table 6 the firings are arranged in order of increasing E.

The values found for E for works-fired specimens are not given. It should be noted, however, that the general relationship between E, σ_{bend}, and σ_{com} is satisfactorily maintained (Figs. 6, 7); this suggests that quality control is possible by this method. Similar results were obtained for body samples from the Artem works. 200 specimens fired at different regions of the scove kiln and of the cars in the tunnel kiln (Table 7) were tested by the sonic method.

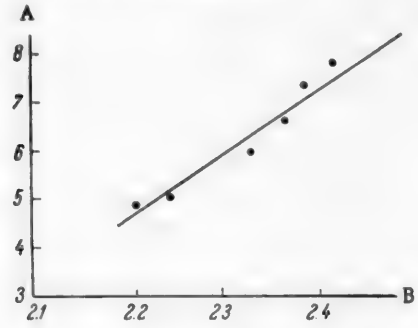

Fig. 4. Variation of E with R for works bodies: A) $E \cdot 10^{-5}$ (kg/ cm^2); B) R (g/ cc).

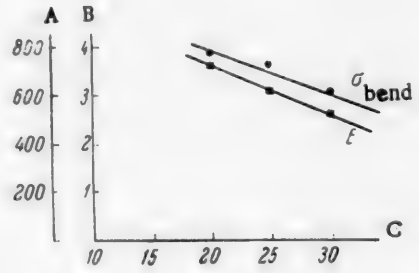

Fig. 5. Variation of E with composition (suspension tests): A) σ_{bend}(kg/ cm^2), B) $E \cdot 10^{-5}$ (kg/ cm^2), C) quartz content (%).

TABLE 7

Elasticity Modulus of Artem Works Specimens Fired in the Tunnel Kiln and Scove Kiln at 1320-1330°

Kiln	Position of specimen in kiln	Elasticity modulus $E \cdot 10^{-5}$ (kg/ cm^2)
Scove kiln	Center, floor	5.759
	Center, middle	8.320
	Center, top	5.730
	Along radius, burner	5.450
	Along radius, middle	5.990
Tunnel kiln	Burner	5.747
	Bottom row, center	6.070
	Middle row, center	5.950
	Top row, center	5.720

TABLE 8

Variations of Elasticity Modulus Under Different Cooling Conditions

Cooling	No. of specimens	Elasticity modulus $E \cdot 10^{-5}$ (kg/ cm^2)
Usual, during 10 hours	5	4.24
In air stream down from temperature of (°C):		
800	6	1.38
700	5	1.84
500	6	4.19
In water from 600°	4	1.99
In sand from 600°	3	3.685
Retarded with partly open kiln door, from 500°	6	4.39
Retarded in air without air blast, from 600°	3	4.19

Each value of E (Table 7) represents the average for a batch of 25 specimens. Pyrometric determinations of the firing temperatures indicated that there are considerable temparature differences over the volume of the kiln, leading to the production of specimens differeing in quality. This is confirmed by the results of mechanical strength and water absorption tests.

Determination of the effect of the stressed state on the elastic properties (the modulus E) of porcelain was another problem considered in the present investigation.

To create a state of stress in the porcelain it was cooled rapidly in a current of air from a fan at a velocity of 7-8 m/ second. Porcelain specimens of the dimensions given above were cooled down from 800, 700, and 500° after extraction from a Silit furnace (after firing at 1320°); other specimens were placed in water or sand for cooling. Table 8 contains average results of 5-6 values of E; the variations were 5-7%.

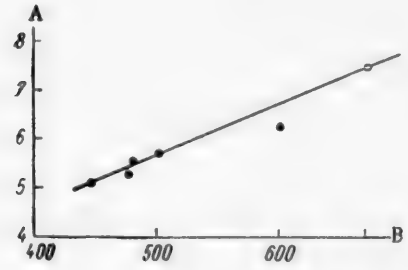

Fig. 6. Variation of E with σ_{bend}: A) $E \cdot 10^{-5}$ (kg/ cm²), B σ_{bend} (kg/ cm²).

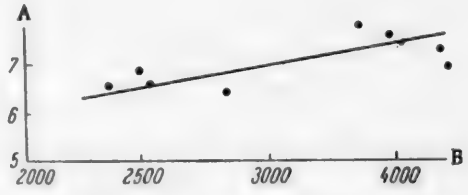

Fig. 7. Variation of E with σ_{com}: A) $E \cdot 10^{-5}$ (kg/ cm²), B) σ_{com} (kg/ cm²).

Although the data in Table 8 are qualitative rather than quantitative, they nevertheless indicate that more rapid cooling corresponds to lower values of E. For example, for porcelain cooled down from 600° in water $E = 1.99 \cdot 10^{-5}$, whereas after cooling in sand it is $-3.68 \cdot 10^{-5}$ and after 10 hours of cooling in the kiln it is $-4.24 \cdot 10^{-5}$. Cooling down from a higher temperature is more rapid and the value of E is then lower than that found for cooling from 500°.

Since we assume that the cooling rate determines the intensity of the stressed state of the ceramic material, these data show that the modulus E can serve as a characteristic of the stressed state.

SUMMARY

1. Increase of the quartz content of insulator porcelain to 25% results in an increase of its elasticity modulus E. Further increase of the quartz content results in a decrease of E.

2. The relationships found between E, σ_{bend}, σ_{com}, and the bulk density of insulator porcelain can be used as the basis of a method of quality control.

3. The value of E may reflect the conditions of cooling of the porcelain and its stressed state.

LITERATURE CITED

[1] G. N. Voronkov, Trans. State Res. Inst. of Electrical Ceramics 1 (1956).

[2] G. M. Rushchuk, Papers at the 1958 Conference of the Mozhaiskii LVVIA [in Russian].

[3] A. S. Gurvich, Trans. Sci. Res. Inst. Constructional Ceramics 12 (1957).

[4] Yu. S. Chatinyan and I. G. Drozdov, Electricity 2, 32 (1955).

[5] L. G. Genin, Glass and Ceramics 4 (1958).

[6] H. Marzahl, Coll. Translations from the Foreign Periodical Literature, Chemistry and Technology of Silicates, 1 [in Russian] (1956); Ber. Dent. Keram. Res. 32, No. 7, 203 (1955).

[7] Z. I. Veselova, Refractories 5, 221 (1956).

[8] T. N. Keshishyan and M. B. Épel'baum, Glass and Ceramics 7, 11 (1958).

Received September 19, 1958

STUDY OF THE CRYSTALLIZABILITY (DEVITRIFICATION) OF GLASSES IN THE SYSTEM $K_2O-ZnO-P_2O_5$

T. I. Veinberg

Phosphate glasses, which have certain special properties which distinguish them from silicate glasses, are becoming increasingly known and the demand for them increases from year to year. However, the phosphate glasses known at present have considerable disadvantages: a high tendency to crystallization, or low chemical durability, or both simultaneously. These disadvantages cause serious difficulties in the technological production of such glasses, and therefore studies of the possibility of obtaining phosphate glasses with a low crystallization tendency and increased resistance to moist atmospheres are of considerable topical significance.

Phosphate systems which yield glasses have been studied very little as yet.

It is known from earlier work in this field [1-3] that melts containing enough or more than enough phosphoric anhydride for formation of metaphosphates of their constituent basic elements can be obtained in glass form. If the amount of phosphoric anhydride is insufficient to combine with all the basic oxides, glasses are not formed as a rule; complete crystallization occurs even during the melting. In presence of excess phosphoric anhydride the glasses formed are hygroscopic and are of indefinite composition, as the uncombined phosphoric anhydride partially volatilizes during the melting, and the cooled glass absorbs moisture from the air. Therefore, formulations of phosphate glasses were usually based on mixtures of metaphosphates of alkaline-earth and alkali metals, and of zinc and aluminum [4-9]. Attempts to lower the devitrification tendency were based on the use of more complex compositions, but despite this glasses based on metaphosphates have a high tendency to crystallization.

The results of investigations of two-component phosphate systems by ourselves and others [10-13] show that only zinc and beryllium phosphates can be obtained in the glassy state if the content of phosphoric anhydride is less than 50 molar%. We also found that if alkali-metal metaphosphates are added to metaphosphates of bivalent metals the crystallization tendency of the glasses diminishes. It was therefore of interest to study the crystallizability of three-component glasses in the systems $K_2O-ZnO-P_2O_5$ and $Na_2O-ZnO-P_2O_5$ in order to investigate the possibility of obtaining glasses with a low tendency to crystallization.

EXPERIMENTAL

The glasses were melted in one or two kilogram lots in quartz crucibles. The melting temperature was between 800 and 1200°, in accordance with the composition of the glass. The finished glasses were cast in the form of slabs so that the region of the maximum crystallization rate could be passed as rapidly as possible, and then annealed in an electric muffle furnace. The annealing temperatures were determined approximately for groups of glasses of similar compositions. The cooled slabs were broken up, and glass fragments 0.25-0.5 cc in size were put into procelain boats and subjected to enforced crystallization in a temperature-gradient furnace in the 450-850° range. Most of the glasses were kept in this furnace for 3 hours.

These experiments showed that in the two-component system $ZnO-P_2O_5$ the boundary of the glassy state lies close to the composition $65ZnO \cdot 35P_2O_5$ (in molar %), in the system $K_2O-P_2O_5$ crystallization takes places during the melting even at the composition $40K_2O \cdot 60P_2O_5$, and in the system $Na_2O-P_2O_5$ at the composition $52Na_2O \cdot 48P_2O_5$. Although glasses are formed near these compositions, they crystallize completely

after exposure of only one hour in the furnace. Zinc metaphosphate crystallized very strongly and yet is slightly hygroscopic. Zinc phosphates containing less than 50 molar % P_2O_5 are not hygroscopic. Glassy alkali phosphates are hygroscopic at all oxide ratios.

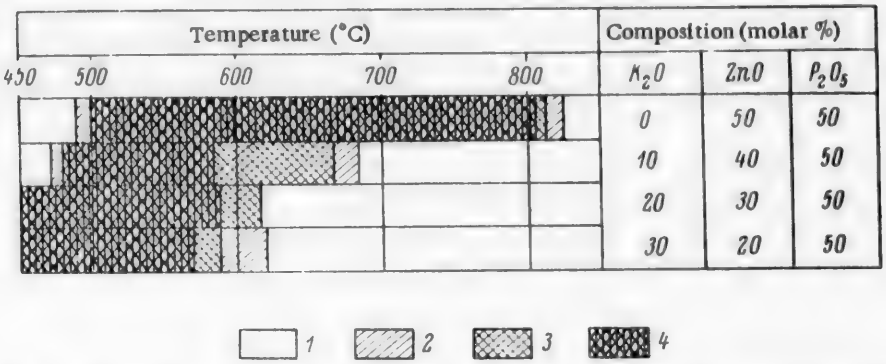

Fig. 1. Crystallization tendency of glasses with the composition $nK_2O \cdot mZnO \cdot 50P_2O_5$. 1) Does not crystallize, 2) weak crystallization, 3) strong crystallization, 4) total crystallization.

The crystallization tendency of three-component glasses in the system $K_2O-ZnO-P_2O_5$ with 50 molar % P_2O_5 is considerably lower than that of zinc metaphosphate. Figure 1 shows graphically variations of the degree of crystallization with temperature for a number of glasses containing 50 molar % P_2O_5. It can be seen that replacement of only 10 molar % ZnO by 10 molar % K_2O makes the crystallization region considerably narrower. On further increase of the K_2O content at the expense of ZnO, the crystallizability of the glasses remains almost unchanged.

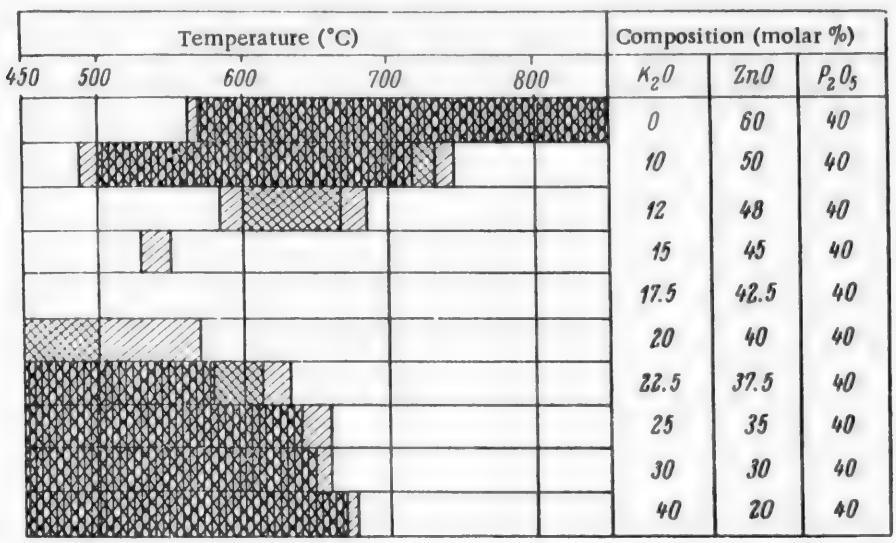

Fig. 2. Crystallization tendency of glasses with the composition $nK_2O \cdot mZnO \cdot 40P_2O_5$. (Designations as in Fig. 1).

In studies of the crystallizability of glasses with 40 molar % P_2O_5, it was unexpectedly found that this series includes a region of glasses which do not crystallize at all during three hours of exposure. Crystallization data for this series of glasses are presented in Fig. 2.

The boundaries of the region of noncrystallizing glasses were established more precisely by crystallization experiments, in the gradient furnace, on a large group of glasses with compositions around this region. Figure 3 represents the crystallizability of all glasses in the ternary system $K_2O-ZnO-P_2O_5$. In distinction from the preceding diagrams, different forms of shading represent the width of the temperature range in which the glasses crystallize within three hours, rather than the degree of crystallization.

Part 4 of this diagram represents the limits of compositions which crystallize even more the melting process. It follows from Fig. 3 that the glasses which do not crystallize within three hours lie within a narrow range of compositions, in the limits of 15-20% K_2O, 40-50% ZnO and 40-45% P_2O_5. It was later found that these glasses do not crystallize within 6 hours either. The wide region of noncrystallizing compositions containing more than 50 molar % P_2O_5 is of no interest because they are highly hygroscopic. Noncrystallizing glasses containing 40-45 molar % P_2O_5 are entirely nonhygroscopic despite the relatively high contents of alkali oxide.

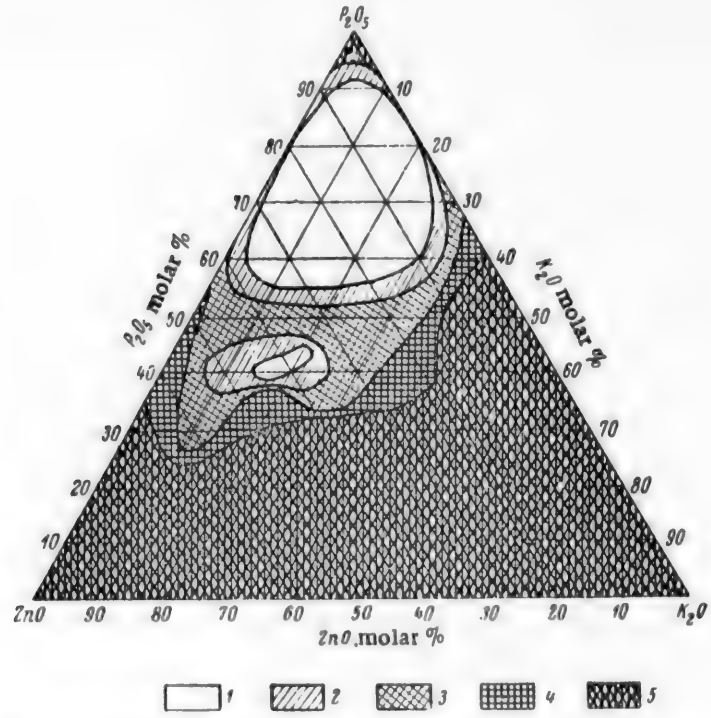

Fig. 3. Crystallization tendency of glasses with the composition $K_2O-ZnO-P_2O_5$. 1) Does not crystallize; width of the crystallization region: 2) 150°, 3) from 150 to 250°; 4) from 250 to 400°; 5) crystallizes during melting.

The ternary system $Na_2O-ZnO-P_2O_5$ was investigated similarly. Since binary sodium phosphate glasses have a lower tendency to crystallization than the corresponding potassium phosphate glasses, it was expected that in the ternary system $Na_2O-ZnO-P_2O_5$ the region of noncrystallizing glasses would be wider or might be displaced toward lower contents of alkali oxide or phosphoric anhydride, i.e., toward glass compositions more resistant to a moist atmosphere. However, the experiments showed that in the composition region where potash glasses do not crystallize at all the crystallization of soda glasses is still considerable. Figure 4 represents the crystallization tendency of glasses in the system $Na_2O-ZnO-P_2O_5$. It is seen that noncrystallizing glasses lie in the composition region with a very high Na_2O content (of the order of 30-40 molar %). Such glasses are known to be very hygroscopic and are of no practical interest. This region was therefore not investigated in greater detail. The diagram also shows that the region of glasses with a relatively low tendency to crystallization differs in configuration from the corresponding region for the potash glasses, and is shifted considerably toward a higher content of basic oxide.

This investigation showed that noncrystallizing and nonhygroscopic glasses can be obtained in the ternary system $K_2O-ZnO-P_2O_5$ with phosphoric anhydride contents of the order of 40-45 molar % and with definite ratios of zinc oxide to potassium oxide. Zinc-containing glasses with less than 50 molar % P_2O_5 are obtainable

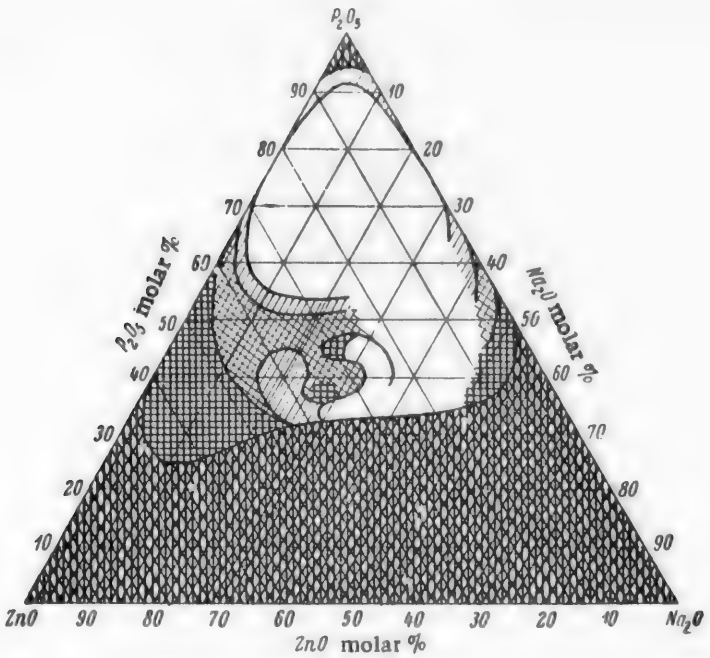

Fig. 4. Crystallization tendency of glasses with the composition $Na_2O-ZnO-P_2O_5$. (Designations as in Fig. 3).

because under these conditions zinc is a glass former and part of it enters into the glass structure with a coordination number of 4 and not 6. The deficiency of phosphoric anhydride evidently prevents formation of metaphosphates or other phosphates of zinc and potassium which might pass into the crystalline state under favorable temperature conditions. This very important fact was subsequently used for practical formulation of more complex phosphate glasses which have been produced industrially.

SUMMARY

1. In the system $K_2O-ZnO-P_2O_5$, a region of compositions has been found giving nonhygroscopic glasses which do not crystallize during prolonged exposure in the 400-850° temperature region.

2. In the system $Na_2O-ZnO-P_2O_5$, compositions which do not crystallize under the same conditions were found only at very high contents of the alkali oxide, i.e., in the region of glasses of very low chemical stability.

3. The explanation for the low crystallization tendency of certain alkaline zinc phosphate glasses is that at definite oxide ratios zinc may act as a glass former and enter the glass structure with a coordination number of 4 rather than 6.

4. The possibility of obtaining nonhygroscopic potassium zinc phosphate glasses with a low crystallization tendency was utilized in formation of phosphate glasses of more complex compositions for practical purposes.

LITERATURE CITED

[1] H. P. Hood, Glass Ind. 7, 287 (1956).

[2] D. Starkie and W. Turner, J. Soc. Glass Techn. 12, 306 (1928).

[3] J. E. Stanworth, J. Soc. Glass Techn. 30, 381 (1946).

[4] Glastechn. Tabellen (1932).

[5] U. S. Patent 1,570, 202 (1926).

[6] French Patent 724,267 (1931).

[7] U. S. Patent 2,423,128 (1947).

[8] French Patent: Silikattech. 10 (1955).

[9] German Patent; Glastech. Ber. H 1 (1956).

[10] E. Kordes, Z. phys. Ch., B 50, 194 (1941).

[11] E. Kordes and H. Becker, Z. anorg. allg. Ch. 185 (1949).

[12] E. Kordes, W. Vogel, and R. Feterowsky, Z. Elektroch. B 57, 4, 282 (1953).

[13] W. Vogel, Silikattech. 12, 510 (1955).

Received December 23, 1957

THE NATURE OF OPACIFYING PARTICLES IN FLUORIDE AND PHOSPHATE OPAL GLASSES

S. I. Sil'vestrovich and É. M. Rabinovich

Earlier x-ray structure investigations of fluoride opal glasses indicate that the opacifying effect is caused by crystallization of fluorides of alkali and alkaline-earth metals only [1-3]; formation of crystals of the fluorides of aluminum, zinc, or lead, or of double aluminum and sodium fluorides was not detected, although the possibility of such formation has been suggested [4-7]. Investigations in this region were concerned mainly with opacified two- and three-component glasses in systems of the types Al_2O_3–R_2O, SiO_2–RO–R_2O.

The nature of the opacifying particles in phosphate opal glasses has not been studied experimentally. It has been suggested that opacity in these glasses is caused by deposition of droplike crystal formations of calcium orthophosphate [8], or by liquation of silicate and phosphate glasses in the system without crystal formation [9].

Our investigations of the structure and properties of fluoride and phosphate opal glasses, close in composition to commercial glasses, yielded new data on the nature of the opacifying particles in such glasses.

TABLE 1

Compositions of the Investigated Opal Glasses and Dimensions of the Opacifying Particles

Glass code No.	Contents of oxides (wt. %)							Nature and amount of opacifier (wt. parts per 100 g of glass)		Acidity coefficient K**	Average size of opacifying particles in glass (μ)
	SiO_2	Al_2O_3	MgO	CaO	Na_2O	K_2O	Σ	F	P_2O_5		
I-8	72	2	3	7	16	—	100	—	8	2.66	6.5
II-4	77	1.65	2.46	5.75	13.14	—	100	8	—	3.45	1.7
II-8 *								—	8		—
III-4	82	1.29	1.93	4.50	10.28	—	100	8	—	4.68	6
III-7								—	6		~0.5
III-8 *								—	8		—
IV	69.05	6.00	2.88	6.72	15.35	—	100	10	—	2.75	—
V	77.44	2.14	3.22	—	17.20	—	100	8	—	3.65	~1
VI-a	80	2.22	—	—	17.78	—	100	10	—	4.72	5
VI-b								—	10		3
VII-a	80	2.22	—	—	—	17.78	100	10	—	7.17	5
VII-b*								—	10		—

* Glass crystallized.

** The acidity coefficient $K = \frac{SiO_2 + Al_2O_3}{R_2O + RO}$, where the amounts of oxides are in molar percentages.

The glasses (Table 1) were melted in a laboratory kerosene furnace at 1450-1500° for 4 hours and subsequently cooled in air. The opacifiers were introduced as relatively unstable ammonium salts – NH_4F and $(NH_4)_2HPO_4$ (analytical grade).

The x-ray structure and microstructure analytical methods were used in this investigation to determine the nature and size of the opacifying particles.

The x-ray patterns were taken by the Debye-Scherrer powder method in a camera 86 mm in diameter designed in the MGU Institute of Physics. The x-ray patterns of the glasses II-4, III-4, IV, V, VI-a, VII-a (fluorine-containing) and I-8, II-8, VI-b (phosphate-containing) were taken.

A list of the crystalline substances found in these glasses by x-ray analysis is given in Table 2.

TABLE 2

Crystalline Formation in the Investigated Glasses

Opacifier	Code No. of glass, from Table 1	Crystalline substances detected in glasses
F	II-4	NaF, CaF_2, $3NaF \cdot AlF_3$, AlF_3
	III-4	NaF, CaF_2, AlF_3
	IV	NaF, CaF_2, AlF_3, $3AlF_3 \cdot 5NaF$
	V	NaF, AlF_3, $3AlF_3 \cdot 5NaF$
	VI-a	NaF, $3NaF \cdot AlF_3$
	VII-a	KF
P_2O_5	I-8	$Ca_3(PO_4)_2$, $Ca_2P_2O_7$, $Mg_2P_2O_7$, $Na_4P_2O_7$, $Na_3(PO_3)_3$
P_2O_5	VI-b	$Na_3(PO_3)_3$, $AlPO_4$
P_2O_5	II-8 (devitrified)	$Na_2O \cdot 2CaO \cdot 3SiO_2$, $MgSiO_3$ (4 modification) Ca_2SiO_4 (α, β, γ), Ca_3SiO_5, $Al_2O_3 \cdot SiO_2$, $2CaO \cdot MgO \cdot 2SiO_2$, α-quartz $Ca_2P_2O_7$, $Ca_3(PO_4)_2$, $Mg_2P_2O_7$, $Na_4P_2O_7$, $Na_3(PO_3)_3$, $NaPO_3$ – II (insoluble) $Na_6P_6O_{18}$ – I (obtained during fusion)

It follows from Table 2 that in all the investigated fluoride opal glasses in which Na_2O is the alkaline oxide, crystalline compounds of fluorine with aluminum were detected: aluminum fluoride-AlF_3, cryolite-$3NaF \cdot AlF_3$ and chiolite-$3AlF_3 \cdot 5NaF$. It was only in the potassium aluminosilicate glass VII-a that known compounds of this type (AlF_3, $3KF \cdot AlF_3$, $AlF_3 \cdot KF$) were not detected, although more than half of the lines in the x-ray pattern of this glass could not be identified.

The values of the interplanar spacings calculated from the x-ray patterns of the investigated fluoride opal glasses, relating to the above-mentioned fluorine compounds of aluminum, are given in Table 3, which also contains values of interplanar spacings and line intensities taken from the literature [10, 11].

From the chemical standpoint, formation of these aluminum fluorides in glasses opacified by means of fluorine is quite probable. It is known [12] that aluminum oxide forms a fluoride in the reaction with hydrogen fluoride at 400-700°, and cryolite can be formed by treatment of Al_2O_3 with ammonium fluoride in an alkaline medium. Therefore, the following reactions are possible in opacification of glasses by fluorine:

$$NH_4F \rightarrow NH_3 + HF,$$

$$Al_2O_3 + 6HF \rightarrow 2AlF_3 + 3H_2O,$$

$$Al_2O_3 + 12NH_4F + 3Na_2O \rightarrow 2(3NaF \cdot AlF_3) + 12NH_3 + 6H_2O.$$

Table 2 shows that the results of x-ray structural analysis also confirm the formation of alkali-metal and calcium fluorides in fluoride opal glasses. Studies of polished sections of II-4 and III-4 glasses (Fig. 1) under

TABLE 3

Interplanar Spacings d and Line Intensities I for Aluminum Fluorides CuKα, λ_{av} = 1.539, 30 kv, 20 ma, d (in A)

Glasses investigated																Standards					
II-4			III-4			IV			V			VI-a			AlF_3		$3Na \cdot F \cdot AlF_3$		$3AlF_3 \cdot 5NaF$	
lines No.	d	I	lines No.	d	I	lines No.	d	I	lines No.	d	I	lines No.	d	I	d	I	d	I	d	I
1	4.48	1															4.51	20		
2	3.92	1															3.88	20		
									2	3.48	3								3.48	0.3
						2	2.89	8											2.90	1.0
4	2.71	1										3	2.70	1			2.75	67		
						4	2.43	1	3	2.50	2								2.46	0.3
5	2.32	6							4	2.35	10	4	2.37	6			2.33	40	2.32	0.7
6	2.13	5	8	2.17	2	5	2.17	1	5	2.14	10	5	2 15	10	2.13	1.0	2.15	13	2.16	0.5
						6	1.98	6	6	1.98	1								1.990	0,7
7	1.92	10							7	1.91	1	6	1.95	1			1.94	100	1.934	0.2B
			10	1.79	10	7	1.79	10	8	1.79	4				1.758	1.0			1.789	0.7
8	1.72	1															1.72	13		
						8	1.68	4	9	1.68	2								1.684	0.2
10	1.60	1	12	1.58	7										1.588	1.0	1.60	20		
11	1.57	1				9	1.54	7	10	1.55	9	9	1.53	9			1.57	53	1.553	0.7
			13	1.43	1	10	1.44	1	11	1.44	2				1.424	0.7				
12	1.36	3															1.375	13		
14	1.25	3	14	1.26	1	12	1.27	4							1.254	0.9				
15	1.235	1							12	1.235	3				1.230	0.6	1.229	5		
			15	1.175	1										1.171	0.5				
16	1.160	1				13	1.163	4							1.161	0.7				
17	1.114	5													1.118	0.5				
18	1.070	2													1.067	0.6				
19	1.048	2	16	1.048	4	15	1.040	5							1.043	0.6				
20	1.006	1													1.007	0.6				
						16	0.978	4							0.984	0.9				
23	0.921	2				17	0.945	1							0.933	0.9				
									14	0.884	2				0.877	0.5				
						19	0.857	4							0.857	0.7				
25	0.835	1													0.838	0.6				

Note. The line intensities for the glasses are assessed on a 10-point scale (visually); for $3NaF \cdot AlF_3$ on a 100-point scale, and for AlF_3 and $3AlF_3 \cdot 5NaF$ in fractions of unity.

the microscope show that most of the opacifying particles in them belong to the cubic system, while investigation of immersion specimens of these glasses shows that they are crystals of sodium fluoride.* Therefore, microscope studies give reason to believe that sodium fluoride predominates among the opacifying particles in glasses of this type. The size of the opacifying particles in the investigated fluoride glasses varied from 1 to 6 μ, and increased with increasing acidity of the glass (Table 1, Fig. 1) within the range of compositions cc taining the same alkaline oxide (Na_2O).

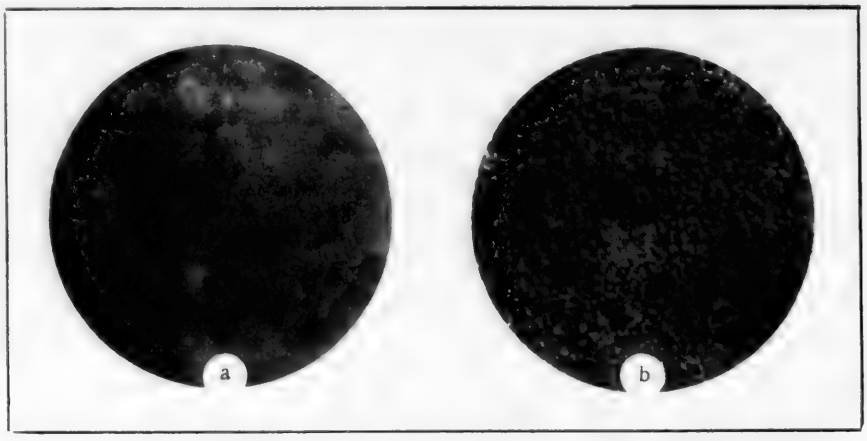

Fig. 1. Microstructure of fluoride opal glasses II-4 (a) and III-4 (b); nonpolarized light, × 672.

The chemical and mineral composition of the opacifying particles in glasses opacified by phosphoric anhydride was determined in detail from the results of x-ray structural analysis of these glasses. It was found (Table 2) that these particles are crystalline formations of ortho-, pyro-, meta-, and other phosphates of metals the oxides of which were contained in the glass. Thus, the hypothesis that opacification of phosphate glasses is the consequence of liquation only was not confirmed. It is possible, however, that liquiation is a primary process which precedes formation of phosphate crystals. This is all the more probable since phosphate glasses of the general empirical formula $Na_{n+2}P_nO_{3n+1}$ are known [13]. The compounds $Na_4P_2O_7$ (glass I-8) and $Na_5P_3O_{10}$ (glass II-8) detected in two phosphate-containing glasses correspond to this formula; they can evidently be regarded as the crystallization products of phosphate glasses of this type.

The size of the particles in the investigated phosphate opal glasses varied from 0.5 to 6.5 μ, decreasing with increasing acidity of the opacified glass (Table 1), probably because of the increase of the melt acidity on introduction of P_2O_5.

Photographs of polished sections of glasses III-7 and III-8 are given in Fig. 2. In the first (Fig. 2,a) the extremely microgranular structure, due to crystallization of phosphates in the opacified glass, may be noted. In the second, devitrified glass (Fig. 2, b), although the particles are larger than in the first, they are still considerably smaller than the usual crystallization products of silicate glasses. When this section was examined in polarized light it was noticedthat the polarizing crystalline particles form large aggregates. It follows that the presence of opacifying particles in a phosphate-containing glass substantially changes the character of its crystallization, causing the formation of a microcrystalline structure. These results are in good agreement with the results obtained by analysis of the x-ray pattern of glass II-8 (Table 2), of analogous composition and also devitrified, which show that in addition to alkali and alkaline-earth phosphates it also contains a large variety of crystallization products of alkali and alkaline-earth dsilicates and α-quartz.

* The immersion liquid was saturated NaF solution, the refractive index of which is identical with the refractive index of crystalline NaF (n_D = 1.32).

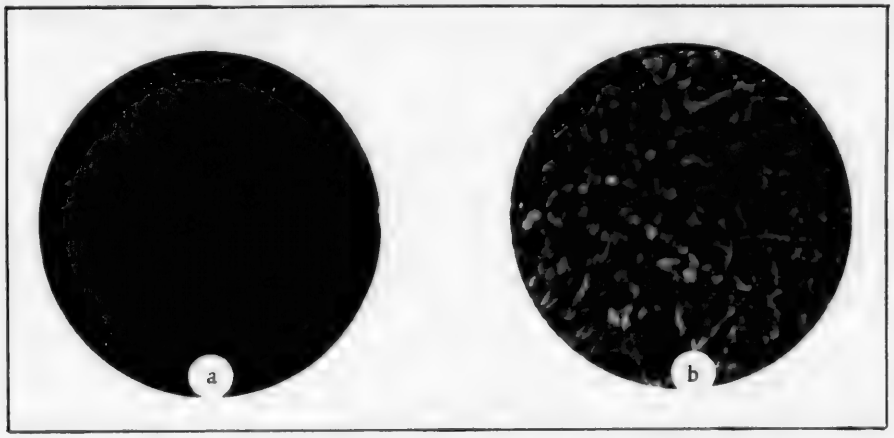

Fig. 2. Microstructure of phosphate-containing glasses – opal III-7 (a) and devitrified III-8 (b); nonpolarized light, × 672.

SUMMARY

1. Opacity in 3-, 4-, and 5-component fluoride opal glasses is caused by formation not only of sodium and calcium fluoride crystals, but also by formation of crystals of aluminum fluoride, cryolite $3NaF \cdot AlF_3$, and chiolite $3AlF_3 \cdot 5NaF$. However, NaF crystals predominate as the opacifying particles in these glasses. The view that AlF_3 and $3NaF \cdot AlF_3$ are not segregated in glasses of this type is unfounded.

2. Opacity in glasses containing phosphoric anhydride is caused by formation of crystals of ortho-, pyro-, meta-, and other phosphates of calcium, magnesium, sodium, and aluminum. Crystal formation can probably be preceded by phase separation (liquation) of silicate and phosphate melts.

3. The size of the opacifying particles in fluoride opal glasses increases with increasing acidity of the glass. The inverse relationship applies to opacifying particles in phosphate-containing glasses.

LITERATURE CITED

[1] J. Ryde and D. Yates, J. Soc. Glass Techn., X , 39, 274, (1926).

[2] H. F. Krause, Keramische Rudschau, 17 (1953).

[3] R. J . Callow, J. Soc. Glass Techn. 36, 172, 266 (1952; Glass Industry, 34, 2, 82 (1953).

[4] R. Vondracek, Sprechsaal, 23 (1909).

[5] F. Doerinckel, Glast. Ber. 5, 268,74 (1931).

[6] E. I. Orlov, Glazes, Enamels, Ceramic Colors and Bodies, 2nd Ed. (State Tech. Press, Leningrad, 1931) [in Russian].

[7] F. Jochmann, Glas-Email-Keramo-Technik, 5, 11-12 (1954).

[8] I. I. Kitaigorodskii, Coloration and Opacification of Glass (ONTI, Moscow, 1935) [in Russian].

[9] R. Dralle and G. Keppeler, Production of Glass, 1 (State Light Industry Press, 1938) p. 210 [in Russian].

[10] A. I. Kitaigorodskii, X-ray Structure Analysis of Microcrystalline and Amorphous Substances (State Tech. Press, Moscow-Leningrad, 1952) [in Russian].

[11] Alphabetical Index of X-ray Diffraction Patterns, Am. Soc. for Testing Materials, Ph., June, August (1945).

[12] H. J. Emeleus, in the Book: Fluorine and Its Compounds [Russian translation] 1 (IL, Moscow, 1953)p.37.

[13] W. Dewald and H. Schmidt, Referat. Zhur. Zhim. 6, 265, 20560 (1956).

Received July 19, 1958

KINETICS OF SPONTANEOUS DECOMPOSITION OF AMMONIUM SULFITE–BISULFITE SOLUTIONS

B. A. Chertkov

Ammonium sulfite–bisulfite solutions are used in the production of caprolactam and paper, for extraction of sulfur dioxide from dilute gases, for concentration of sulfur dioxide, and for other purposes.

Owing to the thermodynamic instability of sulfite–bisulfite solutions, under certain conditions reactions of autoxidation or, as they are often termed, spontaneous decomposition may develop in them, leading to formation of by-products –sulfate, thiosulfate, trithionate, and sometimes elemental sulfur. The mechanism of the spontaneous decomposition process has been studied in detail in the case of sodium sulfite–disulfite by Foerster and his associates [1]. According to their scheme, the spontaneous decomposition of bisulfite proceeds in two sharply-separated stages; in the first stage bisulfite is converted into sulfate, thiosulfate, and polythionates, and in the second the remaining bisulfite and the thiosulfate and polythionates are converted into sulfate and elemental sulfur.

The consecutive chain of reactions in the first stage is of the most interest for a theoretical explanation of the course of bisulfite decomposition. By Foerster's scheme, in absence of selenium* these reactions develop as follows. The first step is apparently decomposition of the bisulfite anion into compounds containing sulfur in higher and lower states of oxidation:

$$2HSO_3^- \rightarrow SO_4^{--} + SO + H_2O. \quad (1)$$

The unstable sulfur monoxide immediately combines with further bisulfite molecules to form trithionate molecules:

$$SO + 2HSO_3^- \rightarrow S_3O_6^{--} + H_2O. \quad (2)$$

Combining Equations (1) and (2), we have

$$4HSO_3^- \rightarrow SO_4^{--} + S_3O_6^{--} + 2H_2O. \quad (3)$$

However, trithionate is hydrolyzed

$$S_3O_6^{--} + H_2O \rightleftarrows SO_4^{--} + S_2O_3^{--} + 2H^+ \quad (4)$$

and the total result of the initial stage in the spontaneous decomposition of bisulfite can be represented by the following aggregate equation:

$$4HSO_3^- \rightleftarrows 2SO_4^{--} + S_2O_3^{--} + 2H^+ + H_2O. \quad (5)$$

After a definite concentration of hydrogen and thiosulfate ions has been reached, the process can be further accelerated automatically by the following reactions:

$$5S_2O_3^{--} + 6H^+ \rightarrow 2S_5O_6^{--} + 3H_2O, \quad (6)$$

$$2S_5O_6^{--} + 2HSO_3^- \rightarrow 2S_4O_6^{--} + 2S_2O_3^{--} + 2H^+ \quad (7)$$

* Selenium is a powerful catalyst of the spontaneous decomposition of sulfite–bisulfite solutions, and the sequence of reactions which develop in its presence differs considerably from that given below.

and, further, after analogous conversion of $S_4O_6^{--}$ into $S_3O_6^{--}$ and hydrolysis of $S_3O_6^{--}$ in accordance with Equation (4), new quantities of $S_2O_3^{--}$ and H^+ ions are formed; these interact in accordance with Equation (6), etc.

In practice, owing to the reversibility of Reaction (4), the solution may contain, in addition to thiosulfate, a certain amount of trithionate, which increases with increasing H^+ ion concentration.

It must be pointed out that the above equations for the formation of thiosulfate, trithionate, and higher polythionates, and for their interconversions, are consistent with D. I. Mendeleev's theory of the structure of thionates, which has been confirmed by a number of recent investigations [2]. According to D. I. Mendeleev, thionic acids are sulfo acids formed by replacement of H atoms in hydrogen sulfides by the sulfo group HSO_3 (thiosulfate, $HS(HSO_3)$; trithionate, $S(HSO_3)_2$; tetrathionate, $S_2(HSO_3)_2$, etc.).

The above-indicated directions of the spontaneous-decomposition reactions are also confirmed by thermodynamic data. For example, if we take literature data [3] for the free energies of formation of ions taking part in the reactions, we find that the total changes of free energy in the above reactions have the following values.

Reaction	ΔF^0 (in kcal)
(3)	−15.7
(4)	−15.63
(5)	−31.35
(6)	− 7.07
(7)	−27.6 (−13.8 kcal per 1 molecule of $S_5O_6^{--}$)

The negative values of ΔF^0 show that all the reactions proceed with decrease of free energy and are therefore fully feasible in principle. It follows that the direction of the reactions is indicated correctly and it is to be expected that as the result of chemical changes in the salt system under consideration just the compounds which figure in the reaction sequence given above will be formed.

Spontaneous decomposition of ammonium sulfite–bisulfite solutions of various concentrations was studied in the Scientific Research Institute of Gas Purification by Golyand and Berdyanskaya [4]. They found that these solutions decompose in accordance with the scheme postulated by Foerster for sodium sulfite–bisulfite solutions, and that the process of spontaneous decomposition is extremely slow (5-6 months) in pure solutions in the cold. The process is accelerated by heating, but takes a fairly long time in absence of catalysts; for example, at 100° complete decomposition requires from 60-70 to 1000 hours, in accordance with the initial composition of the solution.

In the publication cited above, only the initial and final characteristics of the state of the system were given, but the kinetics of the reactions during the first state in the spontaneous decomposition of the solutions was not studied separately. Nevertheless, these are just the data primarily required for assessment of the possible service life of solutions of various compositions under particular industrial conditions. The purpose of the present investigation was to obtain such data.

Kinetics of Spontaneous Decomposition of Solutions of Different Compositions under Laboratory Conditions* at 25°

The investigation procedure was as follows: sulfite–bisulfite solutions of particular initial compositions were poured into a series of similar vessels (open or closed in accordance with the problem under consideration) kept under strictly constant conditions. Changes taking place over given time intervals were determined by analyses of the solution in individual vessels.

The following notation is used to denote the solution components: C_{SO_2}, the total SO_2 content (moles/liter) in ammonium sulfite and bisulfite and in the form of free sulfurous acid (formely often denoted

* The experimental work was performed by D. L. Puklina, T. I. Pekareva, and T. T. Garina.

by S); $C_{NH_3 eff}$, the ammonia content (moles/liter) in ammonium sulfite and bisulfite (formely often denoted by C); $C_{NH_3 tot}$, the total ammonia content in the solution (moles/liter); $C_{SO_2}/C_{NH_3 eff}$, the molar ratio of total SO_2 to effective ammonia in the solution (this is 1 for pure bisulfite and 0.5 for pure sulfite); $C_{SO_4^{--}}$, the ammonium sulfate content (moles/liter); $C_{S_2O_3^{--}}$ the ammonium thiosulfate content (moles/liter); $C_{S_3O_6^{--}}$, the ammonium trithionate content (moles/liter); $g_{S_2O_3^{--}}$ the rate of formation of thiosulfate or of the sum of thiosulfate and trithionate (in moles/liter per 100 hours).

Data on the variations of solution composition with time in a number of the cases studied are plotted in the graphs presented below.

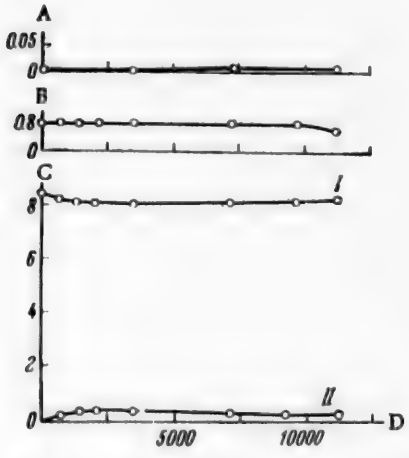

Fig. 1. Changes of solution composition with time: artificial solution in closed vessels, $C_{NH_3 tot}$ = 8.4 moles/liter, temperature 25°; A) $(NH_4)_2S_2O_3$ content (moles/liter), B) $C_{SO_2}/C_{NH_3 eff}$ ratio, C) contents of NH_3 as ammonium sulfite and bisulfite (I) and as ammonium sulfate (II) (moles/liter), D) time (hours.

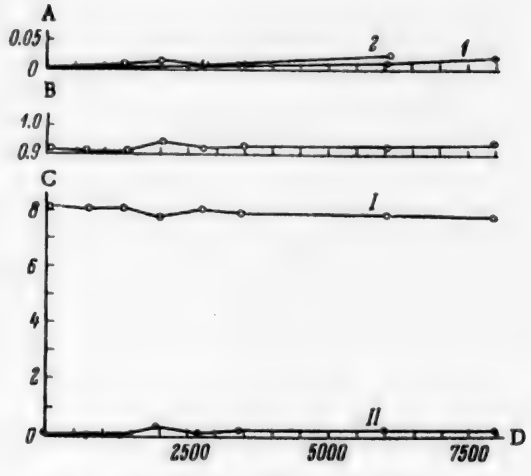

Fig. 2. Changes of solution composition with time: artificial solution in coal vessels, $C_{NH_3 tot}$ = 8.2 moles/liter, temperature 25°; A) contents of $(NH_4)_2S_2O_3$ (1) and $(NH_4)_2S_3O_6$ (2) (in moles/liters; remaining ordinates and curves designated as in Fig. 1.

First we consider the variations in time of the composition of sulfite–bisulfite solution kept in closed vessels and not subjected to the action of atmospheric oxygen; i.e., we consider the process of spontaneous decomposition itself, not complicated by the parallel process of oxidation of the solution.

If the vessels contain pure sulfite-bisulfite solution free from impurities, with an initial $C_{SO_2}/C_{NH_3 eff}$ ratio of 0.78-0.80,* it remains unchanged for a very long time, and at 25° spontaneous decomposition reactions do not develop in it to any practical extent (Fig. 1). If the vessels contain a similarly pure solution, but with an initial $C_{SO_2}/C_{NH_3 eff}$ ratio of 0.92,** certain changes take place, though very slight, associated with slow formation of ammonium thiosulfate and trithionate (Fig. 2). If the vessel contain a working liquor which already contains some ammonium sulfate, thiosulfate, and trithionate,*** then at an initial $C_{SO_2}/C_{NH_3 eff}$

* Close in composition of the regenerated liquor fed to the last absorption stage in the cyclic ammonia process for removal of SO_2 from flue gases.

** Close in composition to the saturated liquor formed in the cyclic ammonia process for removal of SO_2 from flue gases.

*** And also an inhibitor, paraphenylenediamine, added to the liquor to reduce its oxidation rate.

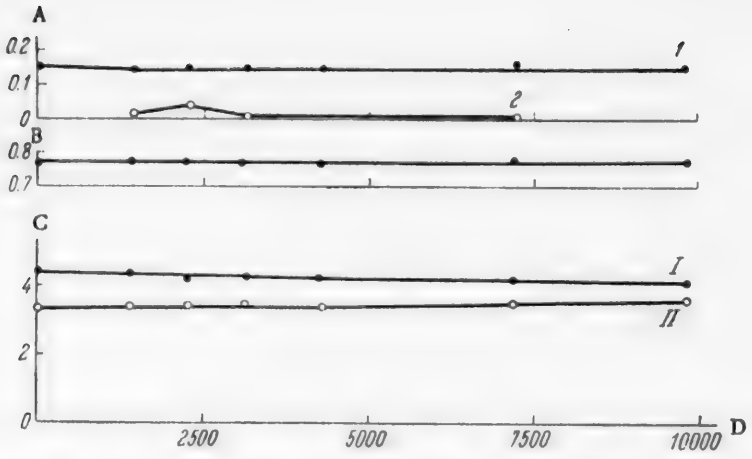

Fig. 3. Changes of solution composition with time: working liquor in closed vessels, C_{NH_3tot} = 8.2 moles/ liter temperature 25°. Ordinates and curves designated as in Fig 1 and 2.

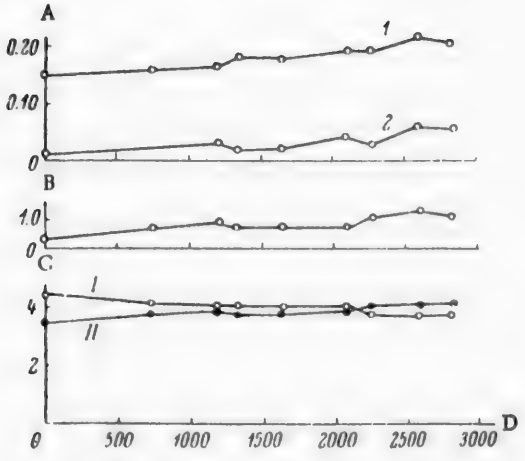

Fig. 4. Changes of solution composition with time: working liquor in closed vessels, C_{NH_3tot} = = 8.2 moles/ liter, temperature, 25°. Ordinates and curves designated as in Fig. 1 and 2.

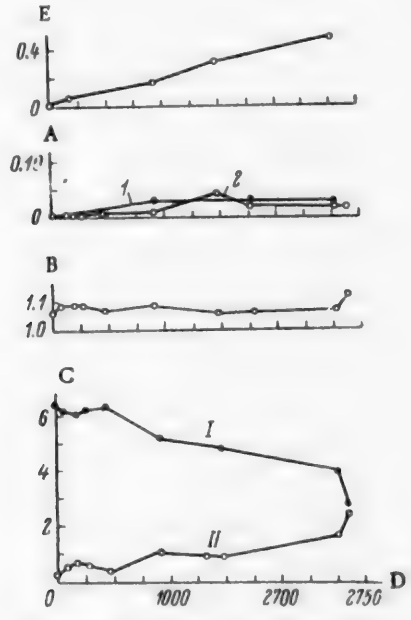

Fig. 5. Changes of solution composition with time: artificial solution in closed vessels, C_{NH_3tot} = 6.6 moles/ / liter, temperature 25°; E) $(NH_4)_2S_4O_6$ content (moles/ liter); remaining designations as in Fig. 1 and 2.

ratio of 0.78 the reactions of spontaneous decomposition again fail to develop (Fig. 3). In contrast to this, if the vessels contain the working liquor, but with an initial C_{SO_2}/C_{NH_3eff}, ratio of 0.93, fresh quantities of ammonium thiosulfate and trithionate are formed quite noticeably, although slowly (Fig. 4). It is also noticeable that the C_{SO_2}/C_{NH_3eff}, ratio increases during spontaneous decomposition of the solution. This is entirely to be expected; the reason is that the molecule of sulfuric acid formed during hydrolysis of trithionate in

accordance with Equation (4) converts 2 molecules of sulfite into bisulfite, so that the general result of the first stage of spontaneous decomposition in the sulfite–bisulfite system may be represented by the equation

$$2NH_4HSO_3 + 2(NH_4)_2SO_3 \rightarrow 2(NH_4)_2SO_4 + 2(NH_4)_2S_2O_3 + H_2O. \quad (8)$$

Since sulfite and bisulfite are expended in equal amounts during spontaneous decomposition, and the solution consists mainly of bisulfite, the relative content of the latter increases appreciably, so that the ratio $C_{SO_2}/C_{NH_3\,eff}$ increases also.*

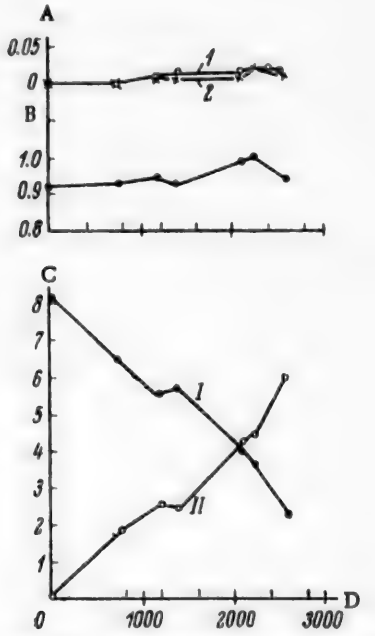

Fig. 6. Changes of solution composition with time: artificial solution in open vessels, $C_{NH_3\,tot}$ = 8.2 moles/liter, temperature 25°. Ordinates and curves designated as in Fig. 1 and 2.

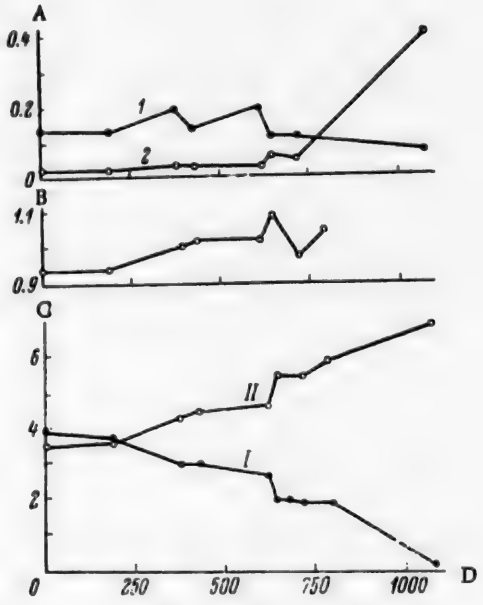

Fig. 7. Changes of solution composition with time: working liquor in open vessels, $C_{NH_3\,tot}$ = 7.75 moles/liters, temperature 25°. Ordinates and curves designated as in Fig. 1 and 2.

If the vessels contain a solution in which the initial $C_{SO_2}/C_{NH_3\,eff}$ ratio exceeds 1,** then the spontaneous decomposition reactions develop rapidly, and because of the high H^+ ion concentration polythionates are predominantly formed by Reactions (6) and (7), while hydrolysis of trithionate by Reaction (4) naturally slows down (Fig. 5).

Thus, the data in Fig. 1-5 show that at 25° in closed vessels the reactions of spontaneous decomposition are extremely slow, although they are accelerated appreciably with increase of $C_{SO_2}/C_{NH_3\,eff}$ ratio and with increasing contents of the products of spontaneous decomposition.

We now consider the changes taking place with time in a sulfite–bisulfite solution in open vessels, when the spontaneous decomposition is accompanied by oxidation under the influence of atmospheric oxygen.

If the vessels contain pure sulfite–bisulfite solution, then the spontaneous decomposition is slow, as it is in closed vessels (Fig. 6). However, as Fig. 6 shows, the solution is oxidized fairly rapidly and by the time

* The relationship between the $C_{SO_2}/C_{NH_3\,eff}$ ratio and the solution pH is given in an earlier paper [5].

** This means that the solution contains some free sulfurous acid in excess of the ammonium bisulfite content.

only about 0.03 mole/ liter of thiosulfate and trithionate* has accumulated in the solution most of the ammonium sulfite–bisulfite has already been oxidized to ammonium sulfate. In working liquors with C_{SO_2}/C_{NH_3eff} ratio of 0.92 both spontaneous decomposition and the oxidation processes are much more rapid than in the previous case (Fig. 7). If the vessels contain solutions with high thiosulfate content and with C_{SO_2}/C_{NH_3eff} ratio greater than 1, the reactions of spontaneous decomposition proceed at the highest rate, irrespectively of whether a working liquor (Fig. 8) or an artificial solution (Fig. 9) is used. Thus, experiments with open vessels also confirm that the rate of spontaneous decomposition of ammonium sulfite–bisulfite solutions increases appreciably with increase of the C_{SO_2}/C_{NH_3eff} ratio and with increasing contents of the products of spontaneous decomposition in the solution.

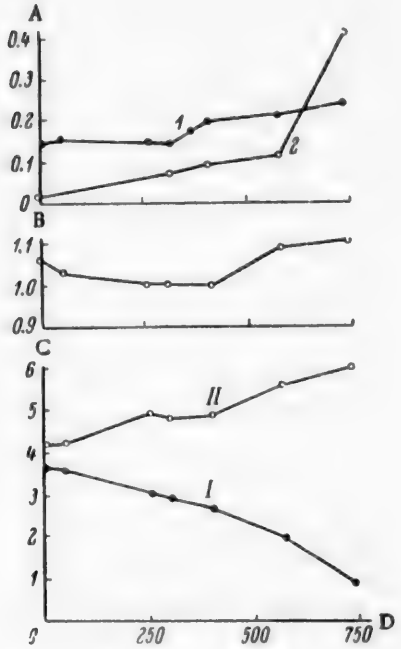

Fig. 8. Changes of solution composition with time: working liquor in open vessels, C_{NH_3tot} = 8.1 moles/ liter, temperature 25°. Ordinates and curves designated as in Fig. 1 and 2.

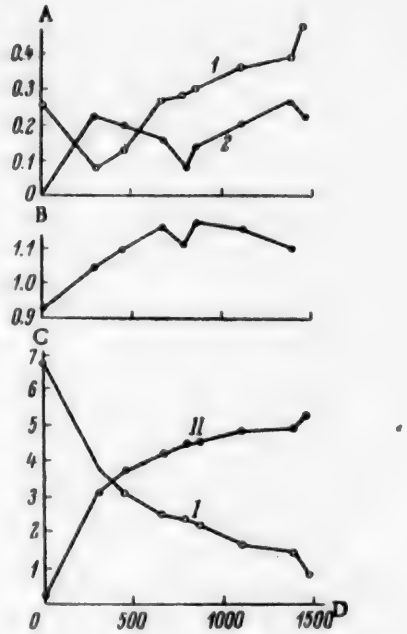

Fig. 9. Changes in solution composition with time: artificial solu- in open vessels, C_{NH_3tot} = 7.1 moles/ liter, temperature 25°. Ordinates and curve designated as in Fig. 1 and 2.

In these experiments the concentration of the sulfite–disulfite solutions was varied over a fairly wide range, corresponding to variations of C_{NH_3eff} from 7-8 to 1.5-2 moles/ liter. Although ammonium sulfite–bisulfite concentration undoubtedly has some influence on the rate of spontaneous decomposition, it is not a determining factor in the process.

The results are summarized in Table 1, where the criterion of comparison is the average rate of formation of the products of spontaneous decomposition $g_{S_2O_3}^{\bullet\bullet}$— (in moles/ liter per 100 hours).

* When C_{SO_2}/C_{NH_3eff} is less than 1, i.e., when sulfite is still present in the solution, higher polythionates cannot be present, since only the known exchange reaction $S_4O_6^{--} + SO_3^{--} \rightleftharpoons S_3O_6^{--} + S_2O_3^{--}$, takes place, and this shifted far to the right in presence of a large excess of sulfite.

** Subsequently, for brevity, the subscript $S_2O_3^{--} + S_3O_6^{--}$ is replaced by $S_2O_3^{--}$, but this implies the total rate of formation or total concentration of thiosulfate and trithionate.

Table 1 shows that values of $g_{S_2O_3^{--}}$ vary over a very wide range.

If from each group experiments are selected, carried out at the same average $C_{SO_2} / C_{NH_3\,eff.}$ ratio and the results are plotted (Fig. 10), a definite relationship is seen to exist between $g_{S_2O_3^{--}}$ and $C_{S_2O_3^{--}}$. The nature of the curves suggests that in this case the relationship between $g_{S_2O_3^{--}}$ and $C_{S_2O_3^{--}}$ should correspond to a power function with a fractional exponent, represented in general form by the equation

$$g_{S_2O_3^{--}} = aC^m_{S_2O_3^{--}} \qquad (I)$$

where a and m are constants.

TABLE 1

Average Data on the Spontaneous Decomposition of Ammonium Sulfite–Bisulfite Solutions at 25° (Variation ranges of $C_{NH_3\,tot}$ – 7–9 moles/liter; of $C_{NH_3\,eff.}$ 1.5–8 moles/liter)

Experimental conditions	Change of thiosulfate and trithionate conc. $C_{S_2O_3^{--}} + S_3O_6^{--}$ in the expt. (in moles/liter)	Average value of $C_{S_2O_3^{--}} + S_3O_6^{--}$ in the expt. (in moles/liter)	Change of ratio $C_{SO_2}/C_{NH_3\,eff.}$	Rate of thiosulfate formation $g_{S_2O_3^{--}} + S_3O_6^{--}$ (in moles/liter per 100 hours)	Value of $g_{S_2O_3^{--}} + S_3O_6^{--}$ in moles/liter per 100 hrs. reduced to $C_{S_2O_3^{--}} = 0.25$
Artificial solution in closed vessels	0—0.05	0.009	0.80—0.80	0.00012	0.0017
	0—0.05	0.014	0.80—0.90	0.00027	0.0027
	0—0.05	0.020	0.8 —0.95	0.00050	0.0035
	0—0.05	0.022	0.92—0.94	0.00050	0.0035
	0—1.00*	0.320*	1.08—1.07	0.02700	0.0220
	0—0.36*	0.190*	1.08—1.09	0.04150	0.0500
	0—1.34*	0.670*	1.08—1.12	0.05150	0.0240
	0.25—0.35	0.283	0.81—0.86	0.00280	0.0023
	0.25—0.35	0.289	0.94—0.97	0.00400	0.0034
	0.25—0.48*	0.375*	0.94—1.05	0.02000	0.0150
Working liquor in closed vessels	0.17—0.18	0.177	0.78—0.78	0	0
	0.17—0.25	0.194	0.93—0.98	0.0023	0.0027
	0.17—0.25	0.185	0.94—0.95	0.0019	0.0024
	0.17—0.49*	0.285*	0.94—1.15	0.0275	0.0250
	0.17—0.25	0.184	0.94—0.95	0.0015	0.0019
	0.17—0.35	0.246	0.94—1.01	0.0145	0.0145
Artificial solution in open vessels	0	0	0.80—0.79	0	0
	0—0.05	0.022	0.80—0.85	0.0007	0.0042
	0—0.10	0.038	0.80—0.92	0.0016	0.0070
	0—0.10	0.042	0.86—0.96	0.0024	0.0096
	0—0.05	0.025	0.93—0.98	0.0027	0.0150
	0—0.05	0.021	0.91—0.84	0.0012	0.0074
	0—0.05	0.026	0.91—0.95	0.0023	0.0124
	0.25—0.35	0.269	0.81—0.89	0.0041	0.0039
	0.25—0.35	0.281	0.81—0.98	0.0089	0.0080
Working liquor in open vessels	0.17—0.18	0.182	0.78—0.83	0	0
	0.17—0.18	0.172	0.94—0.97	0.0041	0.0055
	0.30—0.35	0.324	0.94—0.81	0.0035	0.0026
	0.30—0.35	0.318	0.94—0.89	0.0060	0.0045
	0.25—0.28	0.252	0.92—0.86	0.0044	0.0044
	0.15—0.30	0.202	1.06—1.02	0.0260	0.0325
	0.15—0.65	0.390	1.06—1.10	0.0660	0.0400

* The ammonium tetrathionate present in solution is expressed as thiosulfate on the assumption that 1 mole of $S_4O_6^{--}$ is equivalent to 2 moles of $S_2O_3^{--}$.

In fact, rectification of the curves of Fig. 10 in logarithmic coordinates showed tha the index m varies between 0.7 and 0.9, and can be taken as 0.8 on the average. The coefficient a differs for each individual case and depends on the experimental condions, mainly on the value of $C_{SO_2} / C_{NH_3\,eff.}$

On the assumption that this relationship is valid for all the experiments performed, we applied a correction to the results, reducing them all to the same value of $C_{S_2O_3}$, taken as 0.25 mole/ liter. The reduced values of $g_{S_2O_3}$ are given in the last column of Table 1. As the influence of the factor $C_{S_2O_3}$ is thus eliminated, the relationship between $g_{S_2O_3}$-- and the ratio $C_{SO_2}/C_{NH_3\,eff}$ can now be established.

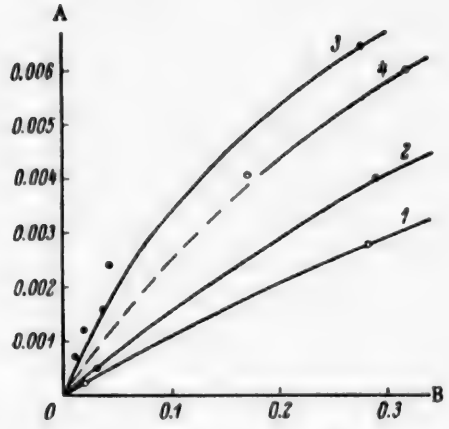

Fig. 10. Variation of the rate of spontaneous decomposition with the existing concentration of thiosulfate and trithionate in solution at 25°: A) Rate of spontaneous decomposition $g_{S_2O_3}$-- (in moles/ liter per 100 hours), B) thiosulfate concentration $C_{S_2O_3}$ (in moles/ liter); artificial solution in closed vessels at $C_{SO_2}/C_{NH_3\,eff}$: 1) 0.85, 2) 0.93-0.95; 3) the same, in open vessels, 0.84-0.88; 4) working liquor in open vessels, 0.92-0.95.

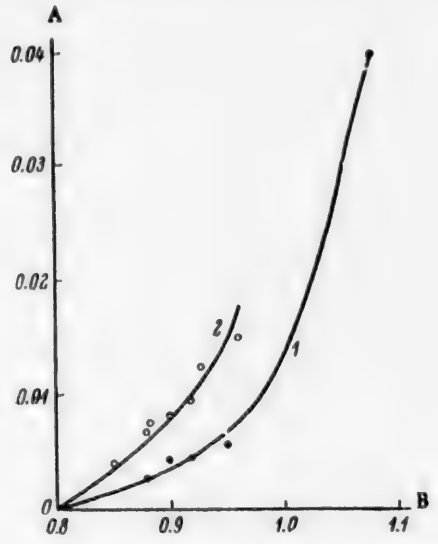

Fig. 11. Variation of the rate of spontaneous decomposition with the $C_{SO_2}/C_{NH_3\,eff}$ ratio at $C_{S_2O_3}$-- = 25 moles/ liter and 25°: A) Rate of spontaneous decomposition $g_{S_2O_3}$-- (in moles/ liter per 100 hours), B $C_{SO_2}/C_{NH_3\,eff}$ ratio; solution in open vessels; 1) working, 2) artificial.

This is done in Fig. 11, based on the results of experiments performed with open vessels, in which unde given conditions the rate of spontaneous decomposition is always higher than in closed vessels; this is in all probability because of the catalytic effect of impurities entering from the surroundings on the reaction rates. In working liquors the rate of spontaneous decomposition is always lower than in artificial solutions, because of the presence of inhibitor, which partially paralyzes the catalytic effect of the thionates present in solution.

It is clear from Fig. 11 that the experimental curves are of a form typical for exponential functions. It is therefore assumed that the relationship between $g_{S_2O_3}$-- and the ratio $C_{SO_2}/C_{NH_3\,eff}$ can be represented in general form by the equation

$$g_{S_2O_3}-- = b \cdot e^{nC_{SO_2}/C_{NH_3}\,eff} \qquad (II)$$

where b and n are constants, and e is the base of natural logarithms.

When the data in Fig. 1 were plotted in semilogarithmic coordinates, it was found that the coefficient n is 14.356, both for the working liquor and the artificial solution. The coefficient b is $8.149 \cdot 10^{-9}$ for the working liquor, and $18.210 \cdot 10^{-9}$ for the artificial solution.

Thus, the influence of $C_{SO_2}/C_{NH_3\,eff}$ on the rate of spontaneous decomposition of ammonium sulfite-bisulfite solutions may be estimated from the following empirical formulas: for a working liquor (with paraphenylenediamine as oxidation inhibitor)

$$g_{S_2O_3}-- = 8.149 \cdot 10^{-9} \cdot e^{14.356C_{SO_2}/C_{NH_3}\,eff} \qquad (III)$$

and for an artificial solution (without inhibitor)

$$g_{S_2O_3^{--}} = 18.210 \cdot 10^{-9} \cdot e^{14.358 C_{SO_2}/C_{NH_3\,eff}}. \quad (IV)$$

By replacing the coefficient a in Equation (1) by its expanded value from Equation (III) or (IV), we can find a generalized empirical expression for the rate of spontaneous decomposition of ammonium sulfite-bisulfite solutions at 25°. Thus, for a working liquor in open equipment variations of $g_{S_2O_3^{--}}$ with changes in the solution composition may be found from the following equation:

$$g_{S_2O_3^{--}} = 8.149 \cdot 10^{-9} \cdot C^{0.8}_{S_2O_3^{--}} \cdot e^{14.358 C_{SO_2}/C_{NH_3\,eff}}. \quad (V)$$

Effect of Temperature on the Rate of Spontaneous Decomposition of Ammonium Sulfite-Bisulfite Solutions

Experiments on the influence of heat on the rate of spontaneous decomposition of ammonium sulfite-bisulfite solutions were performed in a thermostat with automatic temperature regulation, containing flasks

TABLE 2

Data on the Rate of Spontaneous Decomposition of Working Liquor at Various Temperatures (Variation ranges of $C_{NH_3\,tot}$ – 7-10 moles/liter; of $C_{NH_3\,eff}$ – 1.2-5.8 moles/liter)

Experimental temperature (°C)	Change of $C_{SO_2}/C_{NH_3\,eff}$ ratio in the experiment	Average value of $C_{S_2O_3^{--}}$ in the expt. (moles/liter)	$g_{S_2O_3^{--}}$, experimental (moles/liter per 100 hrs.)	$g_{S_2O_3^{--}}$ reduced (moles/liter per 100 hrs.)
50	0.71—0.83	0.210	0.007	0.008
77	0.81—0.80	0.285	0.012	0.011
	0.90—0.95	0.222	0.027	0.030
	0.91—0.88	0.465	0.042	0.026
88	0.81—0.84	0.230	0.035	0.038
	0.89—0.93	0.315	0.100	0.080
103	0.80—0.79	0.416	0.072	0.049
	0.82—0.89	0.561	0.106	0.056
	0.93—0.95	0.251	0.128	0.128
	0.95—0.87	0.410	0.152	0.103
	0.92—0.89	0.414	0.218	0.147
	0.92—0.99	0.548	0.700	0.374
	0.96—0.97	0.286	1.26	1.090

with the solution. In order to diminish losses of NH_3 and SO_2, the volatility of which rises sharply with temperature, in most of the experiments the vapors escaping from the flask were condensed in a water condenser and returned to the flask. Thus, a more or less constant salt concentration was maintained in the solution sample. The increases in the concentrations of the products of spontaneous in the solution, found in separate experiments, are plotted in Fig. 12 (experiments at 77°) and Fig. 13 (experiments at 103°)

The average results are summarized in Table 2.

In order to obtain comparable data, all the experimental values of $g_{S_2O_3^{--}}$ were reduced to the same thiosulfate concentration, 0.25 mole/liter, as in the preceding case.

By selection of experiments carried out with the same $C_{SO_2}/C_{NH_3\,eff}$ ratio it is possible to use these data in order to find the influence of the temperature factor (Fig. 14).

The nature of the curves in Fig. 14 suggests that $g_{S_2O_3^{--}}$ is an exponential function of the temperature, and that the relationship between the two can be represented by an equation of the form:

$$g_{S_2O_3^{--}} = c \cdot e^{pt}, \quad (VI)$$

where c and p are constants.

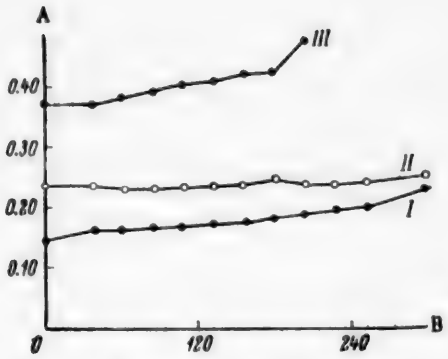

Fig. 12. Increase of thiosulfate concentration in working liquor at 77°: A) Thiosulfate concentration $C_{S_2O_3^{--}}$ (moles/liter), B) time (hours); The ratio C_{SO_2}/C_{NH_3} eff: I) 0.9-0.95, II) 0.8-0.81, III) 0.88-0.91.

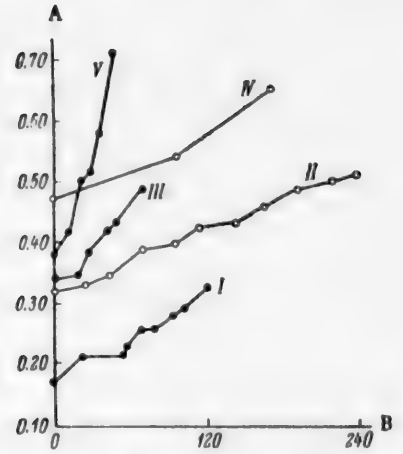

Fig. 13. Increase of thiosulfate concentration in working liquor at 103°: A) Thiosulfate concentration $C_{S_2O_3^{--}}$ (moles/liter), B) time (hours); the ratio C_{SO_2}/C_{NH_3} eff: I) 0.93-0.95, II) 0.80-0.79, III)0.92-0.89, IV)0.82-0,89, V) 0.92-0.99.

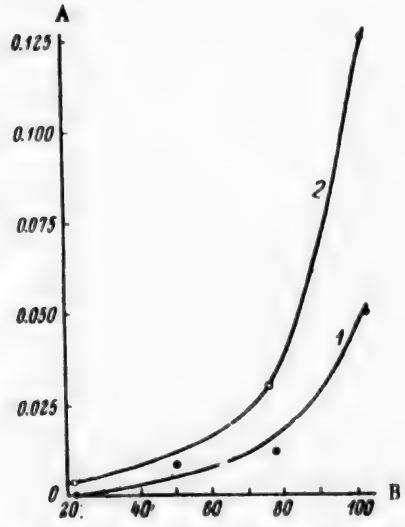

Fig. 14. Effect of temperature on the rate of spontaneous decomposition of working liquor: A) Rate of spontaneous decomposition $g_{S_2O_3^{--}}$ (moles/liter per 100 hours), B) temperature (in °C); the ratio C_{SO_2}/C_{NH_3} eff and concentration $C_{S_2O_3^{--}}$ (in moles/liter) respectively: 1) 0.8 and 0.25, 2) 0.92 and 0.25.

It was found by rectification of the curves in Fig. 14 in semilogarithmic coordinates that the value of the coefficient p, which represents the effect of temperature, is 0.047 for both curves; the value of the coefficient c which depend on other experimental conditions, were naturally different for the two curves. For example, for a solution with an average C_{SO_2}/C_{NH_3} eff ratio of 0.92, Equation (VI) becomes:

$$g_{S_2O_3^{--}} = 0.00104 \cdot e^{0.047t}. \qquad \text{(VII)}$$

Finally, combining the influence of all three principal factors, we derive the following generalized empirical equation which we recommend for determination of the rates of spontaneous decomposition of working liquors of ammonium sulfite-bisulfite in open equipment:

$$g_{S_2O_3^{--}} = 8.149 \cdot 10^{-9} \cdot C_{S_2O_3^{--}}^{0.8} \cdot e^{14.356 C_{SO_2}/C_{NH_3}\text{eff} + 0.047t} \qquad \text{(VIII)}$$

Calculated values of $g_{S_2O_3^{--}}$ found from Equation (VIII) are in most cases in acceptable agreement with experimental data. It must be taken into account, however, that the sensitivity of the spontaneous-decomposition process to the influence of all kinds of impurities

and the specific conditions in each particular case may cause considerable discrepancies between the calculated and the practical data. Nevertheless, the value of these empirical relationships lies in the fact that they can be used for predicting how the average rate of spontaneous decomposition will change under given production conditions if the composition or the temperature of the sulfite–bisulfite solution should change during the process. Moreover, these equations can be used for selecting the most favorable operating conditions, under which the rate of spontaneous decomposition of the solution will be at a minimum.

LITERATURE CITED

[1] F. Foerster and F. Lange, Z. anorg. allg. Ch., 128, 280 (1923); F. Foerster and E. Haufe, Z. anorg. allg. Ch. 177, 17 (1920).

[2] A. I. Brodskii, Progr. Chem. 23, 5 (1954); A. I. Brodskii and R. K. Eremenko, Proc. Acad. Sci. USSR 95, 3, 539 (1954); A. I. Brodskii and R. K. Eremenko, J. Gen. Chem. 1142 (1954).*

[3] W. M. Latimer, Oxidation States of the Elements and Their Potentials in Aqueous Solutions (IL, Moscow, 1954) [Russian translation].

[4] B. A. Chertkov, Trans. Sci. Res. Inst. Gas Purification (Goskhimizdat, 1957).

[5] B. A. Chertkov, J. Appl. Chem. 32, 6, 1385 (1959).*

Received March 19, 1958

* Original Russian pagination. See C.B. Translation.

SPONTANEOUS DECOMPOSITION OF AMMONIUM SULFITE-BISULFITE SOLUTIONS UNDER INDUSTRIAL CONDITIONS

B. A. Chertkov

The results of a laboratory study of the kinetics of spontaneous decomposition of ammonium sulfite–bisulfite solutions were reported previously [1].

In this paper the results of the laboratory investigation are correlated with practical data on the rate of spontaneous decomposition of ammonium sulfite–bisulfite solutions under industrial conditions, determined in a unit for extraction of SO_2 from flue gases in one of the Moscow heating and power plants [2]. Briefly, the technological process in this unit is as follows: after thorough removal of light ashes from the flue gases in an electric precipitator, the gases are cooled by water down to 30° and then interact with ammonium sulfite–bisulfite absorbent liquor, when the following reaction takes place:

$$(NH_4)_2SO_3 + SO_2 + H_2O \rightarrow 2NH_4HSO_3. \quad (1)$$

The resultant saturated liquor is thermally regenerated under vacuum, when the reverse reaction takes place:

$$2NH_4HSO_3 \rightarrow (NH_4)_2SO_3 + SO_2 + H_2O, \quad (2)$$

so that the absorbed sulfur dioxide is released in pure form from the liquor. The regenerated liquor is used again for absorption of SO_2 from flue gases.

The circulating absorbent liquor is therefore alternately heated and cooled, with simultaneous changes in the ratio of ammonium sulfite to bisulfite during the absorption and regeneration stages.

Ammonium sulfate (by oxidation of the liquor) and ammonium thiosulfate (by spontaneous decomposition of the liquor) are formed as by-products in the extraction of SO_2 from flue gases.

In this unit the situation is complicated by the fact that thiosulfate can be formed by absorption of hydrogen sulfide, which occasionally appears in the flue gas when the normal conditions of coal combustion in the boiler furnace are disturbed, as well as by spontaneous decomposition of the solution. However, determinations of the amounts of hydrogen sulfide entering the unit during two months of operation showed that the total amount of hydrogen sulfide absorbed and the equivalent amount of thiosulfate formed corresponds to a very small proportion of the total thiosulfate formed in the system, less than 1%. This can be entirely disregarded for practical purposes and it may be assumed that the main source of thiosulfate in the working liquor lies in the reactions of spontaneous decomposition inherent in the process; the rate of these reactions depends on the operating conditions.

The figure shows the increase of the total content of ammonium thiosulfate in the working liquor during one operating period of the unit. For convenience, three curves are given in the diagram, representing: I) change of thiosulfate concentration in the working liquor (moles/ liter), II) amount of thiosulfate in the system (in kg-moles), and III) the total mount of thiosulfate formed from the start of the period (in kg-moles), with the amount of thiosulfate withdrawn from the system in lost liquor taken into account. From the slope of Curve III it is easy to find the average rate of thiosulfate formation in the working liquor per unit time. These values (3.84, 2.54, 3.86) are also indicated in the diagram against the corresponding portions of the curve.

Data on the average rates of thiosulfate formation for a number of operating periods of the unit, together with the main operating characteristics of the regeneration columns, are given in the table. These data show that the average rate of thiosulfate formation differed considerably in different periods. Thus, during the early periods, when the thiosulfate concentration was low and the $C_{SO_2}/C_{NH_3\ eff}$ ratio was least in the saturated and regenerated liquors, and the boiling point of the liquor at the foot of the column was relatively low, the rate of spontaneous decomposition was at its lowest. Subsequently, with increase of the thiosulfate concentration in the liquor and with rise of boiling point the rate of spontaneous decomposition rose appreciably, in full agreement with the laboratory data.

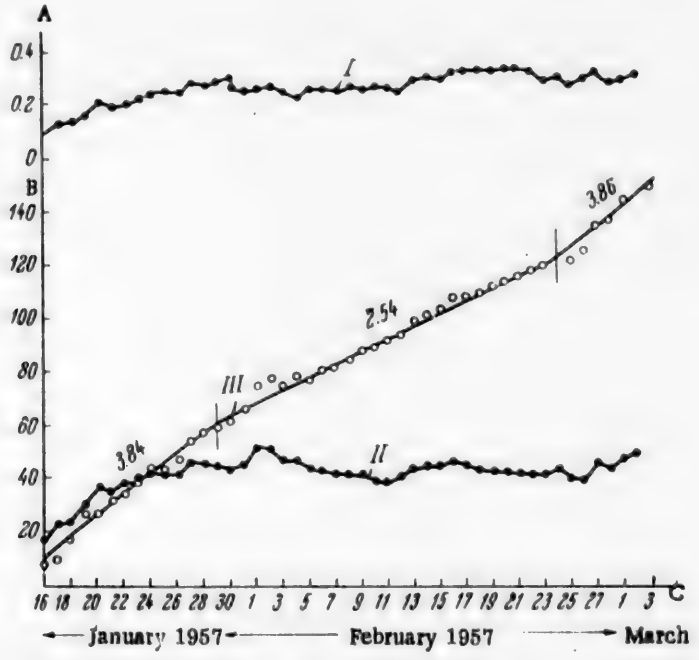

Formation of thiosulfate in the working liquor: A) concentration of $(NH_4)_2S_2O_3$ (moles/ liter), B) amount of $(NH_4)_2S_2O_3$ in the system (in kg-moles), C) time (days); explanations of the curves are given in the text.

During the last periods (see table), when the average thiosulfate concentration was 0.3 mole/ liter and the boiling point of the liquor was raised to 100-104° (by reduction of the vacuum used), the average rate of thiosulfate formation was at the level of 3.7 kg-moles/ day. As the average volume of working liquor in the unit during these periods was 160 m^3, calculation shows that $g_{S_2O_3^{--}}$ was 0.095 mole/ liter per 100 hours.

We now compare this practical value with the rate of the spontaneous decomposition of the liquor calculated from the equation derived in our preceding paper [1]:

$$g_{S_2O_3^{--}} = 8.149 \cdot 10^{-9} \cdot C^{0.8}_{S_2O_3^{--}} \cdot e^{14.356 C_{SO_2}/C_{NH_3 eff} + 0.047t}, \qquad (3)$$

where $g_{S_2O_3^{--}}$ is the average rate of spontaneous decomposition (thiosulfate formation), in moles/ liter per 100 hours, $C_{S_2O_3^{--}}$ is the average thiosulfate concentration in the liquor (moles/ liter), e is the base of natural logarithms, and t is the average temperature (°C).

In a full cycle of the unit 40 m^3 of liquor is circulated per hour. It follows that all the volume of liquor present completes a full cycle in 4 hours. During this time the liquor undergoes the following changes: the ratio $C_{SO_2}/C_{NH_3\ eff}$ changes from 0.83 in the regenerated liquor to 0.95 in the saturated liquor, while

the temperature changes from 30° in the absorption process to about 100° in the regeneration process. Approximate calculations, with the volumes of liquor contained in individual tanks and other equipment taken into account, showed that for about 60% of the time the liquor is in the saturated state and for about 40% in the regenerated state; it is in the heated state for about 40% of the time, and in the cold for about 60%.

Data on Spontaneous Decomposition of Working Liquor in the Sulfur-Collecting Apparatus

Periods	Average rate of thiosulfate formation in the system (kg-mole/day)	Thiosulfate concentration of working liquor (moles/liter)	Liquor feed rate to one column (m^3/hour)	Liquid temperature (°C)		C_{SO_2}/C_{NH_3} eff ratio	
				top of column	bottom of column	saturated liquor	regenerated liquor
9/1 – 9/18/53	0.45	0.03—0.06	12 —15	78—83	78— 83	0.90—0.94	0.79—0.81
9/18 –9/26/53	0.70	0.06—0.07	12.5—18	78—85	78— 83	0.90—0.92	0.77—0.81
11/6 – 11/21/55	1.47	0.01—0.13	17.5—24	65—81	90— 93	0.94—0.96	0.80—0.84
11/21 – 12/4/55	2.93	0.13—0.24	17 —20	77—80	85— 93	0.93—0.96	0.80—0.85
12/4 – 12/17/55	4.45	0.24—0.44	16 —21	78—83	87— 92	0.91—0.93	0.81—0.85
12/17 – 12/28/55	4.80	0.44—0.53	17 —20	80—83	89— 95	0.89—0.96	0.78—0.85
1/16 – 1/29/57	3.84	0.10—0.30	21 —22	80—84	97— 99	0.92—0.93	0.81—0.84
1/29 – 2/24/57	2.54	0.30—0.33	20 —22	81—85	96—100	0.92—0.96	0.82—0.84
2/24 – 3/3/57	3.86	0.33—0.34	20.5—21	77—87	96— 98	0.95—0.97	0.83—0.84
3/12 – 3/21/57	3.80	0.15—0.30	20 —22	80—85	97—102	0.93—0.97	0.82—0.86
3/21 – 4/3/57	3.70	0.27—0.30	20 —21	86—88	100—104	0.92—0.95	0.82—0.83
3/21 – 4/3/57	3.70	0.27—0.30	20 —21.5	86—88	100—102	0.90—0.96	0.82—0.83

To simplify the subsequent calculations we assume that the liquor remains for equal times in the saturated and regenerated states, and also in the heated and cold states. The problem is then to use Equation (3) for calculating the rate of thiosulfate formation at the four limiting regimes indicated below, and to find the average of the results.

C_{SO_2}/C_{NH_3} eff	t°
0.95	100
0.83	100
0.95	30
0.83	30

It is also taken into account that the thiosulfate concentration of the liquor during this period was 0.3 mole/liter.

The corresponding calculations show that $g_{S_2O_3^{--}}$ (in moles/liter per 100 hours) is 0.275 in the first case, 0.056 in the second, 0.010 in the third, and 0.002 in the fourth; hence, the average value of $g_{S_2O_3^{--}}$ is 0.086 mole/liter per 100 hours.

The agreement with the value found in practice (0.095 mole/liter per 100 hours) must be regarded as very good.

Calculations for other periods given in the table also resulted in good agreement between the values found by means of Equation (3) and practical data on the rate of spontaneous decomposition of the liquor in the unit. Hence, our empirical Equation (3) correctly represents the course of spontaneous decomposition of ammonium sulfite–bisulfite solutions under industrial conditions, and it may be used with success for design calculations or if any modifications are introduced into the technological process. However, this does not exhaust the utility of Equation (3). It also indicates at which stage of the process the rate of spontaneous decomposition of the liquor reaches a maximum. It follows from the data presented above that at a low temperature

the rates of spontaneous decomposition are negligibly low in the saturated and especially in the regenerated liquor. It follows that the stage of SO_2 absorption from the gas presents no special risk of development of spontaneous-decomposition reactions.

With rise of temperature, i.e., during regeneration of the liquor, the rate of spontaneous decomposition rises sharply (about 25-fold in the 30-100° temperature range) and becomes very high, especially in the saturated liquor. Evidently, this is the stage of the process on which attention must be concentrated if it is desired to lower the rate of spontaneous decomposition of the working liquor. This result may be achieved either by decrease of temperature of the saturated solution fed into the top of the distillation column, or by a reduction of the time during which the saturated liquor remains in the heat-exchange equipment.

SUMMARY

The results of earlier kinetic studies of the reactions in the first stage of spontaneous decomposition of ammonium sulfite–bisulfite solutions were used to derive an empirical equation which can be used for finding changes in the rate of spontaneous decomposition with variations of the liquor composition and temperature. The results of the laboratory investigation are confirmed by practical data on the spontaneous decomposition of ammonium sulfite–bisulfite under industrial conditions in a unit for extraction of SO_2 from flue gases by the cyclic ammonia process.

LITERATURE CITED

[1] B. A. Chertkov, J. Appl. Chem. 32, 8, 1695 (1959).*

[2] A. P. Andrianov and B. A. Chertkov, J. Chem. Ind. 7, 10 (1954).

Received March 19, 1958

* Original Russian pagination. See C.B. Translation.

THERMOGRAPHIC INVESTIGATION OF ALUMINUM SULFITES

P. V. Dybina

Removal of sulfur dioxide from waste gases from heat and electric power plants burning sulfur-containing coals raises the problem of a method for its most rational utilization. One solution of this problem is the use of SO_2 for decomposition of aluminosilicates with subsequent production of alumina. The thermal stability of the compounds formed in hydrolysis of sulfite solutions has not been studied sufficiently, so that the optimum conditions for thermal dissociation of aluminum sulfites cannot be determined.

Our investigations of the chemical composition of the solid phases formed during hydrolysis in the system $Al_2O_3-SO_2-H_2O$ showed that they rarely correspond to definite stoichiometric formulas. In most cases they are mechanical mixtures either of monobasic and polybasic sulfites, or polybasic sulfite and hydroxide in various proportions.

The formation conditions, chemical composition, and chemical formula of each specimen are given in an earlier paper [1].

One of the methods of physicochemical analysis, thermography, was used to confirm that the solid phases contain aluminum hydroxide in addition to different forms of sulfites. The PK-52 pyrometer was used for the thermographic investigation, with a heating time of 2 hours 30 minutes in the temperature range from 0 to 1100°. The comparison standard was aluminum oxide calcined at 1200°.

The literature contains data on the conditions of formation and thermal conversions of aluminum hydroxide [2-5], but there is no information on the transformations of aluminum sulfites.

The thermal dissociation of monobasic and polybasic aluminum sulfites may be represented by the equations:

$$2AlOHSO_3 \rightarrow Al_2O_3 + 2SO_2 + H_2O, \quad (1)$$

$$Al_2(OH)_4SO_3 \rightarrow Al_2O_3 + SO_2 + 2H_2O. \quad (2)$$

In both cases the heating curves should reveal thermal effects corresponding to decomposition of sulfites and possible transformations of aluminum oxide.

If the solid phase contains aluminum hydroxide in addition to polybasic sulfite, the thermal dissociation may be represented in general form by the equation

$$Al_2(OH)_4SO_3 + 2Al(OH)_3 \rightarrow 2Al_2O_3 + SO_2 + 5H_2O. \quad (3)$$

In that case the thermograms should reveal an additional effect corresponding to decomposition of hydrargillite.

To clarify this question, it was necessary to compare the heating curves for our precipitates and for aluminum hydroxide. The thermogram for aluminum hydroxide (Fig. 1) has three endothermic effects at 245,330 and 550°, and one exothermic effect at 980°. The endothermic effects at 245 and 330° may be attributed to consecutive removal of two water molecules, and at 550° to removal of the third water molecule. The exothermic effect at 980° is probably associated with conversion of aluminum oxide into the crystalline state.

Of the various samples of aluminum sulfites obtained in stepwise hydrolysis, series 20–23, 24–27, 30–33, 39-42 were subjected to thermal analysis. The proportions of the principal components in these samples are given below.

Sample No.	Hydrolysis temperature	Al_2O_3	SO_2	H_2O
20	82	1	1.44	6.11
21	87	1	0.89	6.76
22	92	1	0.68	5.90
23	97	1	0.11	6.20
24	77	1	1.46	5.00
25	82	1	0.89	6.30
26	87	1	0.69	5.26
27	92	1	0.36	6.68
30	82	1	1.73	5.20
31	87	1	1.02	5.15
32	92	1	0.62	5.47
33	97	1	0.11	6.32
39	82	1	1.70	5.60
40	87	1	1.00	6.46
41	92	1	0.58	6.00
42	97	1	0.13	6.28

Examination of the thermograms for hydrolysis products containing more than 1 mole of SO_2 per mole of Al_2O_3 (Samples No. 20, 24, 30, 39) showed that they all give heating curves of the same type, each with two endothermic and three exothermic effects. The endothermic effects in the 120-140° region are due to liberation of adsorbed moisture, and those at 240-250° to breakdown of the sulfite structure. The exothermic effects in the high-temperature region are due to conversion of aluminum oxide into the crystalline state. At 900-1100° the degree of crystallization greatly increases, so that heat energy is liberated.

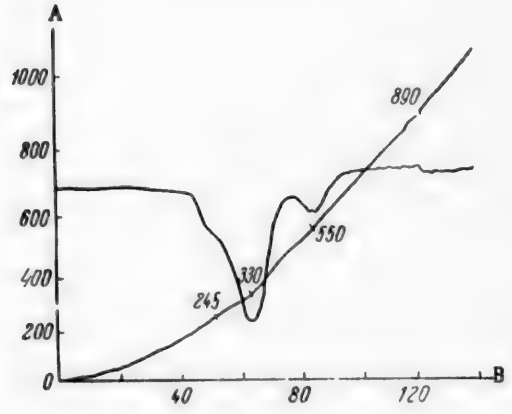

Fig. 1. Thermogram for aluminum hydroxide $Al_2O_3 \cdot 3H_2O$. A) Temperature (°C), B) time minutes).

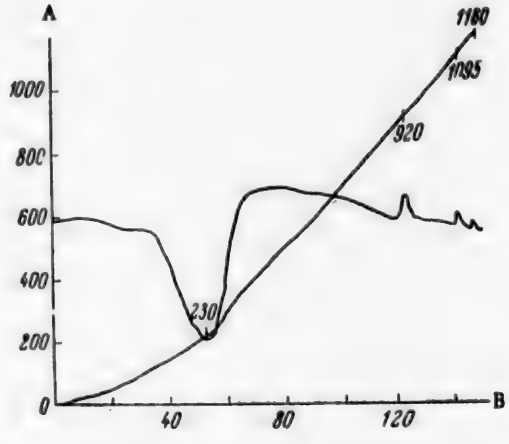

Fig. 2. Thermogram for Sample No. 24. A) Temperature (°C), B) time minutes.

The absence of other effects on the thermograms for these samples indicates that the thermal dissociation of the hydrolysis products isolated at 77-82° proceeds in accordance with Equations (1) and (2).

As a typical example of this series, we consider the heating curve for Sample No. 24 (Fig. 2), with two endothermic effects (at 120 and 230°) and three exothermic effects (at 920, 1095, and 1160°). The endothermic effects may be attributed to removal of adsorbed moisture (at 120°) and breakdown of the sulfite structure (at 230°). The distinct exothermic effects at high temperatures on the differential curve are especially characteristic for this sample.

The heating curves forSamples No. 31 and 40, the compositions of which correspond very nearly to the formula of the polybasic sulfite, are of undoubted interest. The thermograms for these samples differ from the preceding ones in having a smaller exothermic effect corresponding to breakdown of the sulfite structure, and this effect is found at lower temperatures. In addition, the thermograms show small endothermic effects at 900-1000°, apparently compensating the heat effect of alumina crystallization. For a fuller characterization of this series we consider the thermogram for Sample No. 31 (Fig. 3), which has three endothermic effects, at 90, 170, and 900°. The first and second effects are attributable to removal of moisture and to breakdown of sulfite structure respectively. The endothermic effect at 900° indicates the presence of a compound not found in the first series of samples. The smaller thermal effect for breakdown of the sulfite structure and the complete dissociation at 170° indicate that the polybasic sulfite has lower thermal stability than those considered above.

The thermograms for the hydrolysis products containing 0.58-0.69 mole of SO_2 per mole of Al_2O_3 (Samples No. 22, 26, 32, and 41) are somewhat different in character. In addition to the principal effects due to removal of adsorbed water and breakdown of sulfite structure, the heating curves for these samples show a well-defined boehmite effect at 495-550°, corresponding to complete dehydration of hydrargillite. Therefore, aluminum hydroxide as well as polybasic sulfite is formed at 92°. The endothermic effects corresponding to breakdown of sulfite structure are greatly extended, have no pronounced maxima, and lie in the 135-380° range. This suggests that here again the effects of breakdown of sulfite structure and removal of hydration water from hydrargillite are superposed. The endothermic effect in the high-temperature region is greater than for the polybasic sulfite, as comparison with the thermogram for Sample No. 31 shows.

The thermogram for Sample No. 26 (Fig. 4) gives a clear idea of this group of compounds. In the low-temperature region the heating curve does not have a well-defined maximum corresponding to breakdown of aluminum sulfite structure. However, the thermogram shows a distinct boehmite effect at 495°, indicating the presence of hydrargillite. It follows that thermal dissociation of this group of compounds proceeds in accordance with Equation (3).

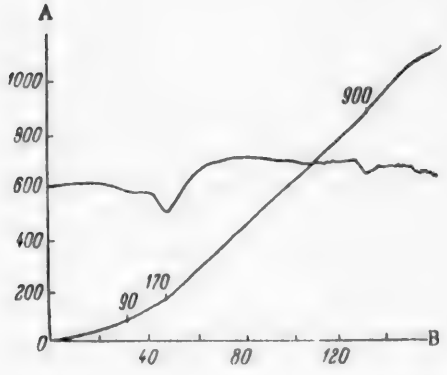

Fig. 3. Thermogram for Sample No. 31. A) Temperature (°C), B) time (minutes).

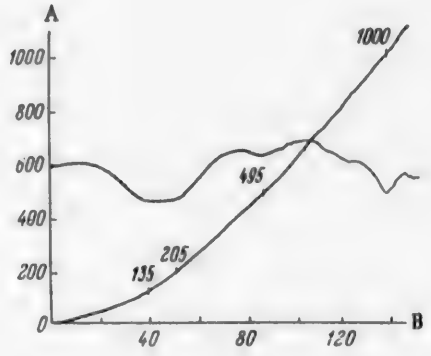

Fig. 4. Thermogram for Sample No. 26. A) Temperature (°C), B) time (minutes).

The last series includes hydrolysis products containing 0.11-0.13 mole of SO_2 per mole of Al_2SO_3 (Samples No. 23, 33, and 42) isolated at 97°. The thermograms for samples in this series are characterized by an extended endothermic effect without a maximum, a boehmite effect, and a high-temperature effect at 960°. Extension of the endothermic effect at 125° to 550° confirms our hypothesis that the effects of breakdown of sulfite structure and removal of hydration water from hydrargillite are superposed.

Sample No. 33, the thermogram for which is given in Fig. 5, is characteristic of this series. Similarly to Samples No. 26 and 31, this product also contains a new phase.

Comparison of the principal endothermic effects for the series of samples considered above shows that the thermal decomposition temperature of the sulfites fall from 230° (Sample No. 24) to 125° (Sample No. 33) with increase of the hydrolysis temperature. If follows that with decrease in the concentration of the hydrolyzed

solution and increase of the hydrolysis temperature the sulfite composition changes, hydrargillite is formed (Samples No. 26 and 33), and also a new compound which gives an endothermic effect in the 900-960° region. In view of the tendency of sulfites to oxidation, we attempted to determine the nature of the endothermic effects for sulfites in the high-temperature region by comparison with the thermogram with aluminum sulfate

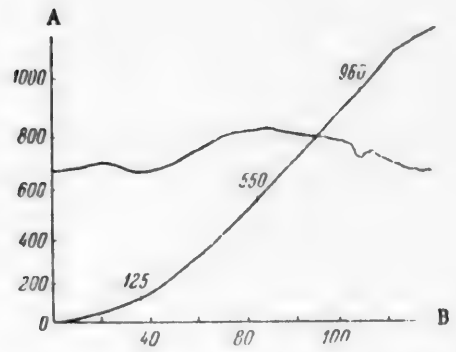

Fig. 5. Thermogram for Sample No. 33. A) Temperature (°C), B) time (minutes).

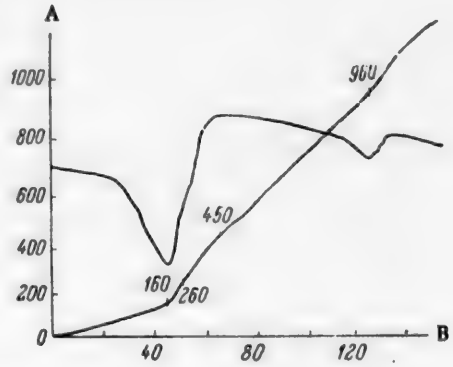

Fig. 6. Thermogram for aluminum sulfate $Al_2(SO_4)_3 \cdot 18H_2O$. A) Temperature (°C), B) time (minutes).

(Fig. 6). The heating curve for aluminum sulfate has a large twinned endothermic effect in the 160-260° region and a small effect at 960°. The former corresponds to removal of hydration water, while the second is the same as the endothermic effects in the 900-960° region for the investigated aluminum sulfites. Therefore, as the hydrolysis temperature is increased, formation of aluminum sulfate begins; its presence could be detected only by thermal analysis.

SUMMARY

1. The heating curves for different sulfite samples depend on their chemical composition; they can therefore be classified by the nature of the thermograms without complicated chemical analyses.

2. The thermal stability of the sulfites diminishes with increase of the hydrolysis temperature of the solutions.

3. The magnitude of the endothermic effect for breakdown of sulfite structure depends on the concentration of the original solution.

4. The thermograms for sulfites obtained by low-temperature hydrolysis (80-82°) show no effects apart from those due to breakdown of sulfite structure and thermal conversions of aluminum oxide. These compounds, consisting of mixtures of monobasic and polybasic sulfites, dissociate in accordance with Equations (1) or (2).

5. The thermograms for precipitates obtained by high-temperature hydrolysis (90-97°) are characterized by extended endothermic effects, which may be regarded as combined effects due to breakdown of sulfite structure and dehydration of hydrargillite. The dissociation of these compounds is represented by Equation (3).

6. Comparison of the heating curves for aluminum sulfites and sulfate shows that the endothermic effects in the high-temperature region are identical in external appearance. This suggests that they represent thermal dissociation of aluminum sulfate. Aluminum sulfate is evidently forming owing to oxidation of sulfur to the hexavalent state.

Our thermographic investigation of the phase composition of aluminum sulfites may be of practical as well as of theoretical significance for determination of the optimum conditions for calcination of sulfites in sulfite decomposition of various aluminosilicates.

LITERATURE CITED

[1] P. V. Dybina, Coll. Trans. VZPI 18 (1957).

[2] N. S. Kurnakov and G. G. Urazov, J. Chem. Ind. 1 (1924)

[3] K. M. Fedot'ev, Trans. Inst. Geol. Sci. Acad. Sci. USSR 120, 35 (1949).

[4] G. Hüttig and Wittgenstein, Z. anorg. allg. Ch. 171, 3.

[5] L. G. Berg, A. V. Nikolaev, and N. Ya. Rodé, Thermography (Izd. An SSSR, 1944) [in Russian].

Received June 16, 1958

ABSORPTION OF NITROGEN OXIDES BY SODIUM CARBONATE SOLUTIONS IN A GAS LIFT APPARATUS

M. L. Varlamov and Ya. I. Starosel'skii

This paper contains the results of laboratory investigations of the absorption of nitrogen oxides at low concentrations (from 0.3 to 1.5% NO, NO_2) by aqueous soda solutions (12.5, 50.5, 87.5 g/ liter) in a high-speed absorber of the gas-lift type. The degree of oxidation of nitric oxide in the gaseous mixture was 0.5-0.9, the flow rate of the gas mixture was from 5 to 30 liters/ minute, corresponding to a linear gas velocity from 1 to 6.4 meters/ second in the rising limb of the apparatus; the immersion depth of the orifice taking the gas to the rising limb was from 20 to 60% of the height of that limb.

Absorption of nitrogen oxides by alkaline solutions in packed and bubbler apparatus and in mechanical absorbers has been studied in a series of investigations [1-10].

Equipment of the gas-lift type is now used for conveying of liquids, mainly in the petroleum industry. Its use for absorption processes has been proposed relatively recently [11]. Such equipment has been used for absorption of SO_2 and CO_2 under laboratory conditions [12, 13].

In addition to the high turbulence of the gas and liquid streams in the reaction space, such equipment is also simple in design, the operating conditions can be varied rapidly over a wide range of gas–liquid ratios, the capital cost is low, there are no pumps for liquid circulation, liquids containing suspended impurities may be treated, etc.

This type of equipment also suffers from the great disadvantage of a high hydraulic resistance; however, this depends to a considerable extent on the design characteristics of the equipment, its layout, and on uniflow of gas and liquid in the rising limb of the apparatus.

The purpose of the present investigation was to determine the influence on the absorption process of such factors as the concetration of the incoming nitrogen oxides, flow rate of the gaseous mixture, gas–liquid ratio (G : L), concentration of the soda solution, temperature, and the immersion depth of the orifice.

The experimental laboratory unit used (Fig. 1) was compact, and it was easy to take gas and liquid samples, to regulate their flow rates, and to maintain a required temperature automatically.

The gas-lift apparatus is shown in Fig. 2. The reaction volume of the apparatus was $2.4 \cdot 10^{-5}$ m^3. The gas inlet tube was connected to the apparatus by a ground-glass joint. The gas and liquid phases were isolated in the separator by means of a special deflector which prevented additional absorption of nitrogen oxides at that point.

To ensure a constant depth of immersion of the orifice during the absorption process, the diameter of the liquid inlet tube was fairly large, regulating stopcocks were used, and a gas connecting tube was fitted.

The gas-lift apparatus was contained in a thermostat in which a given constant temperature was maintained in the gas and liquid to within ±0.5°. The flow rates of the components were measured by means of calibrated rheometers to within ± 2%. The soda solutions used for absorption were brought to a constant temperature in a header vessel. Temperatures and pressures were measured by means of specially installed thermometers and manometers. To obtain gas mixtures with given contents of nitrogen oxides and the required degree

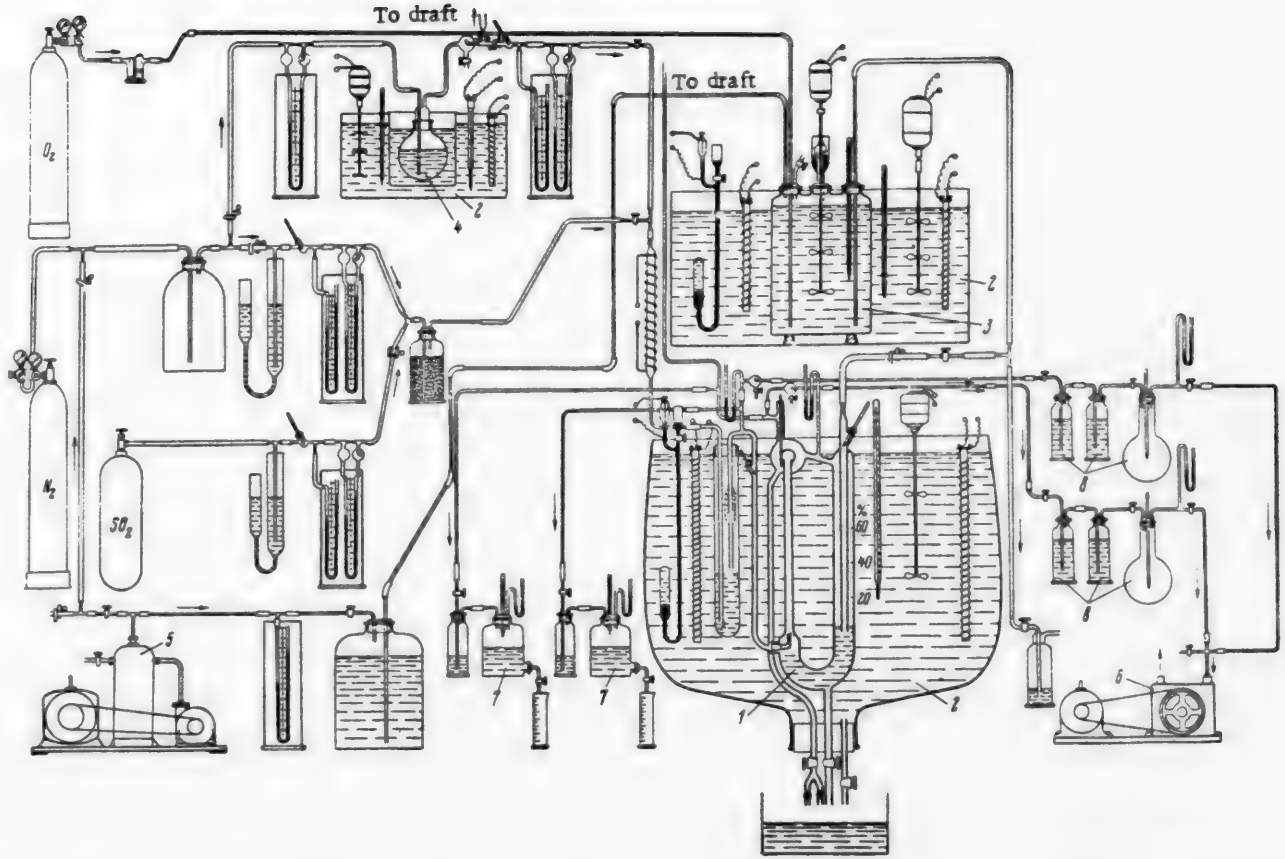

Fig. 1. Experimental absorption unit. 1) Gas-lift apparatus; 2) thermostats; 3) vessel with liquid fed into the gas-lift apparatus; 4) bubbler with nitrose solution; 5) compressor; 6) vacuum pump; 7) sampling of gas for analysis at entry and exit of the gas-lift apparatus (% SO_2 in investigations of mass transfer); 8) sampling of gas at entry and exit of the gas-lift apparatus (% NO, NO_2 in studies of absorption of nitrogen oxides).

of oxidation of nitric oxide, a vessel of about 2 liters in capacity was placed in a thermostat, and filled to about one-third with nitrose solution. Air was bubbled through the nitrose at a constant rate to correspond to the maximum required gas output.

If the nitrose does not contain free HNO_3, the degree of oxidation of the nitrogen oxides blown out from it is $\alpha = 0.5$. It is possible to increase α by addition of free HNO_3 to the solution. With the bubbling height, liquid temperature, and air rate kept constant, the concentration and composition of the nitrogen oxides in the gas remained almost constant during 2-3 experiments, after which the nitrose in the vessel was changed. The required amount of gas was fed into the gas-lift, while the rest was bypassed.

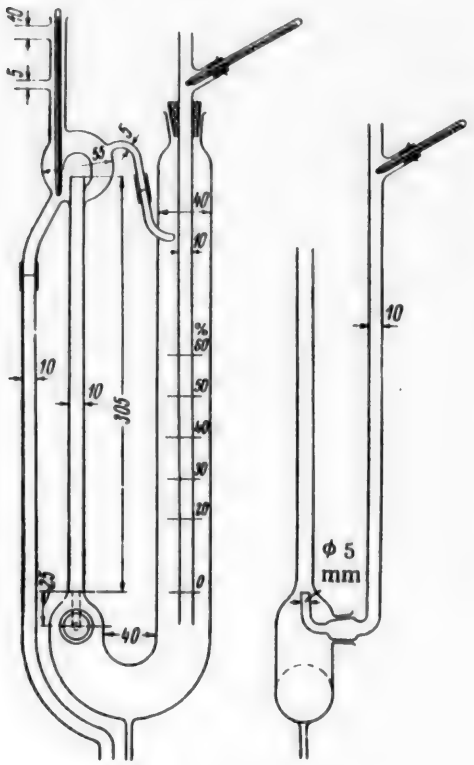

Fig. 2. Gas-lift apparatus.

A recommended method [14, 15] was used for determination of NO_2 and $NO + NO_2$ in the gaseous mixture. Gas samples were taken at the apparatus entry and exit simultaneously; the duration of sampling was a few minutes.

In analysis of the exit gas after alkaline absorption of nitrogen oxides in the gas-lift, the solution was boiled to liberate the carbon dioxide formed in the interaction of nitrogen oxides with the soda solution.

The volume coefficients of the absorption rate of nitrogen oxides in the gas-lift apparatus were calculated from the formula

$$K_G a = \frac{G_{N_2}}{V \Delta P \tau} \left[\frac{\text{kg } N_2}{\text{m}^3 \cdot \text{hr} \cdot \text{atm}} \right], \qquad (1)$$

where G_{N_2} is the amount of absorbed nitrogen oxides calculated as elemental nitrogen (in kg), V is the reaction volume of the apparatus (in m^3) τ is the time of absorption (hours), and ΔP is the driving force of absorption (in atmos).

The mean-logarithmic partial pressure of the oxides at the entry and exit of the apparatus was used for determination of ΔP.

In hydrodynamic studies of the gas-liquid streams in this gas-lift, distilled water was forced by compressed air from a compressor into a header vessel (Fig. 1), from which it entered the apparatus through a siphon. The air passed through a receiver, manostat, rheometer, gas preheater, and a humidifier, and entered the orifice.

At constant air rate the liquid rate increases with increasing immersion depth (h) of the orifice; the maximum is virtually independent of the gas rate for different values of h.

The turbulence of the gas–liquid stream is greatest at the point of maximum liquid rate.

The hydraulic resistance ΔP of the apparatus varied from 70 to 180 mm H_2O at air rates from 5 to 30 liters / minute and orifice immersion depths from 20 to 40%.

Investigations of the influence of the shape of the orifice and of the linear gas velocity at the orifice exit at a given gas rate showed that these factors have no significant effects on the hydrodynamic conditions in the apparatus or the liquid rate.

In addition to ΔP, the performance of the apparatus is characterized by the degree of absorption Δ and by $K_G a$. The influence of the initial concentration of nitrogen oxides in the gas was studied at 25°, soda concentrations of 50.5 and 87.5 g/ liter, at a constant immersion depth h = 20%.

Figure 3 shows variation of $K_G a$ with the flow rate V_g of the gaseous mixture at different concentrations C_{NO, NO_2} of nitrogen oxides.

The experimental points give satisfactorily linear plots in logarithmic coordinates. When V_g is constant $K_G a$ increases with C_{NO,NO_2}. This is represented by the functional relationship

$$K_G \cdot a \approx C^{0.31}_{NO, NO_2}. \quad (2)$$

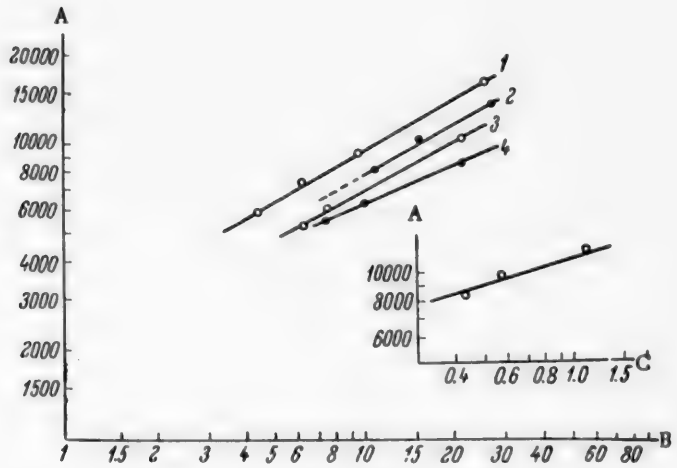

Fig. 3. Variations of the total coefficient of the absorption rate of nitrogen oxides $K_G a$ with % NO, NO_2 in the gas and the gas rate V_g. A) Values of $K_G a$ ($\frac{kg}{m^3 \cdot hr \cdot atm}$), B) volumetric gas rate (liters/ minute), C) concentration of C_{NO, NO_2} (%); values of C_{NO, NO_2} and α respectively: 1) 1.13, 0.8; 2) 0.58, 0.7; 3) 0.43, 0.65; 4) 0.37, 0.65. $C_{Na_2CO_3}$ = 50.5 g/ liter, h = 20%, t = 25.

Figure 4 represents the relationship $\Delta = f(V_g, C_{NO, NO_2})$. Increase of C_{NO, NO_2} results in a considerable increase of the degree of absorption Δ at constant V_g.

The influence of gas rate on Δ and $K_G a$ is clear from Fig. 3 and 4. $K_G a$ increases with increase of V_g; this may be expressed as

$$K_G \cdot a \approx V^{0.57}_g \cdot C^{0.31}_{NO, NO_2}. \quad (3)$$

Equation (3) is valid at V_g = 5-30 liters/ minute, C_{NO, NO_2} = 0.35-1.2% , $C_{Na_2CO_3}$ = 50.5 g/ liter.

Figure 4 shows that Δ decreases with increase of V_g. Thus, Δ is halved when V_g is increased sevenfold.

It is of interest to consider the influence of V_g and C_{NO,NO_2} on the rate of absorption U ($\frac{kg}{m^3 \cdot hr}$) of nitrogen oxides in the gas-lift. For a soda concentration $C_{Na_2CO_3}$, of 87.5 g/ liter it was found that

$$U \approx V^{0.9}_g \cdot C^{1.36}_{NO, NO_2}. \quad (4)$$

The influence of the G : L ratio on Δ is shown in Fig. 5 for $C_{Na_2CO_3}$ = 87.5 g/ liter.

A similar relationship holds at other concentrations of the soda solution. The graphs show that the increase of the G : L ratio, Δ decreases while $K_G a$ increases. At constant G : L ratio, Δ increases with increase of C_{NO, NO_2}.

Variation of $K_G a$ with concentration of the soda solution at different gas rates are plotted in Fig. 6. The initial concentration of nitrogen oxides in the gas and their degree of oxidation were constant for each curve. Increase of $C_{Na_2CO_3}$ leads to some decrease of $K_G a$ and Δ. Thus, when $C_{Na_2CO_3}$ is changed from 12.5 to 87.5 g/ liter, $C_{NO,\ NO_2}$ = 0.55% and V_g = 30 liters/ minute, $K_G a$ decreases from 17,000 to 11,500, or roughly by one third.

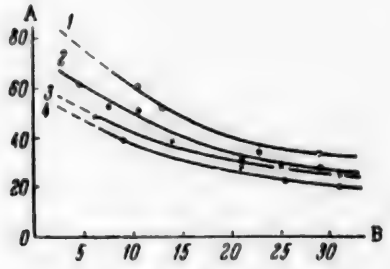

Fig. 4. Variation of the degree of absorption of nitrogen oxides in a gas-lift apparatus with the gas rate and the amount of NO, NO_2 in the gas (in %). A) Degree of absorption Δ (%), B) volumetric gas rate (liters/ minute); values of $C_{NO,\ NO_2}$: 1) 1.5, 2) 1.1, 3) 0.75, 4) 0.6. α = 0.7, $C_{Na_2CO_3}$ = 87.5 g / liter, h = 20% , t = 25°.

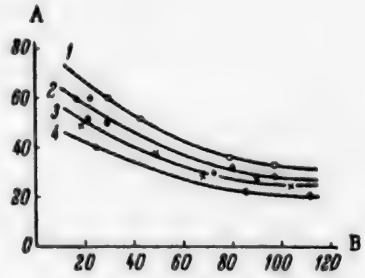

Fig. 5. Variation of the degree of absorption of nitrogen oxides in a gas-lift apparatus with the gas–liquid ratio (G : L) and the amount of NO, NO_2 in the gas (in %). A) Degree of absorption Δ (%), B) G : L ratio; values of $C_{NO,\ NO_2}$: 1) 1.5, 2) 1.1, 3) 0.75, 4) 0.6. α = 0.7, h = 20%, t = 25°, $C_{Na_2CO_3}$ = 87.5 g/ liter.

In Fig. 7 $K_G a$ is plotted against temperature in logarithmic coordinates. Its value decreases considerably with increase of temperature.

Absorption improves at low (< 40%) and high (>60%) immersion depths. However, the hydraulic resistance of the apparatus increases sharply in the latter case.

The results of an experimental study of the effects of the principal factors on physical absorption controlled by diffusion resistances of the gas and liquid phases are presented below, and criterial equations for calculations relating to these processes in the gas-lift apparatus are derived.

Absorption of a sparingly soluble gas was studied for the system oxygen–water, so that volume coefficients of mass transfer in the liquid phase could be calculated.

These coefficients were calculated from the formula

$$K_G a = \frac{G}{V\tau\Delta C}\left[\frac{\text{kg}}{\text{m}^3 \cdot \text{hr} \cdot \frac{\text{kg}}{\text{m}^3}}\right]. \qquad (5)$$

Distilled water was saturated with oxygen and fed into the gas-lift for desorption at the experimental temperature. Technical nitrogen containing from 4 to 8% O_2 was passed through the apparatus in order to increase the driving force of desorption and to improve the analytical accuracy. To avoid evolution of oxygen, the overflow tube of the gas-lift as well as the rising limb was always kept full of outflowing water.

The method used for oxygen determination is based on the easy oxidation of freshly-prepared manganous oxide in an alkaline medium by oxygen dissolved in water [16].

The influence of gas velocity on $K_L a$ has been studied earlier [13, 17]. It was shown that over a wide range of gas velocities (0.08-8 m/ second) $K_L a$ remains constant and is independent of the concentration of the absorbed (or desorbed) gas in physical absorption [17].

$K_L a$ was found to increase with the liquid rate [17].

For gas-lift apparatus the influence of the liquid rate L is represented by the expression [12] $K_L a \approx L^{0.97}$.

According to another paper [13], the $K_L a - L$ graph has a break; up to the break $K_L a \approx L^{0.91}$, and beyond the break $K_L a \approx L^{1.98}$.

Increase of temperature should increase $K_L a$ because of the increase in the coefficients of diffusion and decrease of liquid viscosity.

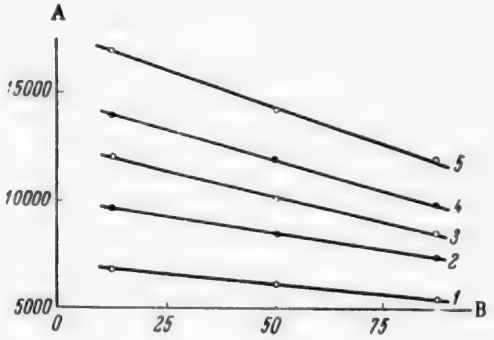

Fig. 6. Variation of $K_G a$ with concentration of soda solution and the gas rate at orifice immersion depth 20%, t = 25°, $C_{NO, NO_2} = 0.55$, $\alpha = 0.7$. Gas rate (liters/ minute): 1) 5, 2) 10, 3) 15, 4) 20, 5) 30. A) $K_G a$ (in kg/ m^3 · hr · atmos), B) concentration of soda solution (in g/ liter).

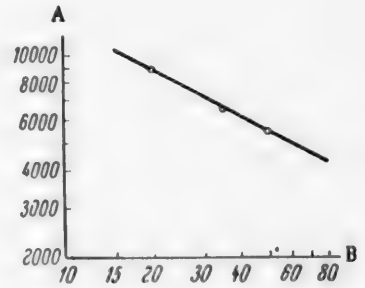

Fig. 7. Influence of temperature on the absorption rate coefficient of nitrogen oxides. A) Absorption rate coefficient $K_G a$ (in kg/ m^3 · hr · atmos), B) temperature (°C). Orifice immersion depth 30.0%; concentration of soda solution 28.5 g/ liter, volumetric gas rate 9.7 liter/ minute, $C_{NO, NO_2} = 0.9$, $\alpha = 0.65$.

The influence of the immersion depth of the orifice is represented by the expression $K_L a \approx L^{-0.5}$ [12] and $K_L a \approx h^{-0.7}$ [13], i.e., $K_L a$ decreases with increasing depth of immersion.

Our experimental data for liquid rates between 0.15 and 1.5 liters / minute at different immersion depths gave the relationship

$$K_L \cdot a = 180 L^{1.25} \cdot h^{-1.94}. \tag{6}$$

The above relationships were correlated with the aid of the similarity principle and presented in the form of power functions of dimensionless criteria; Bol'shakov's method [18] was used. Finally, Equation (7) was derived:

$$Nu'_L = 0.195 Re_L^{1.25} \cdot (Pr'_L)^{0.5} \cdot h^{-1.94}, \tag{7}$$

where

$$Nu'_L = K_L \cdot a \left[\frac{\eta_L^2}{g\gamma_L^2}\right]^{1/3} \cdot \frac{d}{D_L}; \quad Re_L = \frac{w \cdot d \cdot \gamma_L}{\eta_L}; \quad Pr'_L = \frac{\eta_L}{\gamma_L \cdot D_L},$$

η_L is the coefficient of viscosity of the liquid (in $\frac{kg}{m \cdot sec}$), γ_L is the density of the liquid (in kg/ m^3), g is the acceleration due to gravity (m/ sec^2), D_L is the coefficient of diffusion of the gas in the liquid (m^3/ hour), d is the diameter of the lift pipe (m), w is the gas velocity in the lift (m/ second).

For determination of gas-phase mass-transfer coefficients the system SO_2 – water was used [12, 19, 20] with corrections for the diffusional resistance of the liquid phase.

Finally the following expression was obtained:

$$Nu'_g = 0.024 \cdot Re_g^{1.08} \cdot (Pr'_g)^{1/3}, \quad (8)$$

where

$$Nu'_g = \frac{[p_b]_{av} \cdot K_g \cdot a \cdot d}{D_g \cdot \gamma_A} \cdot \sqrt{\frac{\sigma_L}{\gamma_L}},$$

σ_L is the coefficient of surface tension of the liquid, $[p_b]_{av}$ is the average partial pressure of the inert gas in the gas phase, and γ_A is the density of the absorbed component (in kg/ m^3).

Equation (8) is valid at h = 20%, t = 20°, Re_g = 768-5120.

The values given above for the partial and over-all mass-transfer coefficients were used in an attempt to determine H β for the chemical reaction in the liquid phase [21] in the absorption of nitrogen oxides by soda solutions.

The calculations were based on the equation

$$K_G \cdot a = \frac{1}{\frac{1}{K_g a} + \frac{1}{K_L a H \beta}}, \quad (9)$$

where H is the Henry constant and β is the chemical factor.

In particular, at h = 20%, t = 25°, V_g = 5-27 liters/ minute, L = 250-270 ml, H β = 0.4-0.8 $\left(\frac{kg \cdot m}{m^3 \cdot atmos}\right)$.

SUMMARY

1. In an investigation of absorption of nitrogen oxides by soda solutions in a gas-lift apparatus the effects of the concentrations of the nitrogen oxides and soda solution, gas and liquid rates, temperature, and immersion depth of the orifice were studied. The gas-lift apparatus gives rise to intensive absorption, but its hydraulic resistances are greater than in packed towers.

Calculations show that in absorption of nitrogen oxides at low concentrations, as in alkaline absorption in the nitric acid industry, the absorption volume required is decreased 100- to 150-fold while power consumption increases by about 50% in comparison with absorption in packed towers.

2. Equations for mass-transfer coefficients in the gas and liquid phases in the gas-lift apparatus are derived.

LITERATURE CITED

[1] V. I. Atroshchenko, J. Appl. Chem. 12, 2, 167 (1939); 25, 11, 1143 (1952); Ukrain. Chem. J. 10, 443 (1937).

[2] V. I. Atroshchenko and S. I. Kargin, Nitric Acid Technology [in Russian] (Goskhimizdat, 1949).

[3] S. Perel'man and L. Kantorovich, J. Chem. Ind. 6, 3 (1940).

[4] I. N. Kuz'minykh, E. P. Algina, and M. D.Babushkina, Chem. Ind. 8, 266 (1955).

[5] I. N. Kuz'minykh, Chem. Ind. 4 (1956).

[6] V. E. Gorfunkel' and Ya. I. Kil'man, Trans. State Inst. Nitrogen Ind. 5 (1956).

*Original Russian pagination. See C.B. Translation.

[7] N. M. Zhavoronkov et al., Chem. Ind. 7, 35 (1954).

[8] S. N. Ganz, J. Appl. Chem. 28, 2 (1955)*

[9] Proc. Conference of the Scientific Research Institute of Gas Purification on Removal of Nitrogen Oxides from Waste Gases [in Russian] (1957).

[10] M. E. Pozin, B. A. Kopylev, and G. V. Bel'chenko, Trans. Lensoviet Technol. Inst. Leningrad (1956).

[11] É. K. Lopatto, Claim for authors' certif. 399,573(June 6, 1949).

[12] A. G. Bol'shakov and G. O. Grigoryan, Sci. Mem. Odessa Polytech. Inst. 2, 1 (1955).

[13] Yu. N. Gasyuk, Candidate's Dissertation [in Russian] (Odessa Polytech. Inst., 1954).

[14] N. M. Zhavoronkov, Chem. Ind. 3 (1951); 4 (1953); 1 (1955).

[15] I. N. Kuz'minykh, Chem. Ind. 8 (1950).

[16] A. P. Groshev, Technical Analysis [in Russian] (Goskhimizdat, 1953).

[17] A. G. Kasatkin and I. N. Tsiparis, Chem. Ind. 7 (1952); M. E. Pozin, J. Appl. Chem. 3 (1947); 1 (1948).[USSR].

[18] A. G. Bol'shakov, Sci. Mem. Odessa Polytech. Inst. 2, 2 (1954).

[19] R. H. Haslam and R. L. Hershey, Ind. Eng. Chem. 16, 1224 (1924).

[20] J. C. Vivian and R. P. Whitney, Chem. Eng. Prog. 5, 323 (1949).

[21] V. M. Ramm, Absorption Processes in Chemical Industry [in Russian] (Goskhimizdat, 1951).

Received March 3, 1958

* See C.B. Translation.

THE VISCOSITY–TEMPERATURE RELATIONSHIP OF NITRIC ACID

G. L. Antipenko and E. S. Beletskaya

State Institute of Applied Chemistry

Some data on the viscosity of liquid nitric acid in the 0-75° range have been published in the literature [1-3]. The results of earlier determinations of the viscosity of liquid nitric acid and its aqueous solutions [5-8] are less accurate, and were therefore not used in the present investigation.

In the course of a systematic study of the physicochemical properties of the three-component system HNO_3-N_2O_4-H_2O it was necessary to study variations of the viscosity of liquid nitric acid with temperature over a wider temperature range than that reported in the literature. Apart from practical objects, the results of the experimental measurements were of theoretical interest for obtaining further information on the existence of ionic equilibria in nitric acid, which has now been demonstrated quite convincingly.

METHOD AND APPARATUS

The kinematic coefficient of viscosity was determined experimentally between −40 and +20° by the method described in GOST 33-46. The Ostwald viscosimeter was fitted with a device to prevent absorption of moisture from the surrounding air. Two viscosimeters were used in the determinations, with capillaries about 0.6 and 0.8 mm in diameter. The viscosimeter, filled with the solution under test, was placed in thermostat in which the temperature was maintained constant to the nearest ±0.05°. The efflux time of the volume of solution between the marks, measured to the nearest ±0.02 second by means of a seconds clock, was 60-100 seconds. At least five parallel determinations were carried out on each of the two tested samples of pure nitric acid. The average of these determinations was taken as the required value at the given temperature.

The main source of error in the viscosity determinations was the calibration of the viscosimeter. The kinematic viscosity ν was found from the relationship.

$$\nu = C \cdot t, \qquad (1)$$

where t is the efflux time (seconds).

The viscosimeter constant C was found from the viscosities of water, acetone, and absolute alcohol, taken from the literature [9], and from the experimentally determined efflux times at −40, −30, −20, −10, 0, 10, and 20°. The values found for the constant were smoothed graphically in C–t coordinates. The observed deviations from linearity did not exceed ±0.5%.

Nitric acid was prepared by fractional vacuum distillation of a mixture of concentrated nitric and sulfuric acids, followed by further distillation under vacuum. The substance so obtained contained traces of nitrogen oxides and water, as shown by an analytical check by the method developed by Markov [10].

The freezing point of the nitric acid prepared by this method was between −41.2 and −41.5°; the density at 0° was 1.5495 g/cc.

RESULTS

The experimental data on the kinematic viscosity and density of liquid nitric acid in the range of −40 to +20°. are presented in the table. The same table also gives the absolute viscosity of nitric acid, both calculated from the experimental data and reported in the literature.

Data on the density of nitric acid were reported by us earlier [11].

The experimental and literature data available were used in an attempt to determine the viscosity–temperature relationship for nitric acid between −40 and +50°. The graphical method with the use of the functional scale (F scale) [12, 13] was used. In construction of the F scale, literature data [9] on the viscosity of ethylene bromide were used as the standard data.

Kinematic Coefficient of Viscosity, Density, and Absolute Viscosity of Nitric Acid

Temperature (°C)	Kinematic viscosity ν (in centistokes)	Density (in g/cc)	Absolute viscosity η (in centipoises) from data of		
			this paper	Mason [3]	Bingham [1]
−40	1.707	1.6224	2.769	—	—
−30	1.276	1.6042	2.047	—	—
−20	1.008	1.5858	1.598	—	—
−10	0.832	1.5676	1.304	—	—
0	0.713	1.5492	1.105	1.092	1.094
10	0.621	1.5309	0.951	—	—
20	0.561	1.5126	0.849	—	—
25	—	—	—	0.746	0.750
40	—	—	—	0.617	—
50	—	—	—	—	0.602
75	—	—	—	—	0.398

The original data for construction of the F scale from the $\eta_{be} = f(t)$ relationship, and experimental and literature data on $\eta_{HNO_3} = f(t)$ are presented in Fig. 1. It is seen that the viscosity–temperature relationship for nitric acid in the range from −40 to +50°, plotted in a graph with a functional scale, is represented by a straight line, so that interpolation is possible to an accuracy of hundredths of a centipoise, at least.

The observed deviations of the experimental point (at 20°) and one point taken from the literature (at 50°) should be attributed to errors in direct determinations of viscosity.

DISCUSSION OF RESULTS

As much complete and sufficiently reliable data on the viscosity and density of nitric acid were available, it was desirable to attempt to obtain information on the influence of temperature on the equilibrium reactions in nitric acid.

It has been shown quite convincingly [14-16] that in nitric acid HNO_3 molecules are ionized, and probably exist predominantly in the form of solvated $(HNO_3)_2$:

$$(HNO_3)_2 \rightleftarrows NO_2^+ + NO_3^- + H_2O. \qquad (2)$$

According to literature data, the dgree of ionization of HNO_3 molecules is relatively high; it is about 3.4% at temperaturesclose to the freezing point [17].

Each of the ions and molecules appearing as the result of Reaction (2) is solvated by two molecules of nitric acid, for which about 10% more of the nitric acid molecules is required. There is reason to believe [3, 18, 19] that these solvation products are in equilibrium with their constituents. This assumption leads to

the conclusion that the sum total of the equilibrium reactions in nitric acid may be represented by the following over-all scheme:

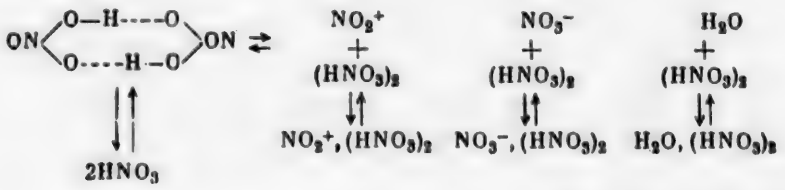

(3)

Change of temperature would evidently cause shifts in these equilibria, and it is therefore to be expected that the degree of association of nitric acid would be changed and there would be some degree of rearrangement

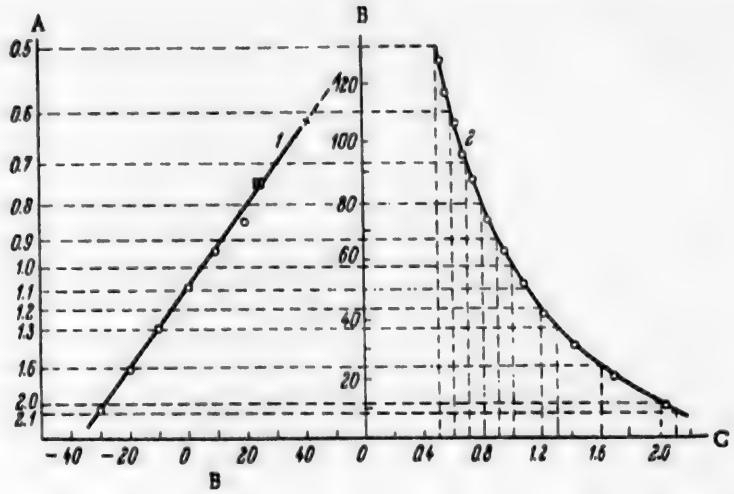

Fig. 1. Viscosity–temperature relationship of nitric acid: A) viscosity (centipoises), F scale, bromoethylene standard; B) temperature (°C); C) viscosity $\eta \cdot 10^3$ (centipoises); 1) nitric acid, 2) standard (bromoethylene).

in the structure of the liquid. Accordingly, for analysis of the effects of temperature on the viscosity and density of NHO_3, two well-known formulas derived by Bachinskii [20] were used:

$$\eta = \frac{A}{(t+\alpha)^3}, \tag{4}$$

$$\eta = \frac{C}{v - W}, \tag{5}$$

(where A and α are constants, C is the modulus of viscosity, v is the specific volume, and W is the limiting volume), together with the formula derived from Frenkel's theory [21]:

$$\eta = Ae^{\frac{U}{kT}}, \tag{6}$$

where A and U (activation energy) are certain functions of pressure and temperature.

When the first of these formulas was used in studies of the viscosity–temperature relationships of liquids was used it was discovered that for a number of substances the straight line in the graph shows a sharp break with

change of temperature. According to Bachinskii, the existence of such a break indicates that the structure of the liquid undergoes a change at the given temperature. Since the structure determines a number of physical properties of liquids, determination of this point for nitric acid was of undoubted interest.

Figure 2 is a plot of the viscosity–temperature relationship for nitric acid in accordance with this Bachinskii equation. It is seen that as the temperature increases from near the freezing point (at −40°) to 50°, there are several breaks on the fluidity–temperature line; namely, at −30, −10, and 25°.

If we accept Bachinskii's view that this course of the straight line is determined by changes in the structure of the liquid, then the observed points of inflection in this case should be interpreted as follows. At temperatures close to the freezing point the molecules of nitric acid are arranged in space in individual groups, and the structure of these groups is evidently very close to the structure of nitric acid in the solid state.

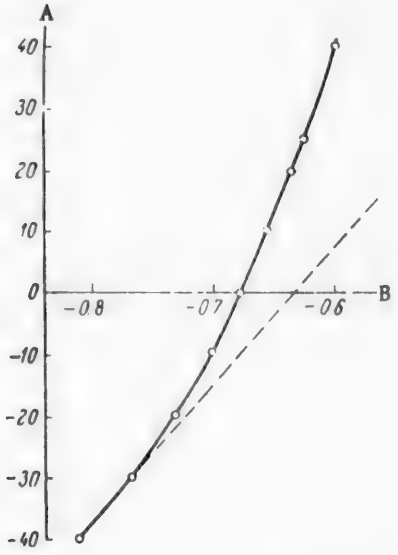

Fig. 2. $\log \sqrt[3]{\varphi} = f(t)$ relationship for nitric acid: A) temperature (°C), B) $\log \sqrt[3]{\varphi}$.

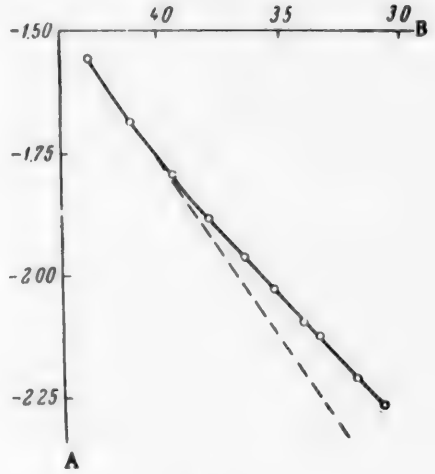

Fig. 3 $\log \eta = f\left(\frac{1}{T}\right)$ relationship for nitric acid: A) $\log \eta$, B) $\frac{1}{T} \cdot 10^3$.

It is known [22] that by the Maxwell distribution law a liquid at a given temperature consists of separate groups, most of which contain equal numbers of molecules of the substance. From this we may conclude that each break on the fluidity–temperature plot for nitric acid represents a change in the number of molecules in the individual groups. It is natural to assume that each of the molecules in an individual group vibrates at a definite frequency. Such a molecular complex can be stable only up to a definite temperature, above which the vibration energy becomes so large that the group disintegrates or a certain number of molecules becomes detached from it. On further increase of temperature a group with a smaller number of molecules becomes stable, etc.

In the light of Frenkel's concept of a liquid as a "damaged" crystal, we may conclude that in the case under consideration at the above-mentioned "characteristic" temperatures there should be a change in the activation energy of displacement of HNO_3 molecules from one state into another. To clarify this point, Fig. 3 shows the viscosity–temperature relationship for nitric acid in accordance with Formula (6). It is seen that in $\log\eta - \frac{1}{T}$ coordinates this relationship is represented by a straight line with breaks at the same temperature points as before, with the exception of the point corresponding to 25°. Figure 4 shows variations of the activation energy U with temperature, calculated from the $\log\eta - \frac{1}{T}$ graph.

In the light of the foregoing considerations it can be assumed with a high degree of probability that increase of temperature results in an abrupt change of the number of molecules in the "damaged" crystals present in nitric acid. This picture of the changes in the structure of liquid nitric acid with temperature is very much simplified, as it does not take into account the influence of temperature shifts of the equilibria represented in the over-all scheme given above. Evidently, such shifts must also have some sort of influence on the structure of the solution, and therefore on its viscosity.

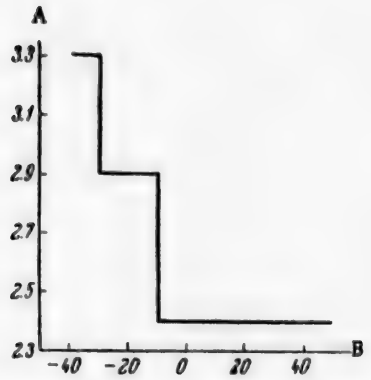

Fig. 4. Effect of temperature on the activation energy of displacement of HNO_3 molecules from one equilibrium state into another: A) activation energy U (cal/ mole), B) temperature (°C).

The influence of the temperature shift in the equilibrium reactions on the viscosity of liquid nitric acid can be estimated, in the first approximation, from the variations of viscosity and density with temperature, plotted in Fig. 5. The first of these relationships corresponds to Formula (5), which, as is known, gives a linear plot in fluidity–specific volume coordinates in the case of nonassociated liquids. In the present instance this relationship for nitric acid is represented by a curve, which increasingly deviates from a straight line with rise of temperature. The observed increase of fluidity must be attributed to shifts in the equilibrium reactions, represented above in the form of an over-all scheme, toward decomposition of the solvation products, which is quite probable.

Consideration of the V = f(t) curve leads to a similar conclusion. For approximately the same temperature (−10°) the increase of specific volume is represented by a curve which deviates increasingly from linearity with increase of temperature (dash line, Fig. 5). This accelera-

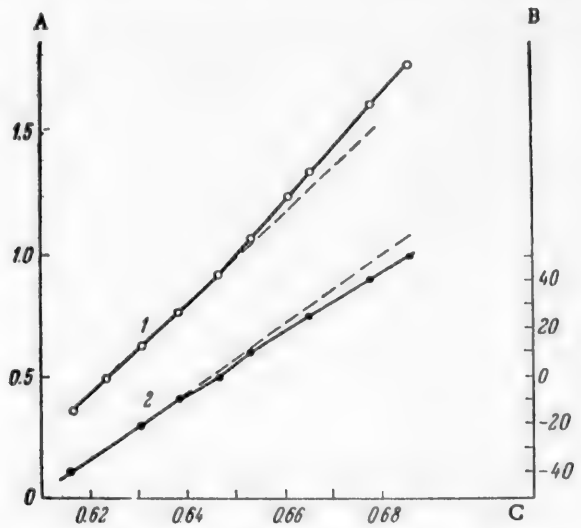

Fig. 5. Fluidity and specific volume of nitric acid at various temperatures: A) fluidity $\varphi \cdot 10^2$, B) temperature (°C), C) specific volume V (in cc / g); 1) $\varphi = f(V)$, 2) $V = f(t)$.

tion of the rate of increase of the specific volume of nitric acid is probably due to an increase in the number of free molecules in the liquid. Hence, the earlier conclusion, based on viscosity data, concerning the influence of temperature on the equilibrium reactions in nitric acid is consistent with the conclusion drawn from a consideration of the density-temperature relationship.

LITERATURE CITED

[1] E. C. Bingham and S. B. Stone, J. Phys. Chem. 27, 701 (1923).

[2] F. H. Rhodes and H. B. Hodge, Ind. Eng. Chem. 21, 142 (1929).

[3] D. M. Mason, J. Petker, and S. P. Vango, J. Phys. Chem. 59, 511 (1955).

[4] D. Schofield, Bull. Chem. Soc. (Peru), 6, 7 (1935).

[5] F. W. Küster and R. Kremman, Z. anorg. Chem. 41, 1 (1904).

[6] M. C. Chevenceau, Comp. rend., 155, 154 (1912).

[7] M. le D'Poiseuille, Ann. chim. phys. 21, 76 (1847).

[8] W. R. Bousfield, J. Chem. Soc., 107, II, 1781 (1915).

[9] Technical Encyclopedia, Handbook of Physical, Chemical, and Technical Data [in Russian] (Moscow, 1931).

[10] E. V. Valikova and S. S. Markov, Scientific-Technical Instruction, State Inst. Applied Chemistry [in Russian] 6 (1958).

[11] G. L. Antipenko, E. S. Beletskaya, and A. G. Krylova, J. Appl. Chem. 31, 6, 859 (1958).*

[12] E. P. Irany, J. Amer. Chem. Soc. 60, 2106 (1938); 61, 1734 (1939).

[13] V. T. Slavyanskii, J. Phys. Chem. 27, 12, 1776 (1953).

[14] C. K. Ingold and D. J. Millen, J. Chem. Soc. 2612 (1950).

[15] J. Chedin Ann. chim. 8, 243 (1937); J. Phys. Radium 10, 945 (1939); J. Chim. Phys. 49, 109 (1952).

[16] J. Chedin and D. Pradier, Compt. rend. 203, 772 (1936).

[17] R. J. Gillespie, E. D. Hughes, and C. K. Ingold, J. Chem. Soc. 2552 (1950).

[18] J. Chedin and V. Vandoni, Compt. rend. 227, 1232 (1948).

[19] G. L. Wilson and F. D. Miles, Trans. Farad. Soc. 36, 356 (1940).

[20] A. I. Bachinskii, "Some prospects in the science of liquid viscosity," paper presented at the Conference on Liquid Viscosity, II, p. 104 [in Russian] (Izd. AN. SSSR, 1944).

[21] Ya. I. Frenkel', "Relationship between various theories of the viscosity of liquids," paper presented at the Conference on Liquid Viscosity, II, p. 24 [in Russian] (Izd. AN SSSR, 1944).

[22] E. Baum, Kolloid-Zeitung, 135, 3, 176 (1954).

Received July 12, 1958

*Original Russian pagination. See C.B. Translation.

STUDY OF THE MECHANISM AND KINETICS OF THE OXIDATION OF THE SULFIDE BY ATMOSPHERIC OXYGEN

D. N. Klushin and O. V. Nadinskaya

It was shown in earlier investigations [1-3] of a process for extraction of tin from lean ores that conversion of the tin to sulfide and sublimation in that form is the most promising method for processing of raw materials of this type.

The present paper is concerned with a study of the mechanism and kinetics of oxidation of SnS by atmospheric oxygen and determination of the process conditions, lacking in the literature, for conversion of sulfide sublimates in order to obtain a product (stannic oxide) suitable for subsequent treatment by the existing standard pyrometallurgical process.

EXPERIMENTAL

An apparatus in which a constant pressure was automatically maintained in the system, with continuous gas circulation, was used for studies of the mechanism and kinetics of the oxidation of tin sulfide in air and pure oxygen. The apparatus is shown schematically in Fig. 1.

The gas was circulated by means of a circulating pump with an electromagnetic coil. The sulfur dioxide liberated during the reaction, the amount of which was a measure of the extent of the reaction, was absorbed in a system of absorption flasks. This system consisted of five rows of paired flasks connected in parallel. The exit gases could be directed into either row by a system of stopcocks. With the aid of this absorption system it was possible to perform determinations and estimate the reaction rate at any time intervals.

The pressure was maintained constant in the system by the following principle: the pressure changes in the system due to absorption of sulfur dioxide in the absorption flasks are transmitted to the electromagnetic coil of the circulating pump; this varies the rate of oscillation of the core in accordance with pressure variations in the system, resulting in greater or lesser rarefaction in the tube through which oxygen or air is drawn into the system. The circuit diagram of the pressure regulator is shown in Fig. 2.

The amount of air of oxygen passed during an experiment was recorded by means of a gas meter of the GSB type with 0.02 dm^3 scale divisions.

Pure oxygen was further purified by means of platinized asbestos (heated to 350°), "askarit"*, and phosphorus pentoxide.

The experiments were performed as follows: a 1.5 g weighed sample in tin sulfide was placed in a corundum crucible previously heated to constant weight and weighed. The crucible with the sample was placed in a reaction tube. When the furnace temperature was 50° above the required level, the furnace was moved onto the reaction tube, and the instant at which the required temperature was reached was taken as the start of the experiment.

The furnace temperature, maintained to an accuracy of ±5°, was measured by means of a platinum–platinum/rhodium thermocouple and an electronic potentiometer.

* Asbestos impregnated with KOH and calcined – Translator's note.

In studies of the oxidation of tin sulfide in pure oxygen the whole system was rinsed out with pure oxygen before the experiments.

At the end of an experiment the furnace was moved off the reaction tube, and the latter was cooled in a current of oxygen or air. The cooled crucible was weighed, and the cinder was analyzed for tin compounds by x-ray structural, mineralogical, and phase analysis.

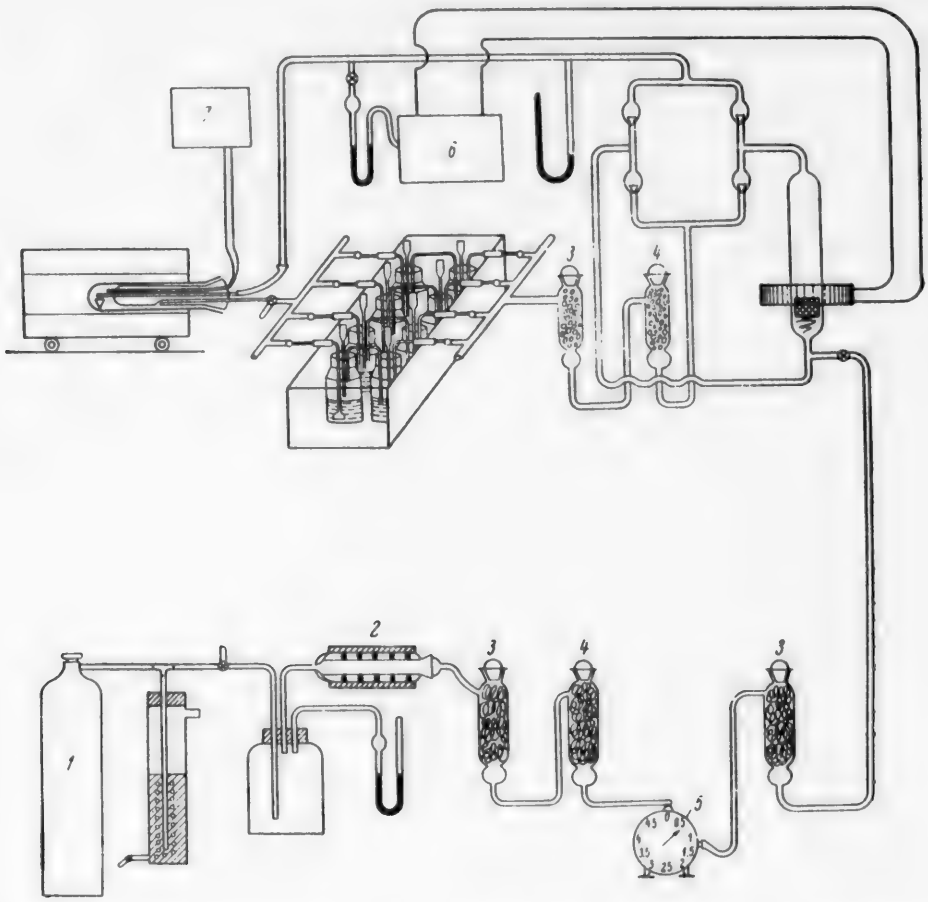

Fig. 1. Apparatus for investigation of the reaction $SnS + O_2$: 1) oxygen, 2) platinized asbestos, 3) askarit, 4) P_2O_5, 5) gas meter, 6) apparatus for automatic pressure regulation, 7) potentiometer.

Oxidation of Tin Sulfide by Atmospheric Oxygen

The experiments were performed at 600, 700, 800, 900 and 1000°, for times of 15, 30, 60, and 120 minutes, with 1.5 g samples containing 1.173 g of tin and 0.327 g of sulfur.

The results of the experiments are presented in Tables 1 and 2 and in Figs. 3-5.

It follows from the data in Tables 1 and 2 and Fig. 3 that the weight of the sample changes during oxidation of tin sulfide by atmospheric oxygen; in the 600-770° range it increases, reaching 103.5% of the initial weight at 600°, while above 770° there is a weight decrease, which reaches 7.7% at 1000° in an experiment lasting 120 minutes. The weight increase at low temperatures is caused by formation of lead sulfate, and the loss at higher temperature by volatilization, mainly of lead sulfide.

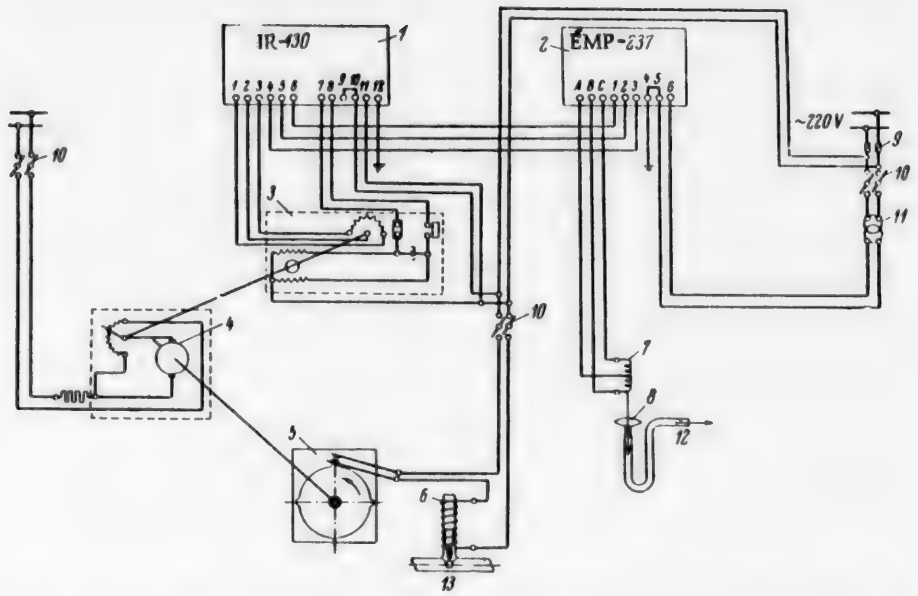

Fig. 2. Electric circuit of the pressure regulator: 1) proportional integral regulator, 2) electronic bridge, 3) actuating mechanism, 4) direct-current micromotor, 5) breaker, 6) solenoid valve, 7) induction coil, 8) corrugated membrane, 9) PR-1 fuse, 10) package switch, 11) stepdown transformer, 12) lead to gas line, 13) gas line.

TABLE 1

Weight Changes and Total Tin Contents of Cinders at Different Temperatures and Experimental Times

Temperature (°C)	Duration (min)	Wt. of sample (g)	Wt. change (%)	Total tin content of cinder	
				in %	in g
600	60	1.555	+3.7	75.0	1.17
	120	1.550	+3.5	—	1.17
700	60	1.525	+1.5	—	—
	120	1.508	+0.5	79.3	1.19
800	15	1.498	−0.7	76.8	1.15
	30	1.487	−0.8	78.5	1.17
	60	1.491	−0.6	30.0	1.19
	120	1.494	−0.3	79.0	1.18
900	15	1.484	−1.0	74.8	1.11
	30	1.493	−0.5	78.5	1.17
	60	1.471	−1.9	79.3	1.17
	120	1.451	−3.2	78.5	1.14
1000	15	1.459	−2.7	78.2	1.14
	30	1.418	−5.5	78.5	1.11
	60	1.408	−6.2	79.0	1.11
	120	1.384	−7.7	79.3	1.10

The data in Table 2 and Fig. 4 show that the tin sulfide content of the cinder decreases and the tin oxide content increases with rise of temperature and increased duration of the experiment. The tin sulfate content decreases with rise of temperature.

Mineralogical and x-ray structural analyses of the cinders showed that they contain SnS, Sn_2S_3, SnS_2, Sn_{met}, SnO_2, $SnSO_4$. The quantitative proportions of these components vary with the temperature and duration of the experiment. Thus, at 900 and 1000° in experiments of 15 minutes the cinders contain SnS, Sn_2S_3 and

TABLE 2

Changes in the Phase Composition of the Cinders in Oxidation of Tin Sulfide by Atmospheric Oxygen

Temperature (°C)	Duration (min)	Composition of cinder								Discrepancy (%)
		Sn_{met}		$SnSO_4$		SnS, Sn_2S_3, SnS_2		SnO_2		
		in g	in %	in g	in %	in g	in %	in g	in %	
600	60	0.1	0.6	0.177	7.5	0.25	16.0	1.17	75.2	—0.7
	120	0.009	0.6	0.216	1.7	0.10	6.4	1.36	87.7	—3.6
700	120	0.009	0.6	—	—	0.014	0.9	1.49	97.7	—0.8
800	15	0.006	0.5	—	—	1.08	71.6	0.37	24.5	—3.6
	30	0.005	0.3	—	—	0.604	40.3	0.73	52.1	—7.3
	60	0.01	0.7	—	—	0.629	42.3	0.81	54.5	—2.5
	120	0.01	0.7	—	—	0.01	0.7	1.41	94.4	—5.2
900	15	0.008	0.5	—	—	1.0	67.4	0.37	24.9	—8.2
	30	0.008	0.5	—	—	0.477	31.9	0.95	63.6	—4.0
	60	0.016	1.08	—	—	0.037	2.5	1.34	91.1	—5.3
	120	0.008	0.5	—	—	0.021	1.4	1.43	98.5	+0.4
1000	15	0.007	0.5	—	—	0.668	45.8	0.67	45.9	—7.8
	30	0.01	0.7	—	—	0.148	10.4	1.2	84.6	—4.3
	60	0.008	0.6	—	—	0.028	1.9	1.31	93.0	—4.5
	120	0.007	0.5	—	—	0.013	0.9	1.28	92.5	—6.1

SnO_2, whereas at the same temperatures in experiments of 60 and 120 minutes the main constitutent is SnO_2, with a small amount of SnS; there is no Sn_2S_3.

With increasing duration of the experiments the tin oxide formed passes from the amorphous to the crystalline state.

The results of mineralogical analysis of cinders formed at 800-1000° in 15-minute experiments shows that they contain amorphous SnO_2; in experiments lasting 120 minutes at the same temperature, SnO_2 is present in a crystalline form in the cinders.

The micrograph of a polished section of the cinder (Fig. 5) formed by oxidation of tin sulfide by atmospheric oxygen at 600° in 60 minutes gives a fairly full idea of the mechanism of oxidation of tin sulfide by oxygen.

The photograph (Fig. 5) shows that the grains of the original tin sulfide, situated in the center, are surrounded by grains of tin sesquisulfide (Sn_2S_3), while at the SnS–Sn_2S_3 boundary there is metallic tin, evidently formed in the reaction

$$3SnS = Sn_2S_3 + Sn.$$

Beyond the band formed by the Sn_2S_3 grain there are grains of SnS_2, and at the boundary between them microscopic examination reveals metallic tin (not recorded in the microphotograph) which under these conditions is evidently formed in the reaction

$$2Sn_2S_3 = 3SnS_2 + Sn.$$

The tin disulfide edges are surrounded by the crystals of tin oxide. The absence of a tin phase in the micrograph is due to the fact that tin sulfate is leached out during preparation of the section.

Thus, the results of mineralogical, phase, and x-ray structural analysis indicate that the mechanism of oxidation of tin sulfide by oxygen can be represented as follows.

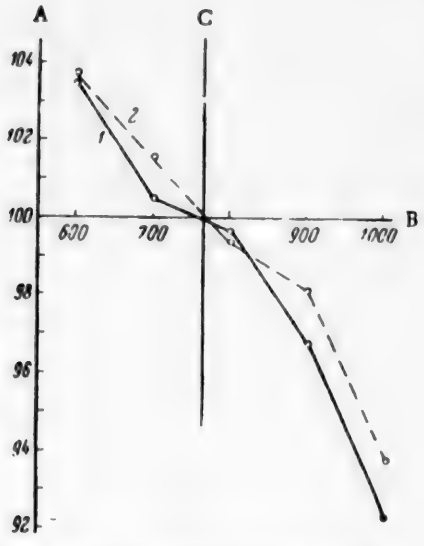

Fig. 3. Effect of temperature on the weight of the cinder: A) change of weight (of % of the original sample), B) temperature, C) decomposition of tin sulfate; duration of experiment (minutes): 1) 120, 2) 60

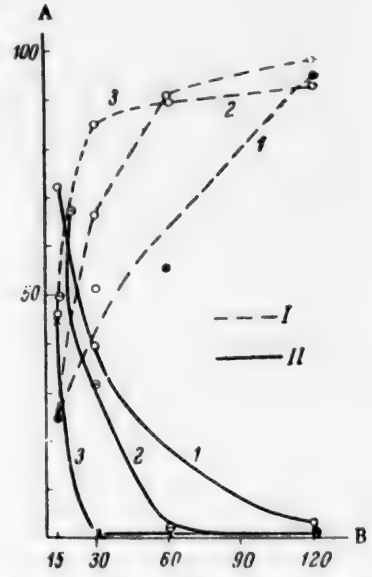

Fig. 4. Effect of the duration of the experiment on the contents of a mixture of tin sulfide and tin oxide in the cinder: A) contents of $SnSO_3$, SnS in the cinder (%), B) duration of experiment (minutes); temperature (°C): 1) 800, 2) 900, 3) 1000. I) SnO_2, II) SnS.

At low temperatures (up to 800°)

$$3SnS = Sn_2S_3 + Sn,$$
$$2Sn_2S_3 = 3SnS_2 + Sn,$$
$$2SnS_2 + 6O_2 = SnSO_4 + SnO_2 + 3SO_2.$$

At high temperatures (above 800°)

$$3SnS = Sn_2S_3 + Sn,$$
$$2Sn_2S_3 = 3SnS_2 = Sn,$$
$$3SnS_2 + 3O_2 = SnO_2 + 2SO_2.$$

Figures 6-9 show the degrees and nominal rates of oxidation of tin sulfide by atmospheric oxygen.

Figure 6 shows that the degree of oxidation of tin sulfide by atmospheric oxygen increases smoothly with duration and temperature of the experiment.

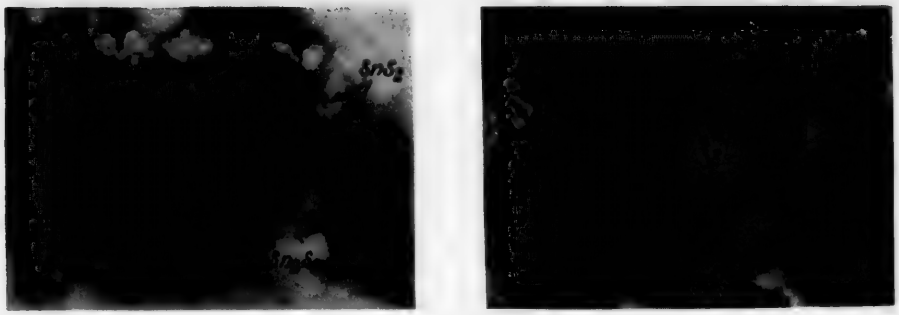

Fig. 5. Microphotograph of a polished section of the cinder.

Because of the very complex oxidation mechanism, the nominal rate of oxidation of tin sulfide was calculated, not referred to unit surface area. It is clear from Fig. 7 that the nominal rate increases with temperature and has two maxima; it is also seen in Fig. 7 that the maxima occur earlier with increase of temperature.

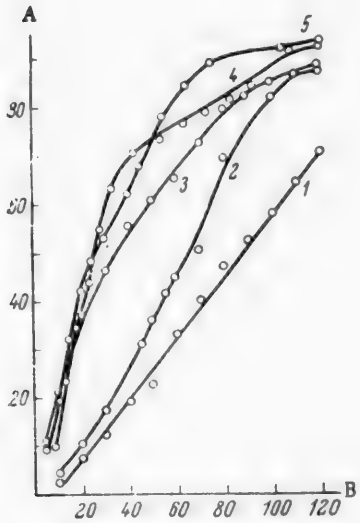

Fig. 6. Variation of the degree of oxidation of tin sulfide by atmospheric oxygen with the duration of the experiment: A) degree of oxidation (%), B) duration of experiment (minutes); temperature (°C): 1) 600, 2) 700, 3) 800, 4) 900, 5) 1000.

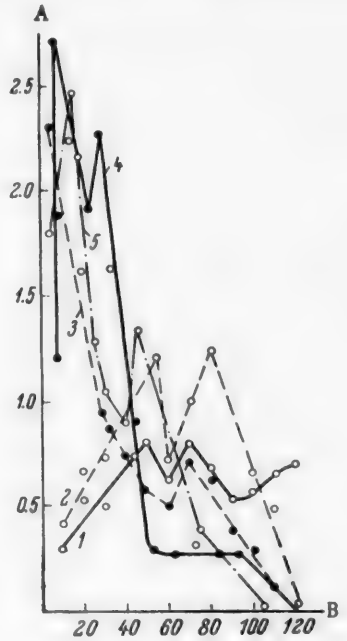

Fig. 7. Variation of the nominal rate of oxidation of tin sulfide by atmospheric oxygen with the duration of the experiment: A) nominal rate of oxidation (degree of oxidation/ minute), B) duration of experiment (minutes); temperature (°C): 1) 600, 2) 700, 3) 800, 4) 900, 5) 1000.

For example, at 600° the first maximum is reached after 50 minutes, whereas at 900° it is reached after 8 minutes.

The curves for the variation of the nominal rate of oxidation of tin sulfide with temperature in Fig. 8 show that when the temperature is increased in the 600-1000° range the oxidation rate is at a maximum at 900°.

This effect is evidently the result of a definite regrouping of the atoms and changes of bond strengths between the molecules at that temperature, leading to an increase of the reactivity of the compound

A connection has been established [4, 5] between changes of the electrical properties of metals, alloys, sulfides, oxides, and other compounds and the atomic states and variations in the bond forces between the atoms.

Kochnev [6, 7] has shown that changes of the physical constants and physical and chemical properties of substances (heat capacity, vapor pressure, rates of oxidation and reduction) at definite temperatures correspond to changes of electrical conductivity of these substances at the same temperatures.

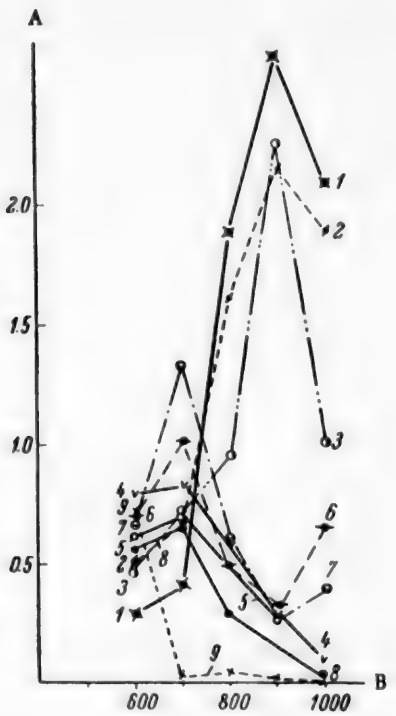

Fig. 8. Variation of the nominal rate of oxidation of tin sulfide with the temperature: A) nominal oxidation rate (degree of oxidation/ minute), B) temperature (°C); duration of experiments (minutes): 1) 10, 2) 20, 3) 30, 4) 50, 5) 60, 6) 70, 7) 80, 8) 100, 9) 120.

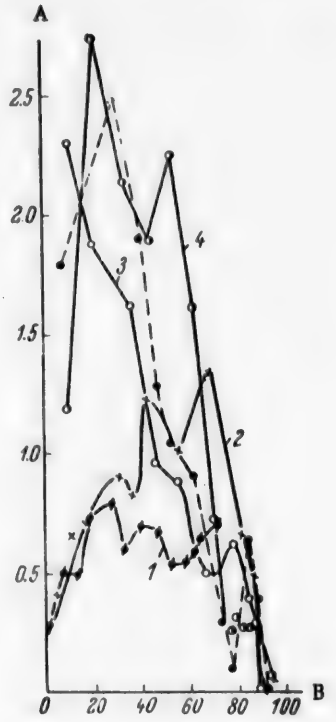

Fig. 9. Variation of the nominal rate of oxidation of tin sulfide with the degree of oxidation: A) nominal oxidation rate (degree of oxidation/minute), B) degree of oxidation (%); temperature (°C); 1) 600, 2) 700, 3) 800, 4) 900.

Our investigation* of the electrical resistance of tin sulfide in the 600-950° range (Fig. 10) confirms these results [4, 5] and shows that at 900° the value of the resistance through a transient maximum and minimum.

This sharp change in the resistance of tin sulfide at 900° corresponds to a sharp increase in its oxidation rate which, as noted earlier (Fig. 8) also occurs at 900°.

The logarithms of the average rates of oxidation of tin sulfide by atmospheric oxygen over a period of 20 minutes at various temperatures, calculated from the data in Fig. 8, are given below.

* This investigation was performed by A. I. Bershak at our request.

Temperature (°C)	600	700	800	900	1000
log V	−0.2924	−0.1739	+0.2068	+0.2788	+0.2788

These data show that at about 800° there is a change in the direction of the curve, corresponding to a change in the reaction order and in its mechanism. Hence it may be concluded that up to 800° the reaction of oxidation of tin sulfide by atmospheric oxygen is in the kinetic region, when its rate depends mainly on the temperature. With increase of temperature the reaction of oxidation of tin sulfide passes into a region intermediate between the kinetic and diffusional regions, when its rate depends on the temperature and on the gas velocity.

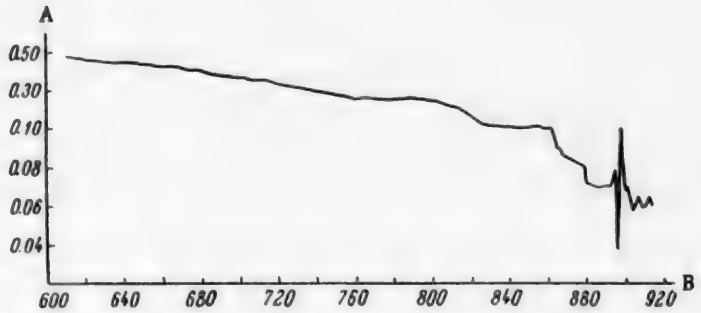

Fig. 10. Variation of the resistance of SnS with temperature: A) resistance (in ohms), B) temperature (°C).

The apparent activation energy can be calculated from the Arrhenius equation.

$$\log K = \ln Z - \frac{E}{RT}.$$

Disregarding small variations of Z and E with temperature, we have

$$\log K = B - \frac{E}{RT},$$

or

$$\log K = B - \frac{A}{T},$$

where

$$B = \ln Z, \qquad A = \frac{E}{2.3R} = \frac{E}{4.575},$$

E is the activation energy, $\log K = B - \frac{A}{T}$ is linear equation in $\log K - \frac{1}{T}$ coordinates, A is the tangent of the angle formed with the abscissa axis.

The calculated apparent activation energy (E) is 106.1 kcal/mole for the kinetic region, and 28.8 kcal/mole for the intermediate region.

SUMMARY

1. Investigation of the oxidation of tin sulfide by atmospheric oxygen in 600-1000° temperature range shows that the oxidation rate of tin sulfide is higher at 900° than at, say, 950 and 1000°.

This anomalous effect is explained, in accordance with available literature data, by changes taking place at 900° in electronic structure of the atoms and bond strengths between the molecules, increasing the reactivity of the substance. This fact must be taken into account when the production process conditions are finally established.

2. The activation energy of the reaction of oxidation of tin sulfide by oxygen has been determined; its values is 106.1 kcal/mole for the intermediate region at 800-1000°.

LITERATURE CITED

[1] D. N. Klushin and O. V. Nadinskaya, J. Appl. Chem. 29, 10, 1493 (1956).*

[2] D. N. Klushin, O. V. Nadinskaya, and K. G. Bogatina, Concentration and Metallurgy of Nonferrous Metals, Coll. Trans. State Sci. Res. Inst. Nonferrous Metals [in Russian] 13, (Metallurgy Press, Moscow, 1957) p. 211.

[3] D. N. Klushin and A. A. Benuni, Bull. Central Sci. Res. Inst. of Nonferrous Metals 11 (1958).

[4] A. F. Ioffe, Jubilee Volume of the Academy of Sciences USSR [in Russian] 1 (1947) p. 305.

[5] I. V. Mochan, J. Tech. Phys. 18, 812 (1948).

[6] M. I. Kochnev, Proc. Acad. Sci. USSR 105, No. 6, 1237 (1955).

[7] M. I. Kochnev, J. Appl. Chem. 21, 12, 1210 (1948).

Received March 1, 1958

* Original Russian pagination. See C.B. Translation.

HYDROGENATION OVER NICKEL CATALYSTS PREPARED BY DECOMPOSITION OF OXALATES

I. B. Rapoport and Yu. V. Vysheslavtsev

Sabatier and Senderens [1] hydrogenated benzene over a nickel catalyst for the first time in 1901. Hydrogenation commences at 70°, and the reaction rate increases with rise of temperature up to 170-200°. Further rise of temperature slows down the hydrogenation reaction. Nickel catalyst prepared by the method of Sabatier and Senderens loses its activity fairly rapidly and at temperatures above 200° causes decomposition of benzene.

According to Zelinskii and Turova-Polyak [2], a nickel catalyst precipitated by carbonates in accordance with the support used catalyzes hydrogenation of benzene to cyclohexane even at about 100°. Taylor and Douherty [3] showed that a nickel catalyst deposited on kieselguhr (containing 11% Ni) has good activity.

Shuikin, Minachev, and Feofanova [4] studied the hydrogenation properties of nickel catalysts containing from 12 to 20% Ni, deposited on various supports.

Finally, mention must be made of the work of Rubinshtein, Novikov, Lapshin, and Shuikin [5] who used nickel in the form of nickel formate deposited on activated carbon for hydrogenation. According to their data, benzene is hydrogenated completely over this catalyst at a low space velocity, namely 0.06 liter/ liter · hour^{-1}.

The next group of nickel-containing hydrogenation catalysts comprises alloy catalysts.

In 1924 Raney published a method for preparation of an active nickel catalyst by leaching of silicon from an alloy by means of aqueous alkali.

Further investigations of alloys showed that a nickel–aluminum alloy is more suitable.

The Raney method, modified by Covert and Adkins [6], involves a stage of prolonged heating at 115°.

Pattison and Degering [6] prepared a Raney-type catalyst from an alloy of nickel and magnesium, dissolving out the latter in acetic acid. An active catalyst was obtained. The most active catalyst of the Raney type was prepared by Adkins and Billica.

Dupont and Piganiol, in an x-ray study of the structure of leached alloy catalyst, found that the dimensions of the nickel particles are in the 40-80 A range, or one tenth of those in nickel made by the method of Sabatier and Senderens.

I. B. Rapoport jointly with Sil'chenko, and later with B. M. Rapoport [7, 8] studied the influence of various factors such as pressure, particle size, and degree of leaching of the catalyst on the activity of Raney-type catalysts in hydrogenation of various compounds.

They also tested various alloy catalysts and showed that Co–Si catalyst is inferior in activity to Co–Al catalyst.

Rapoport [9] studied the hydrogenation of various compounds over leached and alloy catalysts in a current of hydrogen at atmospheric pressure at 190-195°.

Several publications have recently appeared dealing with studies of catalysts prepared by decomposition and reduction of mixed crystals or salts of organic acids. The general method for preparation of mixed catalysts

so far prepared is as follows: a solution of salts of several metals is mixed with ammonia, alkali, or soda, and the resultant mixtures of hydroxides or carbonates are subjected to further treatment. Generally, the gel particles or crystalline particles of the components are situated side by side. Reduction of these particles yields a coarsely-dispersed metallic catalyst. More finely-divided metallic catalysts may be prepared by reduction of mixed salts of a noble and a base metal. In such a catalyst the noble-metal ions are at large distances apart, as they are separated by extraneous ions [10].

According to Langenbeek and Giller [10], magnesium was used as the base metal because Ni and Mg have the same ionic radius (0.78 A). Catalysts containing 8.2 and 16.2% Ni are considerably more active than Raney catalyst.

Langenbeek, Dreyer, and Vehring [11] prepared a highly-active catalyst by decomposition of mixed nickel and magnesium oxalates. They precipitated the oxalates from an aqueous solution of the nitrates by oxalic acid solution at 50°. The catalyst was reduced in a current of hydrogen at 350° for 4 hours. Nickel oxalate decomposes under these conditions with formation of metallic nickel, while magnesium oxalate decomposes at a higher temperature.

The catalyst so prepared hydrogenated cyclohexene at room temperature and was 5 times as active as Raney catalyst.

Danes and Jiru [12] described a mixed catalyst (Ni/ MgO) prepared by decomposition of the corresponding oxalates under a high vacuum at 430°. This catalyst contains 24.4% nickel. The activity of the catalyst was determined from the degree of hydrogenation of benzene to cyclohexane at atmospheric pressure. The degree of hydrogenation of benzene to cyclohexane was 22.7% at 26.2°, and 93% at 54°.

Cabicar, Gubner, and Klier [13] reported the preparation of an active catalyst by deposition of nickel oxalate on kieselguhr followed by reduction at 320°. Danes et al. [14] prepared highly active catalysts by decomposition of oxalates under a high vacuum. Langenbeek [15] gives more detailed information on some aspects of the development and use of mixed catalysts. Langenbeek's catalyst is nearly 5 times as active as Raney catalyst.

Rinacker, Birrenstaedt, and Tachel [16] published data on the specific surface and activity of a Ni/ MgO catalyst prepared from the formate and oxalate, in relation to the reduction temperature. The results show that catalysts made from oxalates have considerably greater surface area than catalysts made from formates. The specific activity of the catalysts decreases with increase of reduction temperature.

It follows from this brief survey of the literature that catalysts made from mixed salts with organic anions are not inferior in properties to catalysts used up to now, and in some cases are even better.

The publications cited above do not deal with a number of aspects which, in our opinion, must be considered for a deeper study of the properties of these catalysts. The present investigation is an attempt to fill some of the gaps in this very interesting field.

EXPERIMENTAL

Starting materials and catalysts. The starting materials for catalyst preparation were salts of the chemically-pure grade. The catalysts were prepared by precipitation, by saturation with subsequent precipitation, and by mixing.

Catalyst preparation by the precipitation method. The catalyst was prepared by precipitation from a mixture of nickel and magnesium nitrates by ammonium oxalate at 50°, with vigorous stirring. The powdered support was introduced into the precipitate stirred by a high-speed electric stirrer. The mixture was stirred for some time, after which the precipitate was filtered off and washed with warm distilled water to a negative reaction for NO_3. The precipitate was dried in a drying cabinet at 120-140°, powdered, and mixed into a doughlike mass with addition of 1% starch solution; the doughlike mass was pressed through a sieve of 1.5-2.0 mm mesh. The pieces were dried in a drying oven at 120-140°.

Catalyst preparation by the saturation method with subsequent precipitation. The support was ground down to 3-4 mm grains and added to a solution of nickel and magnesium nitrates. It was left in the solution for 24 hours. The solution was then evaporated to dryness on a water bath and the residue was dried in a drying oven at 120-140°.

The support, saturated with nickel and magnesium nitrates, was immersed in a heated saturated solution of ammonium oxalate. The solution was evaporated to dryness on a water bath. The catalyst was dried in a drying oven at 120-140°, and then washed with warm distilled water to a negative reaction for NO_3 and dried in a drying oven at 120-140°.

When the catalysts were pared by the first and second method part of the nickel went into solution during the washing. For accurate determination of the losses of nickel these solutions were analyzed and a correction applied to the catalyst composition.

Catalyst preparation by the mixing method. The oxalates were mixed mechanically in a porcelain mortar. 1% starch solution was added to the mixture until a doughlike mass was obtained, which was then pressed through a sieve of 1.5-2 mm mesh. The pieces were dried in a drying oven at 120-140°

Experimental conditions. The experiments were performed in an apparatus of the flow type in the 60-200° temperature range. The activity of the catalyst was estimated from the degree of conversion of benzene to cyclohexane at a definite temperature. The benzene used for the experiments was free from thiophene; b.p. 80-81°; ρ_4^{20} 0.879, $n^{20}D$ 1.5020.

The degree of hydrogenation was determined from the refractive index measured in an Abbe refractometer. In some cases the product was investigated in greater detail.

RESULTS AND DISCUSSION

Effects of different supports on the activity of Ni/ MgO catalyst in hydrogenation of benzene were studied with catalyst samples made by the precipitation method with subsequent addition of the support. The catalyst usually contained Ni ~ 46% , MgO 6%, support ~48%. The supports used were alumina, kieselguhr, asbestos, and pumice, previously finely powdered.

The catalysts were reduced in 50 ml lots by hydrogen at 450°.

Determinations of the activity of different catalyst samples were carried out in a current of hydrogen at 200° at space velocities from 1.5 to 1.9 vol/ vol. catalyst · hour, and at 140° at space velocities from 0.76 to 0.97.

TABLE 1

Effects of Different Supports on the Activity of Ni–MgO Catalysts Prepared From the Metal Oxalates. (Catalyst composition: Ni ~46%, MgO ~ 6%, support ~48%; reduction time 4 hours, hydrogen space velocity 1000-2000 vol./ vol.catalyst · hour)

Support	Volume of catalyst after reduction (ml)	Hydrogenation temperature (°C)			
		140		200	
		space velocity	contents of C_6H_{12} (%)	space velocity	contents of C_6H_{12} (%)
Al_2O_3	29.4	0.76	77	1.52	44
Kieselguhr	40.4	0.96	66	1.92	38
Asbestos	41.0	0.97	38.5	1.94	27
Pumice	25.5	0.80	23	1.48	14
Silica gel	26.1	0.80	60	1.60	15

The results in Table 1 show that the catalyst deposited on powdered alumina is the most active. Catalyst deposited on pumice has the lowest activity. The catalyst deposited on kieselguhr is exceptional; at 140° its activity approaches that of the catalyst deposited on alumina.

The influence of temperature on the degree of hydrogenation of benzene over Ni–MgO–Al_2O_3 catalyst is clear from the data in Table 2. The greatest degree of conversion of benzene into cyclohexane is observed at 140°; at higher or lower temperatures the degree of hydrogenation is less.

Effect of the decomposition and reduction temperature on catalyst activity. It follows from the data in Table 3 that the optimum reduction temperature for this catalyst is 350°. The catalyst activity is lowered somewhat if the reduction temperature is lowered to 250° or raised to 400-450°; this is especially clear from the data for hydrogenation of benzene to cyclohexane at 60°.

Tests of a catalyst prepared by saturation of aluminum oxide with solutions of nickel and magnesium nitrates with subsequent precipitation by ammonium oxalate. A distinctive feature of this catalyst is the low contents of nickel and magnesium oxides, namely: Ni ~ 6%, MgO ~1% and Al_2O_3 93%. Its activity was compared with that of a catalyst made by the precipitation method.

TABLE 2

Effect of Temperature on the Degree of Hydrogenation of Benzene to Cyclohexane (Catalyst reduced at 450°, reduction time 4 hours)

Hydrogenation temperature (°C)	Contents of C_6H_{12} (in %) at space velocity (vol./vol·catalyst·hour)	
	1.5	0.75
200	44	—
140	59	74
100	52	72
65	27	—
60	—	19
50	5	—

TABLE 3

Effects of Decomposition and Reduction Temperatures on Catalyst Activity (Reduction time 4 hours, space velocity in reduction 1000-2000 vol./ vol.catalyst · hour)

Temperature of catalyst reduction (°C)	Contents of C_6H_{12} (%)		
	space velocity 1.5, temperature 140°	space velocity 0.75, temperature 140°	space velocity 0.75, temperature 60°
250	43	76	40
300	60	90	76
350	79	74	83
375	55	75	75
400	54	75	24
400	56	—	5

Comparison of the hydrogenation results with the two catalysts shows that the catalyst prepared by saturation of Al_2O_3 and subsequent precipitation is not inferior to the corresponding catalyst sample made by the precipitation method in hydrogenation at 140° at a space velocity of 0.48-0.24 vol./ vol.catalyst · hour. The degree of hydrogenation varies from 74 to 95% in accordance with the space velocity. If the hydrogenation temperature is lowered to 60° the activity of the catalyst made by saturation of Al_2O_3 and subsequent precipitation by ammonium oxalate falls sharply to 7% as compared with 83% for the catalyst made by the precipitation method. The probable explanation lies in the low nickel content in the catalyst made by saturation of Al_2O_3 and subsequent precipitation. The catalyst made by saturation of Al_2O_3 and subsequent precipitation with ammonium oxalate is highly active at 140°, has high mechanical strength, and is convenient to use.

These factors prompted a more detailed investigation of the catalyst.

Effect of the reduction time on the activity of a catalyst made by the saturation method with subsequent precipitation by ammonium oxalate. The catalyst samples were reduced during periods of 1 to 10 hours. The catalyst reduced for 2-4 hours had the highest activity. The degree of hydrogenation of benzene to cyclohexane over this catalyst , at a space velocity of 0.24 vol./ vol.catalyst . hour was 86-91%, and at a space velocity of 0.48 it was 74-78%. This catalyst was used for experiments on hydrogenation of various organic compounds. Some of the results are presented below.

Hydrogenation of Various Compounds Over a Catalyst of the Composition 6% Ni, 1% MgO, and 93% Al_2O_3.

Hydrogenation of unsaturated compounds. The results of hydrogenation of some unsaturated hydrocarbons, given in Table 4, show that at 140°, atmospheric pressure, and space velocities from 0.12 to 0.48 hr^{-1}, unsaturated compounds in gasoline and kerosene fractions are 90-100% hydrogenated in presence of this catalyst. It was noticedthat the activity of the catalyst falls by 10-12% as a result.

It was found that after hydrogenation of unsaturated compounds in gasoline and kerosene the activity of the catalyst can be restored by treatment with hydrogen at 330-350°.

Hydrogenation of benzaldehyde to benzyl alcohol. The original benzaldehyde boiled at 179-181° and had $n^{20}D$ 1.5450 and d^{20}_4 1.042; the correct values are $n^{20}D$ 1.5463 and d^{20}_4 1.050.

Benzaldehyde was hydrogenated at 140° and a space velocity of 0.12. The catalyzate yield was 80%. The hydrogenation product was dried and distilled. A fraction boiling at 202-205° was collected; it had $n^{20}D$ 1.5395 and d^{20}_4 1.040. The values for benzyl alcohol are b. p. 204.7°, $n^{20}D$ 1.5396 and d^{20}_4 1.0453.

TABLE 4

Hydrogenation of Olefinic Hydrocarbons at 140°

Substance hydrogenated	Starting material			Space velocity ~ 0.48 hr^{-1}			~ 0.24 hr^{-1}			~ 0.12 hr^{-1}		
	d^{20}_4	n^{20}_D	iodine number	d^{20}_4	n^{20}_D	iodine number	d^{20}_4	d^{20}_D	iodine number	d^{20}_4	n^{20}_D	iodine number
C_{10} fraction containing olefins	0.741	1.4180	25.5	0.731	1.4150	2.0	0.729	1.4150	1.58	—	1.4160	1.4
180-320° fraction enriched with olefins	0.768	1.4375	44.1	0.765	1.4340	8.13	0.740	1.4340	3.5	—	—	—
40-180° gasoline fraction enriched with olefins	0.718	1.4220	188	0.714	1.4040	0	0.715	1.4020	0	—	—	—
C_9 fraction from paraffin cracking distillate, containing olefins	0.730	1.4060	112	—	—	—	—	—	—	0.720	1.4110	0

Hydrogenation of aromatic hydrocarbons. Toluene of b. p. 110-112°, $n^{20}D$ 1.4960 and d^{20}_4 0.866 was taken for hydrogenation. The hydrogenation was performed at 140° and a space velocity of 0.12 vol./vol.catalyst · hour. The catalyzate yield was 100%. The product boiled at 100-102° and had $n^{20}D$ 1.4235 and d^{20}_4 0.770; the constants for methylcyclohexane are b. p. 101°, $n^{20}D$ 1.4230 and d^{20}_4 0.769.

A sample of p-xylene of b. p. 136-138°, $n^{20}D$ 1.4940 and d^{20}_4 0.8615 was hydrogenated.

The hydrogenation was performed at 140° and a space velocity of 0.12. The catalyzate contained 50% of p-dimethylcyclohexane; after it had been treated with sulfuric acid, washed with alkali and water, dried, and distilled it boiled at 119-121° and had $n^{20}D$ 1.4290, d^{20}_4 0.7610; the constants for p-dimethylcyclohexane are b. p. 119.5, $n^{20}D$ 1.4290 and d^{20}_4 0.7625.

SUMMARY

1. Of various mixed catalysts deposited on different supports, the most active was Ni–MgO–Al_2O_3, reduced at 350° at a space velocity of 1000-2000 hr^{-1} for 2-4 hours.

2. The optimum temperature of hydrogenation of aromatic and unsaturated hydrocarbons over this catalyst is 140°; in some instances it can be lowered to 60°.

3. The activity at 140° of a mixed Ni–MgO–Al_2O_3 catalyst prepared by the saturation method with subsequent precipitation by ammonium oxalate, containing 6% Ni, is close to that of a catalyst prepared by the precipitation method and obtaining 46% Ni. The catalyst containing 6% Ni was used for hydrogenation of benzene under atmospheric pressure for 150 hours without loss of activity.

4. A catalyst containing Ni 6%, MgO 1% and Al_2O_3 93%, prepared by saturation of alumina with subsequent precipitation by ammonium oxalate had high activity in hydrogenation of benzene, its homologs, and certain oxygen-containing compounds.

LITERATURE CITED

[1] P. Sabatier and J. Senderens, Compt. rend. 132, 210, 556 (1901).

[2] N. D. Zelinskii, Collected Works, III [in Russian] (Izd. AN SSSR, 1955).

[3] H. S. Taylor, and G. Douherty, J. Phys. Chem. 27, 531 (1923).

[4] N. I. Shuikin, Kh. M. Minachev, and L. M. Feofanova, Bull. Acad. Sci., Div. Chem. Sci. 1, 96 (1933).

[5] A. M. Rubinshtein, S. S. Novikov, Z. Ya. Lapshin, and N. I. Shuikin, Proc. Acad. Sci. USSR, 74, 77 (1950).

[6] Catalysis and Catalysts of Organic Reactions (IL, 1956) [Russian translation edited by A. A. Balandin].

[7] I. B. Rapoport and E. I. Sil'chenko, J. Appl. Chem. 10, 1427 (1937).

[8] I. B. Rapoport and B. M. Rapoport, J. Appl. Chem. 11, 723 (1938).

[9] I. B. Rapoport, J. Appl. Chem. 11, 1656 (1938).

[10] W. Langenbeek and A. Giller, Z. anorg. alg. Ch. 272, 64 (1953).

[11] W. Langenbeek, H. Dreyer, and D. Vehring, Naturw, 41, 362 (1954).

[12] V. Danes and P. Jiru, Chem. Listy, 50, 32 (1956).

[13] H. S. Taylor, J. Phys. Chem. 27, 531 (1923).

[14] B. Danes, J. Cabicar, K. Klier, P. Gubner, and P. Jiru, Chem. Listy, 50, 1048 (1956).

[15] W. Langenbeek, Ang. Ch. 4, 453 (1956).

[16] G. Rinäcker, J. Birrenstaedt, and G. Tachel, J. pr. Chem. 4, 190 (1956).

Received March 21, 1958

STUDY OF NICKEL CATALYSTS PREPARED BY DECOMPOSITION OF ORGANIC SALTS*

I. B. Rapoport and I. Par

The first communication contained a description of the preparation of an active Ni–MgO/Al_2O_3 catalyst for hydrogenation of aromatic and oxygen-containing compounds, by decomposition of nickel and magnesium oxalates [1].

The present communication deals with the effects of different proportions of nickel and magnesium oxide, different anions, and preparation conditions on catalyst activity.

An attempt was also made to compare the catalyst prepared from oxalates with catalysts developed by N. D. Zelinskii and V. A. Komarevskii.

EXPERIMENTAL

Effects of different Ni : MgO ratios on the activity of catalysts prepared from nickel and magnesium oxalates and deposited on active alumina. The catalyst activity was determined from the degree of hydrogenation of benzene to cyclohexane under the same process conditions, i.e., at equal space velocities, constant benzene-hydrogen ratio, and equal hydrogenation temperatures. The reduction temperature of the catalyst was 430-450°. At this temperature nickel and magnesium oxalates decompose in a current of hydrogen to give Ni and MgO respectively.

The experiments were performed at atmospheric pressure and space velocities of 0.86 and 0.43 vol./vol.-catalyst · hour.

It follows from the data in Fig. 1 and 2 that the most active catalyst has the composition 35Ni–15MgO–$50Al_2O_3$.

The catalyst activity diminishes with decreasing nickel content.

Isotherms for hydrogenation of benzene to cyclohexene at 70, 100, and 140° show a conversion maximum with 35% of nickel in the catalysts.

The maximum degree of hydrogenation of benzene to cyclohexane in presence of the catalyst of the composition 35Ni–15MgO–$50Al_2O_3$ at space velocities of 0.86 and 0.44 vol./vol. catalyst · hour is observed at 140°; it is 70% in the first case, and 87% in the second. The cyclohexane yield decreases if the temperature is raised to 200°. The degree of conversion also decreases, but to a smaller extent, if the temperature is lowered to 100°.

The decrease of cyclohexane yield at 200° is probably due to changes in adsorption conditions on the catalyst surface.

To confirm this, we dehydrogenated a mixture of benzene and cyclohexane, containing 25% benzene, at various temperatures. The results, presented in Table 1, show that dehydrogenation in presence of the cata-

* Communication II in the series on active catalysts.

lyst begins at temperatures above 250°. There was no decomposition at temperatures up to 300°.

Effect of reduction temperature on the activity of Ni–MgO–Al_2O_3 catalyst prepared from oxalates. Experiments on determination of the optimum reduction temperature were carried out with a catalyst of the composition 35Ni–15MgO–50 Al_2O_3 at a space velocity of 0.43 vol./ vol.catalyst · hour. The $H_2 : C_6H_6$ ratio in the experiments was 5 : 1. The catalyst activity was determined after reduction at 330-340, 360-370, 420, 430-450°. At 420 and 430-450°, which are above the decomposition temperatures of nickel and magnesium oxalates, the catalyst contains Ni and MgO. If the reduction is performed at 330-340 and 360-370°, only the nickel oxalate is decomposed while magnesium oxalate is unchanged, as its decomposition temperature is ~420°. Therefore, two types of catalysts are obtained in accordance with the reduction temperature: 1) Ni–MgO on Al_2O_3 at reduction temperatures of 420 and 430-450°; 2) nickel on magnesium oxalate and aluminum oxide at reduction temperatures below 420°.

TABLE 1

Dehydrogenation of Cyclohexane over Ni–MgO/ Al_2O_3 Catalyst at a Space Velocity of 0.43 vol./ vol.catalyst · hour

Dehydrogenation temperature (°C)	200	255	250	275	300
Refractive index $n^{20}D$	1.4288	1.4286	1.4395	1.4455	1.4500

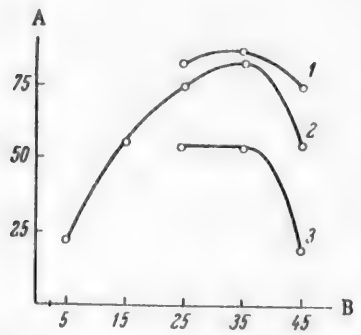

Fig. 1. Effect of Ni content on the yield of cyclohexane in presence of Ni–MgO–Al_2O_3 catalyst at a space velocity of 0.43 ml / ml catalyst · hr, T_r* = 430-450°, Q_r* = 4 hours; A) degree of hydrogenation of benzene (%), B) Ni content (%); reaction temperature (°C): 1) 140, 2) 100, 3) 70.

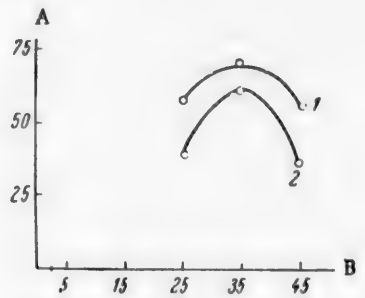

Fig. 2. Effect of Ni content on the yield of cyclohexane in presence of Ni–MgO–Al_2O_3 catalyst at a space velocity of 0.86 ml/ ml catalyst · hr; T_r = 430-450°, Q_r = 4 hours; A) degree of hydrogenation of benzene (%), B) Ni content (%); reaction temperature (°C): 1) 140, 2) 100.

The experiments showed that the most active catalyst was obtained at a reduction temperature of 330-340° (Fig. 3).

* Here and subsequently T_r is the reduction temperature of the catalyst, Q_r is the reduction time, and V is the space velocity.

The degree of conversion of benzene at hydrogenation temperatures of 100 and 140° in presence of catalysts reduced at 330-340, 420, and 430-450° is high; it lies in the 81-92% range. The reduction temperature has a sharp influence on the degree of conversion of benzene only in hydrogenation at 70° and lower.

Comparison of the activities of catalysts prepared by mixing of oxalates and by precipitation from nitrates by ammonium oxalate. The effect of the method used for catalyst preparation was studied with catalyst samples of the composition (%): 35Ni -15MgO-50Al_2O_3, prepared by precipitation by ammonium oxalate and by direct mixing of the oxalates. The catalysts were reduced at 450°. The catalyst activities were determined at a space velocity of 0.48 and $H_2 : C_6H_6 = 5 : 1$. The results of these experiments confirmed that catalysts made by simple mixing of oxalates with aluminum oxide are less active than precipitated catalysts (Table 2).

The catalyst made by the mixing method showed a sharp fall in activity in hydrogenation at 100°. Under these conditions the degree of conversion of benzene was less than 10%.

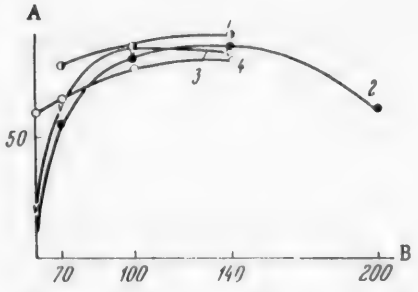

Fig. 3. Effect of reduction temperature on the activity of Ni-MgO-Al_2O_3 catalyst at Q_r = 4 hours, V = 0.46 ml/ ml catalyst · hour; A) degree of hydrogenation of benzene (%), B) temperature (°C); Reduction temperature (°C); 1) 330-340, 2) 430-450, 3) 420, 4) 360-370.

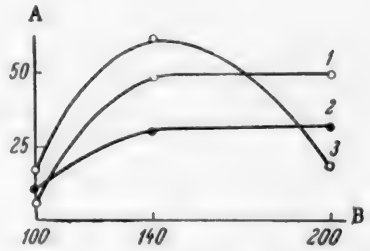

Fig. 4. Effect of the cation in the oxalate used on catalyst activity at T_r = 430-450°, Q_r = 4 hours; A) degree of hydrogenation of benzene (%), B) temperature (°C); cation in oxalate: 1) Ni/ Al_2O_3, 2) Co/ Al_2O_3, 3) Fe-Ni-MgO-Al_2O_3.

These results show that catalysts made by the precipitation method have higher activity than catalysts made by mixing of the salts, but apparently only because, first, simple mixing of nickel and magnesium oxalates with Al_2O_3 cannot give such good mixing of all three components as coprecipitation, and second, the catalyst lattice is formed during the precipitation process, and this does not occur when oxalates are mixed with aluminum oxide.

However, the activity of the catalyst made by the mixing method is high, and in some instances catalysts made by the mixing method may be used for studies of various factors.

Comparative tests on catalysts made from the oxalates of Co, Ni, Fe, and Cu. The catalysts were prepared by mixing of oxalates with aluminum oxide and reduced at 430-450°. The catalysts were so prepared that the ratio of metal to support was always about 7 : 10. In the hydrogenation, benzene was passed at a space velocity of 0.43 vol./ vol.catalyst · hour, and 5 : 1 ratio of hydrogen to benzene. The most active catalyst was Ni/ Al_2O_3, which gave 50% conversion of benzene at 200° and 46% at 140°. The activity of the Co/ Al_2O_3 catalyst was considerably lower (Fig. 4).

Cu/ Al_2O_3 and Fe/ Al_2O_3 catalysts were tested; these gave negative results under the experimental conditions used.

Special attention was paid to the reduction conditions for the Fe/ Al_2O_3 catalyst. Iron oxalate on Al_2O_3 was therefore reduced at 250, 350, 450, and even 620°. The catalysts so obtained were inactive in hydrogenation of benzene. Tests on catalysts with small amounts of added Fe showed that additions of up to 5% iron to Ni do not have an adverse effect on catalyst activity.

Effects of salt anions on the activity of nickel catalysts deposited on aluminum oxide. Above we considered the influence of different cations on the activity of catalysts prepared from oxalates. It was equally interesting to determine the effects of salts with different anions on the activity of Ni/ Al_2O_3 catalyst. The Ni : Al_2O_3 ratio was 7 : 10 for all the catalysts. The catalysts were prepared by mixing of the salts and were reduced at 430-450°; their activity was determined from the degree of hydrogenation of benzene at 100, 140, and 200°.

TABLE 2

Effect of Preparation Method on Activity of 35Ni–15MgO–50Al_2O_3 Catalyst (Reduction time 4 hours at 430-450°, space velocity 0.40-0.43 vol./ vol.catalyst · hour, catalyst volume 28 ml)

Data	Mixing			Precipitation		
Hydrogenation temperature (°C)	200	140	100	200	140	100
Degree of benzene conversion (%)	–	61	8	62	88	83

The results (Fig. 5) show that the catalyst made from nickel carbonate was the most active. This catalyst is not inferior in activity to Zelinskii's catalyst at hydrogenation temperatures of 70-140°. Catalysts made from nickel acetate and formate are more active than the catalyst from nickel oxalate. This is probably due to the

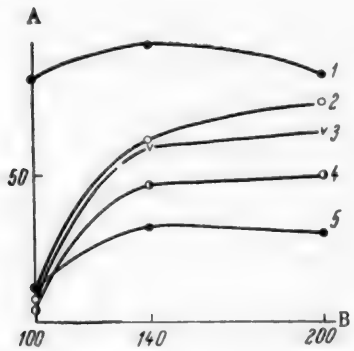

Fig. 5. Effects of different anions on the activity of nickel catalysts at T_r = 430-450°, Q_r = 4 hours, V = = 0.43 ml/ ml catalyst · hr; A) degree of hydrogenation of benzene (%), B) temperature (°C) salts: 1) $NiCO_3$, 2) $Ni(HCOO)_2$, 3) $Ni(CH_3COO)_2$, 4) NiC_2O_4, 5) $Ni(NO_3)_2$.

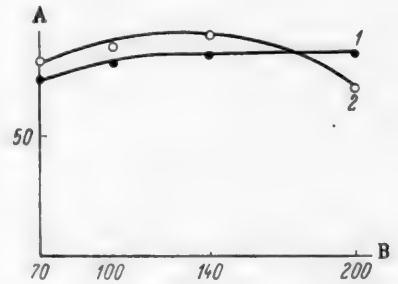

Fig. 6. Comparison of the activities of Ni–MgO–Al_2O_3 (35–15/ 50) catalyst and Zelinskii's catalysts at Q_r = = 4 hours, V = 0.43 ml/ ml catalyst · · hr; A) degree of hydrogenation of benzene (%), B) temperature (°C); catalysts: 1) Zelinskii's, T_r = 320-330°; 2) Ni–MgO/ Al_2O_3, T_r = 330-340°.

relatively good solubility in water of nickel acetate and formate (on addition of aqueous starch solution) and formation of mixed crystals even in the course of mixing, which does not occur when the catalysts are prepared from oxalates. The catalyst made from nickel nitrate is the least active.

Comparison of activities of the 35Ni–15MgO–50Al_2O_3 catalyst and Zelinskii's catalyst. The literature on mixed catalysts prepared from salts of organic acids [2] contains comparative data on the activities of a mixed catalyst and Raney catalyst. In the present investigation the activities of a catalyst made from oxalates by the precipitation method and the Zelinskii's catalyst were compared. Zelinskii's catalyst and the Ni–MgO–Al_2O_3 catalyst made from oxalates were reduced at 330°. Hydrogenation was performed under the same conditions,

TABLE 3

Apparent Activation Energy of the Catalyst 35Ni–15MgO–50Al_2O_3

Temperature (°C)	Values of activation energy (kcal/ mole) at reducing temperatures (°C)	
	330-340°	430-450°
70-100	2960	–
100-140	105	4390

namely: the benzene was fed at 12 ml/ hour, the catalyst volume was 28 ml, and the hydrogen–benzene ratio was 5 : 1. The experimental temperature varied from 70 to 200° in accordance with the required conditions.

The Ni–Mg–Al_2O_3 catalyst made from oxalates was more active than the Zelinskii catalyst at hydrogenation temperatures of 70-140°. At 200° benzene is 85% hydrogenated in presence of Zelinskii's catalyst, and only 60% in presence of the Ni–MgO–Al_2O_3 catalyst (Fig. 6).

Determination of the apparent activation energy of hydrogenation of benzene to cyclohexane in presence of Ni–MgO–Al_2O_3 catalyst. The apparent energy of activation was determined for two catalysts of the same composition, but reduced at 430-450° (Sample No. 1) and 330-340° (Sample No. 2) respectively. The catalyst composition (%) was 35Ni, 15MgO, 50Al_2O_3.

The hydrogen–benzene ratio in hydrogenation was 5 : 1.

For calculation of the activation energy, isotherms were plotted showing variations of the degree of conversion of benzene into cyclohexane with the reciprocal space velocity for catalyst Samples No. 1 (Fig. 7) and No. 2 (Fig. 8).

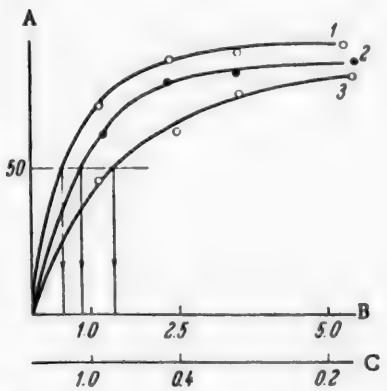

Fig. 7. Hydrogenation of benzene over Ni–MgO/ Al_2O_3 (35–15/ 50) catalyst at various temperatures and space velocities at T_r = 430-450°, Q_r = 4 hours: A) degree of hydrogenation of benzene (%), B) reciprocal space velocity, C) space velocity (ml/ ml catalyst · hr^{-1}); reaction temperature (°C) 1) 140, 2) 100, 3) 200.

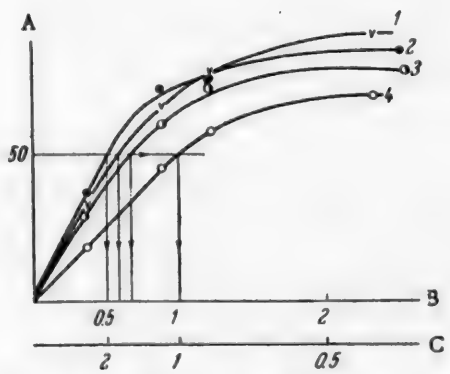

Fig. 8. Hydrogenation of benzene over Ni–MgO/ Al_2O_3 (35–15/50) catalyst at various temperatures and space velocities at T_r = 330-340°, Q_r = 4 hours: A) degree of hydrogenation of benzene (%), B) reciprocal space velocity, C) space velocity (ml/ml catalyst · hr^{-1}); reaction temperature (°C): 1) 140, 2) 100, 3) 70, 4) 200.

The apparent activation energies given in Table 2 were calculated by means of the Arrhenius equation.

These results show that at the same space velocity hydrogenation of benzene proceeds up to 100° to a greater extent over the catalyst reduced at 330-340°. Increase of temperature to 140° is accompanied by a decrease in the degree of hydrogenation of benzene, and on further increase of temperature to 200°, the degree of hydrogenation of benzene is still less.

The degree of hydrogenation of benzene at 70-100° over a catalyst reduced at 430-450° is considerably lower than over the catalyst reduced at 330-340°.

It was observed that when the reduction temperature is raised to 450° there is a shift in the activity toward an increase of the temperature required for hydrogenation, i.e., the reaction must be carried out at a somewhat higher temperature in order to attain the same degree of conversion of benzene into cyclohexane over the catalyst reduced at 430-450°.

The influence of temperature on the degree of conversion of benzene into cyclohexane is associated with changes in chemisorption on the catalyst surface. It is known that, apart from other factors, in the chemisorption of benzene considerable forces due to the conjugation effect of its atoms (34 kcal) must be overcome [2]. Therefore, chemisorption of benzene can take place only at the most active centers, with the greatest heat of adsorption.

Hydrogen may be activated at less active centers where benzene cannot be activated [3]. Renäcker and Birekenstaedt [2] reported that with increase of the reduction temperature to 450° the specific surface of a catalyst made from oxalate is half that of a catalyst reduced at 350°.

The decrease in the specific surface of a catalyst reduced at 450° is probably due to partial sintering and disturbance of the active centers on the surface, which is accompanied by a decrease in the adsorption of benzene at lower temperatures.

This probably accounts for the fact that, under otherwise equal conditions at 100-140° the degree of conversion of benzene into cyclohexane was higher in presence of the catalyst reduced at 330-340° than in presence of the catalyst reduced at 430-450°.

This difference increased sharply at 70 and 60°. It seems likely that changes in the specific surface (and therefore of pore size) change the degree of sorption of benzene and hydrogen, and hence the activity of the catalyst.

SUMMARY

1. An active catalyst of the composition 35Ni–15MgO–50Al_2O_3 is prepared by simultaneous precipitation of nickel and magnesium from nitrate solutions by ammonium oxalate, with subsequent reduction at 330-340°.

2. Precipitated catalysts are the most active.

3. Studies of the hydrogenation of benzene over various metals prepared by decomposition of oxalates and deposited on active alumina showed that nickel is the most active, and cobalt is less active. Iron with various additives is inactive. Additions of up to 5% iron to nickel do not reduce the activity of the catalyst.

4. Nickel catalysts prepared from different salts differ in activity. Catalyst prepared from nickel carbonate is the most active, followed by catalysts prepared from nickel formate, acetate, and oxalate.

5. The activity of the Ni–MgO–Al_2O_3 catalyst at 70-140° is 8-10% higher than that of Zelinskii's catalyst. In hydrogenation at 200° the degree of conversion of benzene is 15% higher in presence of Zelinskii's catalyst than in presence of Ni–MgO–Al_2O_3 catalyst made from oxalates.

6. The apparent energy of activation for hydrogenation of benzene to cyclohexane at 70-100° in presence of catalyst of the composition 35Ni–15MgO–50Al_2O_3 reduced at 330-340° is 2960 kcal/ mole, and at 100-140° with catalyst reduced at 430-450° it is 4390 kcal/ mole.

LITERATURE CITED

[1] L. B. Rapoport and Yu. V. Vysheslavtsev, J. Appl. Chem. 32, 8, 1738 (1959)*

[2] G. Renäcker, J. Birekenstaedt, and G. Tachel, J. pr. Chem. 4, 190 (1956).

[3] R. M. Flid, Trans. Lomonosov Inst. Fine Chemical Technology, Moscow [in Russian] (Goskhimizdat, 1956), p. 61.

Received March 21, 1958.

*Original Russian pagination. See C.B. Translation.

LIQUID–VAPOR EQUILIBRIA IN THE SYSTEM METHYLCYCLOHEXANE–n-HEPTANE*

I. N. Bushmakin and N. P. Kuznetsova

The Leningrad (Order of Lenin) State University

The system methylcyclohexane–n-heptane was proposed by Fenske et al. in 1934 [1] for determination of the efficiency of rectification columns. Since that time this system has always been used for the most accurate efficiency determinations.

The history of the liquid–vapor equilibrium data for this system is as follows. In 1933 Bromiley and Quiggle [2] studied these equilibria. The values of relative volatility (α) calculated by us from their data are marked in the diagram by crosses. Calingaert and Beatty [3] considered their data to be wrong and put forward the opinion that direct determination of liquid–vapor equilibria for systems with such low values of α are impossible until the determination technique has been improved. They therefore investigated variations of total vapor pressure in this system with solution concentration at constant temperature and found that this relationship is almost linear (the behavior of the system is almost ideal). On this basis they determined the vapor pressures of the pure components at their boiling points under atmospheric pressure and then used the P_2^0/P_1^0 ratio to calculate the end values of α. By the data of Calingaert and Beatty, with 100% methylcyclohexane α = 1.0728, and with 100% heptane α = 1.0710. In the figure the dotted line (the one in the middle) joins these end values of α.

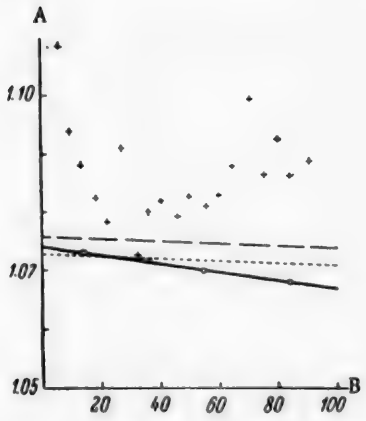

Variations of the relative volatility (α) in the system methylcyclohexane–n-heptane with the concentration of n-heptane in the liquid: A) relative volatility, B) x, the content of n-heptane in the liquid (in molar %). Explanation in text.

Willingham and Rossini [4] decided in 1946 to check the data of Calingaert and Beatty; they measured very accurately the vapor pressures of the pure components at their boiling points and found α = 1.07584 for 100% methylcyclohexane, and α = 1.07380 for 100% heptane. In the figure these end values of α are joined by the dash line (the upper).

Willingham and Rossini's vapor-pressure data are undoubtedly very accurate, but the end values calculated from them apply to an ideal system. In a real system, even if very close to ideal, the end values of α differ somewhat from those for an ideal system; it follows that calculations of efficiency from data for an ideal system are always to some extent incorrect. We therefore performed a direct investigation of liquid–vapor equilibria in the system methylcyclohexane–n-heptane (it will be seen that our technique was a considerable improvement on that of Bromiley and Quiggle).

* Communication XI.

Two samples of methylcyclohexane and two samples of n-heptane were available for the investigation. The first sample of methylcyclohexane was left over from a study of liquid–vapor equilibria in the system methylcyclohexane–2,2,4-trimethylpentane [5]. This sample was additionally rectified in a column of 120 theoretical plates (calculated for the benzene–carbon tetrachloride system), the first portion of the distillate and the still residue being rejected, and then tested for purity in a 120-plate column [6]. This sample of methylcyclohexane had $n^{20}D = 1.42307$. The second sample was prepared from toluene. Toluene was purified by rectification in columns. The purified toluene had $n^{20}D = 1.4968$ (determined in a refractometer of the Abbe type). The toluene was hydrogenated. Methylcyclohexane was separated from unchanged toluene by rectification. It was then washed with concentrated sulfuric acid (to a negative formalite reaction), sodium carbonate solution, and water, carefully rectified in 120-plate columns, and tested for purity in a column of the same efficiency. The refractive index of this sample coincided exactly with that of the first sample.

The samples of n-heptane were obtained from the same source, but at different times. They were prepared from synthine. The two samples (separately) were carefully rectified in 120-plate columns and tested for purity in the same columns. Both samples had exactly the same refractive index $n^{20}D = 1.38767$.

One pair of liquids was used for the investigations, and the results were checked with the other pair.

Two distillation units of the old design were used for equilibrium determinations for the first pair of liquids. They differed in dimensions. The liquid capacity of the still in Apparatus I was 75 ml, and in Apparatus II, 200 ml. An apparatus of the new design was used for the checks. The capacity of the still of this apparatus (III) was 60 ml. Descriptions of the distillation equipment were given earlier [7].

The apparatus was connected to a manostat during the experiments.

The compositions of the liquid and equilibrium vapor were determined from differential readings on the scale of a Pulfrich refractometer. Scale reading–concentration graphs were first plotted for the concentration regions in which the investigations were to be carried out. New graphs were plotted before the verification of the equilibrium data. The error in the refractometer scale readings was ±0.1', which corresponds to a concentration error of ±0.03 molar %. In the experiments 8 to 12 scale readings were taken for each liquid (condensate and the still contents), and therefore the average error in determinations of liquid composition was of the order of ±0.01 molar %. Corrections were applied to the decomposition of the liquid in the still because liquid samples were taken from the cooled apparatus [7].

Equilibria were determined in three concentration regions. Table 1 illustrates the degree of agreement obtained. It includes the results of both the main and the check experiments. Our values of α are indicated in the diagram by circles. The straight line $\alpha = f(x)$ drawn through these points can be represented by the equation

$$\alpha = 1.074 - 0.00007x. \qquad (1)$$

It should be noted that the end value of α for 100% methylcyclohexane in this system exactly coincided with the end value of α for 100% methylcyclohexane (1.074) found by us with the system methylcyclohexane–2,2,4-trimethylpentane [5].

Equation (1) was used to calculate interpolated values for the liquid–vapor equilibria. The results are given in Table 2.

For the system methylcyclohexane–n-heptane the slope of the line $\alpha = f(x)$ is so small that in determinations of column efficiency the number of theoretical plates can be calculated accurately from the equation

$$\frac{y'}{100 - y'} = \alpha^n \frac{x'}{100 - x'}, \qquad (2)$$

where x', y' are the contents of n-heptane in the still and condenser (in molar %), n is the number of theoretical plates, and α corresponds to the middle of the x'–y' range. The discrepancy between the numbers of theoretical plates calculated from Equation(2) and determined by exact methods [5] does not exceed 0.2%, even for such a wide concentration range as 0.01-99.99 molar %. However, it is more convenient to use number of plates–concentration diagrams than to perform calculations by Equation (2) in each efficiency determination. Data for the plotting of such diagrams were therefore calculated (Table 3).

The range of 0.01-99.99 molar %, according to Table 3, includes 271 plates, and according to Willingham and Rossini, it includes 255 plates.

For determinations of column efficiency with the aid of the data in Table 3, the concentrations of n-heptane in the condensate and still liquids (in the 5-95 molar % range) can be found by means of a refractom-

TABLE 1

Liquid–Vapor Equilibria in the System Methylcyclohexane–n-Heptane, Determined in Single-Evaporation Apparatus P = 760 mm

Apparatus	Content of n-heptane (molar %)		α
	liquid	vapor	
I	13.81	14.66	1.072
	14.26	15.14	1.073
III	14.35	15.24	1.073
I	52.83	54.50	1.070
	53.12	54.78	1.069
II	53.71	55.37	1.069
	54.38	56.07	1.071
	54.43	56.10	1.070
III	54.94	56.64	1.071
I	83.97	84.84	1.068
	84.08	84.94	1.068
III	84.03	84.89	1.068

TABLE 2

Liquid–Vapor Equilibrium Data for the System Methylcyclohexane–n-Heptane Interpolated from the α = f(x) Graph P = 760 mm

Content of n-heptane (molar %)		Content of n-heptane (molar %)	
liquid	vapor	liquid	vapor
1.00	1.07	60.00	61.61
2.00	2.14	70.00	71.39
5.00	5.35	80.00	81.04
10.00	10.65	85.00	85.82
15.00	15.92	90.00	90.57
20.00	21.15	93.00	93.41
30.00	31.48	96.00	96.24
40.00	41.66	98.00	98.12
50.00	51.70	99.00	99.06

eter of the Abbe type (to an accuracy of $\pm 1 \cdot 10^{-4} \cdot n^{20}D$). The relationship between $n^{20}D$ and concentration is given in the paper by Bromiley and Quiggle [2]. Our more accurate data for this relationship are presented in Table 4.

To test for the absence of any systematic error in the liquid–vapor equilibrium data so obtained, we determined the compositions of the liquids in the condenser and still during operation of the column (with total

TABLE 3

The System Methylcyclohexane–n-Heptane Data for Plotting of Number of Plates – Concentration Diagrams (P = 760 mm, n-heptane concentration in still 0.01 molar %)

Conc. of n-heptane in condenser reflux (molar %)	Number of plates	Conc. of n-heptane in condenser reflux (molar %)	Number of plates	Conc. of n-heptane in condenser reflux (molar %)	Number of plates
0.01	0	35	120.9	98.4	192.4
0.1	32	45	127.0	98.8	196.9
0.3	47.7	55	132.9	99.0	199.8
0.5	54.9	60	135.9	99.2	203.2
0.8	61.5	65	139.1	99.4	207.7
1.0	64.7	70	142.5	99.5	210.5
1.5	70.4	75	146.3	99.6	214.0
2.0	74.5	80	150.6	99.7	218
4	84.5	85	155.9	99.8	225
6	90.5	90	162.9	99.9	235
8	94.9	93	168.9	99.92	239
12	101.3	95	174.4	99.94	243
16	106.0	96	178.0	99.96	250
20	109.9	97	182.6	99.98	260
25	114.0	98	188.9	99.99	271

reflux) in different concentration regions, and then found the corresponding numbers of plates* from the diagrams (Table 3). For comparison, the numbers of plates were also calculated from the same data and Willingham and Rossini's values of α. The results of these determinations and calculations are given in Table 5.

TABLE 4

Effect of Concentration of Refractive Index of Methylcyclohexane–n-Heptane Solutions

Conc. of n-heptane (molar %)	n_D^{20}	Conc. of n-heptane (molar %)	n_D^{20}
0.0	1.4231	55	1.4024
5	1.4212	60	1.4007
10	1.4192	65	1.3990
15	1.4172	70	1.3973
20	1.4152	75	1.3957
25	1.4132	80	1.3941
30	1.4114	85	1.3925
35	1.4096	90	1.3909
40	1.4077	95	1.3893
45	1.4060	100	1.3877
50	1.4042		

Table 5 shows that the number of plates calculated from our data remains constant for all the concentration ranges. Calculations based on Willingham and Rossini's values of α give some decreases in the number of plates with increase of the n-heptane concentration in the still. This means that the slope of the $\alpha = f(x)$ line plotted from Willingham and Rossini's data is too small. However, such a conclusion can be drawn only if Columns 4 and 5 in Table 5 are compared. Without such comparison the small decrease in the number of plates in Column 4 might be attributed to experimental error. From the data of Column 4 alone it is impossible to decide whether Willingham and Rossini's data are correct or not. It can only be said that the true $\alpha = f(x)$ line is also straight, but it cannot be decided whether the line being checked coincides with the true line or whether it lies above or below it.

Thus, here we have some limitations of the potentialities of our proposed method for verification of liquid-vapor equilibrium data [6]. If the $\alpha = f(x)$ plot is linear, the method may indicate if it is incorrect but may not confirm that it is correct. If the number of theoretical plates for a given column differs in different concentration ranges, that means that the $\alpha = f(x)$ line is incorrectly plotted; if the number of plates is the same, this only means that the true $\alpha = f(x)$ line is also straight; to establish its location on the α, x diagram it is necessary to determine liquid–vapor equilibria experimentally for at least two concentrations. Such cases, unfavorable for our method, are extremely rare.

TABLE 5

Verification of Liquid–Vapor Equilibrium Data for the System Methylcyclohexane–n-Heptane (P = 760 mm)

Range	Contents of n-heptane in liquid (molar %)		Number of plates	
	in still	in condenser	from Willingham and Rossini's α	from our α
I	10.2	51.9	31.1	32.5
II	32.5	81.7	30.9	33.0
III	83.3	97.55	29.1	31.9
IV	95.23	99.40	29.7	32.6

SUMMARY

The system methylcyclohexane–n-heptane is very nearly ideal. In the α, x diagram the difference between the end values of α for the ideal and real systems respectively is $2 \cdot 10^{-3}$ on the methylcyclohexane side and $7 \cdot 10^{-3}$ on the n-heptane side; the number of theoretical plates calculated from α for the real system is 4-10% higher than that calculated from α for the ideal system (the extent depends on the location of the concentration range).

* The liquid compositions were determined from differential readings on the scale of the Pulfrich refractometer.

LITERATURE CITED

[1] M. R. Fenske, C. O. Tongberg, and D. Quiggle, Ind. Eng. Chem. 26, 1169 (1934).

[2] E. C. Bromiley and D. Quiggle, Ind. Eng. Ch. 25, 1136 (1933).

[3] G. Calingaert and H. A. Beatty, Ind. Eng. Chem. 26, 504 (1934).

[4] Ch. B. Willingham and F. D. Rossini, J. Research. Nat. Bur. St. 37, 15 (1946).

[5] I. N. Bushmakin, S. P. Versen, and N. P. Kuznetsova, J. Appl. Chem. 32, 6, 1274 (1959).*

[6] I. N. Bushmakin, R. V. Lyzlova, and P. Ya. Molodenko, J. Appl. Chem. 26, 1258 (1953).*

[7] I. N. Bushmakin, J. Appl. Chem. 32, 4, 812 (1959).*

Received April 29, 1958

* Original Russian pagination. See C.B. Translation.

THE HYDRAULIC RESISTANCE OF LAYERS OF GRANULAR MATERIALS

A. A. Komarovskii and V. V. Strel'tsov

The S. Ordzhonikidze Polytechnic Institute, Novocherkassk

Since the time of Darcy, who established his filtration law in 1856, much attention has been devoted to problems of the hydraulic resistance of layers of granular materials by specialists in a great variety of branches of science and technology. However, despite the very large number of publications, a number of questions in this complex problem, which is of great practical importance, remain unsolved to the present day. There is no common approach to correlation of the experimental data, and the calculation formulas given by different authors are very diverse.

The most usual method for correlation of experimental data is based on the hydraulic radius or equivalent diameter of the cross section of the stream, calculated from the diameter of a sphere of the same dimensions, taken to be the linear grain size d_g. However, even this method, which is considered to be the most justified theoretically, cannot take into account all the characteristics of the granular bed – grain shape, surface state, and structure of the bed. Various methods are used to take these individual characteristics into account.

In particular, it has been proposed [1-3] to introduce a correction factor determined experimentally for each type of packing.

The resistance equations can then be written in the form [3]:

$$\Delta p = \zeta_o \cdot \varphi_g \cdot \frac{h}{d_{eq,\,o}} \cdot \rho \cdot v^2, \tag{1}$$

$$\zeta_o = f(Re), \tag{2}$$

$$Re = \frac{v \cdot d_{eq,\,o}}{\nu}, \tag{3}$$

$$d_{eq,\,o} = \frac{4\varepsilon}{\sigma_o} = \frac{2}{3}\,\frac{\varepsilon}{1-\varepsilon}\,d_g, \tag{4}$$

$$\sigma_o = \frac{1-\varepsilon}{d_g}, \tag{5}$$

where Δp is the pressure drop in the bed (in kg/m^2); h is the height of the bed (in m); d_{eq} is the equivalent diameter of the stream cross section (in m); v is the liquid velocity in the bed (in m/second); $Re = \frac{v \cdot d_{eq.\,o}}{\nu}$ is the Reynolds number; d_g is the diameter of the grains in the bed, defined as the diameter of an equivalent sphere (m); ρ is the density of the liquid ($\frac{kg \cdot sec^2}{m^4}$); ζ is the resistance coefficient of the bed; φ_g is the correction factor for the bed; σ is the specific surface of the grains (in m^2/m^3); ϵ is the free volume (voidage) of the bed (in m^3/m^3); ν is the kinematic viscosity coefficient (in m^2/second); the subscript o corresponds to a bed of spherical particles.

The correction factor φ_g (the bed coefficient) is found from the ratio:

$$\varphi_g = \frac{\Delta p}{\Delta p_o} = \frac{\zeta}{\zeta_o}. \tag{6}$$

This paper is primarily concerned with the choice of the form of Function (2) for a bed of spherical particles or of grains of any shape

$$\zeta = f(\mathrm{Re}) . \tag{7}$$

Moreover, in the publications cited above [1-3] the values of φ_g are assumed constant over the entire range of Reynolds numbers. Further, Akopyan [2] proposes the use of data from one experiment for determination of φ_g. We intend to show that this assumption is contrary to theory and to available experimental data. In cases when the assumption that φ_g is constant may be useful (for example, in studies of mass transfer [4]) it is necessary to check carefully that large errors are not thereby introduced into the calculations.

A considerable amount of experimental data has now been published in relation to Equation (2) or (7), covering a wide range of Reynolds numbers both for layers of spheres and of materials in which the grains are not spherical. A number of very important conclusions may be drawn from these experimental data. First, they show that at low Reynolds numbers the resistance coefficient varies linearly; the straight line then passes into a smooth curve which tends to a certain constant value in the turbulent region. The $\zeta = f(\mathrm{Re})$ curve does not have breaks representing transition from streamline to turbulent flow, as in the case of liquid flow in pipes. Deviations from the Darcy linear law occur at Reynolds numbers considerably less than the critical Reynolds number for flow in pipes.

The cause of this change in the resistance is that in the motion of a liquid through a granular bed the linear losses due to viscosity forces are accompanied, even at low Reynolds numbers, by quadratic losses the significance of which increases with increase of Reynolds number. Some workers attribute these losses to true turbulence which gradually develops in channels of different cross section which are present in porous media. They have also been attributed to the increasing influence of inertia forces, which may manifest itself even in the strictly streamline region. Schneebeli [5] investigated the resistance of coarsely granular materials with the aid of colored streams and found that the Darcy law breaks down at much lower Reynolds numbers than those at which turbulence appears.

Although the origin of the quadratic losses is interpreted differently by different investigators, more and more are reaching the conclusion that the resistance of a granular bed can be represented most accurately by a binomial equation. Accordingly, Velikanov [6, 7], Lindquist [8], and Engelund [9] give the following expression for the hydraulic gradient in the bed:

$$i = av_f + bv_f^2, \tag{8}$$

where i is the hydraulic gradient and v_f is the rate of filtration (in m/second).

Ergun and Orning [10, 11] gave a binomial equation for the pressure drop in a granular bed, with energy lost in overcoming viscosity and inertia forces taken into account. Zhavoronkov, Aérov, and Umnik [12], Minskii [13], Mints and Shubert [14], Schneebeli [5], and the present authors [3] used a binomial expression for the coefficient of resistance of a granular bed:

$$\zeta = \frac{A}{Re} + B. \tag{9}$$

Equation (8), like Ergun and Orning's equation, can be easily reduced to the form of (9). Finally, it should be noted that Huitt [15] recently used the Ergun and Orning equation reduced to the form of (9) for successful correlation of the results of a study of the resistance to flow of water in artificial cracks filled with sand.

The table contains values of the constants A and B obtained by different workers and recalculated for the notation used above [Equations (1)-(5)].

It was shown earlier [3] that for a layer of spheres good agreement with the experimental data of many workers is given by the equation derived by Zhavoronkov and his associates [12], with a somewhat corrected value of the constant B:

$$\zeta_0 = \frac{72.6}{Re} + 0.9. \tag{10}$$

Figure 1 shows that Equation (10) is also in good agreement with the experimental data of Leva and his co-workers [16] for flow of air and helium through beds of glass and porcelain spheres at Reynolds numbers up to 33,700.

Values of A and B from Equation (9)

Authors	Material, d_g (mm)	A	B	φ_s	B_0
Lindquist [8]	Lead shot	81.8	1.22	1.13	1.06
Engelund [9]	Sand with angular grains, 1.4 and 2.6	149.3	2.37	2.06	1.15
Ergun and Orning [10, 11]	Spheres	66.7	1.17	0.919	1.27
Zhavoronkov et al. [12]	Spheres: steel 3.19 and 7.15, lead 2.46	72.6	0.80	1.00	0.80
Mints and Shubert [14]	Anthracite:				
	0.937	185.5	3.32	2.56	1.30
	2.08	176.0	2.92	2.43	1.20
	3.46	184.0	2.93	2.53	1.16
	5.10	179.0	2.49	2.47	1.01
	7.79	184.0	2.20	2.53	0.905
	Steel spheres				
	1.664	86.7	1.54	1.19	1.29
	Fine gravel				
	3.665	145.5	2.11	2.01	1.047
Schneebeli [5]	Glass spheres				
	27	77.7	0.78	1.07	0.73
	Granite lumps				
	37	180.7	3.94	2.49	1.58
Komarovskii et al [3]*	Aluminum cylinders:				
	4.52	127.0	1.59	1.75	0.91
	3.72	125.0	1.70	1.73	0.98
	3.46	80.0	1.72	1.10	1.56
	2.32	110.0	1.49	1.52	0.98
	Sand with rounded grains:				
	1.85	145.0	1.50	2.00	0.75
	0.90	87.5	1.37	1.21	1.03
	0.45	64.0	1.14	0.882	1.29

* The values of A and B given in the table for aluminum cylinders and sands differ from the published data [3]. In the earlier paper these values were found from values of A and B for spheres in Equation (10) and the layer coefficient determined experimentally. Here we give values of A and B found directly by experiment from ζ Re – Re graphs [14].

We used Equation (10) to calculate the bed coefficients for the investigated materials and represented the results of all the experiments by a single correlation curve. However, we do not consider that this justifies the assumption that the bed coefficient remains constant over the whole range of Reynolds numbers. The bed coefficient can remain constant only if all the factors on which the resistance of the bed depends influence both the losses due to viscosity forces and the losses due to inertia forces to an equal extent. However, it is well known that surface roughness, which does not influence losses in streamline flow, has a strong effect on losses in turbulent flow. The arrangement of the grains in the bed and its structure may have a similar influence. These considerations are confirmed by experimental data.

Our calculations showed that if the average value of φ_g for a given material is taken as constant over the whole range of Reynolds numbers the calculation errors are increased, sometimes very considerably. For example, for cylinders of d_g = 3.46 mm the average error in determination of the resistance coefficient from the bed coefficient is 12.1%. At the same time, calculations from the constants A and B found directly from experimental data (see table) give an average error not exceeding 5.1%. Moreover, in the first case calculations give high values of the resistance coefficient at lower Reynolds numbers and low values at high Reynolds numbers.

This is well illustrated by Fig. 2. In this graph the continuous curve is plotted from values of the constants A and B given in the table, and the dash curve from values of the constants calculated from φ_g [3]. The values of the coefficients A and B given in the table, which vary over wide ranges, also indicate that there are

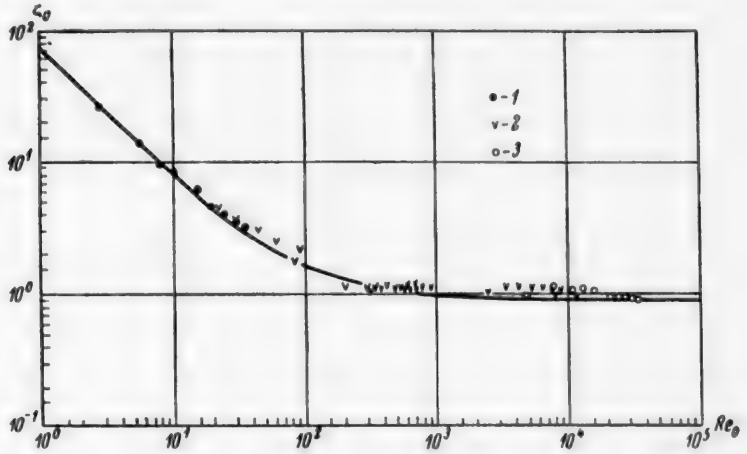

Fig. 1. Variation of the resistance coefficient of a bed of spheres with Reynolds number; curve plotted from Equation (10): points from Leva's experimental data [16]: 1) glass spheres, helium; 2) glass spheres, air; 3) porcelain spheres, air.

several factors which differ in their effects on linear and quadratic losses. Even with grains of the same shape, such as spheres, these coefficients differ quite considerably. These differences are revealed especially clearly if the bed coefficient is calculated from data for streamline flow by means of the expression

$$\varphi_g = \frac{A}{72.6}. \tag{11}$$

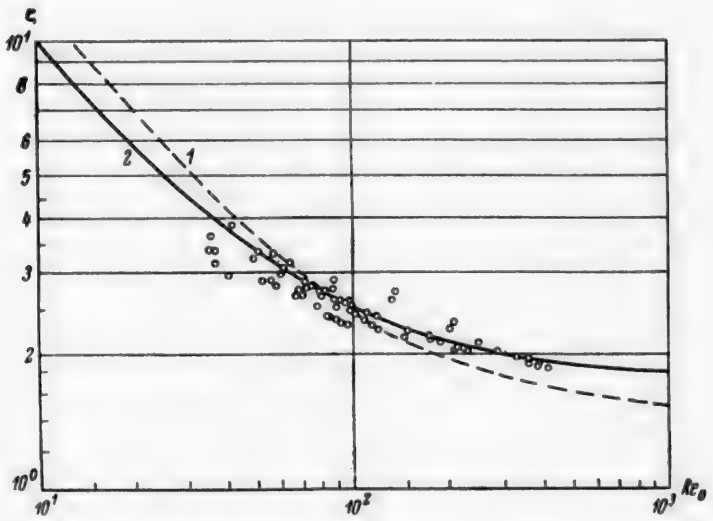

Fig. 2. Variation of the resistance coefficient of a bed of cylinders of d_g = 3.46 mm with Reynolds number: 1) from equation $\zeta = \frac{111.1}{Re} +$ + 1.38 [3], 2) from equation $\zeta = \frac{80.0}{Re} + 1.72$.

Values of φ_g calculated in this manner are given in the table. The bed coefficient φ_g can then be used to find the corresponding values of B_0:

$$B_0 = \frac{B}{\varphi_g}. \tag{12}$$

The data in the table show that these calculations do not give equal values of B_0, and therefore the $\epsilon = f(Re)$ curves, when reduced to a common straight line for streamline flow by means of the bed coefficient

$$\zeta_0 = \frac{\zeta}{\varphi_g} = \frac{72.6}{Re}, \tag{13}$$

would diverge in the transitional and turbulent regions. This is illustrated by Fig. 3, plotted from Mints's data for crushed anthracite.

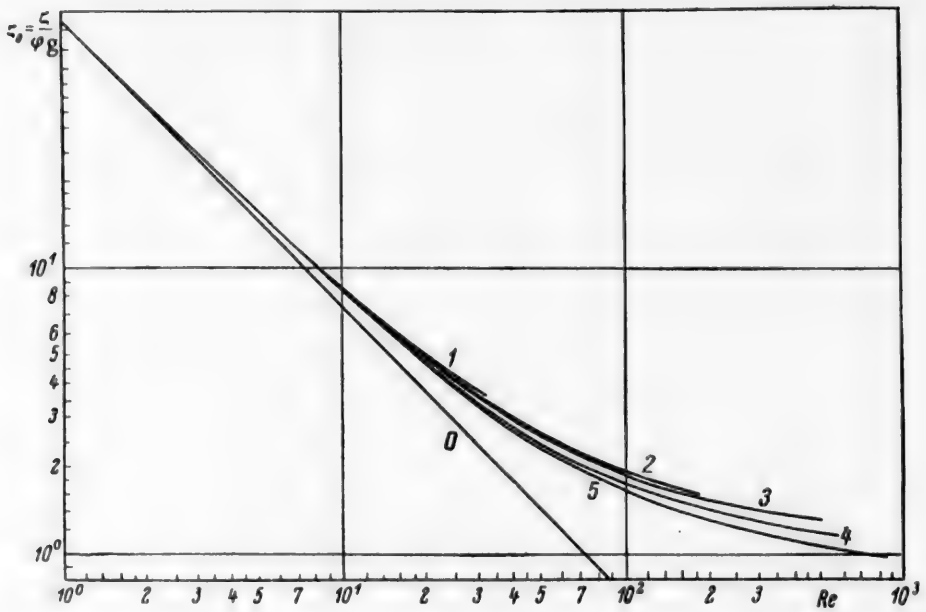

Fig. 3. Variation of the resistance coefficient of crushed anthracite with Reynolds number, from experimental data of Mints [14]: 0) from equation $\zeta = \frac{72.6}{Re}$; grain size d_g (mm): 1 – 0.937, 2 – 2.08, 3 – 3.46, 4 – 5.10, 5 – 7.79.

This divergence of the curves in the transitional and turbulent regions may be due to different causes. Kagan [17, 18] and Leva et al. [16] attribute divergence of the curves for the materials studied by them to the influence of grain roughness. At low Reynolds numbers the experimental points both for smooth and for rough grains can be reduced to a single straight line conforming to the Darcy law. With increase of Reynolds number the $\zeta = f(Re)$ curves diverge from this line and gradually pass into horizontal straight lines which differ for materials of different roughness. The coarser the grain roughness, the higher do these lines lie. Similar results were also obtained by Schneebeli [5] for glass spheres (smooth surface) and crushed granite (acute-angled rough grains). Kagan and Leva note that these results are in good agreement with the results obtained by Nikuradze for the resistance of rough pipes.

At sufficiently low Reynolds numbers roughness does not give rise to quadratic losses which are due to inertia forces. For grains of the same shape (such as spheres) the coefficient A of Equation (9) in this region is the same for any degree of roughness, and when $B \approx 0$ we have the same linear expression for the resistance [13].

In the region of developed turbulence the viscosity term in Equation (9) becomes zero, and the resistance coefficient becomes equal to B. However, the inertia losses differ for material of different roughness. They increase with increase of the relative roughness $\frac{\delta^*}{r}$, and B should increase accordingly. Thus, the general expression for the resistance should be of the form:

$$\zeta = \frac{A}{Re} + B = \frac{A}{Re} + B\left(\frac{r}{\delta}\right). \tag{14}$$

The form of the $B\frac{r}{\delta}$ function cannot be established at the present time. In the most complete data on this question, those of Leva, there is only a qualitative comparison of the roughness of the materials used. Moreover, Leva's experiments with rough materials cover a relatively narrow range of Reynolds numbers in the turbulent region.

These considerations are confirmed by the experimental results of Mints and Shubert for crushed anthracite (table, Fig. 3). They studied 5 samples of anthracite with grains of different sizes. It seems likely that the grains in these samples retain geometric similarity, and the average height of the projections is the same for all. In that case the relative roughness $\frac{\delta}{r}$ is inversely proportional to the linear grain size (d_g or $r = \frac{d_g}{2}$). If the roughness of the smallest grains (d_g = 0.937 mm) is taken as unity, the following relative values of δ_o are obtained for the roughness of the other samples:

d_g (in mm)	δ_o
0.937	1.0
2.08	0.45
3.46	0.27
5.10	0.18
7.79	0.12

Examination of the data shows that despite the wide range of variations of δ the value of A is virtually the same for all the anthracite samples. The inertia term B depends on δ_o, increasing with increase of relative roughness. In Fig. 4, B is plotted against δ_o in logarithmic coordinates. The values of B for the different anthracite samples fit fairly well on one straight line, which suggests that the function $B(\frac{\delta}{r})$ may be represented as a power function.

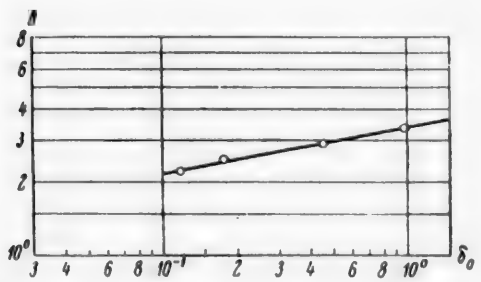

Fig. 4. Variation of B with δ_o for crushed anthracite.

It must also be noted that Kagan [17] used deviations of $\zeta = f(Re)$ curves for estimation of surface roughness of the materials studied.

Analogous conclusions may also be drawn in relation to the influence of the structure of the bed. Zhavoronkov, in his studies of the hydraulics of the scrubbing process [19] showed that the hydraulic resistance of ordered packings depends on the arrangement of the packing elements in the bed.

Martin, McCabe, and Monrad [20], in a study of the effect of arrangement of the spheres in a bed on resistance found that their data can be easily correlated for the streamline region. This was impossible for the turbulent region. These experiments indicate that the bed structure has different effects on linear losses due to viscosity forces and quadratic losses due to inertia forces.

* Here r is the grain radius (m), and δ is the average height of the projections (m).

Finally, it should be noted that Minskii [13], in his binomial equation for resistance in turbulent filtration through porous media, gives the second term as the function $\frac{d_g}{l}$, where l is the average transverse diameter of the pore channels. The ratio $\frac{d_g}{l}$ characterizes the degree of convolution or macroroughness of the pore channels.

SUMMARY

1. Experimental data on the resistance of a granular bed, covering the whole range of Reynolds numbers, can be correlated most effectively by means of the binomial Equation (9). This equation should be regarded as an expression for the general law of resistance.

2. Experimental results show that different factors may have unequal effects on the constants A and B in Equation (9). Foremost among these factors are surface roughness of the grains and the structure of the bed. In particular, the available data indicate that B in Equation (9) should be regarded as a certain function $B\left(\frac{r}{\delta}\right)$ of the relative roughness.

3. To expand this relationship and to derive a generalized expression for the resistance law it is necessary to carry out special experiments over a wide range of Reynolds numbers, covering the streamline, transitional, and turbulent regions for each material.

4. In the absence of a generalized relationship of this type, reliable results can be obtained only by the use of values of A and B in Equation (9) determined experimentally for a given material.

5. The correction factor in the resistance equation (of the type of the bed coefficient φ_g) are not constant over the entire range of the Reynolds numbers, and correlation of experimental data with the aid of such factors is approximate only. If this method is used it is necessary to confirm that the inevitable error does not exceed the permissible limits. The bed coefficient φ_g itself should be determined from the results of a number of determinations in a given range of Reynolds numbers.

LITERATURE CITED

[1] I. M. Fedorov, in the book: Modern Problems of Drying Technology, edited by Prof. M. Yu. Lur'e [in Russian], 2 (GÉI, 1941) p. 64.

[2] L. A. Akopyan and A. G. Kasatkin, J. Chem. Ind. 2, 94 (1955).

[3] A. A. Komarovskii, M. S. Verteshchev, and V. V. Strel'tsov, Trans. Novocherkassk Polytech. Inst. 41 (55), 41 (1956).

[4] V. V. Strel'tsov and A. A. Komarovskii, Trans. Novocherkassk Polytech. Inst 44 / 58, 3 (1957).

[5] G. Schneebeli, La Houille Blanche, 10, 2, 141 (1955).

[6] M. A. Velikanov, Bull. Sci. Melior. Inst. 14, 78 (1926).

[7] M. A. Velikanov, Bull. Acad. Sci. USSR, OTN, 7-8, 638 (1945).

[8] E. Lindquist, Premier Congres des Grands Barrages, V, Stockholm, 81, (1933).

[9] F. Engelund, Trans. Danish Acad. Techn. Sci. 3 (1953).

[10] S. Ergun and A. A. Orning, Ind. Eng. Chem. 41, 6, 1179 (1949).

[11] S. Ergun, Chem. Eng. Progress, 48, 2 89 (1952).

[12] N. M. Zhavoronkov, K. É. Aérov, and N. N. Umnik, J. Phys. Chem. 23, 3, 342 (1949).

[13] E. M. Minskii, Proc. Acad. Sci. USSR 78, 3, 409 (1951).

[14] D. M. Mints and S. A. Shubert, Hydraulics of Granular Materials [in Russian] (Min. Com. Ind. RSFSR Press, 1955).

[15] J. L. Huitt, J. Am. Inst. Chem. Eng. 2, 2, 259 (1956).

[16] M. Leva, M. Weintraub, M. Grummer, M. Pollchik, and H. H. Storch, U.S. Bur. Mines, Bull. 504 (1951).

[17] S. M. Kagan, in the book: New Soviet Power Equipment [in Russian] (Central Sci. Res. Inst. for Boilers and Turbines, Leningrad, 1939) p. 125.

[18] S. M. Kagan, in the book: Investigation of Combustion Processes of Natural Fuel [in Russian] edited by G. F. Knorre (GÉI, 1948), p. 49.

[19] N. M. Zhavoronkov, Hydraulic Principles of the Scrubbing Process and Heat Transfer in Scrubbers [in Russian] (Soviet Science Press, 1944).

[20] J. J. Martin, W. L. McCabe, and C. C. Monrad, Chem. Eng. Progr. 41, 2, 91 (1951).

Received January 23, 1958

EFFECT OF VIBRATORY GRINDING ON THE PROPERTIES OF CARBON BLACK FOR CARBON–GRAPHITE MATERIALS

A. S. Fialkov and I. V. Temkin

During recent years the vibratory method of grinding has become widely used in industry [1-7]. Its most important advantage over other methods is that the material being ground is subjected to high-frequency alternating loads which produce considerable fatigue stresses in it. This method was used by us in production of carbon–graphite materials by simultaneous grinding and mixing of carbonaceous materials and high-temperature coal-tar pitch [8]. The results obtained indicate that the vibratory method for production of carbon–graphite compositions is very promising.

One component which determine the properties of these materials is carbon black. Its use, in particular, in production of electrical brushes containing agglomerated carbon-black structures [9, 10] involves considerable difficulties associated with the persistent instability of their properties.

In the present investigation the influence of vibratory grinding on the properties of carbon black is considered.

EXPERIMENTAL*

Carbon black was ground in an M-10 vibratory mill of the laboratory type, with a cylinder 10 dm^3 in capacity, vibrated at a frequency of 25 cps with an amplitude of 3 mm. The grinding balls weighed 3.3 kg, and the weight of carbon black was 0.5 kg. The grinding was performed at 20-25° in cycles of 5, 10, 15, 20, and up to 70 minutes. The bulk density and absorption for nonpolar kerosene were determined for the treated carbon black. The nominal specific surface was measured by means of the FÉK-M electric photocolorimeter.

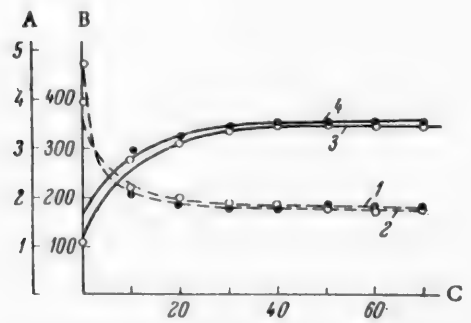

Fig. 1. Effects of grinding time in a vibratory mill on absorption of nonpolar kerosene (1, 2) and bulk density (3, 4) of lamp black: A) absorption of nonpolar kerosene (ml/g), B) bulk density (g/dm^3), C) grinding time (minutes); lamp black: 1) 3-No. 1, 2) 4-No. 2.

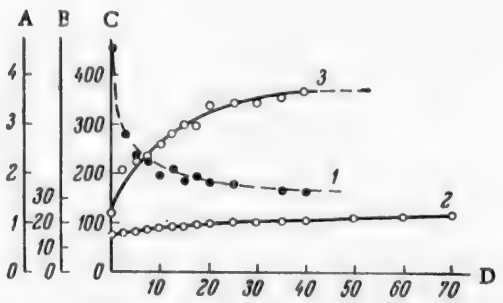

Fig. 2. Effects of grinding time in a vibratory mill on absorption of nonpolar kerosene (1), nominal specific surface (2), and bulk density (3) of lamp black: A) absorption of nonpolar kerosene (ml/g), B) nominal specific surface (m^2/g), C) bulk density (g/dm^3), D) grinding time (minutes).

* E. B. Beletskaya assisted in the experimental work

The results are presented in Fig. 1-4.

It is seen from these results that when lamp black is ground in a vibratory mill the bulk density and kerosene absorption change sharply during the first 1-5 minutes. These properties remain almost unchanged on further treatment (after 30 minutes).

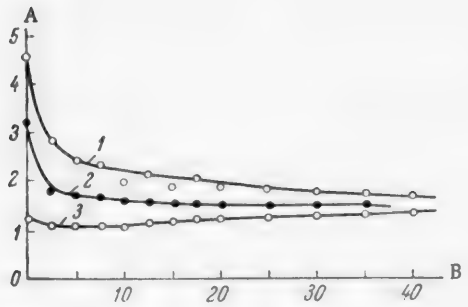

Fig. 3. Comparison of the effect of grinding time in a vibratory mill on bulk density of three types of carbon black: A) bulk density (g/ dm^3), B) grinding time (minutes); carbon black: 1) lamp black, 2) gas channel black, 3) furnace black.

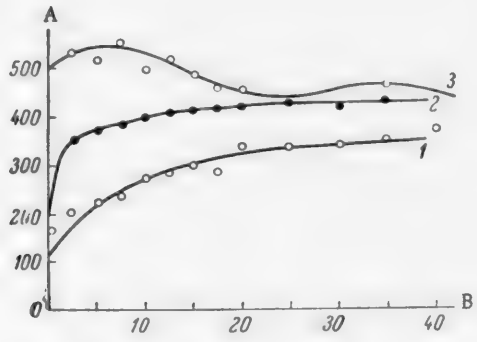

Fig. 4. Comparison of the effect of grinding time in a vibratory mill on absorption of nonpolar kerosene by three types of carbon black; A) absorption of kerosene (g/ dm^3), B) grinding time (minutes); carbon black: 1) lamp black, 2) gas channel black, 3) furnace black.

The bulk density and absorption of kerosene of two samples of lamp black, taken from 2 batches differing in bulk density and kerosene absorption, became almost the same for the two samples after 20 minutes of treatment in the vibratory mill.

The specific surface of lamp black changes only slightly in grinding (Fig. 2).

Electron micrographs (Fig. 5) of samples of lamp black before and after treatment in the vibratory mill, taken at 12000 × magnification in the MÉM-3 electron microscope, showed that the structure of lamp black was broken down after 40 minutes of treatment in the vibratory mill. Thus, the observed changes in the properties of the carbon black are due to extensive disintegration of the chains down ito individual particles.

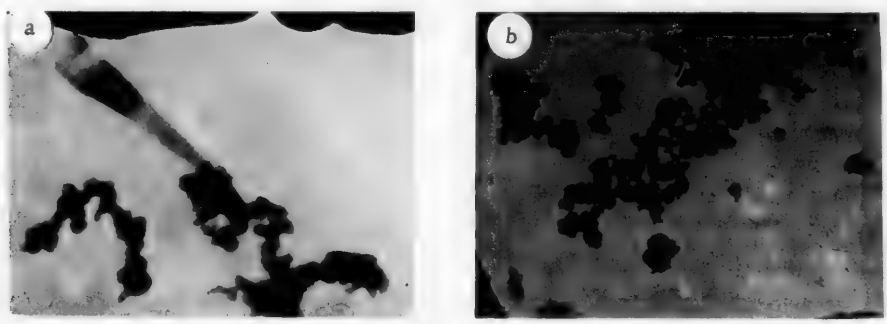

Fig. 5. Electron micrograph of lamp black: a) not ground, b) ground for 40 minutes in M-10 vibratory mill; magnification 9000.

The influence of changes in the structure of lamp black on the properties of carbon–graphite materials was investigated as follows: lamp black from one large batch was divided into two parts. One of these parts, mixed with high-temperature pitch in the proportion of 54.5 vol. % of black to 45.5 vol. % of pitch, was ground

in the M-10 mill for 60 minutes. The density of the lamp black was 1.40 g/cc, ash content 0.06%, kerosene absorption 5.06 ml/g, specific surface 14.16 m^2/g; the high-temperature pitch had a softening temperature of 155°, ash content 0.09%, coke yield 51.7%, free carbon 51.5%.

The other portion was used for preparation of 2 mixtures in the same proportions. The carbon black was mixed with high-temperature pitch, previously crushed in a hammer mill, in a mixer with Z-shaped blades for 60 minutes without heating. All three mixtures were then rolled 4 times in laboratory oil-heated rolls at 195 ± 5°, with a 0.8 mm gap between the rolls. The rolled masses were used for preparation of molding powders of identical grain composition, which were pressed in a mold at 2000 kg/cm^2 into specimens 30 × 40 × × 70 mm in size. The molded specimens were fired in a PA-32 electric furnace at 950° and graphitized in an RS-400 variable-resistance electric furnace at 2600°.

The physical and mechanical properties of graphitized specimens made from treated and ordinary carbon black with the same amounts of binder (high-temperature pitch) are given in the table.

It is seen that specimens made by the vibratory grinding method have considerably greater mechanical strength and hardness.

An important practical result of vibratory grinding for this purpose is that carbon agglomerates of a stable and reproducible structure can be obtained [11]. We attribute this to development of a mechanochemical effect

Physicomechanical and Electrical Properties of Graphitized Intermediate Product Made from Carbon Black and Pitch for Electrical Brushes

Treatment	Ratio of components in dry mixture (vol. %)		Bulk density (g/cc)	Strength (kg/cm^2)		Specific impact viscosity	Hardness H_f	Electrical properties			
	lamp black	pitch		compressive	transverse			specific resistance (ohms · mm^2/m)	wear (mm)	contact potential drop for pair of brushes (v)	coefficient of friction
Combined grinding of carbon black and pitch in M-10 vibratory mill	54.4	45.5	1.83	667	305	1.1	56.6	43.1	0.06—0.04	2.5	0.12
Mixing of carbon black and pitch in mixer with Z-shaped blades	54.5	45.5	1.66	583	168	1.0	17.1	72.0	0.17—0.07	2.2—2.6	0.13
	54.5	45.5	1.57	316	113	1.0	17.1	75.0	0.2 —0.04	2.2—2.5	0.14

of break of the carbon black and pitch structure, which results in the formation of a large number of unsaturated bonds which bind the individual carbon particles into agglomerates.

SUMMARY

1. A study of the effect of vibratory grinding on the properties of carbon black showed that the properties of different batches of carbon black are equalized during grinding.

2. It is shown that high-temperature pitch can be used as a binder in carbon–graphite compositions based on carbon black and pitch; the view is advanced that development of a mechanochemical effect during simultaneous treatment of carbon black and high-temperature pitch in a vibratory mill results in the formation of a considerable number of unsaturated bonds which favor the formation of carbon-black agglomerates.

LITERATURE CITED

[1] D. Bachman, Z. VDI-Beiheft, 2, 3 (1940).

[2] R. Meldau, Z. VDI-Beiheft, 3, 95 (1939).

[3] S. Kiesskalt, VDI-Z., 91, 13, 313 (1949).

[4] M. L. Morgulis, Vibratory Grinding of Materials [in Russian] (Industrial Construction Press, 1957).

[5] P. P. Budnikov and A. S. Mchedlov, J. Appl. Chem. 29, 5, 645 (1956).*

[6] P. A. Rebinder, "Vibratory grinding, the most effective modern method of comminution" [in Russian] Sci. Comm. All-Union Sci. Res. Inst. for Fine Grinding of Structural Materials 17, (1956).

[7] H. Rose, Trans. Inst. Chem. Eng. 35, 2, 98 (1957).

[8] A. S. Fialkov and I. V. Temkin, Authors' Certif. No. 112,831, March 1, 1958.

[9] A. S. Fialkov and P. S. Livshits, Bull Electrical Ind. 5, (1958).

[10] A. S. Fialkov, The Conference of Industrial Carbon (London, 1957).

[11] G. Ya. Tarasov and A. S. Fialkov, J. Appl. Chem. 27, 12, 1296 (1956).*

Received July 5, 1958

*Original Russian pagination. See C.B. Translation.

USE OF GAMMA RAYS FOR DETERMINATION OF SURFACE TENSION AND CONTACT ANGLE AT HIGH TEMPERATURES

D. M. Ziv and B. I. Shestakov

Determination of surface tension at high temperatures involves specific difficulties, and therefore rational selection of a method most suitable for such conditions is of special significance. The choice of method depends on a number of factors: nature of the tested substance, its chemical and physical properties and high temperatures, wetting conditions, viscosity, interface, and the accuracy required. In addition, simplicity of the method and availability of the apparatus are always significant.

For high-temperature determinations static methods [1] for determination of surface tension are more convenient than dynamic, but most of them (the capillary method, the method of maximum bubble pressure, drop counting, surface rupture) require either rather complicated and nonstandard apparatus or capillaries of strictly circular section with constant and accurately determined diameter of total wetting [1]. Under such conditions the sessile- or hanging-drop method is the most suitable, as in such cases the contact angle has no influence on the result (provided that it remains constant around the wetting perimeter), and it is the simplest method experimentally.

Until recently drop contours have been measured either by the optical method by means of a transmitted parallel light beam [2], or by the luminescence of a melted drop [3], or by the solidified-drop method [4]. Whereas by the first of these methods the required accuracy may be attained with some sacrifice of the simplicity of experimental technique, the second method is far from ensuring such accuracy, despite the increased precision of the calculation formulas given in some papers [4].

It has been shown by our experiments and by the work of Popel', Esin, and Gel'd [5] that this method gives discrepancies of up to 20-30% from the values for the surface tension of liquid drops.

Som publications have recently appeared on determinations of interfacial and surface tensions of melted metals with the aid of x-ray photographs of the contours of sessile drops [5-7]. The idea of x-ray photography was used much earlier by Libman [8] for determination of surface tension by the capillary depression method.

This method is very convenient for high-temperature determinations, but the experimental procedure is rather complicated, and therefore the purpose of the present investigation was to test the possibility of using γ-rays for determinations of interfacial and surface tension at high temperatures and in opaque media by the sessile-drop method; this would simplify the experimental technique considerably.

The experiments were performed in a quartz apparatus on graphite or mica supports. The hot junction of a a Pt-Pt/Rh thermocouple was in direct contact with the under side of the support. The apparatus was placed in an ordinary TG-1 crucible tfurnace with a through opening in the direction of the γ-ray beam. The protected γ-ray source was placed on one side of the furnace in the direction of the opening, and the cassette with the film was placed on the other. The apparatus is shown schematically in Fig. 1.

The temperature was regulated by means of ÉPV-01 electronic potentiometer. The experiments were performed in a current of hydrogen. "Roentgen XX" x-ray film with a sensitivity of 35 reciprocal units was used, with lead foil intensifying screens. The distance from the source to the film was 52 cm. The aperture of the lead protection at the exit of the γ-ray beam was 1.5 mm. The γ-ray source in the main experiments

was Eu^{154} with an activity of 740 μ.* The exposure time was 1.5 hours in determinations of surface tension, and about 3 hours in determinations of interfacial tension. The drop dimensions – the maximum diameter d and the height h from it – were determined by means of the MIR-12 microscope.

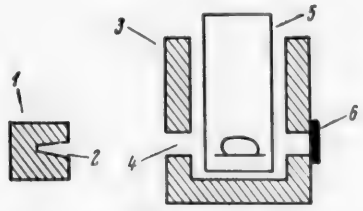

Fig. 1. Diagram of the apparatus: 1) lead protection, 2) radioactive material, 3) TG-1 crucible furnace, 4) opening in furnace, 5) quartz apparatus with drop, 6) cassette with film.

Surface tension was calculated from the formula

$$\sigma = \frac{d^2}{H} \Delta\rho q,$$

where $\frac{1}{H} = f(\frac{d}{2h})$ was found from the tables published by Koshevnik et al. [9], d is the maximum diameter, h is the distance from the maximum diameter to the vertex of the drop, $\Delta\rho$ is the difference between the densities of the drop and the surrounding medium, and q is the acceleration due to gravity.

The following values were determined: the surface tension of mercury, bismuth, tin, and lead; the interfacial tension in the system $Pb-PbCl_2 \cdot KCl$; and the contact angles of mercury on quartz, bismuth, and tin, and of lead on graphite, found to be 137, 143, 120, and 127* respectively. The values of surface tension (average for 2-5 experiments) are compared with literature data in the table.

Results of Surface Tension Determinations

Method	Surface tension σ (dynes/cm)					Literature sources
	air at 20°	hydrogen				
		300°	300*	350°	500°	
Sessile drop	—	563	—	—	—	[10]
	423	—	—	—	—	[5]
	441	—	—	—	—	[11]
Maximum bubble pressure	—	—	—	449	—	[12]
	485	527	388	453	—	[1]
	—	—	383	444	—	[1]
Maximum drop pressure	465	527	376	442	—	[11]
	—	532	—	—	—	[13]
Drop counting	473	—	390	480	—	[14]
	465	—	—	—	—	[11]
Capillary depression	—	—	—	—	226	[15]
Sessile drop	480	530	373	440	235	This investigation

The table shows that the values found for the surface tension are in fairly good agreement with literature data determined by various methods. The experimental error is ±4–7%, and is due to the diffuse nature of the edges of the drop image; the extent of the diffuse region was 0.2-0.3 mm. By analogy with sensitivity in flaw detection in metals by means of γ-rays [16], this value defines the sensitivity of this method as the limiting difference in the blackness of two adjacent regions of the photograph (corresponding to the minimum drop thickness in the direction of the radiation) which can be distinguished by the human eye. Diffuseness of the edges is due to the fact that the difference in the absorption of γ-rays diminishes with decreasing thickness, and the contrast and clarity of the image diminish accordingly. Nevertheless, it is evident that a high degree

* As in original – Publisher's note.

of accuracy in determinations of interfacial tension can be attained only if the difference between the densities of the drop material and the surrounding medium is sufficiently large.

It is natural that the linear attenuation factor increases with decrease of the energy of monochromatic radiation and with increase of the drop thickness and density, and the image contrast increases accordingly. In the case of nonmonochromatic radiation low-energy γ-quanta are absorbed to a greater extent with increase of thickness and density, which has the effect of increasing the hardness of the radiation so that the effective attenuation factor diminishes and the image becomes more diffuse. Therefore, of the three γ-ray sources available – Co^{60}, Cs^{137} and Eu^{154} – the last was chosen after preliminary experiments. Of the γ-ray sources produced in this country [16] this condition is best satisfied by Ir^{192}, Tm^{170}, and partly by $Eu^{154, 152}$. The first two are also convenient because the protection required with their use is 2 to 3-fold less than that required with Co^{60}, but for the same reason their activity must be 6-8 times that of Co^{60} to give the same density in the negative. Moreover, the harmful influence of scattered radiation, with increasing thickness of the material, must be taken into consideration; since its energy is lower than that of the main radiation, the contrast of the image is diminished. Its harmful effects can be partly prevented by the use of lead foil and by restriction of the width of the γ-ray beam to the permissible minimum; this is effected by reduction of the angle of taper of the opening in the protective case for the source.

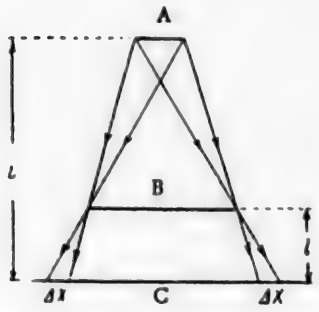

Fig. 2. Effect of geometrical factors on sharpness of this image: A) source of x-rays, B) drop, C) film.

The sharpness of the image is also influenced by geometrical factors such as the dimensions of the source, its distance from the film (the focal length), and the distance from the drop to the film.

It is clear from Fig. 2 that the dimensions of the penumbra Δx are connected with the source dimensions A, focal length L, and distance between the drop and the film l by the expression

$$\Delta x = A\frac{l}{L-l}.$$

The expression shows that the edges of the image become more diffuse with decrease of focal length L; at constant source size A and focal length L, the image becomes more diffuse with increasing distance between the drop and the film. Unfortunately, this factor depends on the furnace dimensions, and sharpness can be increased only by increase of the focal length L and decrease of the source size A. It is therefore desirable to use sources of the highest possible specific activity, which give beams of γ-rays of high intensity. Of the sources available commercially, this condition is best satisfied by Ir^{192}, which has a very high neutron-capture cross section, and partly by Eu^{154}.

The sensitivity–focal length graphs given in Tatochenko's book [17] may be used for tentative selection of focal length. The sharpness of the image also depends on the density of the photograph; it increases with the exposure time if the other factors remain constant. Exposure monograms [16], with data for this source and drop material taken into account, were used for approximate selection of the exposure time, as is done in γ-ray defectoscopy. The exposure time can be reduced 1.5 to 2-fold by the use of "Roentgen XX" film (rather than "Roentgen X" [16]) and of intensifying screens. Lead foil 0.1-0.2 mm thick and fluorescent screens are used for this purpose; the latter shorten the exposure 2 to 3-fold as compared with the use of lead foil, and 5 to 6-fold as compared with direct photography on the film [16], but they reduce sharpness of the image.

Finally, the quality of the photographic processing is also important. The developers specially recommended for this purpose [16] must be used, and the conditions must be strictly followed.

SUMMARY

It is shown that γ-rays can be used in determinations of the surface tension of substances at high temperatures. The method can also be applied to determinations of contact angles at high temperatures and in opaque

media. The method is especially suited for determinations of interfacial tensions in opaque systems at high temperatures: because of deviations, the Antonow rule cannot be always applied without qualification. This method may therefore prove suitable for studying various metallurgical and high-temperature extraction processes.

Of the sources of γ-rays available commercially, Eu^{154} and Ir^{192} are the most suitable for this purpose.

The advantage of the method is its simplicity, while its defects are the considerable time required and the not very high accuracy (4-7%)error). However, if all the necessary conditions are fulfilled the accuracy may be increased.

LITERATURE CITED

[1] N. K. Adam, Physics and Chemistry of Surfaces (State Tech. Press, 1947) [Russian translation].

[2] A. N. Belyaev, Surface Phenomena in Metallurgical Processes [in Russian] (Metallurgy Press, 1952); I. N. Plaksin, Trans. S. M. Kirov Ural Polytech. Inst. 18 (1944).

[3] A. M. Levin, Electrometallurgy [in Russian] (Metallurgy Press, 1952).

[4] M. Humenik and W. D. Kingery, J. Phys. Chem. 57, 359 (1953); J. K. Davis and F. E. Bartell, Anal. Chem. 20, 12 (1948); R. C. Sangster and J. N. Carman, J. Chem. Soc. 23, 6 (1955); Yu. A. Klyachko and L. L. Kunin, J. Appl. Chem. 13, 7 (1940); B. F. Ormont and V. M. Smirnova, Proc. Acad. Sci. USSR 32, 5 (1952); A. A. Leont'eva, Colloid J. 11, 3 (1949); J. Phys. Chem. 29, 7-8 (1945).

[5] S. N. Popel', O. A. Esin, and P. V. Gel'd, Proc. Acad. Sci. USSR 24, 6 (1950).

[6] Mori and Fodzimura, J. Iron and Steel Inst. Japan 40, 3 (1954).

[7] P. Kozakevitch, S. Chatel and M. Sage, Compt. rend. 236, 2, 2064 (1953).

[8] E. Libman, Pr. Nat. Acad. Sci. 13, 8, 588 (1927).

[9] L. Yu. Koshevnik, I. L. Kusanov, and N. M. Lubman, J. Phys. Chem. 12 (1953) [USSR].

[10] H. Siedentopf, Ann. Phys. 61, 235 (1897).

[11] R. Hogness, J. Am. Chem. Soc. XLII, 7, 1621 (1921).

[12] H. Greenway, J. Inst. Metals (London), 74, 133 (1947).

[13] N. L. Pokrovskii and N. D. Galanina, J. Phys. Chem. 23, 324 (1949).

[14] V. K. Semenchenko, Progr. Chem. 6, 777 (1937).

[15] R. Lorenz, and A. Liebmann, Z. phys. Ch. 83, 459 (1913).

[16] S. V. Rumyantsev and Yu. L. Grigorovich, Testing of Metals by Gamma Rays [in Russian] (Metallurgy Press, 1954).

[17] L. K. Tatochenko and S. V. Medvedev, Industrial Gamma-Ray Defectoscopy [in Russian] (Metallurgy Press, 1955).

Received July 31, 1958

COMPARATIVE EVALUATION OF MATERIAL-BALANCE EQUATIONS FOR PLATE TOWERS

A. G. Evstaf'ev, D. D. Zykov, and N. M. Karavaev

After it had been discovered that in plate towers there is a concentration gradient in the liquid and vapor phases along the path of the liquid [1], attempts were made to represent this effect by mathematical equations [2-4]. These attempts consisted of calculations of the material balance for an element of the liquid path, with various assumptions, and subsequent integration for the whole plate length. An attempt is made here to compare these equations and to establish a correlation between them.

Comparison of Symbols Used by Lewis [2], Rukenshtein [3], and the Present Authors [4]

Our symbols	x_{nm}	y_{nm^*}	$y_{(n-1)m^*}$	W	E_{vl}	m
Lewis	x_n	y_n	y_{n-1}	0	E	—
Rukenshtein	x_n	$y_{l=l_0}$	$y_{l=0}$	L	E	$1-s$

I. The material-balance equation for the more volatile component (MVC) for an element dm of the plate length, given by Lewis [2] is

$$E_{vl} \cdot \left(y^{*}_{nm} - y_{(n-1)m^*}\right) dV = W dx_{nm}, \tag{1}$$

where E_{vl} is the extent to which equilibrium is attained between the liquid and vapor (gas); x_{nm} is the concentration of MVC in the liquid at the n-th plate from the bottom of the column, at a distance m from the point of overflow, where m is the path from the point under consideration to the point of overflow, expressed as a fraction of the liquid path along the plate; $y_{(n-1)m^*}$ is the concentration of MVC in the vapor (gas in equilibrium with liquid of the composition x_{nm}; y_{nm}^{*} is the actual concentration of the vapor (gas) directly over a liquid in which the MVC concentration is x_{nm}; W is the amount of liquid flowing down the column (moles/hour); V is the amount of vapor (gas) passing across the full section of the column (moles/hour).

It is assumed in this equation that there is no agitation of the liquid along its path, and no agitation or complete mixing of the vapor in its movements between the plates [$y_{(n-1)m^*} = y_{nm_{in}}$, where $y_{nm_{in}}$ is the MVC concentration in the vapor (gas) entering a liquid of the composition x_{nm}].

II. The Rukenshtein equation [3] is of the form:

$$W\frac{dx_{nm}}{dm} + \frac{d}{dm}\left[c \cdot \xi \cdot f(m) \cdot l_0 \cdot (D+\varepsilon)\right]\frac{dx_{nm}}{dm} =$$

$$= \left[1 - \exp\left(\frac{sHl_0}{V'}\right)\right] V' \cdot a \cdot f(m) \cdot \left(x_{nm} - x^{*}_{(n-1)m}\right), \tag{2}$$

where D is the diffusion coefficient; l_0 is the height of liquid on the plate; f(m) is the width of the plate; ξ is the fraction of the area $l_0 \cdot f(m)$ occupied by the liquid; s is the contact surface between the phases

per unit volume; H is the transfer coefficient; V' is the molar discharge of vapor per unit surface; $x^{*}_{(n-1)m}$ is the molar fraction of MVC in a hypothetical liquid in equilibrium with the vapor reaching the n-th plate; c is the total molar concentration in the liquid; ϵ is the convective mass-transfer coefficient.

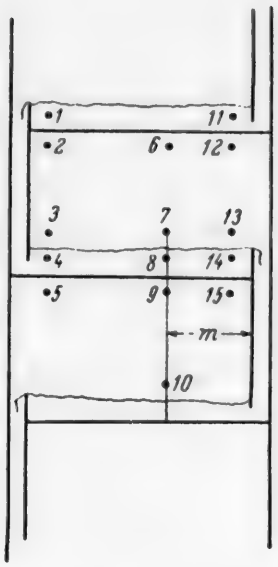

Schematic representation of the concentrations of liquid and vapor (gas) phases in the column: points: 1) $x_{(n+1)0}$, 2) y_{n1}, 3) y_{n1}^{*}, 4) x_{n1}, 5) $y_{n1,in}$ 6) y_{nm}, 7) y_{nm}^{*}, 8) x_{nm}, 9) $y_{mm\ in}$, 10) $y_{(n-1)m}^{*}$, 11) $x_{(n+1)1}$, 12) y_{n0}, 13) y_{n0}^{*}, 14) x_{n0}, 15) $y_{n0\ in}$.

For convenience in comparison, we transform Equation (2). First we place the plate width f(m) by its average value $\overline{f(m)} = h$.

We note that Rukenshtein [3] gives

$$1 - \exp\left(\frac{s \cdot H \cdot l_0}{V'}\right) = E_{Vl} \tag{3}$$

$$a \cdot \left(x_{nm} - x^{*}_{(n-1)m}\right) = y^{*}_{nm} - y_{(n-1)m^{*}}, \tag{4}$$

$$V' \cdot h \cdot dm = dV. \tag{5}$$

We put

$$h \cdot c \cdot \xi \cdot l_0 (D + \varepsilon) = \Theta. \tag{6}$$

In the first approximation it may be assumed that Θ = const.

Substitution of Equation (3)-(6) into Equation (2) and rearrangement gives

$$E_{Vl} \cdot \left(y^{*}_{nm} - y_{(n-1)m^{*}}\right) dV = W dx_{nm} + \Theta \cdot d\left(\frac{dx_{nm}}{dm}\right). \tag{7}$$

It is seen that Equation (7) differs from Equation (1) in the right-hand side, which includes the additional term $\Theta \cdot d \cdot (d\,x_{nm}/\,dm)$, which takes into account agitation of the liquid along its path on the plate.

However, Equation (7), like Equation (1), suffers from the defect that it does not take into account agitation of the vapor in its motion between the plates.

III. The equation proposed by us [4]:

$$E_{Vl} \cdot \left(y^{*}_{nm} - y_{nm\ in}\right) dV = \frac{W}{1 - E_l} \cdot dx_{nm}, \tag{8}$$

where E_l is the degree of equalization of MVC concentrations in the liquid.

As before, we perform certain rearrangements for more convenient comparison.

In accordance with our data [4]

$$y_{nm\ in} = y_{n\,av,\,in} \pm L_{n-1} \cdot (m - 0.5), \tag{9}$$

$$y_{(n-1)m^{*}} = y_{n\,av.\,in} \pm L_{(n-1)^{*}} \cdot (m - 0.5), \tag{10}$$

$$\frac{L_{(n-1)^{*}} - L_{n-1}}{L_{(n-1)^{*}}} = E^{*}_{V}, \tag{11}$$

where: $y_{n\ av.\,in}$ is the average MVC concentration in the vapor (gas) reaching the n-th plate; L_n is the slope of the line representing the change of concentration in the vapor (gas) in the direction of the motion; L_n^{*} is the same, immediately over the liquid; E_V is the degree of equalization of MVC concentrations in the vapor (gas).

We use Equations (9)-(11) and express

$$y_{nm\ in} = \varphi\left(y_{(n-1)m^{*}}\right)$$

as

$$y_{nm\ in} = y_{(n-1)m^*} \mp E_v L_{(n-1)^*} \cdot (m - 0.5). \tag{12}$$

Substituting the value of $y_{nm\ in}$ from Equation (12) into Equation (8) we have

$$E_{vl} = \left[y^*_{nm} - y_{(n-1)m^*} \mp E_v \cdot L_{(n-1)^*} \cdot (m - 0.5)\right] \cdot dV = \frac{W}{1 - E_l} dx_{nm}. \tag{13}$$

Comparison of Equation (13) with Equation (1) shows that Equation (13) differs from Equation (1) not only in the right-hand side, as is the case with Equation (7), but also in the left-hand side.

The right-hand side of Equation (13) contains the additional term E_l, which represents agitation of the liquid; the left-hand side has the term $\mp E_v \cdot L_{(n-1)^*} \cdot (m - 0.5)$ which takes into account, on the one hand, the variable composition of the vapor along the plate, $L_{(n-1)^*}$ and, on the other agitation of the vapor in the space between the plates as it moves away from the plate, E_v.

Thus, Equation (13) is more complete than Equation (1) and (7) and represents the processes taking place both on the plate and in the space between the plates.

It is interesting to note that the same effect of liquid agitation is taken into account in the right-hand sides of Equations (7) and (13). The problem is solved in different ways in the two cases: in the first case by introduction of the term $\Theta \cdot d\,(dx_{nm}/dm)$ and in the second, by introduction of E_l.

Evidently, if we equate the right-hand sides of Equations (7) and (13), we can readily derive the relationship between E_l and $\Theta \cdot d(dx_{nm}/dm)$; then

$$E_l = \frac{\frac{\Theta}{W} d\left(\frac{dx_{nm}}{dm}\right)}{dx_{nm} + \frac{\Theta}{W} d\left(\frac{dx_{nm}}{dm}\right)}. \tag{14}$$

This equation may be written in the form:

$$E_l = \frac{1}{\frac{W}{\Theta} \cdot \frac{\left(\frac{dx_{nm}}{dm}\right)}{\left(\frac{d^2x_{nm}}{dm^2}\right)} + 1}. \tag{15}$$

Since the function x = f(m) is exponential, the ratio of the derivatives is

$$\frac{\left(\frac{dx_{nm}}{dm}\right)}{\left(\frac{d^2x_{nm}}{dm^2}\right)} \approx 1. \tag{16}$$

In this case

$$E_l = \frac{1}{\frac{W}{\Theta} + 1}. \tag{17}$$

The present authors [4] regard E_l as the ratio:

$$E_l = \frac{dX_{nm} - dx_{nm}}{dX_{nm}}, \tag{18}$$

where dX_{mn} is a certain hypothetical change of concentrations over the region nm which would occur if the liquid was not agitated along its path.

From Equations (14) and (18) we have

$$dX_{nm} = dx_{nm} + \frac{\Theta}{W} d\left(\frac{dx_{nm}}{dm}\right), \tag{19}$$

or, in simplified form

$$dX_{nm} = dx_{nm} \cdot \left(1 + \frac{\Theta}{W}\right). \tag{20}$$

Consideration of Equation (14) and (19) shows that the effect of liquid agitation along the plate is taken into account in more detail in the Rukenshtein equation than in the others, so that E_l and dX_{nm} can be interpreted to a certain extent. In this respect Equation (7) is undoubtedly the most general.

However, it must be pointed out that the use of the term $\Theta \cdot d(dx_{nm}/dm)$ to account for the effect of liquid agitation introduces considerable difficulties in the solution of the differential equation in finite differences. Introduction of E_l for the same purpose makes solution simple.

As already noted, Equation (7) gives a more detailed description of the agitation of the liquid along its path but fails entirely to reflect the processes taking place in the vapor phase between the plates. In this respect Equation (13) is more complete, as in addition to describing the process of liquid agitation [although in less detail than Equation (7)] it describes mass transfer in the vapor phase between the plates [the left-hand side of Equation (13)].

LITERATURE CITED

[1] E. Kirshbaum, Chem. Fabrik, 6 (1933).

[2] W. Lewis, Ind. Eng. Ch. 28, 4 (1936).

[3] E. Rukenshtein, J. Appl. Chem. 30, 7, 1012 (1957).*

[4] A. G. Evstaf'ev, D. D. Zykov, and N. M. Karavaev, Bull. Acad. Sci. USSR, OTN, 8 (1955).*

Received November 10, 1957

* Original Russian pagination. See C.B. Translation.

ELECTROLYTIC TREATMENT OF SINTERED-ALLOY DIES*

N. V. Sokolov and A. I. Levin

The S. M. Kirov Polytechnic Institute of the Urals.

Compact sintered-metal alloys have exceptional hardness, and they are therefore widely used in many branches of industry for cutting tools, punches, drills, and dies for wire drawing.

The mechanical abrasive method of sharpening, cutting, and grinding of superhard alloys is very laborious and involves the use of costly grinding materials. Therefore new electrical and electrochemical methods for treatment of hard metals and alloys have been used in industry in recent years. Mention should be made of the electric spark method proposed by Lazarenko [1], based on the action of high-frequency impulse discharges on the treated metal.

In Gusev's anodic-mechanical process [2] electrochemical (anodic) dissolution is combined with mechanical removal of the dissolution products.

An important defect of these methods is that the cathode undergoes breakdown and wear during the treatment, so that articles of very inaccurate dimensions are obtained. For example, in treatment of sintered-metal dies, wear of the cathode makes it difficult to obtain a channel of specified profile, i.e., of definite taper angle, in the die. Because of this, these methods have not been widely accepted for treatment of dies with circular orifices.

At the same time, dies made by powder metallurgy are the main and most commonly-used tools for wire drawing; hundreds of thousands are in use.

For production of high-quality wire the die must have a definite channel profile, which depends on the degree of reduction and cold working and other important characteristics of the drawing process. In addition, energy requirements in drawing are determined by the finish and properties of the surface of the deforming portion (hole) of the die.

It is clear that improvement of die quality by improvements in methods of die treatment is an important problem in modern production of steel wire and various alloy wires.

The high standards required in die production are best satisfied by the electrolytic finishing method in the form in which it was widely adopted in industry after a number of improvements.

It must be emphasized that electrolytic treatment of metals and alloys is in principle a new method which cannot be regarded as a simple variation of the anodic-mechanical process, although the two have a number of features in common [2, 3].

Although the use of electrolytic process of metal finishing has grown very rapidly, the mechanism and characteristic of this process have been studied very little, so that the potentialities of the anodic dissolution process cannot be fully utilized or assessed. A special study of electrolytic finishing of sintered-carbide alloys was therefore carried out. The apparatus is shown schematically in Fig. 1.

The sintered alloys VK3, VK6, and VK8 consist mainly of tungsten carbide and cobalt (Table 1).

* L. I. Shchetkin took part in the experimental work.

TABLE 1

Chemical Composition of Sintered Alloys

Alloy	Contents of elements (%)			
	WC	W	C	Co
VK3	97	91	6	3
VK6	94	88.3	5.7	6
VK8	92	86.5	5.5	8

Anodic dissolution of tungsten conforms to the equation [4]

$$W + 8OH^- - 6e \rightarrow WO_4^{2-} + 4H_2O. \quad (1)$$

Since tungsten (in the form of WC) is the principal element in these alloys, alkaline electrolytes were used for their treatment. It is true that it is reported in the literature [5] that certain organic acids (oxalic, citric, acetic) may be used for revealing tungsten carbide by electrolytic etching. However, these reagents are clearly unsuitable for mass finishing of dies because of their high cost.

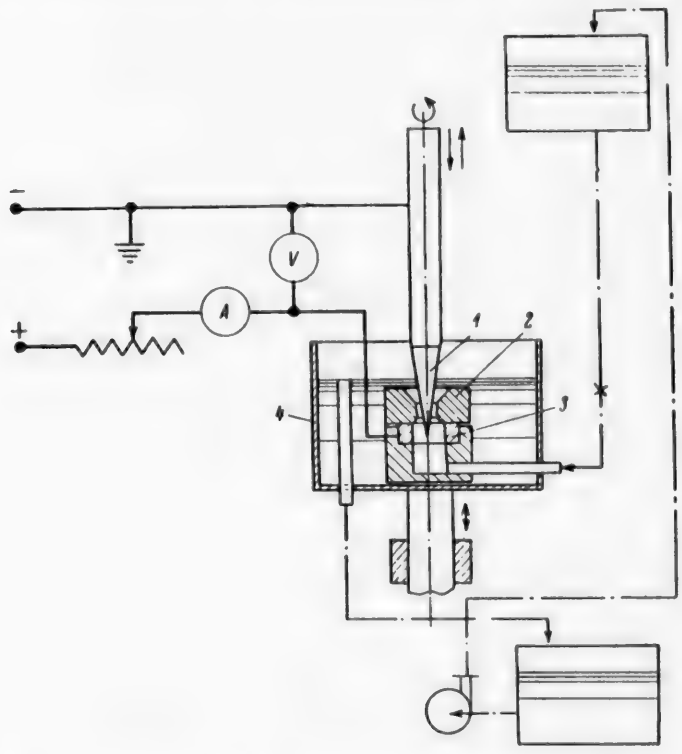

Fig. 1. Diagram of unit for electrolytic treatment of dies: 1) conical cathode, 2) treated die (anode), 3) contact plate, 4) electrolytic cell.

Tungsten and cobalt, like chromium [6], tend to become passive, and therefore it is probably necessary to introduce depassivators into the solution for successful anodic dissolution of these metals at a fairly high current efficiency. The chloride ion is the most powerful depassivator [7]. It may be introduced into the electrolyte in the form of soluble salt (NaCl, KCl, and others).

Analysis showed that in treatment of the sintered alloys ionization of the alloy components is accompanied by liberation of carbon dioxide. It was therefore decided that NaOH or KOH should not be used, as they would be rapidly converted into carbonates. Therefore a solution of soda ash mixed with common salt was used as the electrolyte. Solutions containing 20-100 g Na_2CO_3 and 20-100 g NaCl were tested.

Analysis of the products formed by ionization of the sintered alloy showed that when tungsten dissolves, the compound Na_2WO_4, readily soluble in water, is formed. Cobalt, on the contrary, gives sparingly soluble carbonates of the type $CoCO_3$ and $Co_2(OH)_2CO_3$. The experiments showed that carbon is oxidized to CO_2 during anodic treatment. The dissolution of tungsten carbides was particularly favored by liberation of oxygen at the anode according to the equation

$$2OH^- - 2e \rightarrow H_2O + \frac{1}{2} O_2. \qquad (2)$$

The calculated quantities of electricity required to dissolve the individual elements in VK6 alloy are given in Table 2.

The data in Table 2 show that the electrochemical equivalent of VK6 alloy corresponds to 0.75 g/amp-hr; 38% of the electricity is consumed for conversion of carbon into CO_2.

TABLE 2

Consumption of Electricity for Dissolution of the Individual Elements in VK6 Alloy

Elements	Contents of elements in alloy (%)	Electrochemical equivalent (in g/amp-hr)	Quantity of electricity required to dissolve the elements in 100 g of alloy	
			in amp-hr	in %
W	88.3	1.145	77.2	57.8
Co	6.0	1.10	5.5	4.1
C	5.7	0.112	50.8	38.1
Alloy ...	100.0	0.75	133.5	100.0

Note. The electrochemical equivalent of carbon was calculated for the reaction $C + 2O \rightarrow CO_2$.

Copying power of electrolyte for anodic treatment. In treatment of dies, a channel profile of the required configuration can be obtained with the aid of a cathode of definite shape. This is achieved most simply if the channel (anode) exactly reproduces the shape of the anode as the result of the treatment. Thus, whereas in electroplating the principal aim is to obtain a uniform distribution of current and metal over the coated article (cathode), in anodic treatment the opposite effect is desired; this consists of maximum irregularity of current distribution. In that case, the worse the throwing power of the electrolyte the better its copying power, which gives rise to the required channel profile which reproduces the complex shape of the cathode.

The equation for current distribution [8] can be used to derive an expression for the copying power K_e of the electrolyte,

$$K_e = \frac{\Delta l}{\varkappa \frac{\Delta \varphi}{\Delta i} + l}, \qquad (3)$$

where Δl is the difference between the distance from the cathode to separate regions of the treated anode; l is the distance between the electrode; $\varkappa$ is the specific conductance of the electrolyte solution; $\Delta\phi/\Delta i$ is the rate of change of polarization with the current density at the anode.

It follows that the copying power of the electrolyte increases with decrease of the specific conductance κ of the electrolyte and of the distance l between the electrodes.

Whereas in electroplating the distance between the electrodes is usually several centimeters, in anodic treatment of dies the distance should be as small as possible; it is determined mainly by the design characteristics and the accuracy to which the apparatus for electrolytic treatment can be set. For example, in the units installed in one plant the distance between the electrodes is only 0.1-0.3 mm. It is true that short circuiting mayoccur with such short interelectrode distances, but this difficulty is eliminated in practice by specially accurate setting.

It also follows from Equation (3) for copying power that the copying process improves with decrease of anode polarization. It follows that copying should be improved by intensive circulation of the electrolyte and by the presence in the electrolyte of depassivating ions which suppress polarization at the anode (die). Nevertheless increase of the electrolyte temperature, which also diminishes polarization, is not advisable, as it raises the specific conductance of the electrolyte and has an adverse effect on the surface finish of the die channel.

Determination of the optimum conditions for anodic treatment of dies made from VK6 alloy. The effects of treatment conditions on copying of the cathode profile, amount of alloy dissolved, and the surface finish of the conical hole were studied with an electrolyte containing 20 g of Na_2CO_3 and 20 g of NaCl per liter.

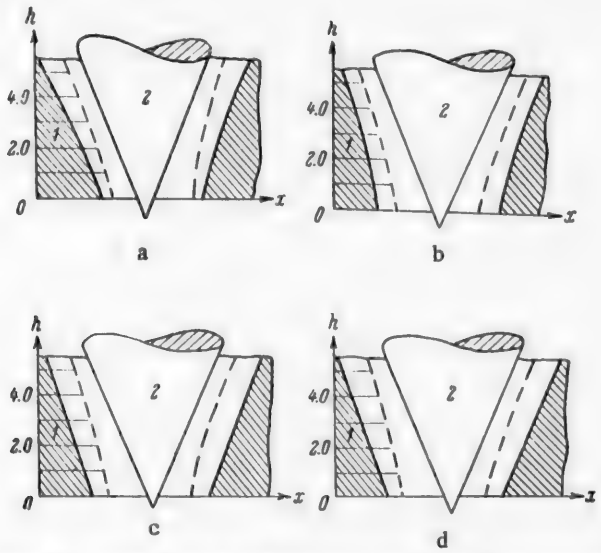

Fig. 2. Effect of the rate of circulation of the electrolyte on the accuracy of copying of the cone (cathode) profile: circulation rate v (ml/ minute): a) no circulation, b) 80, c) 160, d) 400; the dash lines indicate the channel profile before the electrolytic treatment. 1) Dies, 2) conical cathode.

The copying accuracy of the cathode profile was determined by means of a microscope with a special optical system. The profile of the conical channel was determined before and after treatment. The surface finish was studied by means of an interference microscope (MIS-11). The amount of alloy dissolved was found from the weight loss of the dies after treatment and from the quantity of electricity passed.

The effect of the circulation rate of the electrolyte is shown in Fig. 2.

It follows from Fig. 2 that copying of the cathode profile improves with increasing rate of circulation of the electrolyte. At a higher temperature (55°) copying deteriorates, as selective dissolution of individual alloy

components takes place. The electrolyte temperature apparently should not exceed 45°. As already noted, decrease of the interelectrode distance to 0.13 mm results in an improvement in the surface finish of the die cone.

The results of an investigation of the effects of certain other factors in electrolysis on the amount of alloy dissolved are given in Table 3.

TABLE 3

Variation of the Amounts of VK6 Alloy (in g/amp-hr) Dissolved at the Anode with the Electrolyte Composition and Conditions of Treatment of the Die Cone; Treatment Time 10 minutes

Factors studied	Average current strength (amp)	Average amount of alloy dissolved (in g/amp-hr)
Electrolyte composition (g/liter):		
fresh – Na_2CO_3 20, NaCl 20	3.5	0.84
W 8.2	3.6	0.68
W 13.8	4.5	0.56
Cathode rotation rate (rev/min):		
0	4.9	0.71
300	4.7	0.76
660	3.5	0.79
Cathode vibration amplitude (mm):		
0	4.3	0.71
1	4.3	0.70
2	4.3	0.74
3	4.3	0.85

Note. The electrolyte was circulated through the die channel (Fig. 3) in all experiments.

It is evident from the experimental data that the anodic current efficiency falls considerably as the original electrolyte becomes richer in tungsten. On the other hand, increase of the rotation rate and vibration amplitude of the cathode raise the anodic current efficiency. At the same time increase of the cathode amplitude has an adverse effect on copying.

Thus, all these factors must be taken into account when the process conditions for anodic treatment of dies are established.

Possible acceleration of anodic treatment of dies. It is known [9] that any electrochemical process can be intensified by the use of higher current densities, but when the possibilities of such increase have been exhausted the electrolytic treatment can be evidently accelerated by some other means, such as improvements of methods for removal of the electrolysis products from the narrow die channel. In this connection special attention was paid in the investigation to improvement of methods of electrolyte circulation, on the assumption that the better the circulation the more rapidly are the anodic reaction products removed from the treatment zone.

Four methods of electrolyte circulation, tested in die treatment, are shown schematically in Fig. 3.

In the method shown in Fig. 3, a, electrolyte circulation was effected by movement of the cathode only. Figure 3, b shows circulation of the electrolyte effected within the bulk of the electrolyte which did not flow through the die channel. This method had little effect (in comparison with that of Fig. 3, a) on the treatment of the die channel, but it did ensure more stable temperature conditions in the cell.

A circulation method which ensured electrolyte flow directly through the die channel is shown in Fig. 3,c; this circulation method is now used in one plant in all the units for electrolytic die treatment. This method has improved the quality of the finish and raised the output of the units.

However, increase of electrolyte circulation as shown in Fig. 3, c is not entirely satisfactory, as the normal process of anodic treatment is disturbed by removal of the die from the contact plate by the strong stream of electrolyte.

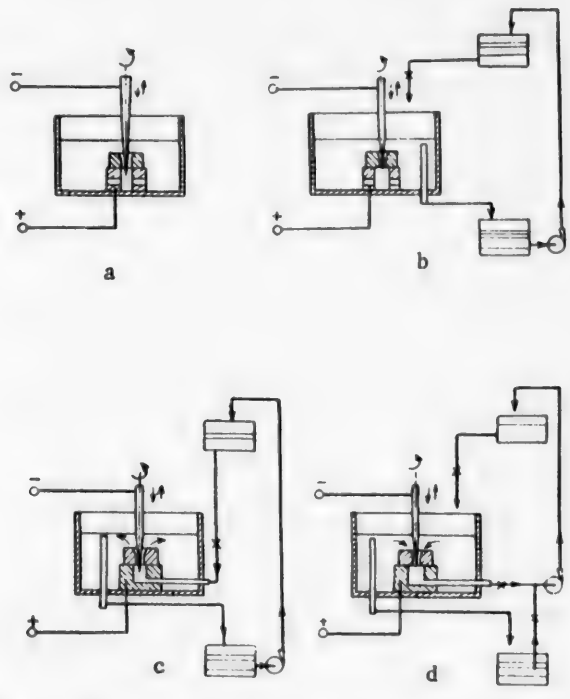

Fig. 3. Electrolyte circulation systems: a) by motion of the cathode, b) circulation outside the die channel, c) flow of electrolyte through die channel, d) forced circulation (by means of a vacuum pump) of electrolyte through the die channel.

Figure 3, d represents a new and improved system of electrolyte circulation, recently suggested and tested. In this system the electrolyte and electrolysis products are withdrawn from the die channel by way of a special vacuum pump. This circulation method gives much higher rates of electrolyte flow through the die channel and at the same time allows the use of particularly high current densities (5 to 10 times as high as in the system shown in Fig. 3, c), so that the dissolution rate of the alloy is raised from 0.02 to 0.15 mm/ minute. At the same time the vacuum fixes the die firmly by suction to the contact plate, which undoubtedly favors more accurate finishing of the tapered channel.

The vacuum system of electrolyte circulation gives a much better surface finish, which reaches a rating of 9 or 10. In treatment by the system 3, c the surface finish is generally not better than class 8.

Use of enforced electrolyte circulation by the new system solves the problem of treatment of dies with particularly small orifice diameters (less than 0.8-1.0 mm).

Electrolytic treatment of dies results in a considerable saving of resources and abrasive materials in comparison with mechanical abrasive grinding. The speed of electrolytic finishing proved to be considerably higher than that of mechanical abrasive finishing; the durability of the dies was also increased by a factor of approximately 1.5.

SUMMARY

1. The anodic dissolution of sintered alloys (of the VK6 type) in alkaline media is considered, conditions for good copying of the cathode are discussed, and the advantages of the electrolytic method for treatment of sintered-alloy dies over mechanical abrasive grinding are demonstrated. Experimental data are presented confirming that channels of very complex configuration and of predetermined dimensions can be produced.

2. Systems of electrolyte circulation are considered. The considerable advantages of a new circulation system with removal of electrolyte from the die channel by means of a vacuum pump are demonstrated.

LITERATURE CITED

[1] B. R. Lazarenko and N. I. Lazarenko, Electric Spark Treatment of Metals [in Russian] (Gosenergoizdat, 1950).

[2] V. N. Gusev, Anodic–Mechanical Treatment of Metals [in Russian] (Mashgiz, 1952).

[3] A. G. Sarkisov, Physicochemical Principles of Anodic–Mechanical Cutting of Metals [in Russian] (Kuibyshev, 1952).

[4] S. Glasstone, Introduction to Electrochemistry (IL, Moscow, 1951) [Russian translation].

[5] L. Ya. Popilov and L. P. Zaitsev, Electrolytic Polishing and Etching of Metallographic Sections [in Russian] (Metallurgy Press, 1955).

[6] A. I. Levin and A. I. Falicheva, J. Phys. Chem. 28, 1952 (1954); 29, 91 (1955).

[7] A. I. Levin, Coll. Trans. Urals Polytech. Inst. 43,(1953).

[8] A. T. Vagramyan and T. B. Il'ina-Kakueva, Current Distribution on Electrode Surfaces in Electrodeposition of Metals [in Russian] (Metallurgy Press, 1955).

[9] A. I. Levin and O. A. Esin. Trans. Urals Industrial Inst. 27, 79 (1947).

Received March 28, 1958

METHOD FOR DETERMINATION OF EXCHANGE CURRENT AT A SOLID METAL SURFACE BY MEANS OF RADIOACTIVE TRACERS

V. L. Kheifets and S. E. Vaisbrud

The "Gipronikel'" Planning and Scientific Research Institute, Leningrad

The use of radioactive isotopes for studying exchange between phases and, in particular, exchange across metal–electrolyte interfaces was initiated by the work of Hevesy [1] who demonstrated, in the case of lead, the existence of exchange between metal atoms and its ions in solution. The first electrochemical investigation in this field was performed by Groh [2], who studied exchange between amalgams of lead and bismuth and solutions of the corresponding salts. His values for exchange rates are very inaccurate because of the serious faults in the method used. In studies of exchange between metallic silver and $AgNO_3$ solution Rollin [3] found that the number of atomic layers involved in the exchange depends on the method used for previous treatment of the metal, and varies from 10 to 150 layers calculated for the geometrical surface. According to Coffin and Tingley [4], exchange on silver affects from 10 to 1000 atomic layers; this result is not in agreement with the data of Rollin or of Simnad and Ruder [5], and is in all probability due to increase of the true surface area when metals are dissolved in acid solutions. According to Simnad and Ruder, who studied exchange between cobalt and solutions of its ions, exchange affects 5-6 atomic layers calculated for the geometrical surface.

The first attempt at quantitative analysis of the exchange process from the kinetic aspect by direct study with the aid of radioactive tracers was made by Haissinsky and his co-workers [6-12]. The data obtained for exchange between metals and solutions conform to an empirical equation which, however, cannot be derived on general kinetic considerations [13].

According to Haissinsky's data, exchange at a solid metal surface involves hundreds or thousands of atomic layers. This result, which he attributes to disturbance of the structure in the course of exchange, may be the consequence of changes in the surface as the result of the corrosion of metallic specimens in acid solutions. Conclusions were drawn concerning the influence of the nature of the anion on the rate of exchange; this also depends on the nature of the metal and, for a given metal, on the concentration of the anion and the time of contact between the metal and solution [7]. At the same time it is known [14] that if anions do not have a tendency to specific adsorption then the rate of transfer of ions from solution to metal and back depends on the thermodynamic activity of the given ion in solution (and also of the metal in the amalgam) and the potential difference at the metal–solution boundary; that is, it depends, in the final analysis, on the nature of the exchanging metal and the activity of its ions in solution. Consequently the influence of the anion must reduce to its influence on the activity of the exchanging cation in solution; such an influence can hardly be expected in dilute solutions.

Haissinsky's results in all probability involve a number of experimental errors to which attention was drawn in discussion of his work [13]. Therefore, Haissinsky's data and conclusions should be treated with caution.

Miller and Pleskov [15] were the first to measure the exchange current directly. For lead, bismuth, and zinc amalgams they obtained values of 0.04 to 0.1 amp/ cm^2 for the exchange current. The calculations were performed by means of the equation

$$i_0 = \frac{1}{QSt} \cdot \frac{AB}{A+B} \cdot \ln \frac{n_\infty}{n_\infty - n}, \qquad (1)$$

where i_0 is the exchange current, Q is the electrochemical equivalent, S is the interfacial area, A and B are the amounts of exchanging metal in the amalgam and solution, and n and n_∞ are the activities of the solution at time t and after equilibrium distribution of the radioactive isotope between the vigorously agitated phases has been reached. The derivation of Equation (1) indicates that exchange between volume phases was studied; this is also shown by the use of an amalgam as the original active phase. The electrocapillary maximum was shifted by the use of amalgams instead of individual metals. These two factors - exchange between the volume phases and shift of the electrocapillary maximum - caused the value of the exchange current at amalgam electrodes to be so high. Therefore, we cannot accept the view [16] that the exchange current should be greater for pure metals than for amalgams.

It has been suggested [17] that the equation for the rate of exchange at an amalgam electrode can also be used for determination of exchange current at a solid electrode. The use of an equation for heterogeneous exchange between liquid phases cannot be regarded as valid in the case of a solid electrode, as here the distribution conditions of the labeled atoms in the metallic phase are quite different because of the extremely low rate of self-diffusion in metals at low temperatures.

In studies of exchange on solid metallic silver, Gerischer et al. [18, 19] concluded that equilibrium distribution of radioactive atoms between metal and solution, determined by exchange as such, is reached very rapidly and that the exchange affects 1-2 atomic layers. The exchange current was estimated at about 0.01 amp/ cm^2. This value was obtained from an approximate equation for the steady process at an electrode undergoing exchange and anodically polarized.

$$c = \frac{i}{\frac{C_0}{C} \cdot \frac{C_0^*}{C^*} - 1}, \qquad (2)$$

where i_c is the cathodic-current density, i is the polarizing-current density, C is the concentration of silver ions in the double layer, C_0 is the corresponding concentration at the equilibrium potential, C^* is the concentration of labeled atoms at the metal surface, and C_0^* is the corresponding concentration after isotopic equilibrium has been reached (at the equilibrium potential). It was found that, despite the precautions taken, exchange which occurs at equilibrium potential cannot be completely avoided after the current is switched off. The results [19] show that the final radioactivity of the specimen is determined to a great extent by this exchange stage. As a result C^* approaches C_0^*, which should give high results, as Equation (2) shows.

It follows that the data presented above do not provide a solution to the problem of exchange current at a solid metallic surface.

General Form of the Equation for Exchange Between Liquid and Solid Phases

When a metal plate is immersed in a solution containing its own ions, labeled by a radioactive isotope, three processes occur simultaneously: transfer of ions from solution to the metal surface, transfer of ions from the metal surface into solution, and decay of radioactive ions. The surface of the plate may become richer or poorer in the isotope, in accordance with the ratio of the specific activities of the solution and the metal surface. This process continues until isotopic equilibrium is reached. Since the electrode surface is not large while the solution volume is fairly large, the number of labeled atoms passing across the interface in the course of exchange has virtually no effect on the total content of labeled atoms in the solution. Therefore, the concentration of labeled atoms in solution may be taken as constant during the entire experiment.

Consider a metal plate in such a solution at a certain instant t, and assume that the product of decay is not radioactive; this is generally the case in decay of artificial radioactive isotopes. The concentration of labeled atoms in the layer at the electrode should change during the exchange process. However, if not one but 20-30 ionic layers are involved in the exchange from the solution side, then calculations shows that the concentration of labeled atoms in the layer near the electrode may be assumed constant with sufficient accuracy. Since the coefficients of diffusion in the liquid are fairly large, it may be assumed that affects of least 20-30 ionic layers of the liquid side. Thus, the concentration of labeled atoms in solution must depend almost entirely on their decay. At the same time, at temperatures far from the melting point, when the coefficient of self-

diffusion in the metal is very small, only the surface layer of metal atoms should be involved in the exchange.

We adopt the following symbols: S_n, the total number of atoms per cm^2 of electrode surface, C_n, the number of labeled atoms per cm^2 of electrode surface, and m, the concentration (in atomic fractions) of labeled ions in solution.

If the volume concentration n of the metal is much greater than the volume concentration n^* of labeled ions in solution, and since $m = n^* / n + n^*$, then $m = m_0 e^{-\lambda t}$, where m_0 is the concentration of labeled ions in solution at the instant of immersion of the plate, and λ is the decay constant.

Transfer of labeled ions from solution to the metal is proportional to their concentration in solution and to the exchange current. Radioactive decay is proportional to the decay constant. Therefore the rate of change of the number of labeled atoms per unit area of the metal is given by the equation

$$\frac{dC_n}{dt} = i_0 m_0 e^{-\lambda t} - i_0 \frac{C_n}{S_n} - \lambda C_n, \tag{3}$$

where i_0 is the exchange current.

Integration of Equation (3) gives

$$C_n e^{\left(\frac{i_0}{S_n} + \lambda\right) t} = m_0 S_n e^{\frac{i_0}{S_n} t} + \text{const.}$$

When $t = 0, C_n = C_{n_0}$, then $\text{const} = -m_0 S_n + C_{n_0}$, and hence

$$C_n e^{\left(\frac{i_0 t}{S_n} + \lambda t\right)} = m_0 S_n \left[e^{\frac{i_0}{S_n} t} - 1\right] + C_{n_0} \tag{4}$$

and finally

$$x_t = m_0 e^{-\lambda t} \cdot \left[1 - e^{-\frac{i_0}{S_n} t}\right] + \frac{C_{n_0}}{S_n} \cdot e^{-\lambda t} \cdot e^{-\frac{i_0 t}{S_n}}, \tag{5}$$

where $x_t = \frac{C_n}{S_n}$ is the concentration (as an atomic fraction) of labeled atoms per unit electrode area.

Methods of Using Equation (5) for Calculation of Exchange Current

Case 1. $C_{n_0} = 0$. Equilibrium distribution of labeled atoms between electrode and solution reached rapidly. At equilibrium the concentration of labeled atoms on the electrode surface is equal to their concentration in solution:

$$x_\infty = m_0 \cdot e^{-\lambda t_\infty}.$$

It follows from Equation (5) that when $C_{n_0} = 0$ the following expression is true for any time interval

$$x_t = m_0 \cdot e^{-\lambda t} \cdot \left[1 - e^{-\frac{i_0}{S_n} \cdot t}\right]$$

hence

$$\frac{x_t}{x_\infty} = e^{\lambda(t_\infty - t)} \cdot \left[1 - e^{-\frac{i_0}{S_n} t}\right]. \tag{6}$$

If isotopic equilibrium is reached rapidly, then the values of t and t_∞, and especially the differences between them, are so small that $e^{\lambda(t_\infty - t)}$ is close to unity. Then

$$i_0 = -\frac{S_n}{t} 2.3 \log\left(1 - \frac{x_t}{x_\infty}\right). \qquad (7)$$

The ratio $\frac{x_t}{x_\infty}$ when $C_{n_0} = 0$, is equal to $\frac{C_{nt}}{C_{n\infty}}$, and can be defined as the ratio of electrode activities at taime t and equilibrium; hence, Equation (7) can be used to calculate the exchange current.

Case 2. $C_{n_0} = 0$. Equilibrium distribution of labeled atoms between electrode and solution reached after a long interval of time. In this case, determination of x_∞ is difficult and it is desirable to have means for determining the exchange current from measurements over shorter time intervals.

By determining C_n for two time intervals t and 2t, we have, analogously to (6)

$$\frac{C_{n_1}}{C_{n_2}} = \frac{x_1}{x_2} = e^{\lambda t} \cdot \frac{\left(1 - e^{-\frac{i_0}{S_n} t}\right)}{\left(1 - e^{-\frac{i_0}{S_n} 2t}\right)}.$$

Denoting $e^{-\frac{i_0 t}{S_n}}$ by k, we have, after substitution and solution of the equation for k

$$k = e^{\lambda t} \cdot \frac{C_{n_2}}{C_{n_1}} - 1,$$

hence

$$i_0 = -\frac{S_n}{t} 2.3 \log\left[e^{\lambda t} \frac{C_{n_2}}{C_{n_1}} - 1\right]. \qquad (8)$$

Equation (8) can be used to calculate the exchange current from two determinations of the electrode activity provided that at the initial instant the electrode surface was free from labeled atoms.

Case 3. $C_{n_0} \neq 0$. Equilibrium distribution of labeled atoms between electrode and solution reached after a long interval of time. The activity of the plate is measured after three time intervals t, 2t, and 3t.

We put $e^{\frac{i_0}{S_n} t} = l$. Then, in accordance with Equation (4), we can put

$$\frac{C_{n_2}}{C_{n_1}} l e^{\lambda t} = \frac{m_0 S_n [l^2 - 1] + C_{n_0}}{m_0 S_n [l - 1] + C_{n_0}}$$

and

$$\frac{C_{n_3}}{C_{n_1}} l^2 e^{2\lambda t} = \frac{m_0 S_n [l^3 - 1] + C_{n_0}}{m_0 S_n [l - 1] + C_{n_0}}.$$

We put $\frac{C_{n_2}}{C_{n_1}} e^{\lambda t} = A$ and $\frac{C_{n_3}}{C_{n_1}} e^{2\lambda t} = B$.

Then

$$Al - 1 = \frac{m_0 S_n (l^2 - l)}{m_0 S_n (l - 1) + C_{n_0}} \qquad (9)$$

and

$$Bl^2 - 1 = \frac{m_0 S_n (l^3 - l)}{m_0 S_n (l - 1) + C_{n_0}}. \tag{10}$$

Division of Equation (9) by (10) gives

$$\frac{Al - 1}{Bl^2 - 1} = \frac{1}{l + 1},$$

and hence

$$l = \frac{A - 1}{B - A}.$$

After substitution and suitable rearrangement we have

$$i_0 = \frac{S_n}{t} 2.3 \log \frac{C_{n_2} \cdot e^{\lambda t} - C_{n_1}}{C_{n_3} \cdot e^{2\lambda t} - C_{n_2} e^{\lambda t}}. \tag{11}$$

Equation (11) can be used for determining the exchange current i_0 from three determinations of plate activity both if an inactive plate was immersed in the solution and if the plate was initially active.

Case 4. $C_{n_0} \neq 0$. No labeled atoms are present in solution. Let the metal plate contain a certain amount C_{n_0} of labeled atoms as the result of previous immersion in a solution containing the radioactive isotope. The plate is then immersed in a solution of a salt of the metal without the radioactive isotope. Exchange between the electrode and solution results in a decrease of plate activity. In this case $m_0 = 0$ and Equation (4) becomes

$$C_n \cdot e^{\left(\frac{i_0 t}{S_n} + \lambda t\right)} = C_{n_0},$$

hence

$$i_0 = \frac{S_n}{t} \left(2.3 \log \frac{C_{n_0}}{C_n} - \lambda t\right). \tag{12}$$

Equation (12) can be used for determination of exchange current from the decrease of plate activity during contact with an inactive solution. The solution must flow past the plate, as otherwise labeled atoms would accumulate in it, so that the assumption of constant concentration of labeled atoms in solution (zero in this instance) is not valid and Equation (12) is not applicable.

If the half life of the isotope is considerably greater than the duration of the experiment decay may be disregarded and all the equations are simplified accordingly.

Equations for the case in which the activity of the solution and not of the metal surface is the dependent variable can be derived analogously. Since in this case the experiment is so performed that the activity of the solution changes with time, the concentrations of labeled atoms both on the metal surface and in solution change simultaneously, and an equation for the rate of heterogeneous exchange analogous to Equation (1) is obtained. It is therefore possible to determine the exchange current on a solid metallic surface from determinations of solution activity, but the sensitivity of the method is considerably lower in this case.

SUMMARY

The possibility of using radioactive tracers for determinations of exchange current at a solid metallic surface is considered and four particular solutions of a general kinetic equation are given; these correspond to

four different variants for determination of exchange current from experimental determinations of radioactivity.

LITERATURE CITED

[1] G. von Hevesy, Phys. Z. 16, 52 (1915).

[2] I. Groh, Z. phys. Ch. 128, 449 (1927).

[3] B. V. Rollin, J. Am. Chem. Soc. 62, 86, (1940).

[4] M. C.Coffin and Y. Y. Tingley, J. Chem. Phys. 17, 502 (1949).

[5] M. T. Simnad and R. C. Ruder, J. Electroch. Soc. 98, 301 (1951).

[6] M. Haissinsky and B. Pullman, J. phys. 8, 33 (1947).

[7] M. Haissinsky, M. Cottin, and B. Verjabedian, J.Chim. Phys. 45, 213(1948).

[8] M. Haissinsky, J. Chim. Phys. 45, 224 (1948)

[9] M. Haissinsky, and M. Cottin, J. Chim. Phys. 46, 476 (1949).

[10] M. Cottin, Compt.Rend. 231, 697 (1950).

[11] M. Anta and M. Cottin, Compt. Rend. 234, 1686 (1952).

[12] M. Haissinsky, Cahier phys. 51, 53 (1954).

[13] R. Audubert, J. Chim. Phys. 45, 228 (1948).

[14] A. N. Frumkin, V. S. Bagotskii, Z. A. Iofa, and B. N. Kabanov, Kinetics of Electrode Processes [in Russian] (Izd. MGU, 1952).

[15] N. B. Miller and V.A. Pleskov, Proc. Acad. Sci. USSR, 64, 323 (1950).

[16] V. A. Pleskov and N. B. Miller, Proceedings of Conference on Electrochemistry [in Russian] (Izd. AN SSSR, Moscow, 1953).

[17] V. V. Losev, Trans. Inst. Phys. Chem. Acad. Sci. USSR, 6, 20 (1952).

[18] H. Gerischer and W. Vielstich, Z. Electroch. Ber. Bunsenges. phys. Chem. 56, 380 (1952).

[19] H. Gerischer and R. P. Tischer, Z. Elektroch. Ber. Bunsenges. phys. Chem. 58, 819 (1954).

Received September 18, 1958

PECULIARITIES OF CATHODIC REDUCTION OF PLATINUM METALS FROM COMPLEX ELECTROLYTES

A. I. Levin and B. A. Pankratov

The S. M. Kirov Polytechnic Institute of the Urals

Electrical deposition of metals of the platinum group from mother liquors involves a number of difficulties, caused mainly by changes in the composition of such electrolytes both with regard to contents of component and with regard to salt saturation. The latter factor is associated with shifts of ionic equilibria in the layers of electrolyte near the electrode during electrolysis [1]. This conclusion is not only consistent with the characteristics of electrodeposition of metals from solutions containing complex anions of variable composition [2], but it follows directly from the physicochemical properties of the platinum metals. These metals, in comparison with most other metals, can vary their chemical properties and charge over very wide ranges. It is known, for example, that some metals of this group have derivatives corresponding to valence states from 1 to 8 [3]. In addition to a strong tendency to complex formation [4], all the metals of the platinum group have high catalytic activity and are capable of forming stable colloidal solutions of different degrees of dispersion [5]. In view of these circumstances there are as yet no reliable data on the laws governing the electrolytic extraction of metals of the platinum group; these metals have been studied very little from the electrochemical aspect. This is illustrated by the contradictory data in the literature on the standard potentials of platinum, palladium, and iridium (Table 1).

The difficulties in determining exact physicochemical constants, including the reversible electrode potentials, is due to the very complicated composition of the complex compounds and the absence of full data on shifts of ionic equilibria in absence of current and during electrolysis in these solutions. This is clearly demonstrated by the values of the potential of palladium in certain solutions of its complex salts, given in Table 2.

TABLE 1

Standard Potentials of Pt, Pd, and Ir on the Hydrogen Scale at 25°

Author	Standard potential (v)		
	Pt	Pd	Ir
Latimer [6]	1.2	0.987	1.15
Muller [7]	0.88	0.72	–

TABLE 2

Potentials of Palladium in Solutions of Its Complex Salts in Absence of Current

Electrolyte	Concentration of Pd^{2+} g-equiv/liter)	φ° (v)
$PdCl_2$	–	+0.8
K_2PdCl_4	$10^{-4.3}$	+0.6
$K_2[Pd(NO_2)_4]$	$10^{-8.6}$	+0.1
$[Pd(NH_3)_4]Cl$	$10^{-16.5}$	−0.35

It is clear from Table 2 that the potential of palladium varies sharply with the composition and concentration of the complex electrolyte. Thus, the stability of the ions predetermines the values of the electrode potentials as well as retardation of dissociation of the complexes.

We investigated shifts of potential in absence of current in various electrolytes containing metals of the platinum group. The determinations were performed by the usual compensation potentiometric method. The values of the potentials at different dilutions in absence of current at 20° are given in Table 3.

As was to be expected (Table 3), the potentials of the platinum metals in solutions of their complex compounds in absence of current depend to a considerable extent on the salt content and concentration of the solution containing the platinum metal, and shift in the negative direction with increasing dilution. The determinations showed that in most cases the potentials are nonequilibrium in character and are not established immediately.

The mother liquors often reach saturation concentrations with respect to various salts. The main components of these solutions are chloride, sulfate, ammonium and nitrate compounds of the noble metals and of metals of the platinum group. Their concentrations vary over very wide limits, from 5-15 mg/liter to 0.5-1 g/liter.

TABLE 3

Changes in the Potentials φ^0 of the Metals of the Platinum Group with Electrolyte Dilution in Absence of Current at 20°

Electrolyte composition	Metal concentration (g/liter)	φ^0 (v)	Metal concentration (g/liter)	φ^1 (v)
H_2PtCl_6	0.486	0.749	0.0486	0.711
H_2PdCl_4	0.500	0.663	0.0500	0.624
H_3RhCl_6	0.500	0.577	0.0500	0.548
H_3IrCl_6	0.479	0.774	0.0479	0.725
$RuCl_6$	0.400	0.396	0.0400	0.350

The contents of base metals (Fe, Ni, Cu, Pb, Sn, As, Sb, Se, Te, etc.) in such solutions may be from 0.5 to 15 g/liter. We studied two groups of mother liquors (Table 4).

One of the most important factors influencing energy consumption in electrolysis of mother liquors is their conductivity. Thus, it was found experimentally* that the specific conductance of solutions of Group I

TABLE 4

Qualitative and Quantitative Compositions of the Mother Liquors

Solution group	Acidity (g/liter)	Concentration (mg/liter)							Concentration (g/liter)				
		Pt	Pd	Rh	Ir	Ru	Au	Ag	Ni	Fe	Pb	Cu	Se+Te
I	8.1	25.7	295.1	59.1	14.09	6.34	1.83	0.04	0.1	3.2	0.1	0.5	1.15
II	14.3	16.0	40.0	8.0	6.0	3.4	0.4	239.0	0.16	8.2	0.65	0.07	0.4

is $\kappa = 0.07678\ ohm^{-1} \cdot cm^{-1}$, and of Group II it is $\kappa_2 = 0.07698\ ohm^{-1} \cdot cm^{-1}$. The close values for the conductivities of the solutions indicate that the part played by compounds of the metals of the platinum group in transport of current is probably negligible. To confirm this, conductivities of pure synthetic solutions of

* Conductivities were determined by means of a bridge with a high-frequency alternating-current generator and a cathode-ray oscillograph as the null instrument [8].

complex compounds of Pd, Pt, Rh, Ir, Ru at concentrations up to 500 mg / liter were determined individually. It was found that the specific conductance of such solutions varies between 0.0022 and 0.0085 $ohm^{-1} \cdot cm^{-1}$. It follows that the conductance of the mother liquors of the compositions given in Table 4 is due mainly to compounds containing base metals.

The data on the composition of the mother liquors show that these electrolytes contain considerable amounts of substances capable of taking direct part in cathodic reduction reactions. This naturally creates certain difficulties in explaining the electrode processes for individual metals. Some new data concerning the mechanism of electrolytic reduction of complex compounds of metals of the platinum group are probably provided by studies of concentrational changes in the catholyte of a solution containing compounds of one of the platinum metals (in a small excess of complex former). Systems containing complex compounds of palladium are of considerable interest. This metal has higher chemical activity than the other platinum metals, and is soluble not only in aqua regia but also in concentrated nitric and hot sulfuric acids.

The complex ions of palladium in Table 2 are not the only ones possible in the mother liquors under investigation. However, here we shall consider only the simplest, namely K_2PdCl_4. The cell in question can then be represented schematically as: $\overline{Pb} \mid K_2PdCl_4, KCl, H_2O \mid \overset{+}{C}$.

The electrolyte could contain the following ions:

$$K_2PdCl_4 \rightarrow 2K^+ + PdCl_4^{2-},$$
$$KCl \rightarrow K^+ + Cl^-,$$
$$H_2O \rightleftarrows H^+ + OH^-.$$

Let x be the fraction of the current carried in the electrolyte by ions of the complex compound K_2PdCl_4, and (1−x) the fraction carried by ions of KCl. Further, let n_1 and n_2 be the transference numbers of the anions in these salts, and A and (1−A) the current efficiencies for Pd and H_2. Then, on the assumption that $PdCl_4^{2-}$ and H^+ ions can be discharged simultaneously at the cathode, we have the following cathode balance which indicates the directions of the changes in the concentrations of individual substances in the catholyte.

Discharge:

$$\left.\begin{aligned} A PdCl^{2-} + 2A\bar{e} &\rightarrow APd + 4ACl^- \\ 2(1-A)\,H_2O &\rightarrow 2(1-A)\,H^+ + 2(1-A)\,OH^- \end{aligned}\right\} \quad (a)$$
$$2(1-A)\,H^+ + 2(1-A)\,\bar{e} \rightarrow (1-A)\,H_2 \quad (b)$$

Transport of current by ions:

$$K_2PdCl_4 \quad 2x(1-n_1)\,K^+ - xn_1 PdCl_4^{2-} \quad (a)$$
$$KCl \quad 2(1-x)(1-n_2)\,K^+ - 2(1-x)\,n_2 Cl^- \quad (b)$$

Total:

$$(A + xn_1)\,K_2PdCl_4 + 2(2A - n_2 - xn_2)\,KCl +$$
$$+ 2(1-A)\,KOH - 2(1-A)\,H_2O - 2\bar{e} + APd + (1-A)\,H_2.$$

It must be pointed out that a number of simplifying assumptions was made in the balance. For example, the effects of diffusion and circulation of the electrolyte, which tend to equalize the solution concentration, were disregarded; nevertheless, even the somewhat distorted picture given by the approximate calculations show that an appreciable rise of pH and increase of KOH concentration would occur at the cathode during electrolysis. This result indicates that the change taking place in the composition and contents of the starting substances in the catholyte layers do not consist merely of loss of K_2PdCl_4, but are more complex. This is due to reduction of $PdCl_4^{2-}$ ions as shown in the balance, i. e., simultaneous deposition of metallic palladium at the cathode.

Concentration changes at the anode can be similarly assessed if it is taken into account that discharge of chloride anions is accompanied by discharge of hydroxyl ions. The anode balance then is of the following form.

Discharge:

$$2A'Cl^- - 2A'\bar{e} \rightarrow A'Cl_2 \quad \text{(a)}$$

$$\left.\begin{aligned} 2(1-A')\,H_2O &\rightarrow 2(1-A')\,H^+ + 2(1-A')\,OH^- \\ 2(1-A')\,OH^- - 2(1-A')\,\bar{e} &\rightarrow (1-A')\,H_2O + \frac{1}{2}(1-A')\,O_2 \end{aligned}\right\} \quad \text{(b)}$$

Transport of current:

$$K_2PdCl_4 \quad -2x(1-n_1)\,K^+ + xn_1PdCl_4^{2-} \quad \text{(a)}$$

$$KCl \quad -2(1-x)(1-n_2)\,K^+ + 2(1-x)n_2Cl^- \quad \text{(b)}$$

Total:

$$xn_1K_2PdCl_4 + 2(1-A')\,HCl - 2(1+n_2x-n_2)\,KCl - \\ - H_2O + 2\bar{e} + \frac{1}{2}(1-A')\,O_2 + A'Cl_2,$$

where A' is the current efficiency for Cl^-, and (1-A') is the current efficiency for oxygen.

It follows that under practical conditions the acidity in the main mass of the electrolyte does not decrease but increases somewhat because of simultaneous discharge of Cl^- and OH^- ions at the graphite anode. Practical data show that, with side processes disregarded, about 65-70% of hydroxyl ions and 30-35% of acid ions (Cl^-) are discharged at the anode.

It should be noted in returning to consideration of cathode processes in mother liquors of more complex composition that cathodic polarization in joint electrodeposition of metals of the platinum group diminishes rapidly with increase of temperature and rate of stirring, and therefore, under otherwise constant conditions, increase of temperature should favor preferential deposition (before hydrogen) of the platinum metals. For a fuller elucidation of electrode processes in the investigated electrolytes we studied electrode polarization accompanying simultaneous discharge of metals of the platinum group from mother liquors.

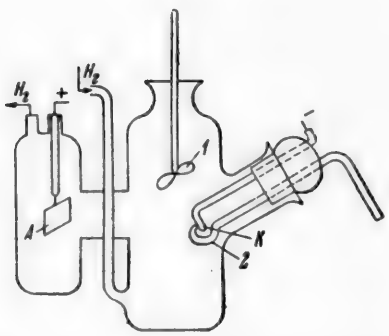

Fig. 1. Cell for measurement of cathodic polarization: A) anode, K) cathode, 1) stirrer, 2) electrolytic bridge.

The polarization curves were determined by the direct compensation method [8, 9]. The cell shown in Fig. 1, 300 ml in capacity with platinum electrodes, was used for electrolysis. The cathode area was approximately 1 cm^2, and its inactive side was coated with glass. A saturated calomel half cell was used as the reference electrode. Hydrogen was passed for 30 minutes before each $i-\varphi$ curve was determined. The cell was contained in a thermostat with temperature regulation (to within ±0.2°). Each determination was repeated several times.

Mother liquors of the composition given in Table 4 were taken for the investigation. The results are plotted in Fig. 2 and 3. The following conclusions may be drawn from analysis of the polarization curves: to reduce polarization the electrolysis must be performed at fairly high temperatures (80-85°) with vigorous stirring. The current efficiency for the platinum metals increases appreciably with increase of temperature and stirring rate.

Examination of the polarization curves obtained for electrolysis of different solutions containing platinum

metals [10] leads to the conclusion that cathodic polarization depends on the acidity of the electrolyte. During the electrochemical process the potential of hydrogen evolution is reached even at low current densities. Evolution of hydrogen lowers current efficiency for the metals and diminishes the rate of extraction of platinum metals from the mother liquors.

Accordingly, a series of pH determinations was carried out during electrolysis of these solutions. It was found that electrochemical deposition of metals of the platinum group is extremely sensitive to the content and concentration of hydrogen ions. For example, at 20°, despite the fact that the deposition potentials of the platinum metals are far more positive than the potential of hydrogen evolution, the cathodic polarization increases by 0.12-0.15 v on increase of acidity to 40 g/ liter (Fig. 3, curve 5). On further increase of the amount of free acid the cathodic polarization increases further, and the deposition potential of the metals of the platinum group is shifted so appreciably in the negative direction that hydrogen liberation begins before the limiting-current region has been passed. This is clearly shown by the data in Fig. 4. Evidently, in this case there is an effect

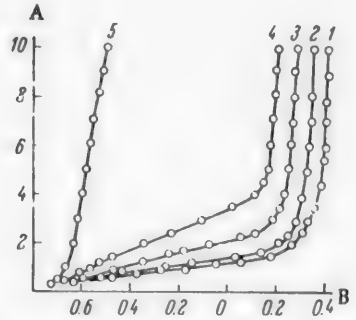

Fig. 2. Polarization curves for solutions of Group I*: A) current density i_c (amp/ dm^2), B) cathode potential φ (v); at temperature (°C): 1) 20, 2) 40, 3) 60, 4) 80, 5) 80 with stirring.

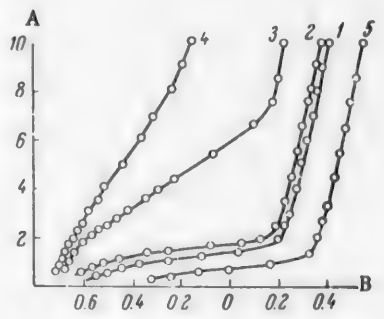

Fig. 3. Polarization curves for solutions of Group II*: A) current density i_c (amp/ dm^2), B) cathode potential φ (v); at temperature (°C): 1) 20, 2) 40, 3) 60 with stirring, 4) 80 with stirring, 5) 20 without stirring, acidity 40 g/ liter.

associated with shift of the dissociation equilibrium toward formation of weakly dissociated complex ions. Moreover, increased acidity has a considerable influence on the redissolution of platinum metals deposited at the cathode. In addition, intensified corrosion occurs because the spongy metal formed on the cathode partially falls to the bottom of the cell, loses electrical contact with the cathode, and is attacked by the acid [11].

It was calculated that the total amount of platinum metals redissolved in 12 hours changes from 0.2% when the acidity is 10 g/ liter to 2% when the acidity is 40 g/ liter. This effect is probably due to the lower chemical stability of platinum metals in the form of microcrystalline sponge (black) as compared with compact deposits. It follows that the acidity of the mother liquors should be as low as possible in extraction of platinum metlas. To increase conductance neutral conducting salts which do not influence the electrode reactions should be added to the electrolyte.

To decrease the amount of metals redissolved, the freshly-deposited spongy material must not be allowed to remain for a long time in contact with the electrolyte, especially in acid solutions.

Another important conclusion was drawn from the experimental data: small amounts of copper ions have a strong influence on the course of the cathode process. A Group II solution (Table 4) with an initial copper content of 0.07 g/ liter was taken for the investigation. It was found that the deposition potentials of the platinum metals become more positive with increasing concentration of copper cations, evidently because of the

* See Table 4.

depolarizing effect of these cations due to their simultaneous discharge with the platinum metals. The results of determinations of cathodic polarization in presence of copper ions are plotted in Fig. 5

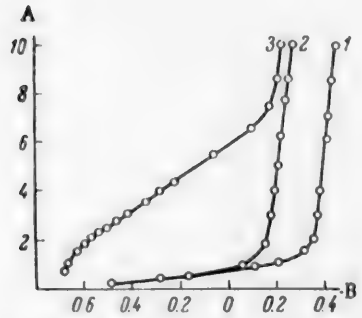

Fig. 4. Polarization curves for solutions of Group II* at 60° with stirring, for different concentrations of hydrochloric acid: A) current density I_c (amp/dm^2), B) cathode potential φ (v); HCl concentration (g/liter): 1) 80, 2) 40, 3) 14.3.

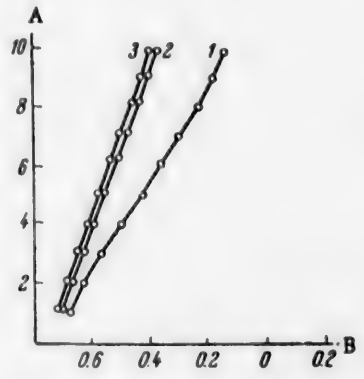

Fig. 5. Polarization curves for solutions of Group II* at 80° with stirring: A) current density I_c (amp/dm^2), B) cathode potential φ (v); copper content (g/liter): 1) 0.07, 2) 0.2, 3) 1.

The greatest depolarizing effect was obtained with a copper content of 0.5 g/liter.

SUMMARY

1. It was found in an examination of the theoretical principles and a study of practical possibilities of electrochemical extraction of platinum metals from solutions of their complex compounds that cathodic reduction of metals of the platinum group is very strongly influenced by the composition, temperature, and acidity of the original mother liquors.

2. The most satisfactory explanation of the appreciable concentrational changes taking place in the catholyte is based on the assumption that complex anions containing metals of the platinum group are discharged directly at the cathode.

3. Simultaneous discharge of acid anions (such as Cl^-) and hydroxyl ions is shown to occur at the anode.

4. The electrode polarization in cathodic reduction of platinum metals is diminished in presence of copper in the complex electrolyte. This effect of copper cations is due to their simultaneous discharge and depolarization of the cathode process.

LITERATURE CITED

[1] A. I. Levin, J. Gen. Chem 27, 1748 (1957)**

[2] A. I. Levin and E. A. Ukshe, Proc. Acad. Sci. USSR 88, 697 (1953).

[3] B. N. Nekrasov, Course of General Chemistry [in Russian] (Goskhimizdat, 1954) p. 788; M. P. Slavinskii, Physicochemical Properties of the Elements [in Russian] (Metallurgy Press, 1952).

[4] A. A. Grinberg, Introduction to the Chemistry of Complex Compounds [in Russian] (Goskhimizdat, 1951).

* See Table 4.

** Original Russian pagination. See C.B. Translation

[5] M. N. Polukarov, Proceedings of Conference of Electrochemistry [in Russian] (Izd. AN SSSR, 1953) p. 488.

[6] W. M. Latimer, Oxidation States of the Elements and Their Potentials in Aqueous Solutions (IL, 1954) [Russian translation].

[7] E. Muller, Z. phys. Ch. 65 (1909).

[8] A. I. Levin, A. V. Pomosov, and E. A. Ukshe, Laboratory Handbook of Theoretical Electrochemistry, 1 [in Russian] (Ural Polytech. Inst. Press, 1957).

[9] A. I. Levin, J. Phys. Chem. 32, 472 (1958).

[10] V. I. Lainer and N. G. Kudryavtsev, Principles of Electroplating, 2 [in Russian] (Metallurgy Press, 1946).

[11] A. I. Levin and S. A. Pushkareva, J. Phys. Chem. 31, 1938 (1957).

Received June 30, 1958.

POLYMERIZATION OF VINYL COMPOUNDS AT APPROXIMATELY ROOM TEMPERATURES

M. P. Tikhomolova, M. M. Koton, and A. N. Baburina

Institute of High Polymers, Academy of Sciences USSR

In recent years there have been numerous studies of polymerization of acrylic monomers at approximately room temperatures in presence of various oxidation–reduction systems. Thus, Bredereck and his associates [1] described a large number of α-hydroxy- and α-amino sulfones and sulfinates of organic bases, which in presence of benzoyl peroxide catalyzed rapid polymerization (5-30 minutes) of methyl methacrylate at +20°. However, the available literature data [2] give only a qualitative assessment of polymerization of vinyl compounds in presence of oxidation–reduction systems.

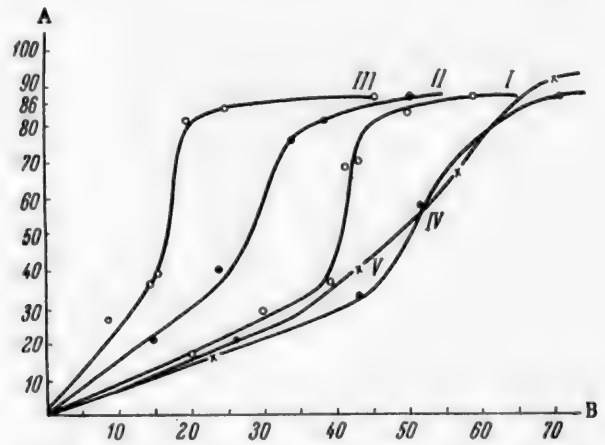

Course of the polymerization of methyl methacrylate (at 20°) and styrene (at 50°): A) conversion (%), B) time (hrs.); catalyst systems; for methyl methacrylate: I) 2% S + 2%BP, II) 2% HMTS + 2% BP, III) 1% HBTS + 1% BP, IV) 2% HP + + 2% HBTS; for styrene: V) 0.5% HMTS + 0.5% BP.

We investigated bulk polymerization of methyl methacrylate and styrene at 20-50°, with determinations of the degree of conversion (in %) of monomer into polymer. The following oxidation–reduction systems were used: 1) benzoyl peroxide (BP) and p-toluenesulfinic acid (S) or its condensation products with aldehydes (formaldehyde, OFTS, and butyraldehyde, OBTS) [3], 2) isopropylbenzene hydroperoxide (HP) and α-hydroxymethyl-p-tolyl sulfone (HMTS), 3) benzoyl peroxide and bis(p-tolylsulfonmethyl)amine (SMA), and 4) benzoyl peroxide and dimethylaniline.

The results of our studies of the polymerization of methyl methacrylate at 20° and of styrene at +50° in presence of various oxidation–reduction systems up to the maximum possible conversions of monomers to

polymers are presented in the diagram and Table 1. These results show that the "boundary of conversion" of methyl methacrylate monomer into the polymer at +20° is at about 86% conversion. For styrene at +50° this "conversion boundary" corresponds to 95% conversion of monomer into polymer. After the conversion boundary has been reached at a given temperature the polymer yield does not increase further, regardless of the time of polymerization (Table 1) despite the fact that this polymerizing mass contains considerable amounts of catalyst.

TABLE 1

Polymer Yields of Polymerization of Methyl Methacrylate (at 20°) in Presence of Various Catalyst Systems

Monomer	Catalyst system	Polymerization time (hours)	Conversion (in %)
Methyl methacrylate	0.5% HBTS + 1% BP	49	85—87
		340	85—87
	1% HBTS + 1% BP	25	85—86
		240	85—87
	2% S + 2% BP	50	83—85
		240	86—87
	2% HMTS + 2% BP	48	85—87
		240	85—87
		5 months	86
	4% HMTS + 4% MP	39	84—86
		52	84—86
	2% SNA + 2% BP	48	86
		96	85
Styrene	0.5% HMTS + 0.5% BP	70	93—95
		480	95

Thus, in polymerization of methyl methacrylate at 20° in presence of a system consisting of 2% benzoyl peroxide and 2% α-hydroxymethyl-p-tolylsulfone (Fig. , curve 1) the polymerization mass contained up to 1.5% benzoyl peroxide even after 5 months from the start of polymerization, while the yield of polymethyl methacrylate was 86%. In polymerization of styrene at 50° in presence of catalyst system consisting of 0.5% benzoyl peroxide and 0.5% α-hydroxymethyl-p-tolyl sulfone (Fig., curve V), after 20 days of polymerization the mass contained 0.2% benzoyl peroxide, and the yield of polystyrene was 93-95%. The glass transition temperature of the polymethyl methacrylate samples in our experiments was in the 20-23° range. It has been shown [3, 4] that the coefficient of diffusion in the polymer is decreased 1000 to 10,000-fold on transition through the glass transition temperature (T_g). Therefore, below T_g the monomer molecules lose mobility in the polymer to such an extent that the chain polymerization reaction cannot develop.

Of the oxidation-reduction systems studied, the most active in polymerization of methyl methacrylate at 20° is the system consisting of 1% α-hydroxybutyl-p-tolyl sulfone and 1% benzoyl peroxide (Fig., curve III). However, this system is of no practical value because of the instability of the reducing agent, which must be used as soon as prepared. The molecular weights of the methyl methacrylate polymers obtained in presence of different oxidation-reduction systems were determined (Table 2). Table 2 shows that the polymers obtained differed considerably in molecular weight. The lower molecular weight of polymethyl methacrylate formed in presence of the system consisting of 2% benzoyl peroxide and 2% p-toluenesulfinic acid is probably the consequence of participation of p-toluenesulfinic acid in chain transfer. Comparison of the experimental results in Table 1 and 2 shows that although the molecular weights of the methyl methacrylate polymers vary from $5 \cdot 10^5$ to $17 \cdot 10^5$ the final conversion of monomer to polymer remains the same (about 85-87%) at room temperature (+20°), and does not alter even after 5 months.

The blocks formed in polymerization of methyl methacrylate in presence of these oxidation-reduction systems at 20° were transparent and colorless, and did not change on keeping.

Polymerization of methyl methacrylate and butyl methacrylate in presence of the system consisting of 2% benzoyl peroxide and 1% dimethylaniline proceeds at a high rate (in 3 hours at 20°), and the temperature of the polymerizing mass at the point of gelation reaches 102°. With lower concentrations of the catalyst mixture (1.0% benzoyl peroxide and 0.5% dimethylaniline) the process slows down, and is completed in 48 hours. In this case the blocks of polymethyl methacrylate have a yellow color.

TABLE 2

Average Molecular Weights of Reprecipitated Polymethyl Methacrylate Formed in Presence of Different Catalyst Systems

Catalyst system	η	$M \cdot 10^{-5}$
1% α-hydroxybutyl-p-toluene sulfone + 1% benzoyl peroxide	4.4	11.05
2% α-hydroxymethyl-p-toluene sulfone + 2% benzoyl peroxide	6.3	17.00
2% p-toluenesulfinic acid + 2% benzoyl peroxide	2.3	4.97

The blocks of polystyrene formed by polymerization at 50° in presence of various oxidation-reduction system became "silvery" after 2-3 days and lost their transparency.

EXPERIMENTAL

Benzoyl peroxide was purified by recrystallization, and contained 99.5% of the theoretical amount of active oxygen. Technical isopropylbenzene hydroperoxide, purified by conversion into the sodium salt [5], contained 99.8% of the theoretical amount of active oxygen and boiled at 78-80° (2 mm). p-Toluenesulfinic acid was prepared from its sodium salt directly before the experiments, by the method of Oxley et al. [6] with certain modifications.

A solution of 70 g of anhydrous sodium sulfite in 250 ml of water was heated to 70-80°, and a mixture of 44 g of sodium bicarbonate and 50 g of p-toluenesulfonyl chloride was added during 1-1.5 hours; the mixture was then heated at 80° for 1 hour. When the mixture was cooled to 35-40° crystals of sodium p-toluenesulfinite were precipitated. If the solution is cooled to a lower temperature, the product is contaminated with inorganic salts. To liberate free p-toluenesulfinic acid the sodium salt was dissolved in the minimum amount of water and the solution was carefully acidified with 60% sulfuric acid. The precipitated crystals of the acid were separated from the solution, washed with a small amount of water, and recrystallized from water at 60-70° in a nitrogen atmosphere. Very pure acid melting at 83-84° was obtained.

The methods of Bredereck and Bäder [7] were used for preparation of α-hydroxymethyl and α hydroxybutyl sulfones and of bis(p-tolylsulfonmethyl)amine.

The experiments on polymerization of methyl methacrylate and styrene were performed in sealed glass tubes in a nitrogen atmosphere. Temperature variations during polymerization were recorded by means of a copper-constantan thermocouple in the polymerization mass.

The polymer yield was determined by reprecipitation in the case of methyl methacrylate, while in the case of styrene, residual monomer was determined by bromination. In some samples, residual benzoyl peroxide was determined by the iodometric method.

We offer our thanks to B. A. Dolgoplosk and S. E. Bresler for their interest and valuable advice.

SUMMARY

1. In bulk polymerization of methyl methacrylate at +20° and of styrene at +50° in presence of various

oxidation-reduction systems the "boundary of conversion" of monomer into polymer is at 86% conversion of methyl methacrylate and 95% conversion of styrene.

2. After the conversion boundary has been reached the polymer yield does not increase further, irrespective of the polymerization time, despite the fact that the polymerization mass contains considerable amounts of catalyst.

LITERATURE CITED

[1] H. Bredereck, E. Bäder, and N. Nübling, Marcromol. Chem. 12, 100 (1954); E. Bäder and H. Herman, Ber. Deut. Chem. Ges. 88, 41 (1955); H. Bredereck, E. Bäder, and N. Nübling, Macromol. Chem. 18/19, 431 (1956).

[2] G. Braun and F. Burns, J. Polymer Sci. 19, 311 (1956); German Patent 927,052; Chem. Abs. 10870 (1955); M. Imoto and S. Choc, J. Polymer Sci. 15, 485 (1955).

[3] G. Ya. Ryskin, J. Tech. Phys. 25, 458 (1955).

[4] U. Melville, Proc. Roy. Soc. 237, 149 (1956).

[5] M. S. Kharasch, A. Fono, W. Nudenberg, J. Org. Chem., 16, 113 (1951).

[6] P. Oxley, M. W. Partridge, T. D. Robson, and W. E. Short, J. Chem. Soc. 767 (1946).

[7] H. Bredereck and E. Bäder, Ber. 87, 129 (1954).

Received April 16, 1958.

PREPARATION OF POLYELECTROLYTES FROM METHACRYLIC AND ACRYLIC ACID DERIVATIVES

M. N. Savitskaya

In recent years communications [1] have appeared in the foreign press on the use of polyelectrolytes for stabilization of soil structure. A crumbly soil structure is important for high yields of agricultural crops. More than sixty synthetic polyelectrolytes used for improving on soil structure are named in patents. Most of them are polymers of copolymers of the vinyl series (acrylonitrile, acrylamide, vinyl acetate, and their hydrolysis products). Several brands of polyelectrolytes of the Krilium type (derivatives of methacrylic and acrylic acids) are produced for agricultural purposes in the United States of America. The best known of these are the copolymer of vinyl acetate and maleic anhydride, and hydrolyzed polyacrylonitrile. Polyelectrolytes are also used for coagulation in the mining industry [2]. Coagulants known as "DT-120," "Separan-2610", "Aerofloc-548", and others are used in Germany and the United States. However, methods for preparation of these polyelectrolytes are not described in the literature.

The present communication deals with methods for preparation of polyelectrolytes based on derivatives of acrylic and methacrylic acids and their polymers.

EXPERIMENTAL

The materials used for preparation of polyelectrolytes were polymers of methacrylic acid, sodium methacrylate, and acrylamide, and copolymers of methacrylic acid with amides (methacrylamide or acrylamide). Syntheses of the monomers used are described in the literature and present no difficulties.

Preparation of methacrylamide. Methacrylamide [3, 4] was prepared by the action of excess ammonia on methyl methacrylate by the reaction:

$$CH_2=\overset{\displaystyle CH_3}{\overset{|}{C}}-COOCH_3 + NH_3 \rightarrow CH_2=\overset{\displaystyle CH_3}{\overset{|}{C}}-CO-NH_2 + CH_3OH.$$

Methyl methacrylate was placed in a glass vessel with 3 times the quantity of 23% ammonia and shaken for 3 days. The resultant homogeneous solution was cooled in a mixture of solid carbon dioxide and acetone down to −50°; methacrylamide was precipitated in the form of crystals. The crystals were filtered off on a Buchner funnel and recrystallized from ethyl alcohol. The properties of the methacrylamide so prepared are given in Table 1.

Preparation of acrylamide. Acrylamide was prepared by saponification of acrylonitrile [5] by sulfuric acid by the reaction

$$CH_2=CHCN + H_2O \xrightarrow[100°]{H_2SO_4} CH_2=CHCONH_2.$$

A three-necked flask fitted with a stirrer, thermometer, and reflux condenser contained 116 parts by weight of 84.5% sulfuric acid containing 0.2 parts by weight of copper powder. The acid was stirred and 53 parts by weight of acrylonitrile was added. The mixture was warmed up steadily to 100° during 50 minutes and held

at 100° for 45 minutes, when the reaction was terminated. Two methods were used for isolation of acrylonitrile from the reaction mass. In the first method the reaction mass was cooled to 60° and diluted threefold with isopropyl alcohol. Gaseous ammonia was passed through the solution to neutralize sulfuric acid. The precipitated ammonium sulfate was filtered off and isopropyl alcohol was distilled off under vacuum. The separated acryl-

TABLE 1

Properties of Monomers

Monomer	Method for purification of monomer	Melting point (in °C)		Monomer yield (%)
		found	literature data	
Methacrylamide	Recrystallization from ethyl alcohol	110	110	70
Acrylamide		85	85	60
Acrylamide	Percolation through "ÉDÉ-10" anion exchange	85	85	80

amide was recrystallized from ethyl alcohol. In the second method the cooled reaction mass was diluted with water in 1 : 1 ratio and the solution was percolated through a column with "ÉDÉ-10" anion exchanger. The acrylamide content of the filtrate was checked. The properties of the acrylamide so prepared are given in Table 1.

It is seen in Table 1 that the melting points of the monomers agree with literature data.

The best method for purification of acrylamide is percolation of the diluted reaction mass through "ÉDÉ-10" anion exchanger. This method is convenient because it shortens the purification time and eliminates a whole sequence of operations. Solvents are not required for this method, which makes it cheaper and eliminates fire and toxicity hazards.

TABLE 2

Composition and Properties of Methacrylic Polymers

Contents (%)		Solubility in water	Relative viscosity at 20°
Na salt of methacrylic acid	methacrylic acid		
–	100	Sparingly soluble	
100	–	Readily soluble	1.73
25	75	Readily soluble	2.54
10	90	Soluble	1.46
5	95	Soluble	1.46

Polymerization of methacrylic acid and acrylamide. There is little information in the literature on polymerization and copolymerization of these monomers. According to the literature [5], methacrylic acid polymerizes in presence of potassium persulfate. The methacrylic acid used by us for polymerization was of

plant manufacture. It was distilled under vacuum before polymerization. It was polymerized in 10% aqueous solution in presence of 0.2% potassium persulfate at 90°. The reaction proceeded with liberation of heat up to 96° and was rapidly completed. The polymerized methacrylic acid was precipitated in gel form. To improve the solubility of polymethacrylic acid in water, polymerization of methacrylic acid partially neutralized by caustic soda has been described. Sodium methacrylate and partially-neutralized methacrylic acid polymerize under the same conditions as methacrylic acid. The compositions and solubilities of the polymers obtained are given in Table 2.

Table 2 shows that partial or total neutralization of methacrylic acid before polymerization improves the solubility of the polymer in water. The relative viscosity of the polymers is low.

It is reported in the literature [1] that acrylamide polymerizes in an oxidation-reduction system (ammonium persulfate and sodium hydrosulfite in equimolecular proportions) with formation of polymers with maximum intrinsic viscosity of 3.8. Polyacrylamide is also formed [6] in presence of hydrogen peroxide; its molecular weight is 10,000. Polyacrylamide of higher molecular weight has not been described in the literature.

It is known that polymerization of acrylonitrile has the peculiar feature that at elevated temperatures cross linking may occur, owing to mobility of the hydrogen atom in the α-position to the carbon atom, and the polymer becomes insoluble. If the polymerization is effected in an oxidation-reduction system the temperature of the polymerization reaction may be lowered, and a polymer of high molecular weight can be obtained if the components are chosen correctly.

TABLE 3

Effect of the Amount of Catalyst on the Intrinsic Viscosity of the Polymer*

Expt. No.	Catalyst composition (g)			[η] at 20° in water
	$K_2S_2O_8$	$Na_2S_2O_4$	$N(CH_2CH_2OH)_3$	
1	0.0010	0.0002	0.0005	Does not polymerize
2	0.0030	0.0006	0.0015	Low viscosity
3	0.0050	0.0014	0.0025	4
4	0.0200	0.0056	0.0100	3

* 20 ml of 5% solution.

In our experiments acrylamide was polymerized in presence of an oxidation-reduction system in an aqueous medium. The oxidizing agent was potassium persulfate, and the reducing agents were sodium hydrosulfite and triethanolamine. The components were used in the following proportions: 0.4 mole of sodium hydrosulfite and 0.9 mole of triethanolamine were taken per mole of potassium persulfate. Potassium persulfate reacts simultaneously with both reducing agents at 50-60° to form free radicals which cause polymerization of acrylamide. Acrylamide was polymerized in an atmosphere of nitrogen. Acrylonitrile in the form of 5% aqueous solution was put into a flask and triethanolamine was added; a mixture of aqueous solution of potassium persulfate and sodium hydrosulfite was then added at once with stirring. The mixture was heated at 50° for 8 hours and then at 60° for 6 hours. The propoerions of the catalysts and their influence on the intrinsic viscosity of polyacrylamide are given in Table 3.

TABLE 4

Effect of Polymerization Conditions on Polymer Yield

Polymerization time (hrs.) at		Relative viscosity at 20°	Polymer yield (%)
50°	60°		
10	–	279	–
12	–	280	–
8	6	297	100

It follows from Table 3 that polyacrylamide of highest molecular weight is obtained with the following proportions of catalysts: potassium persulfate 0.5%, sodium hydrosulfite 0.14%, and triethanolamine 0.25% on the weight of dry acrylamide (Experiment No. 3).

The polymerization of acrylamide in presence of the optimum amount of catalyst was studied with variations of temperature and duration of the experiment. In all the experiments the relative viscosity of 0.5% aqueous solution was determined in an Ostwald viscosimeter at 20°. When the viscosity of the polymer ceased to increase, the polymer yield was determined.

The results of some of the experiments are given in Table 4.

Thus, as Table 4 shows, polymerization of acrylamide is completed if the mixture is heated first for 8 hours at 50° and then for 6 hours at 60° in presence of the optimum amount of catalyst. The degree of polymerization of acrylamide depends on the purity of the monomer. Table 5 shows that polyacrylamide made from monomer passed through "ÉDÉ-10" anion exchanger has the highest intrinsic viscosity.

TABLE 5

Effect of Purity of Acrylamide Monomer on the Degree of Polymerization

M.p. of acrylamide (°C)	Method of purification of acrylamide	$[\eta]$ in water at 20°
83-84	Single recrystallization from ethyl alcohol	3
84	Twofold recrystallization from ethyl alcohol	4
84-85	Threefold recrystallization from ethyl alcohol	5.1
85	Single percolation through "ÉDÉ-10" anion exchanger	6.5

The resultant aqueous solution of polyacrylamide is a highly viscous colloid. When the polymer solution is poured into acetone the polymer is precipitated in fibrous form. The specific gravity of the dry polymer is 1.27. Its nitrogen content is 18%.

TABLE 6

Compositions and Solubilities of Copolymers

Expt. No.	Amounts (%) of		Nitrogen contents (%)		Relative viscosity of 1% solutions
	methacrylic acid	methylacrylamide	found	calc.	
1	3	97	10.44	15.59	2.0
2	25	75	10.43	12.35	1.90
3	60	40	6.07	6.58	4.99
4	50	50	6.64	8.23	—
5	40	60	8.06	9.87	—
6	75	25	3.86	4.11	—
7	50	50*	12.04	9.83	—

*Acrylamide.

Copolymerization of methacrylic acid with amides (acrylamide and methacrylamide). Copolymers of methacrylic acid with acrylamide and methacrylamide were made by polymerization in an aqueous medium with 1% potassium persulfate at 65° for 18 hours. The compositions and solubilities of the copolymers are given in Table 6.

The copolymers of methacrylic acid with methacrylamide were soluble in 1% ammonia solution and insoluble in water. Copolymers of acrylamide and methacrylic acid were soluble in water.

The nitrogen contents, determined by the Dumas micromethod in the analytical laboratory of the Institute of High Polymers, show that in most of the experiments less than the calculated amount of acrylamide was copolymerized. The found and calculated contents of amide coincided only when 60% methacrylic acid and 40% methacrylamide was taken. This polymer was of the highest molecular weight.

Trials of the polymers. All the polymers were tested as soil-conditioning agents by the Lenin Agrophysical Institute in the soil structure laboratory under the guidance of Prof. P. V. Vershinin. The trials showed that copolymers of methacrylic acid and methacrylamide (Experiment No. 3) gave positive results. Particularly good results were obtained with the polyacrylamide of high molecular weight. Polyacrylamide was also tested as a coagulant in the mining industry (in the Institute of Halurgy of the Ministry of Chemical Industry, State Scientific Research Institute of Nonferrous Metals, and the Leningrad State Institute for the Planning of Mine Developments in the Coal Industry). The tests gave positive results in all cases.

I offer my deep gratitude to M. M. Koton for valuable advice in the course of this work, and to P. V. Vershinin, A. B. Zdanovskii, and E. I. Lyakhovskaya for testing the polymers.

SUMMARY

1. Polyacrylamide and copolymers of methacrylic acid with methacrylamide are suitable for improving soil structure; polyacrylamide gives the best results.

2. Polyacrylamide is a good coagulant for the mining industry.

LITERATURE CITED

[1] A. S. Michaels, Ind. Eng. Chem. 46, 7, 1485 (1954).

[2] E. Teichmann, Glückauf, 35/36, 1033 (1956).

[3] S. H. Pinner, J. Polymer Sci. X. 4, 379 (1953).

[4] C. L. Arcus, J. Chem. Soc. 2732 (1949).

[5] C. E. Schildknecht, Vinyl and Related Polymers, (N. Y. 1952) p. 317.

[6] J. W. Sholton, Macromol. chem. 14, 169 (1954).

Received June 18, 1958

INVESTIGATION OF THE LUMINESCENCE OF LIGNIN FROM COTTON-PLANT WASTES (STEMS AND BOLLS)

S. N. Vil'kova

The problem of rational utilization of lignin still remains unsolved. Hundreds of tons of lignin are burned, although it might be a valuable raw material for a number of industries. Lignin of cotton-plant wastes is also burned together with these wastes, and its chemical composition has not been studied at all.

In order to obtain at least a general preliminary idea of the chemical structure of cotton-plant lignin, it was studied by means of luminescence analysis.

Manskaya, Bardinskaya, and Kochneva showed that lignin in the solid state in plant cells gives a bluish green and greenish blue luminescence in ultraviolet light [1, 2]. They observed the luminescence of lignin by means of the luminescence microscope [3]. The luminescence of lignin may serve as one proof of the presence of aromatic groups in the lignin complex [4, 5]; indeed, chemical investigations have shown that various aromatic compounds (vanillin, syringaldehyde, protocatechuic acid, and some phenylpropane derivatives) can be obtained from lignin of mature wood [6, 7]. Recent investigations have shown that lignin is not an individual chemical substance but a mixture of aromatic substances – derivatives of pyrocatechol and pyrogallol [8].

On the assumption that the same constituent parts of lignin molecules of different origins would exhibit luminescence of the same color, we studied the luminescence of lignin from cotton-plant wastes; to eliminate the element of subjectivity, lignin was investigated in the dissolved state and its luminescence was photographed on film. For comparison, luminescence spectra of lignin obtained from sawdust were photographed together with the luminescence spectra of lignin from cotton-plant wastes.

Lignin was extracted from the wastes by 5% alkali solution. To insure that the lignin was free from impurities, the wastes were subjected to special preliminary treatment; they were shredded and treated consecutively in Soxhlet extractors with ethyl alcohol, benzene, and ether until waxes and resins had been completely removed. Water-soluble substances were then extracted. The chemical composition of these substances has not been adequately studied. It is known that they contain tannins, sugars, etc. [9]. To extract them, the cotton wastes were covered with water and heated at 70-75° for 24 hours with stirring.

For extraction of humic acids the wastes were then covered with 5% sodium bicarbonate solution and heated at 70-75° for 24 hours with stirring. After bicarbonate had been washed out thoroughly, the material was spread in a thin layer on a sheet of filter paper and dried at room temperature. From this product lignin was extracted by 5% alkali solution at 70-75° for 9 hours. This yield was dark brown extract to which concentrated hydrochloric acid was added in order to precipitate lignin. The lignin was filtered off on a Schott filter, dissolved in alkali, and again precipitated from the alkaline solution by hydrochloric acid. This reprecipitation was performed six times in order to purify the lignin as much as possible. It was then washed free from acid by decantation to a neutral reaction, filtered off on a Schott filter, and dried in a vacuum desiccator. The resultant lignin was a velvety brown powder soluble in alkali.

Lignin was extracted from sawdust in exactly the same manner.

The ISP-51 spectrograph was used for the experiments.

Luminescence of cotton-waste lignin dissolved in 5% aqueous alkali was induced by ultraviolet radiation passed through a blue filter which absorbed all the lines of the mercury spectrum with the exception of the line at 405 mμ, which induces luminescence. The luminescence spectrum of cotton-waste lignin was detected in the region from 4800 to 6500 A (Fig. 1, Curve 1); it broke off so abruptly toward the infrared region of the spectrum that it seemed very probable that the luminescence spectrum of lignin continues in the infrared region, and that this sharp termination was due to insensitivity of the "isopanchrome" film used in the infrared region. The spectrum is of complex structure with a single maximum. The structure of the luminescence spectrum of lignin obtained for sawdust (Fig. 1, Curve 2) has almost exactly the same structure.

The almost total similarity of the luminescence spectra of lignins from cotton-plant wastes and wood lignin indicates that the luminescent centers (which may be aromatic rings of some kind, radicals, etc.) in the molecules of the two lignins are either identical or very similar.

To determine whether the luminescence of lignin conforms to the basic law of luminescence, experiments were performed in which luminescence of lignin was induced by light of different wave lengths, namely: 365, 436, 546, and 578 mμ. The luminescence spectra induced by these wave lengths did not differ essentially from each other either for lignin from cotton wastes or for lignin from sawdust; this shows that the luminescence of lignin conforms to Vavilov's law, according to which the luminescence spectra of complex molecules are independent of this wave length of the exciting light [10].

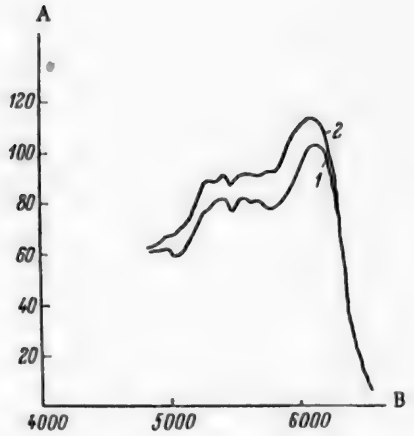

Fig. 1. Luminescence spectra of lignins from cotton-plant wastes and sawdust:* A) $\log \frac{I}{I_0}$, B) wave length (λ).

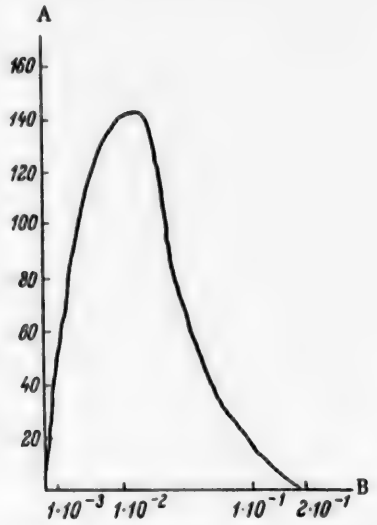

Fig. 2. Concentrational extinction of the luminescence of lignin. A $\log \frac{I}{I_0}$, B) concentration (%).

Experiments were then carried out in order to determine whether the luminescence of lignin is subject to concentrational extinction. If we start with very dilute solutions of a luminescent substance, then the intensity of the luminescence at first increases with increase of concentration because of the increase in the amount of excitation energy absorbed by the solution; at a certain concentration of the dissolved substance the intensity reaches a maximum, and with further increase of concentration it first remains unchanged and then begins to decrease, i.e., concentrational extinction begins. For some substances the intensity begins to decrease immediately after the maximum has been reached.

In our experiments the luminescence intensity was measured over a fairly wide concentration range, from

*Explanations of the curves in all the figures are given in the text.

$1 \cdot 10^{-4}$ to $2 \cdot 10^{-4}$%. The results were used for plotting a curve for luminescence intensity as a function of concentration (Fig. 2), which shows that the intensity increases with concentration up to a certain limit, when concentrational extinction characteristic of luminescence occurs.

The energy distribution in the luminescence spectrum of lignin was investigated by comparison with a standard source of a known energy distribution. The standard source was a tungsten-filament lamp calibrated for a color temperature of 2850 ± 20° K. The spectrum of this lamp was photographed through an optical wedge. Above and below the spectrum of the standard lamp were photographed the mercury-vapor spectrum from a quartz mercury lamp and the neon spectrum from a neon lamp. The lines of these spectra were used for determining the wave lengths of individual regions of the spectrum of the standard lamp. For determination of the spectral sensitivity of the film, the spectrum of the standard lamp photographed through an optical wedge was measured photometrically by the degree of attenuation in different regions, corresponding to different wave lengths. For each wave length a blackening curve was plotted, the maximum ordinate of which was proportional to the radiation energy for the given wave length. The maximum ordinates were then used for plotting blackening intensity a, proportional to the energy E emitted by the standard lamp at the given wave length, against

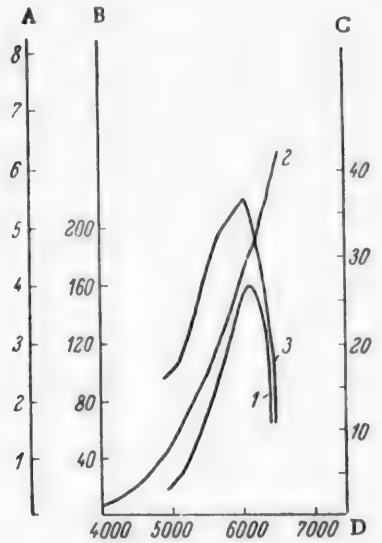

Fig. 3. Energy distribution in the spectrum of the standard lamp: A) radiation energy (E), B) log I/I_0, C) blackening intensity (a), D) wave length (λ).

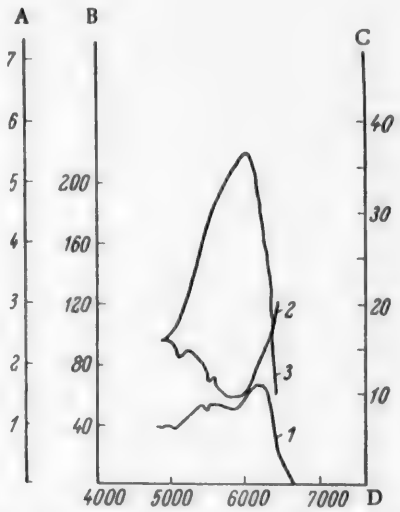

Fig. 4. Energy distribution of the luminescence spectrum of lignin: axes as in Fig. 3.

the wave length (Curve 3, Fig. 1). To convert blackening into terms of energy, an additional curve was plotted (Fig. 3, Curve 2) showing the spectral energy distribution for an incandescent tungsten filament at a color temperature of 2850 ± 20° K [11]. The ordinates of various points in Curve 1 were drawn and continued to their intersection with Curve 2, which gave the corresponding energies for these points. The ratio of the blackening intensity to the energy corresponding to this blackening gives the curve for the spectral sensitivity of the film (Fig. 3, Curve 3).

In order to have an ideal of the nature of the energy distribution in the luminescence spectrum of lignin, the blackening intensity (proportional to the energy of luminescence) was plotted against the wave length (Fig. 4, Curve 1), and the curve for the spectral sensitivity of the photographic film from Fig. 3 was then superposed (Fig. 4, Curve 3). By relating the blackening to the corresponding sensitivity we find Curve 2, which represents the energy distribution in the luminescence spectrum of lignin.

The energy distribution in the luminescence spectrum of lignin is complex in character; this is further evidence for the complex structure of the lignin molecule, and the right-hand side of the curve ascends steeply

in the infrared direction, which again indicates that the luminescence spectrum of lignin extends into the infrared region, and that this fact cannot be detected only because the film is insensitive in the infrared region the spectrum. The same ISP-51 spectrograph was used for determining the absorption spectra of the two lignins; like the luminescence spectra, they proved to be almost identical.

SUMMARY

1. It is shown that lignin exhibits luminescence not only in the solid state (in sections of the plant tissues) but also in the dissolved state; the luminescence spectra of lignin from sawdust and from cotton-plant wastes are quite similar, which indicates that the luminescent centers in the molecules of the two lignins are similar in structure.

2. The nature of the luminescence spectra and energy-distribution curves for the two lignins indicates that the luminescence spectra of both lignins extend into the infrared region of the spectrum.

3. The absorption spectra of the two lignins also show them to be similar.

LITERATURE CITED

[1] S. M. Manskaya and M. N. Kochneva, Proc. Acad. Sci. USSR 62, No. 4, 505 (1948).

[2] M. S. Bardinskaya, Proc. Acad. Sci. USSR 76, 3, 435 (1951).

[3] N. I. Nikitin, Chemistry of Wood [in Russian] (Moscow–Leningrad, 1951) p. 226.

[4] M. A. Konstantionova-Shlezinger, Lumenescence Analysis [in Russian] (Moscow–Leningrad, 1948) p. 150.

[5] M. A. Konstantinova-Shlezinger, Trans. P. N. Lebedev Phys. Inst. 2, 7, 122.

[6] M. S. Bardinskaya, Proc. Acad. Sci. USSR 73, No. 1, 133 (1950).

[7] S. M. Manskaya, M. S. Bardinskaya, and M. N. Kochneva, Proc. Acad. Sci. USSR 76, No. 5, 707 (1951).

[8] N. I. Nikitin, S. D. Antonovskii, and M. A. Mikhailova, J. Appl. Chem. 30, 5, 750 (1957).

[9] F. P. Komarov, Laboratory Manual of Wood and Cellulose Chemistry [in Russian] (Leningrad–Moscow, 1932) p. 36, 37.

[10] V. A. Levshin, Photoluminescence of Liquids and Solids [in Russian] (Moscow–Leningrad, 1951) p. 92.

[11] N. I. Chechik, S. M. Fainshtein, and T. M. Lifshits, Electron Multipliers [in Russian] (Moscow, 1954) p. 39.

Received April 9, 1958

SYNTHESIS OF NITROACETOPHENONES BY OXIDATION OF NITROETHYLBENZENES

P. M. Kochergin, R. M. Titkova, V. A. Zasosov, and A. M. Grigorovskii

The S. Ordzhonikidze All-Union Pharmaceutical Scientific Research Institute

At the start of our work (in 1955) on oxidation of ethylbenzene derivatives by potassium permanganate to give aryl methyl ketones, literature information on the subject was rather scanty [1-4]. Subsequently, several more papers [5, 6] and patents [7, 8] were published. However, a number of questions, including the selection of a buffer for the optimum conditions for oxidation of ethyl groups to acetyl, remained unclarified.

Since p-nitroacetophenone is widely used as an intermediate in the synthesis of levomycetin, the purpose of the present investigation was a fuller study of the conditions for oxidation of p-nitroethylbenzene, already reported in a brief communication [9]. It was also desired to extend this reaction to preparation of other nitroacetophenones.

It follows form the literature sources cited above that the main condition for satisfactory yields of aryl methyl ketones is oxidation of ethylbenzene derivatives by potassium permanganate in weakly acidic or neutral solutions. To conform to this condition, the reaction was effected in presence of buffers – salts of strong acids and weak bases (nitrates of magnesium, calcium, and zinc; sulfates of magnesium and zinc).

A series of experiments (Table 1) was performed in order to study the influence of the chemical nature of the buffers on the yields of p-nitroacetophenone and p-nitrobenzoic acid in oxidation of p-nitroethylbenzene by potassium permanganate in aqueous solution. The buffers used were water-soluble sulfates and nitrates of metals of groups I-III and V-VIII of Mendeleev's periodic system. The other reaction conditions were kept constant. It follows from the results of these experiments that the nature of both the cation and the anion in the buffer is important in oxidation of ethyl to acetyl groups. In oxidation of p-nitrobenzene in presence of nitrates the yield of p-nitrobenzene (calculated on the alkyl benzene taken) is generally 1-24% lower, and the yield of the reaction by-product (p-nitrobenzoic acid) 1.5-20% higher than in presence of sulfates of the corresponding metals. The best results (61-65% yield of p-nitroacetophenone) are obtained by oxidation of p-nitroethylbenzene by potassium permanganate in presence of aluminum and magnesium sulfates and ammonium ferric alum. The best buffer was aluminum sulfate, which is also the most readily available and cheapest material. The reaction then proceeds according to the equation

$$9\,O_2N{-}C_6H_4{-}CH_2CH_3 + 12KMnO_4 + 2Al_2(SO_4)_3 \rightarrow$$
$$\rightarrow 9\,O_2N{-}C_6H_4{-}COCH_3 + 12MnO_2 + 4Al(OH)_3 + 6K_2SO_4 + 21H_2O.$$

If p-nitroethylbenzene is oxidized in presence of a large excess of aluminum sulfate, the p-nitroacetophenone formed (yield 43.3%) must be washed with sodium carbonate solution in order to remove p-nitrobenzoic acid. It was found (Table 2) that if the amount of aluminum sulfate corresponds to 100% of the theoretical required for p-nitrobenzene the yield of p-nitrophenone reaches 56-65% on the amount of p-nitroethyibenzene taken for the reaction and 82.9-93.5% on the amount converted. Under these conditions, with some excess of potassium permanganate, the oxidation reaction proceeds near the end at solution pH above 7, and terminates

TABLE 1

Effect of the Nature of the Buffer on Yields of p-Nitroacetophenone and p-Nitrobenzoic Acid

Expt. No.	Chemical formula of buffer	Yields calc. on p-nitroethylbenzene (%)				Amount of p-nitrobenzene recovered (%)
		p-nitroacetophenone		p-nitrobenzoic acid		
		on amt. taken	on amt. converted	on amt. taken	on amt. converted	
1	$CuSO_4$	58.0	74.7	1.8	2.4	22.2
2	$Cu(NO_3)_2$	57.0	79.0	1.2	1.7	27.8
3	$MgSO_4$	61.0	73.5	3.8	4.6	17.7
4	$Mg(NO_3)_2$	55.1	69.2	5.2	6.7	20.2
5	$Ca(NO_3)_2$	43.0	55.2	8.4	10.9	20.0
6	$Sr(NO_3)_2$	50.0	65.8	8.1	10.7	23.5
7	$Ba(NO_3)_2$	1.5	11.4	0.3	2.2	84.3
8	$ZnSO_4$	59.4	69.0	0.5	0.6	13.9
9	$Zn(NO_3)_2$	52.8	64.1	10.9	13.6	17.0
10	$Zn(NH_4)_2(SO_4)_2$	52.9	68.4	0.3	0.4	22.8
11	$CdSO_4$	59.4	74.8	1.5	1.9	20.5
12	$Cd(NO_3)_2$	56.4	84.5	1.5	2.3	37.0
13	$Al_2(SO_4)_3$	64.8	84.5	1.2	1.6	23.0
14	$Al(NO_3)_3$	52.4	67.8	3.9	5.1	22.8
15	$AlNH_4(SO_4)_2$	52.2	86.0	3.6	6.0	39.7
16	$AlK(SO_4)_2$	52.8	76.0	1.4	2.1	32.7
17	$Bi(NO_3)_3$	4.0	8.5	15.3	33.3	49.1
18	$CrK(SO_4)_2$	47.3	70.6	—	—	30.0
19	$MnSO_4$	16.4	32.5	—	—	50.0
20	$Mn(NO_3)_2$	4.2	26.0	3.3	20.0	84.3
21	$Fe_2(SO_4)_3$	41.5	54.2	17.1	22.6	23.2
22	$Fe(NO_3)_3$	17.6	27.1	23.0	36.0	35.1
23	$FeNH_4(SO_4)_2$	63.9	77.3	—	—	17.0
24	$CoSO_4$	10.4	20.8	1.5	3.0	50.7
25	$Co(NO_3)_2$	22.4	39.0	12.6	23.5	42.6
26	$NiSO_4$	58.6	89.4	2.1	3.5	43.3
27	$Ni(NO_3)_2$	50.0	75.2	3.3	5.0	36.5
28	$Ni(NH_4)_2(SO_4)_2$	50.0	73.0	2.9	4.0	31.3

at pH 10. This made it easy to isolate the valuable by-product, p-nitrobenzoic acid, by acidification of the aqueous mother liquor containing its potassium salt. If less aluminum sulfate is used, the yield of p-nitroacetophenone decreases and that of p-nitrobenzoic acid increases. If p-nitroethylbenzene is oxidized in absence of buffer, only p-nitrobenzoic acid is formed.

TABLE 2

Effects of the Amount of Aluminum Sulfate on Yields of p-Nitroacetophenone and p-Nitrobenzoic Acid

Expt. No.	Aluminum sulfate (% of theoretical for p-nitrobenzene)	Yields (%) on p-nitroethylbenzene taken)	
		p-nitroacetophenone	p-nitrobenzoic acid
1	–	–	25.7
2	50	55.4	6.1
3	100	61.5	1.6
4	200	43.3	–

In oxidation of p-nitroethylbenzene the amount of potassium permanganate and the manner in which it is added to p-nitroethylbenzene are of great significance. The optimum amount of potassium permanganate was found to be 125% of the theoretical quantity for p-nitroethylbenzene. If the theoretical amount of oxidizing agent is used, the ketone yield decreases. With 50-100% excess of potassium permanganate the yield of p-nitroacetophenone hardly increases at all, the yield of p-nitrobenzoic acid is increased 2 to 3-fold, and much less of the original p-nitroethylbenzene is recovered. If potassium permanganate is added to an emulsion of p-nitroethylbenzene in aqueous aluminum sulfate solution (at 60-62°) by portions, as each successive amount is reduced, reaction time is extended to 60-70 hours.

If potassium permanganate is all added at once, because of the high concentration of oxidizing agent at the start of the process and the low concentration at the end of the reaction the yield of p-nitroacetophenone decreases by 5-10% and the yield of p-nitrobenzoic acid increases 1.5 to 2-fold. The time required for oxidation of p-nitroethylbenzene can be reduced sharply (to 14-17 hours) and the yield of p-nitroacetophenone increased by addition of potassium permanganate in the form of powder or warm aqueous solution in 9-11 equal portions at intervals of one hour.

An important factor in the oxidation of p-nitroethylbenzene to p-nitroacetophenone is the temperature at which the reaction is performed. It was found that the most suitable temperature is 60-62°. At higher temperatures (70-97°) the yield of ketone drops sharply and the yield of p-nitrobenzoic acid increases. At a low temperature (40-45°) the reaction time is extended to 35 hours, and the yield of ketone increases somewhat.

Despite the mild conditions chosen for oxidation of p-nitroethylbenzene by potassium permanganate, the course of the reaction is indefinite and it does not go to completion. A considerable amount of p-nitroethylbenzene (20-30%) does not react. This cannot be attributed to the nonhomogeneous reaction conditions, as the same result is obtained if the reaction is effected in aqueous acetone. The by-product is p-nitrobenzoic acid (in 1.9-3.3% yield on the p-nitroethylbenzene taken, and 2.8-4.9% on the amount converted).

The material balance for the reaction with the use of p-nitroethylbenzene of 100% purity comprises 88-93%. It is likely that some of the p-nitroacetophenone and p-nitroethylbenzene is oxidized by potassium permanganate to simpler compounds, with destruction of the benzene nucleus.

The reaction conditions found for oxidation of p-nitroethylbenzene to p-nitroacetophenone were used in preparation of o- and m-nitroacetophenones, 2,4-dinitroacetophenone, and acetophenone by oxidation of the corresponding alkyl benzenes.

EXPERIMENTAL

The potassium permanganate and aluminum sulfate used for the experiments conformed to the specifications of GOST 5777-51 (grade 1) and OST 18180-40 ("extra" grade) respectively.

p-Nitroacetophenone. A three-necked flask 2 liters in capacity, fitted with a stirrer, thermometer, and reflux condenser, was charged with 500 ml of water, 90.6 g of aluminum sulfate, and 90.6 g of p-nitroethylbenzene [9, 10] (97% purity, $n^{20}D$ 1.5459, freezing point −13.5°) The mixture was heated to 60°, and 160.3 g of potassium permanganate (in 10 portions of 16.03 g at intervals of one hour) was added with vigorous stirring. The temperature of the reaction mass was maintained at 60-62° on a heated water bath. After the last portion of oxidizing agent had been added, the reaction mass was stirred at the same temperature until the reaction terminated. After 14 hours from the start of the reaction, samples of the reaction mass were taken at intervals of 30 minutes. The end of the reaction was indicated by absence of a violet color on filter paper when a drop of the reaction mass was placed on it. The duration of the process was 14-17 hours.

Two methods were used for isolation of the p-nitroacetophenone.

1. At the end of the oxidation 500-700 ml of dichloroethane was added to the reaction mass and the mixture was stirred at the same temperature (60-62°) for 1-1.5 hours, then cooled to room temperature and filtered through a Buchner funnel. The residue (mixture of manganese dioxide and aluminum hydroxide) was washed on the filter with 100-120 ml of dichloroethane. The filtrate was transferred to a separating funnel, and the dichloroethane layer was separated from the aqueous layer. The aqueous solution was acidified by mineral acid until acid to Congo Red; 1.8-3.2 g of p-nitrobenzoic acid of m. p. 233-236° separated out (yield 1.8-3.3% on the amount of p-nitroethylbenzene taken, or 2.8-4.9% on the amount converted). After evaporation of dichloroethane under vacuum 86.7-88.8 g of a mixture of nitro compounds remained; this mixture was cooled to between −5 and −10°, the precipitated p-nitroacetophenone was filtered off, washed on the filter with 25-40 ml of ice-cold 76% isopropyl, and dried at 40-45°. The yield of p-nitroacetophenone of m.p. 78-81° was 53.9-60.7 g (56.0-63.1% on the amount of 100% p-nitroethylbenzene taken, or 82.9-93.5% on the amount converted). The p-nitroacetophenone so prepared conforms, without additional purification, to the technical specificiations for this intermediate in levomycetin production. After isolation of p-nitroacetophenone 25-32 g (27.6-35.3%) of p-nitroethylbenzene was recovered; this contained 10-20% of p-nitrcacetophenone and other organic impurities which were not investigated. After vacuum distillation it yielded about 60% of p-nitroethylbenzene

suitable for oxidation to p-nitroacetophenone. An additional amount of p-nitroacetophone can be isolated from the residue in the still.

These conditions were used for oxidation of p-nitroethylbenzene and isolation of p-nitroacetophenone in the experiments, the results of which are given in Tables 1 and 2. All the buffers were used in 100% amounts calculated on p-nitroethylbenzene, or 75% calculated on potassium permanganate.

2. After the end of the oxidation, the reaction mass was heated with stirring on a boiling water bath for one hour; p-nitroacetophenone melted at this stage. The precipitate was filtered off from the reaction mass on a heated Buchner funnel or in a pressure filter (heated, steam pressure 2.5-3 atmos). The residue on the filter was washed several times with hot water (96-98°) until nitro compounds had been washed out completely. The filtrate was cooled to 10-15°, and the crystallized p-nitroacetophenone was filtered off and washed on the filter with water and then with a small amount (25-40 ml) of cold 76% isopropyl alcohol. The yield of p-nitroacetophenone of m. p. 78-81° was 52.0-60.0 g.

The p-nitroethylbenzene recovered from the reaction was separated from the aqueous layer in a separating funnel, added to the residue after evaporation of isopropyl alcohol, and cooled to between −5 and −10°. From 0.5 to 1.5 g of p-nitroacetophenone of m. p. 78.81° separated out. The total yield of p-nitroacetophenone was 53.5-60.5 g, or 55.7-63.0% on the amount of p-nitroethylbenzene taken. When p-nitroethylbenzene of 100% purity was used ($n^{20}D$ 1.5460, freezing point −11.5°), the yield of p-nitroacetophenone reached 64-65% in a number of experiments.

After separation of the ketone 13-25 g (14.3-27.6%) of p-nitroethylbenzene was isolated. The aqueous layer was acidified by mineral acid until acid to Congo Red to liberate 1.6-3.0 g of p-nitrobenzoic acid of m.p. 233-236° (yield 1.6-3.1% on the p-nitroethylbenzene taken).

o-Nitroacetophenone. The preparation was carried out similarly to the preparation of p-nitroacetophenone.

The duration of the process was 20-30 hours. 45.3 g of o-nitroethylbenzene [9, 10] (97% purity, $n^{20}D$ 1.5360, freezing point −12.5°), after evaporation of dichloroethane, gave 43.6 g of a mixture of nitro compounds which was fractionated under vacuum. This gave 19.4 g of the original o-nitroethylbenzene of b. p. 76-82° (1.5 mm) and 20.3 g of o-nitroacetophenone of b. p. 117-123° (1.5 mm, m.p. 22-23°, yield 41.5% on 100% pure o-nitroethylbenzene taken, or 71.5% on the amount converted).

m-Nitroacetophenone. This was prepared similarly to p-nitroacetophenone. The duration of the oxidation was 17 hours. 8 g of m-nitroethylbenzene [11] (practically 100% pure, $n^{20}D$ 1.5390, freezing point −39°) after evaporation of dichloroethane gave 7.7 g of a mixture of nitro compounds which was cooled to 0°. The precipitate was filtered off and washed with a small amount of cold alcohol. 1.7 g of m-nitroacetophenone of m.p. 77-79° was obtained. After distillation of the alcohol the residual mixture of nitro compounds was distilled under vacuum (residual pressure 1-2 mm) to remove m-nitroethylbenzene. 5.4 g of m-nitroethylbenzene was obtained. The residue in the still (0.85 g) was distilled in a small amount of alcohol and heated with activated charcoal; the solution was filtered and cooled. An additional 0.53 g of m-nitroacetophenone of m. p. 77-79° was obtained. The total yield of the ketone was 2.23 g (25.5% on the m-nitroethylbenzene taken, and 85.8% on the amount converted).

2,4-Dinitroacetophenone. This was synthesized by the same method as the ketones described above. The duration of the oxidation was 16 hours. 7 g of 2,4-dinitroethylbenzene [12] (b. p. 126-128° at 2 mm, $n^{20}D$ 1.5673) after evaporation of dichloroethane gave 6.5 g of a mixture of nitro compounds which was fractionated under vacuum. This gave the original 2,4-dinitroethylbenzene of b. p. 103-110° (0.5 mm) and 2,4-dinitroacetophenone of b. p. 184-185° (0.5 mm). The yield was low, as a considerable amount of the ketone resinified during distillation. It is a pale yellow oil, readily soluble in most organic solvents, insoluble in water.

2,4-Dinitrophenylhydrazone forms orange needles (from alcohol), m. p. 194-196°, soluble with difficulty in ethanol and other organic solvents, readily soluble in boiling glacial acetic acid. For analysis it was recrystallized first from glacial acetic acid and then from ethanol. A mixed sample with 2,4-dinitrophenylhydrazone (m. p. 194°) melted at 150-155°.

Found %: C 42.94, H 2.64, N 21.43. $C_{14}H_{10}O_8N_6$. Calculated %: C 43.08, H 2.58, N 21.53.

Acetophenone. Ethylbenzene was oxidized and the reaction mass treated as in the preparation of p-nitroacetophenone. The duration of the process was 14 hours. 106.1 g of ethylbenzene (conforming to the Technical Specification of the Ministry of Chemical Industry No. 3925-54) gave 69.6-72.7g of acetophenone (58.0-61.6% on the ethylbenzene taken), b. p. 83-84° (12 mm). Acidification of the aqueous solution by mineral acid yielded 0.75-0.8 g (0.6-0.65% on the ethylbenzene taken) of benzoic acid of m. p. 119-121°.

LITERATURE CITED

[1] R. Riemschneider, Gazz. chim. ital. 77, 607 (1947).

[2] C. Weygand, Organisch-Chemische Experimentier-Kunst. II. 274-275 (Leipzig, 1948).

[3] R. Riemschneider, Gazz. chim. ital. 81, 479 (1951).

[4] J. Wolf, Przemys. chem. 8, (31), 417 (1952).

[5] A. M. Sladkov and S. V. Vitt, J. Gen. Chem. 26, 1130 (1956).*

[6] Kao Yee-sheng, Pan Pei-chuang, and Lon Shuenhsing, Acta pharm. Sinica, 5, 3, 219 (1957).

[7] J. Wolf, Polish Patent 35876, Przemys. chem. 12 (35), 463 (1956); Chem. and Chem. Technol. 14, 129 (1957).

[8] J. Kucera, Czechoslovakian Patent 85737 and 85738 (1956); C. A. 51, 8791 (1957).

[9] P. M. Kochergin, Medical Ind. USSR, 4, 7, (1956).

[10] H. C. Brown and W. H. Bonner, J. Am. Chem. Soc. 76, 605 (1954).

[11] P. M. Kochergin, J. Gen. Chem. 27, 3204 (1957).*

[12] G. Weisweiller, Monatsh. Chem. 21, 39 (1900).

Received February 25, 1959

* Original Russian pagination. See C.B. Translation.

PRODUCTION OF BRANCHED OLEFINS BY ALKYLATION OF TERTIARY-BUTYL CHLORIDE BY β-BUTYLENE

M. M. Ketslakh, D. M. Rudkovskii, and F. A. Éppel'*

Synthesis of branched olefins is of both theoretical and practical interest. The present communication deals with the production of branched olefins by alkylation of tertiary butyl chloride by β-butylene in presence of magnesium oxide.

The main reaction proceeds as follows:

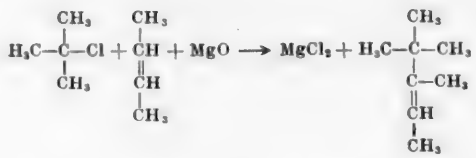

The problem of alkylation of unsaturated hydrocarbons by alkyl halides is not new. As long ago as 1878 Lermontova [1] effected the reaction between tert-butyl iodide and isobutylene and at 100° obtained diisobutylene.

Él'tekov [2] and Kondakov [3] were also interested in alkylation of unsaturated hydrocarbons by alkyl halides, but they did not study the reaction in detail.

Among later publications in the Russian literature, the work of Moldavskii et al. [4] on methylation of hydrocarbons of the olefin series is of interest. They investigated methylation, by means of methyl chloride, of 2-methylbutene-2 and a mixture of butylenes containing about 70% of butene-2, in presence of magnesium oxide. 2,3-Dimethylbutene-1, 2,3-dimethylbutene-2, and 2,3,3-trimethylbutene-1 were identified in the reaction products, and a reaction scheme was proposed to account for the formation of these hydrocarbons.

Also of interest is the paper by Meshcheryakov, Érzyutova, and Petrov [5] on low-temperature alkylation of α- and β-olefins by tertiary alkyl halides in presence of zinc chloride. They showed that in nearly all cases alkylation is accompanied by isomerization. Alkylation of tert-butyl chloride by β-butylene followed by hydrolysis of the chloro alkenes gave a mixture of octenes – 3,4,4-trimethylpentene-2, 2,3,3-trimethylpentene-1, and 2,3,4-trimethylpentene-2 – in a total yield of 35-39% of theoretical (calculated for the converted alkene).

Up to 1948 the foreign literature contained only a few patents on the synthesis of branched olefins. At the end of 1948 Miller and Lovell [6] published their paper on methylation of olefins, and in 1953 Schmerling and Meisinger [7] reported on the condensation of tert-butyl halides with propene, butene-1, and butene-2 in presence of catalysts of the $AlCl_3$ type. These publications were evidently an indication of the interest being displayed in high-octane fuels at that time.

Alkylation of tert-butyl chloride by β-butylene in presence of $FeCl_3$ at 25-35° yielded a mixture of 3-

* The authors thank M. I. Dement'eva for performing the gas analyses.

chloro-2,2,3-trimethylpentane and 2-chloro-3,4,4-trimethylpentane in yields of up to 65% of the theoretical (calculated for the converted butylene); calculated for the corresponding olefins the yield is about 50%. To identify the reaction products, the chlorinated derivatives were either hydrolyzed or dehydrated, and the resultant mixtures of alcohols or olefins were identified by their infra-red absorption spectra.

It is noteworthy that the workers cited [5, 7], who studied alkylation of tert-butyl chloride by β-butylene, observed the formation of various amounts of 2-chloro-3,4,4-trimethylpentane; the other products differed in structure. The probable explanation is that the character of the isomerization differs under different conditions of isomerization. It should also be noted that the total yield of alkenes obtained by hydrolysis of the corresponding chlorides was 39-50% calculated on the butylene converted.

In the present investigation the conditions used for studying the alkylation of tert-butyl chloride by β-butylene differed from those used by the other workers; the reaction was studied at 50-130° in presence of magnesium oxide.

The main aims of the investigation were development of the optimum reaction conditions, identification of the reaction products, and elucidation of the mechanism of their formation.

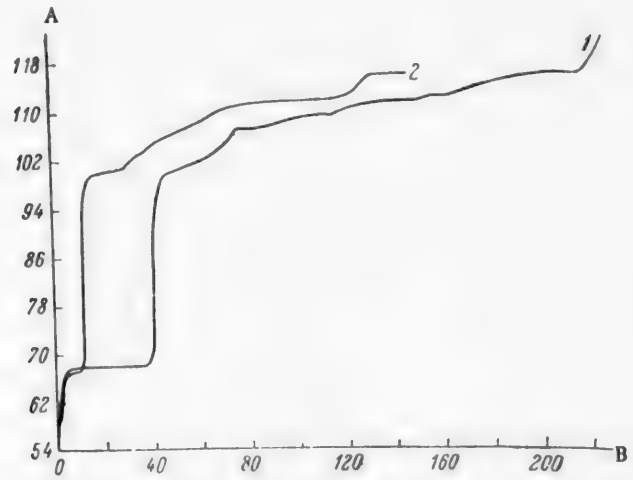

Distillation curves for Experiments No. 44 and 55: A) temperature (°C), B) amount (ml); experiments; 1) No. 44, 2) No. 55.

The results (Table 1, figure) lead to the conclusion that when tert-butyl chloride reacts with β-butylene in presence of magnesium oxide at 100-130° the principal products are dimers of butylene; these are branched octenes, mainly 3,4,4- and 3,3,4-trimethylpentene which comprise about 60% of the dimer fraction, while 2,4,4- and 2,3,4-trimethylpentenes are formed in considerably smaller amounts. The presence of 2,4,4-trimethylpentene-1 in relatively large amounts in comparison with 2,4,4-trimethylpentene-2 (Table 1) indicates that the isobutylene formed by the reaction of butyl chloride with magnesium oxide undergoes polymerization. In addition to these products, secondary-butyl chloride and high-boiling polymers are formed in amounts which increase with rise of temperature (Table 1, 2; Experiments No. 43, 48; figure) and with increase of the molar ratio of tert-butyl chloride to β-butylene. For example, at 2 : 1 ratio of β-butylene to tert-butyl chloride, with a reaction time of 1.5 hours, the dimer–polymer ratio is 1.4 : 1; at 4 : 1 ratio it is 2.6 : 1.

Chlorine determinations in the reaction products obtained under different conditions showed that at 130° with a reaction time of 0.25 hour, about 25% of the octyl chlorides remain unconverted into octylenes and accumulate in the residue together with polymers. As a result, the amount of high-boiling residue increases. The same is found at 50-60° with a reaction time of 3 hours (Table 1; Experiments No. 48, 55). These results show that, as was to be expected, alkylation of tert-butyl chloride by β-butylene is a stepwise process. At the first stage tert-butyl chloride and β-butylene form octyl chloride, and this is followed by formation of dimer

octylenes with liberation of hydrogen chloride. With a reaction time of 1.5-3 hours at 100-130° the reaction products did not contain chlorine.

TABLE 1

Yields of Individual Products under Different Reaction Conditions (Molar ratio of β-butylene to tert-butyl chloride 4 : 1)

Expt. No.	Reaction temperature (°C)	Duration of expt. (hours)	Yields of reaction products, % by weight of theoretically calculated for the converted tert-butyl chloride						Residue from total amt. of reaction products (wt.%)		Dimer-polymer ratio	Yield of dimer fraction, % of theoretical calculated for the converted tert-butyl chloride
			2,4,4-trimethylpentene-1	2,4,4-trimethylpentene-2	3,3,4-trimethylpentene-1	3,4,4-trimethylpentene-1	3,4,4-trimethylpentene-2	2,3,4-trimethylpentene-2	polymers	octyl chlorides		
42	130	1.5	8	2.5	6	4.9	26.4	13	29.3	—	2.5 : 1	59.8
44	100	1.5	8.5	2.1	5.3	3.5	28.5	12	26.8	—	2.8 : 1	60.9
43	90	3.0	11.3	2.9	5.5	4.2	24.7	10.8	28	—	2.6 : 1	59.4
55	60	3.0	8.6	2.3	4.9	3.4	21.6	7.2	19.5	18.4	3.1 : 1	48
48	50	3.0	8.9	1.7	4.4	2.9	20.2	6.9	18	16.2	3.7 : 1	45

Thus, in addition to the main process, formation of 3,4,5-trimethylpentenes, in the alkylation of tert-butyl chloride by β-butylene several side reactions occur: formation of sec-butyl chloride; partial conversion of tert-butyl chloride into isobutylene which, in its turn, is partially polymerized with predominant formation of 2,4,4-trimethylpentene-1 and polymers of high molecular weight and partially reacts with tert-butyl chloride to give rise to 2,4,4-trimethylpentenes; and polymerization of α- and β-butylene.

TABLE 2

Effect of Temperature and Molar Ratio of β-Butylene to tert-Butyl Chloride on Formation of sec-Butyl Chloride

Expt. No.	Reaction temperature (°C)	Molar ratio of β-butylene to tert-butyl chloride	Yield of sec-butyl chloride on the tert-butyl chloride taken (wt. %)
35	100	2 : 1	20.6
44	100	4 : 1	14.4
52	100	4 : 1	Traces
43	90	4 : 1	7.9
46	70	4 : 1	4.2
55	60	4 : 1	3.3
48	50	4 : 1	3.3

• In this experiment sec-butyl chloride was previously added, in an amount corresponding to 12.5% of the tert-butyl chloride taken.

Maximum formation of dimers is prevented mainly by polymerization of olefins with formation of high-boiling residues and by losses due to formation of sec-butyl chloride.

To determine the possibility of suppressing these reactions, it was desired to determine at which stage of

alkylation they occur. Special experiments, performed in a flow-type unit, on gas-phase alkylation of tert-butyl chloride by β-butylene with a short contact time (space velocity of the gaseous raw material,117 liters/ liters of catalyst per hour at 130°, 6 : 1 molar ratio of β-butylene to tert-butyl chloride) showed that sec-butyl chloride and isobutylene (29.6 and 43% respectively on the tert-butyl chloride taken) are formed even at the earliest stages. In addition to these substances, the reaction products also contained 22.4% of unchanged tert-butyl of chloride and 5% of polymerization products; only slight amounts of octyl chlorides were formed. To establish the mechanism of formation of isobutylene and sec-butyl chloride, an autoclave was charged with tert-butyl chloride and magnesium oxide (without β-butylene) in the same proportions as for alkylation (1.1 mole per mole of tert-butyl chloride). The reaction was effected at 110° and continued for 1.5 hours. The reaction yielded the following products, calculated on the tert-butyl chloride taken: sec-butyl chloride 2%, dimers 9%, and polymers 27%.

Thus, in absence of β-butylene sec-butyl chloride is formed in small amounts, and a considerable pr portion of the tert-butyl chloride goes to form the heavy residue; this indicates that formation of sec-butyl chloride is not associated with isomerization of tert-butyl chloride. The considerable amount of polymers formed suggests that reaction of tert-butyl chloride with magnesium oxide yields isobutylene, which is only partially alkylated while most of it polymerizes to products of high molecular weight. Experiments showed that polymers are also formed by polymerization of α- and β-butylenes. Attempts to effect alkylation of tert-butyl chlorides by β-butylene in such a manner that the isobutylene formed as a by-product was completely alkylated by tert-butyl chloride with formation of dimers rather than polymers were unsuccessful. Neither could polymerization of olefins be retarded by introduction of hydrogen under pressure. Formation of sec-butyl chloride could be inhibited by previous introduction of sec-butyl chloride into the reaction mixture, by increase of the molar ratio of β-butylene to tert-butyl chloride, and by decrease of the reaction temperature.

The optimum process conditions, under which the maximum yields of branched dimeric olefins are obtained, are: temperature 100-130°, molar ratio of β-butylene to tert-butyl chloride 4 : 1, and reaction time 1.5 hours; the total yield of branched olefins is then about 61% (calculated on the converted tert-butyl chloride) of the theoretical (Table 3; Experiments No. 42, 44).

TABLE 3

Material Balance for the Alkylation of tert-Butyl Chloride by β-Butylene (Reaction time 1.5 hours, molar ratio of β-butylene to tert-butyl chloride 4 : 1)

Expt. No.	Reaction temperature (°C)	Taken (g)		Obtained (g)							Amt. of tert-butyl chloride reacted (from amt. of chlorine found in magnesium chloride)	Yields, in wt.% (calculated on converted tert-butyl chloride)					
		tert-butyl chloride	butylenes	sec-butyl chloride	unconverted butylenes	2,4,4-trimethylpentenes	3,3,4-trimethylpentene	3,3,4-trimethylpentenes	2,3,4-trimethylpentenes	polymers		2,4,4-trimethylpentenes	3,3,4-trimethylpentenes	3,4,4-trimethylpentenes	2,3,4-trimethylpentenes	polymers	total yield of branched olefins
44	100	240	583	34.6	400.4	24.8	12.4	73	28	49.7	192	11	5	32	12	21	60
42	130	210	515	31.0	390	21.8	12.6	63	27	49.1	168	11	6	31	13	24	61

From the results of this investigation the alkylation mechanism can be represented as follows. In the first state of the process tert-butyl chloride reacts with β-butylene to form octyl chlorides. These octyl chlorides react with magnesium oxide and lose hydrogen chloride to form 3,4,4,-trimethylpentenes. In addition to the main products the dimer fraction contains small amounts of 2,4,4-, 3,3,4-, and 2,3,4-trimethylpentenes. Even at the initial stages of the alkylation process side reactions take place – formation of isobutylene by the reaction of tert-butyl chloride with magnesium oxide, and formation of sec-butyl chloride.

The formation of sec-butyl chloride can be explained by transfer of hydrogen chloride from tert-butyl chloride to β-butylene rather than isomerization of tert-butyl chloride. Therefore alkylation of tert-butyl chloride by β-butylene probably proceeds according to the following scheme:

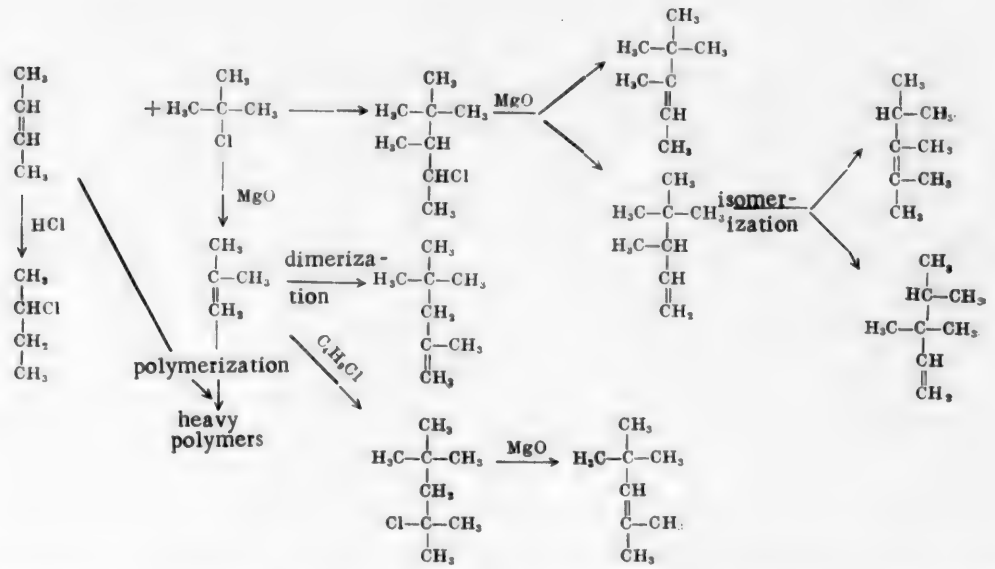

For alkylation of tert-butyl chloride by β-butylene in practice, the use of technical butylene fractions is of interest. These fractions usually contain 25-35% α-butylene and 65-70% β-butylene. If tert-butyl chloride is alkylated by α-butylene, dimethylhexenes (5,5-dimethylhexene-3,5,5-dimethylhexene-2, and others) may be formed. However, dimethylhexenes were not found in the products of alkylation of tert-butyl chloride by butylenes containing 23-25% α-butylene. Analysis of the exit gas showed that α-butylene is recovered almost completely (the amount of α-butylene converted are within the limits of experimental error). because of this selectivity alkylation can be performed by means of a technical gas containing α- and β- (Table 4).

TABLE 4

Butylene Balance in Alkylation of tert-Butyl Chloride by β-Butylene (Molar ratio of β-butylene to tert-butyl chloride 4 : 1)

Expt. No.	Reaction temperature (°C)	Duration of expt. (hours)	Butylenes (g)								
			taken			obtained			converted		
			α	β	i	α	β	i	α	β	i
26	110	3	23.6	76.0	3.4	22.5	54.5	1.8	1.1	21.5	1.6
25	100	3	6.9	28.7	2.4	5.7	18.9	0.5	1.2	9.8	1.9

For synthesis of tert-butyl chloride a mixture of C_4 hydrocarbons even containing small amounts of isobutylene may be used, as the latter reacts selectively with hydrogen chloride under certain conditions to form tert-butyl chloride. Thus, the following procedure may be suggested for practical production of branched olefins by alkylation of tert-butyl chloride β-butylene. A mixture of C_4 hydrocarbons containing isobutylene and α-

and β-butylene is treated with hydrogen chloride under the conditions when tert-butyl chloride is selectively formed. The latter is then alkylated by the unconverted - and β-butylenes in presence of magnesium oxide or calcium oxide.

EXPERIMENTAL

Starting materials. The starting materials for alkylation were tert-butyl chloride (b. p. 50-52°) prepared by the action of hydrogen chloride on isobutylene, and a mixture of α- and β-butylenes prepared by dehydration of n-butyl alcohol over Glukhovo clay. To remove isobutylene, the mixture was subjected to cold polymerization in presence of sulfuric acid. The gas so obtained had the following composition (%): α-butylene 17.2, β-butylene 71.0, isobutylene 5.9, total C_4H_{10} 3.0, liquid residue 2.9.

The material-balance experiments (Table 3) were performed with a gas of the following composition (%): α-butylene 11.19, β-butylene 76, isobutylene 3.7, total C_4H_{10} 7.9, liquid residue 1.

The original gas was analyzed for contents of α- and β-butylenes by low-temperature rectification in a packed column, and isobutylene was determined by the nitrate method [8].

Experimental procedure. An autoclave was charged with finely-ground magnesium oxide (1.1 mole per mole of tert-butyl chloride), and a previously-prepared mixture of the required proportions of tert-butyl chloride and β-butylene was then added with cooling. The reaction mixture was heated at 50-130° for 3 hours for stirring under a pressure of 5-10 atmos (in accordance with the vapor pressure of the reaction mixture at the given temperature).

At the end of the experiment the autoclave was placed in a tilted position and connected to a receiver, a series of condensers cooled in ice and salt, and an evacuated cylinder (5-10 liters in capacity), cooled in solid carbon dioxide, for the gas.

The heavier liquid products were collected in the receiver, and the lighter liquids and unconverted dissolved gas were collected in the condensers. Most of the gas passed into the cylinder. After stabilization in a copper column designed by the All-Union Scientific Research Institute of the Chemical Treatment of Gases [8], the light reaction products were added to the contents of the receiver. To remove substances adsorbed on MgO, the autoclave was placed in the vertical position and the residue, unchanged MgO and small amounts of reaction products, was heated to 80-90°. The reaction were collected and added to the alkylation product.

It must be pointed out that after this treatment the magnesium chloride and unchanged magnesium oxide still contained a certain amount of reaction products. For final removal of the latter, the residue was dissolved in dilute nitric acid and the liberated hydrocarbons were distilled in steam. The amount of magnesium chloride formed from magnesium oxide in the conversion of tert-butyl chloride into olefins was determined by chloride titration by the Volhardt method.

Gas-phase alkylation was carried out as follows: tert-butyl chloride was passed through a dropping funnel into a mixing vessel into which gas containing β-butylene was fed simultaneously. This mixture was passed through a reactor filled with magnesium oxide; the heavy liquid products condensed in the receiver, and the lighter products and unchanged gas were collected in a trap cooled by solid carbon dioxide.

The liquid reaction products formed by alkylation were washed with aqueous sodium carbonate and water, dried by calcium chloride, and were first distilled to give two fractions – up to 120°, and above that temperature; fraction I was then fractionated in a column of about 33 theoretical plates.

The following fractions were collected: up to 72, 72-100, 100-103, 103-108, 108-110, 110-113, 113-115, and 115-120°. The products boiling between 72 and 120° were assumed to be dimers, and the residue boiling above 120° was assumed to consist of polymers.

The composition of the fraction boiling above 120° (polymers) was not investigated in detail; its approximate qualitative composition was determined by fractionation and determinations of the molecular weights of the fractions.

These results indicate that this fraction consisted mainly of trimers.

To determine the composition of the dimer fractions, the above-mentioned individual fractions obtained in experiments under the optimum conditions (as in Experiment No. 44, Table 1 and figure) were combined and redistilled. Close-boiling fractions were collected and their composition determined from their physical

constants and Raman spectra. If these results were insufficient, the individual narrow fractions were hydrogenated and the composition of the saturated hydrocarbons was determined by the methods described above and by the tin-point method [9].

In addition, sec-butyl chloride was fully investigated.

SUMMARY

1. In a study of alkylation of tert- butyl chloride by β-butylene in presence of magnesium oxide it was found that under the optimum process conditions the yield of dimers is 60-61% calculated on the converted tert-butyl chloride. The main products in the dimer fraction are 3,4,4-trimethylpentenes.

2. It is shown that a technical butylene fraction consisting of a mixture of isobutylene and α- and β-butylenes can be used as the raw material.

3. A reaction scheme is given to explain the mechanism by which the products are formed.

LITERATURE CITED

[1] Yu. Ya. Lermontova, J. Russ. Phys.-Chem. Soc. 10, 238 (1878).

[2] A. P. Él'tekov, J. Russ. Phys.-Chem. Soc. 10, 86 (1878).

[3] L. L. Kondakov, J. Russ. Phys.-Chem. Soc. 28, 309 (1896).

[4] B. L. Moldavskii, T. V. Nizovkina, and V. G. Zharkova, J. Gen. Chem. 16, 3 (1946).

[5] L. P. Meshcheryakova, E. I. Érzyutova, and A. P. Petrov, Bull. Acad. Sci. USSR 1, 67 (1956).*

[6] V. A. Miller and M. G. Lovell, Ind. Eng. Chem. 40, 6, 1138 (1948).

[7] L. Schmerling and E.E. Meisinger, J. Am. Chem. Soc. 75, 24, 6217 (1953).

[8] M. I. Dement'eva, Analysis of Hydrocarbon Gases [in Russian] (State Fuel Tech. Press, 1951).

[9] M. M. Ketslakh and F. A. Éppel', J. Anal. Chem. 5, 3, 151 (1950).

Received March 2, 1959

* Original Russian pagination. See C.B. Translation.

SYNTHESIS OF DETERGENTS BY SULFONATION OF OLEFINS BY SOLUTIONS OF SULFUR TRIOXIDE IN LIQUID SULFUR DIOXIDE

K. V. Puzitskii, Ya. T. Éidus, and A. Yu. Rabinovich

The N. D. Zelinskii Institute of Organic Chemistry and the Moscow Branch of the All-Union Scientific Research Institute of Fats

It was shown earlier [1] that olefins present in the products of catalytic hydrocondensation of carbon monoxide with ethylene and propylene can be used for synthesis of sodium alkylbenzenesulfonates with surface-active and detergent properties.

The purpose of the present investigation was synthesis of surface-active and detergent substances by direct sulfonation of olefins with subsequent conversion of the resultant acids into their sodium salts.

The original hydrocarbons used were wide fractions of carbon monoxide–ethylene hydrocondensate, individual polymer fractions obtained from propylene in presence of $ZnCl_2$ catalyst,* and cracking kerosene.

Sulfonation was carried out at temperatures from −30 to −20° by a solution of sulfur trioxide in liquid sulfur dioxide. This sulfonating agent, used earlier for sulfonation of alkylbenzenes [3, 4] is preferable to others in that it excludes the possibility of atmospheric oxidation of the reaction products, and of local overheating causing polymerization and resinification. The sodium salts of the acids so obtained were light in color, from pale cream to bright yellow, whereas sulfonation by concentrated sulfuric acid at 10-15° gave dark resinous products.

EXPERIMENTAL

Fractions of carbon monoxide–ethylene hydrocondensate boiling at 180-230° (C_{10}–C_{12}), 230-300° (C_{12}–C_{17}) and 150-300° (C_9–C_{17}) were used for preparation of the detergents. The properties (physical constants, contents of unsaturated hydrocarbons) of individual fractions of this hydrocondensate are given in the previous paper [1]. Their olefin contents, which increased with decrease of the boiling range, were from 46 to 90%.

The constants of the propylene polymer and cracking kerosene fractions, also used for synthesis of detergents, are given in Table 1.

Freshly-prepared sulfur trioxide (made by distillation from oleum was readily soluble in liquid sulfur dioxide; it dimerized on standing, and its solubility in sulfur dioxide fell sharply. In each experiment 100 ml of the original hydrocarbon fraction and one mole of sulfur trioxide per mole of olefin were used. The average yields of sulfonation products were 70-80% of the theoretical in experiments with ethylene hydrocondensate fractions, 50-60% with propylene polymer fractions, and 60-70% with cracking kerosene. With smaller amounts of sulfur trioxide the yield fell sharply, while with larger amounts a dark product was obtained in higher yield probably owing to formation of di- and polysulfonic compounds, but a part of the unsaturated compounds always remained unchanged. In experiments with cracking kerosene with excess of sulfur trioxide, the aromatic hydrocarbons present in the kerosene entered the reaction in addition to olefins and naphthenes.

The final reaction products usually contained 30-55% of the active substance and 45-70% of sodium sulfate.

*We thank L. I. Antsus for providing the propylene polymer.

The synthesis of detergents by this method from the C_{10}–C_{13} hydrocondensate fraction (b. p. 180-230°, $n^{20}D$ 1.4300, d^{20}_4 0.7606, bromine number 57.0, olefin content 60.2%) is described below.

TABLE 1

Constants of Propylene Polymer and Cracking Kerosene Fractions

Fraction No.	C_n	Boiling range (°C) at 760 mm	n_D^{20}	d_4^{20}	Bromine number	Contents of unsaturated hydrocarbons (%)
			Propylene polymer			
1	C_{10}	150—188	1.4385	0.7912	114.1	102
2	C_{11}	180—200	1.4408	0.7863	127.5	123
3	C_{12}—C_{15}	200—260	1.4481	0.7976	132.3	150
			Cracking kerosene			
1	C_9—C_{17}	150—300	1.4672	0.8354	24.9	30.0

To a solution of 23.3 g of sulfur trioxide in 300 ml of liquid sulfur dioxide, 100 ml of the fraction was slowly added at −30 to −20°; the reaction mass was stirred for an hour at a temperature between −20 and −10° and left overnight. After evaporation of the sulfur dioxide, 110 ml of a dark brown liquid remained; to this 100 ml of water was added, and 130 ml of 20% caustic soda solution for neutralization. Two layers were obtained: an aqueous layer, 250 ml in volume, which was evaporated to dryness to yield 64.3 g of a pale yellow salt (yield 89% of theoretical), and an oil layer 70 ml in volume; this was washed with 20% alkali solution and water and dried over anhydrous copper sulfate; it had b. p. 80-283°, $n^{20}D$ 1.4411, d^{20}_4 0.8164 and bromine number 21.6 (22.7% unsaturated compound).

When olefins are sulfonated by sulfur trioxide the final reaction products may be either alkyl sulfates formed by the reaction

$$RCH{=}CHR' + SO_3 + H_2O \rightarrow RCH_2{-}\underset{\displaystyle R'}{\underset{|}{C}}H{-}OSO_3H,$$

or products of sulfonation of carbon atoms at the double bond, with intermediate formation of compounds of the carbyl sulfate type:

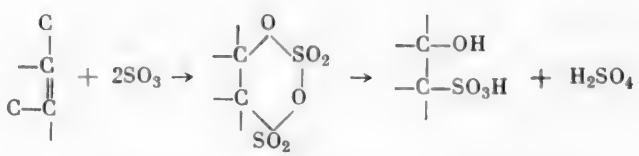

α-Olefins may be sulfonated with retention of the double bond and formation of unsaturated sulfonic acids:

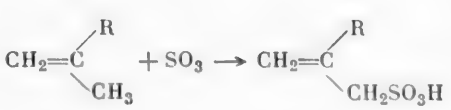

It is reported in the literature [5] that when olefins of sufficiently high molecular weight, with the double bond not at the end of the chain, are treated with a mixture of oleum and acetic anhydride, sulfonic acids and not alkyl sulfates are predominantly formed.

The products obtained in the present investigation are probably sulfonic acid, as shown by their non-saponifiable nature, and considerable amounts of olefins which usually remained in the reaction products. However, further study of this problem is necessary.

The surface-active and detergent properties of aqueous solutions of the products, determined by previously-described methods [6], are given in Tables 2 and 3.

TABLE 2

Surface-Active Properties of Aqueous Solutions of Sulfonated Products from Ethylene Hydrocondensate Fractions

Sulfonated products from hydrocondensate fraction boiling at (°C)	Solution concentration (%)	Solution pH	Foaming power (in ml) at different temperatures		Surface tension (ergs/ cm^2)	Wetting power, cos Θ
			0°	60°		
180—230	0.5	11.7	275/165 *	275/100	35.1	0.56208
	0.25	11.5	270/200	275/150	41.9	0.51803
	0.125	11.2	225/100	175/75	51.9	0.47562
	0.06	10.9	225/150	200/75	61.1	0.43051
	0.03	10.5	140/50	175/50	67.0	0.40514
	0.015	10.2	100/0	0/0	70.2	0.38752
230—300	0.5	7.7	275/165	275/150	33.7	0.62388
	0.25	7.7	275/205	275/175	36.3	0.57358
	0.125	7.4	275/150	260/100	40.6	0.57358
	0.06	7.4	260/150	260/175	46.9	0.56784
	0.03	7.4	255/150	225/100	54.5	0.56353
	0.015	7.2	150/95	140/75	63.7	0.53730
150—300	0.5	7.2	275/210	275/210	33.6	0.54902
	0.25	7.15	265/200	265/140	40.3	0.49697
	0.125	7.15	250/200	260/185	48.3	0.48175
	0.06	7.1	225/165	250/185	56.4	0.47409
	0.03	6.7	160/90	150/80	66.1	0.43680
	0.015	6.5	0/0	0/0	68.8	0.45514

* Here and in Table 3 the numerator represents the original foam volume, and the denominator corresponds to the foam volume after 6 minutes.

Aqueous solutions of sulfonation products obtained from ethylene hydrocondensate fractions (Table 2) are surface-active, but they have low wetting power and emulsifying power of low stability. The foam is of coarsely cellular structure in most cases. The stability to hard water is good – expressed in milliliters of a 1% solution of the substance, it was over 100 both for hard water at 15° and for sea water.

Aqueous solutions of sulfonation products from propylene polymer and cracking kerosene fractions (Table 3) have quite satisfacrory surface activity. They have low surface tension, good wetting power and good resistance to water hardness (above 100), but the emulsifying power is low.

Aqueous solutions of sulfonated products obtained from ethylene hydrocondensate fractions have satisfactory detergent action (Table 4). They are better for washing natural silk than cotton fabric. The best results are obtained when the concentration of active material is 0.25-0.5%.

TABLE 3

Surface-Active Properties of Aqueous Solutions of Sulfonated Products from Fractions of Propylene Polymer and Cracking Kerosene

Boiling range of fraction (°C)	Solution concentration (%)	Solution pH	Foaming power (in ml) at different temperatures		Surface tension (ergs/cm²)	Wetting power, cos Θ
			20°	40°		
Propylene polymer						
150—180	0.5	7.3	250/125	250/150	33.9	0.83549
	0.25	6.7	200/125	250/150	37.1	0.83228
	0.125	6.9	125/100	125/90	39.4	0.78801
	0.06	6.8	125/50	125/70	47.8	0.75471
	0.03	6.5	100/0	100/0	57.4	0.66913
	0.015	6.2	100/0	100/0	64.6	0.68115
180—200	0.5	7.2	250/100	250/100	31.9	0.79512
	0.25	7.4	165/100	240/100	36.4	0.75471
	0.125	7.1	165/100	175/100	38.8	0.65606
	0.06	6.7	160/100	150/100	52.7	0.65276
	0.03	7.0	100/0	75/0	59.2	0.61909
	0.015	6.7	60/0	75/0	67.3	0.57715
200—260	0.5	6.8	250/50	250/100	30.3	0.79512
	0.25	6.9	225/100	250/50	31.5	0.78801
	0.125	6.7	150/50	150/50	35.4	0.75471
	0.06	6.8	100/0	130/0	42.7	0.66044
	0.03	6.8	0/0	0/0	56.1	0.64056
	0.015	6.4	0/0	0/0	61.5	0.59248
Cracking kerosene						
150—300	0.5	6.8	250/100	250/100	34.9	0.82165
	0.25	6.5	200/100	180/100	37.9	0.78801
	0.125	6.5	150/0	125/50	47.8	0.73135
	0.06	6.2	0/0	75/0	61.5	0.71630
	0.03	6.3	0/0	0/0	68.0	0.66913
	0.015	6.3	0/0	0/0	71.8	0.65166

TABLE 4

Detergent Effects of Aqueous Solutions of Sulfonated Products from Ethylene Hydrocondensate Fractions, Expressed as Percentage Whiteness of Washed Fabric* and Percentage of the Detergent Action of Water

Sulfonated product from hydrocondensate fraction (%)	Detergent effects of solutions at concentrations (%)									
	0.5	0.25	0.125	0.06	pH of 0.5% solution	0.5	0.25	0.125	0.06	pH of 0.5% solution
	cotton fabric					natural silk				
180—200	57.5**/320	43.4/240	42.5/145	39.4/109	10.2	64.8/650	55.0/473	40.7/400	—	6.7
230—300	56.3/306	56.3/306	60.6/240	40.4/120	10.1	—	—	—	—	—
150—300	60.3/352	57.4/318	38.9/103	37.2/84	10.0	64.3/650	57.6/522	37.5/143	—	7.3

* The original clean cotton fabric and natural silk had 79.5 and 74.4% whiteness respectively, the artificially soiled had 30.0 and 24.4% , and washed in water had 38.6 and 35.2%.

** The numerator represents the detergent effect in percentage whiteness, and the denominator is expressed as a percentage of the detergent effect of water, taken as 100.

Aqueous solutions of sulfonated products from fractions of propylene polymer and of cracking kerosene (Table 5) are close in their detergent effects and surface-active properties to solutions of alkyl sulfonates made

TABLE 5

Detergent Effects of Aqueous Solutions of Sulfonated Products from Fractions of Propylene Polymer and of Cracking Kerosene, Expressed as Percentage Whiteness of Washed Cotton Fabric*

Sulfonated product from fraction boiling at (°C)	Detergent effect of solution at concentration (%)			
	0.5	0.25	0.125	0.06
150—180 (propylene polymer) . .	42.8	45.1	43.2	43.7
180—200 (propylene polymer) . .	45.9	43.3	44.5	44.3
200—260 (propylene polymer) . .	52.9	50.2	47.4	48.7
150—300 (cracking kerosene) . .	56.9	47.8	49.1	42.8

* The original cotton fabric had 79.3% whiteness in the clean state, 33.8% when artificially soiled, and 45.8% when washed in water.

by sulfochlorination and sulfo-oxidation of the corresponding hydrocarbons, but have better wetting and worse emulsifying powers. Their detergent effects can be improved by certain additives (Na_2CO_3, Na_3PO_4, carboxymethylcellulose), as shown in Table 6.

TABLE 6

Influence of Certain Additives on the Detergent Effects of Aqueous Solutions of Sulfonated Products, Expressed as Percentage Whiteness of Washed Cotton Fabric

Sulfonated product from fraction boiling at (°C)	Solution concentration (%)	Detergent effects of solutions with various additives			
		Na_2CO_3** (1 : 1)	Na_3PO_4 (1 : 1)	$Na_2CO_3 + Na_3PO_4$ (1 : 2 : 2)	20% of carboxymethylcellulose
200—260 propylene polymer	0.5	54.8	58.7	53.1	65.5
	0.25	54.3	54.3	56.1	61.2
	0.125	46.4	56.1	57.6	45.6
	0.06	49.7	—	57.3	47.4
150—300 cracking kerosene	0.5	52.7	51.8	62.0	67.2
	0.25	62.4	55.0	62.2	44.8
	0.125	52.2	44.4	58.1	47.7
	0.06	45.7	—	—	—

** The ratio of the original substance and additive, calculated for active material, is given in parentheses.

SUMMARY

1. The synthesized sulfonated products have surface-active and detergent properties.
2. These products should be used as fatless synthetic detergents in conjunction with useful additives.

LITERATURE CITED

[1] Ya. T. Éidus, K. V. Puzitskii, and A. Yu. Rabinovich, J. Appl. Chem. 32, No. 2, 423 (1959).*

[2] Ya. T. Éidus, N. D. Zelinskii, N. I. Ershov, and M. I. Batuev, Izv. AN SSR, 378 (1950).

[3] D. G. Khomyakov and A. I. Gershenovich, Soviet Patent 77018 (December 12, 1948).

[4] F. N. Baumgartner, Ind. Eng. Ch. 46, 1349 (1954).

[5] A. Schwartz and J. Perry, Surface-Active Agents [Russian translation] edited by A. P. Taubman (IL, Moscow, 1953).

[6] K. V. Puzitskii, A. Yu. Rabinovich, and Ya. T. Eidus, J. Appl. Chem. 32, No. 2, 404 (1959).*

Received June 21, 1958

* Original Russian pagination. See C.B. Translation.

MECHANISM OF THE INHIBITING ACTION OF POLYPHENOLS AND THE ROLE OF OXYGEN*

G. P. Belonovskaya, Zh. D. Vasyutina, and B. A. Dolgoplosk

The inhibiting action of polyphenols in radical reactions is due to the possibility of formation of stable semiquinoid radicals by cleavage of -O-H bonds:

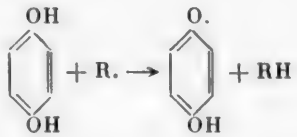

(1)

Earlier investigations [1-4] showed that in hydrocarbon solutions in absence of oxygen, hydroquinone and other polyphenols do not react to any practical extent with free radicals; this is consistent with absence of an inhibiting effect on the polymerization process. Under the same conditions quinones completely inhibit polymerization as the result of reactions leading to formation of semiquinoid radicals:

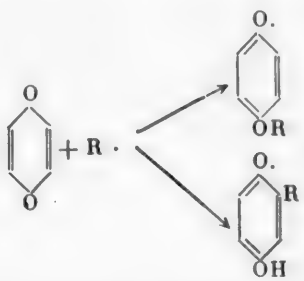

(2)

The occurrence of Reactions (1) and (2) should depend to a considerable extent on the oxidation-reduction potentials of the polyphenols and the corresponding quinones. Introduction of substituents lowers the oxidation-reduction potential; for example, from 0.715 for hydroquinone [5] to 0.554 [6] for di(tert-butyl)hydroquinone. It was therefore to be expected that Reaction (1), which has an inhibiting effect on polymerization, is more probable for the alkyl hydroquinone than for hydroquinone, whereas the reverse is true for the corresponding quinone with regard to Reaction (2). We found in a study of the inhibiting action of di(tert-butyl)quinone on thermal polymerization that it is a relatively weak inhibitor, which merely retards the polymerization of styrene (Fig. 1), whereas benzoquinone under the same conditions causes an induction period proportional to the inhibitor concentration. Figure 1 shows that the inhibiting effect of di(tert-butyl)quinone is similar to that of known relatively weak inhibitors, mono- and dinitrobenzene, and is intermediate between the two.

A similar relationship holds for inhibition of styrene polymerization catalyzed by azobisisobutyronitrile

* Communication XVI in the series of free-radical reactions in solutions.

(Fig. 2). Here again di(tert-butyl)quinone only retards the process to a certain extent, whereas benzoquinone even at a very low concentration causes an induction period with total suppression of polymerization.

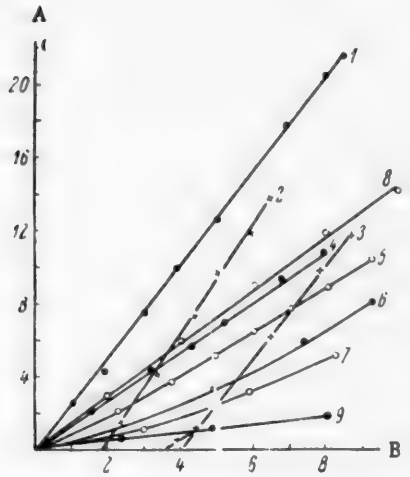

Fig. 1. Thermal polymerization of styrene in presence of benzoquinone and di-(tert-butyl)quinone at 100°; A) polymer yield (%), B) time (hours); 1) without inhibitor; benzoquinone (in molar % on styrene); 2) 0.02, 3) 0.05; di(tert-butyl)-quinone (in molar % on styrene); 4) 0.02, 5) 0.05, 6) 0.1, 7) 0.20; 8) mononitrobenzene, 0.10 molar % on styrene, 9) dinitrobenzene, 0.10 molar % on styrene.

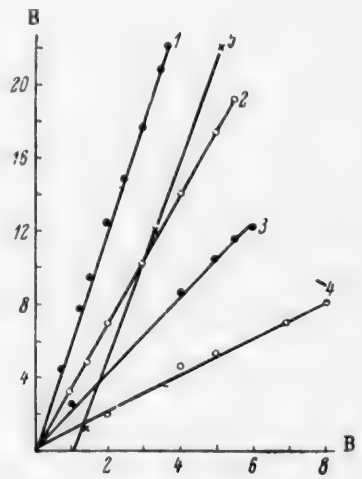

Fig. 2. Polymerization of styrene in presence of azobisiobutyronitrile and di(tert-butyl)quinone at 100°, 0.05 molar % of catalyst on styrene: A) polymer yield (%), B time (hours); 1) without inhibitor; di(tert-butyl)-quinone (molar % on styrene): 2) 0.02, 3) 0.05, 4) 0.10; 5) benzoquinone, 0.0075 molar % on styrene.

It was of definite interest to compare the activities of benzoquinone, the alkyl quinone, and mono- and dinitrobenzene with respect to the free methyl radical formed by thermal decomposition of methylphenyltriazene. The experiments were performed in dry ligroin at 110° by the known method [7]; it was shown that the alkyl quinone is considerably less active than benzoquinone and has approximately the same activity as dinitrobenzene. The results are given in the table.

Influence of Inhibitors on the Yield of Methane in Decomposition of Methylphenyltriazene in Ligroin at 110°

Inhibitor	Concentration in solution (wt. %)		Molar ratio of methylphenyltriazene to inhibitor	Yield of methane (% of theoretical)
	methylphenyltriazene	inhibitor		
Without inhibitor	2.50	—	—	60
Benzoquinone	2.70	2.20	1 : 1	2
	2.60	4.40	1 : 2	0
Dinitrobenzene	2.60	8.28	1 : 2.5	20
Di(tert-butyl)quinone	3.17	5.10	1 : 1	24
Mononitrobenzene	2.64	6.70	1 : 2.5	40

In absence of oxygen di(tert-butyl)hydroquinone, like hydroquinone, merely lowers the rate of styrene polymerization without causing an induction period (Fig. 3).

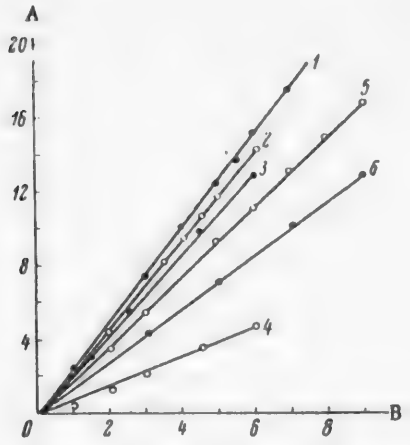

Fig. 3. Polymerization of styrene in presence of di(tert-butyl)hydroquinone and hydroquinone at 100° in nitrogen: A) polymer yield (%), B) time (hours); 1) without inhibitor; di(tert-butyl)hydroquinone (in molar % on styrene); 2) 0.035, 3) 0.07, 4) 0.5; hydroquinone (in molar % on styrene); 5) 0.09, 6) 0.47.

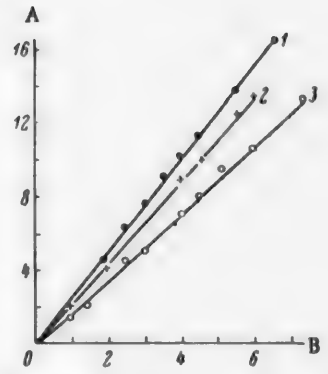

Fig. 4. Polymerization of styrene in presence of di(tert-butyl)hydroquinone and isopropylbenzene hydroperoxide (0.05 molar %) at 80°: A) polymer yield (%), B) time (hours); 1) without hydroquinone; di(tert-butyl)hydroquinone (in molar % on styrene); 2) 0.05, 3) 0.10.

Similar results are obtained for styrene polymerization catalyzed by isopropylbenzene hydroperoxide (Fig. 4).

The inhibiting effect of the dialkyl hydroquinone is more prominent in polymerization of vinyl acetate catalyzed by azobisisobutyronitrile. This is due to the high activity of the polymeric radicals formed, which leads to development of Reactions (1) and (2).

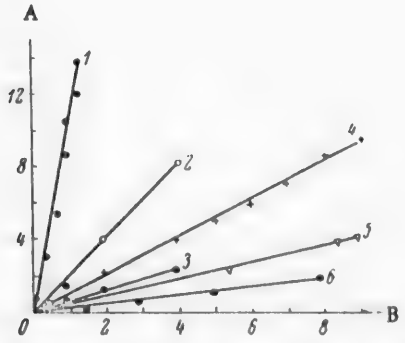

Fig. 5. Polymerization of vinyl acetate at 50° in presence of 0.05 molar % of azobisisobutyronitrile: A) polymer yield (%), B) time (hours); 1) without inhibitor; hydroquinone (in molar % on vinyl acetate); 2) 0.03, 3) 0.11; di(tert-butyl)quinone: 4) 0.02, 5) 0.05, 6) 0.10.

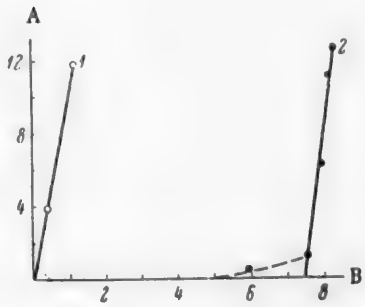

Fig. 6. Polymerization of vinyl acetate at 50° in presence of di-(tert-butyl)quinone and 0.05 molar % of azobisisobutyronitrile: A) polymer yield (%), B) time (hours); 1) without inhibitor, 2) di(tert-butyl)-quinone, 0.025 molar % on vinyl acetate.

Figure 5 shows that hydroquinone and the alkyl hydroquinone retard considerably the polymerization of vinyl acetate, and at equal molar concentrations the alkyl hydroquinone is more effective than hydroquinone.

Di(tert-butyl)quinone in very low concentrations completely inhibits catalyzed polymerization of vinyl acetate, causing a prolonged induction period (Fig. 6). Similar results were obtained in earlier investigations [2] with benzoquinone.

The Role of Oxygen in Inhibition of the Polymerization Process in Presence of Polyphenols

It was shown in earlier investigations that polyphenols inhibit polymerization completely in presence of oxygen. Studies of the effect of di(tert-butyl)hydroquinone on polymerization of styrene in presence of oxygen showed that its inhibiting effect is much more prominent than that of the dialkyl quinone (at the same molar concentrations) in absence of oxygen. Whereas di(tert-butyl)quinone is a relatively weak inhibitor (Fig. 1), di(tert-butyl)hydroquinone is presence of oxygen inhibits the process completely, causing a prolonged induction period (Fig. 7).

This fact shows convincingly that the inhibiting action of the system dialkyl hydroquinone + oxygen is associated with stages preceding formation of the final oxidation product (quinone):

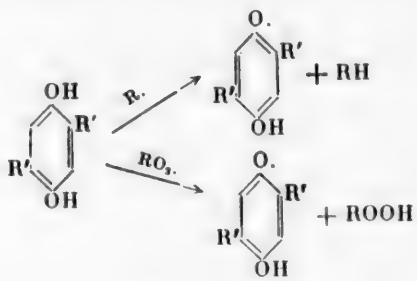

(a)

(b)

Reaction (b) is thermodynamically more advantageous than Reaction (a). If R· radicals, oxygen, and polyphenol are present in the system, inhibition of polymerization is associated with formation of semiquinoid radicals by the reaction of RO_2· radicals with hydroquinone.

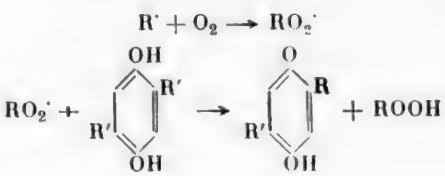

(3)

The existence of RO_2· radicals as an intermediate step in formation of polymeric peroxides in thermal and catalyzed polymerization of styrene in presence of air was demonstrated by Miller and Mayo [8] and in a number of other publications.

It is also well known that $CN-\overset{CH_3}{\underset{CH_3}{C}}-COO\cdot$ radicals are formed by the decomposition of azobisisobutyronitrile in hydrocarbon solution in presence of oxygen. Many workers have reported the interaction of RO_2· radicals with phenols and polyphenols. As long ago as 1947 Bolland [9] suggested that the inhibiting effect of hydroquinone on the oxidation of linoleate catalyzed by benzoyl peroxide is due to its interaction with RO_2· radicals formed in the oxidation of linoleate; benzoquinone is formed as the result of these conversions.

Boozer and Hammond [10] showed in a study of catalyzed oxidation of hydrocarbons that $CN-\overset{CH_3}{\underset{CH_3}{C}}-OO\cdot$, radicals formed in the decomposition of azobisisobutyronitrile in presence of oxygen react with di(tert-butyl)-cresol and other phenols to form compounds of quinoid structure.

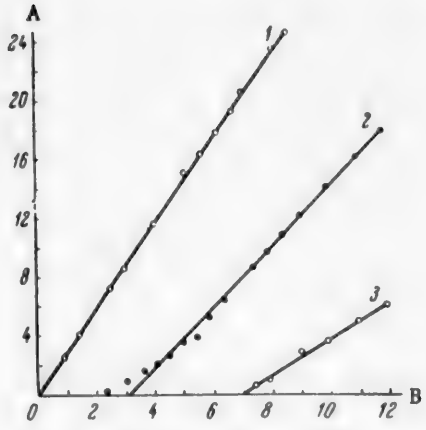

Fig. 7. Polymerization of styrene in presence of di(tert-butyl)hydroquinone and air at 100°: A) polymer yield, B) time (hours); 1) without hydroquinone; di(tert-butyl)hydroquinone (molar % on styrene): 2) 0.02, 3) 0.05.

It has been shown for hydroquinone [2] and, in the present instance, for di(tert-butyl)hydroquinone that dimethylcyanomethyl radicals cannot react with polyphenols in accordance with Equation (1). When di(tert-butyl)hydroquinone is heated with excess azobisisobutyronitrile for 4 hours at 90°, i.e., under conditions when this dinitrile decomposes completely, di(tert-butyl)hydroquinone does not undergo any changes. Under analogous conditions, but in absence of a source of free radicals di(tert-butyl)hydroquinone is not oxidized directly by oxgen.

When di(tert-butyl)hydroquinone is heated with excess of azobisisobutyronitrile in a current of oxygen at 90°, it is completely converted in 4 hours into compounds of the quinoid type. Spectrophotometric determinations of optical density at different wave lengths* showed that the reaction mixture contains no di(tert-butyl)hydroquinone, 30-35% of di(tert-butyl)quinone, and a considerable amount of compounds of the quinoid type, evidently formed by interaction of di(tert-butyl)quinone with the radicals

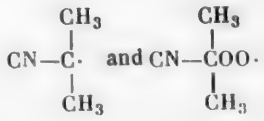

The peroxide compounds formed by oxidation of azobisisobutyronitrile in absence of polyphenols are weaker oxidizing agents. Under our experimental conditions (4 hours, 90°) they convert only 20% of the di-(tert-butyl)hydroquinone into the corresponding quinone.

It is evident from these results that in polymerization of styrene catalyzed by azobisisobutyronitrile the inhibiting effect of hydroquinone in presence of air is mainly due to Reaction (3) as follows:

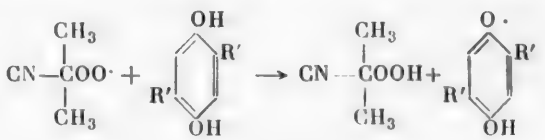

In thermal polymerization in presence of oxygen semiquinoid radicals are formed by interaction of di(tert-butyl)hydroquinone with polymeric peroxide radicals.

EXPERIMENTAL

Di(tert-butyl)hydroquinone was prepared by direct alkylation of hydroquinone. It was purified by recrystallization from 70% ethyl alcohol. It forms crystals of m. p. 211-212°.

Di(tert-butyl)quinone was prepared by oxidation of di(tert-butyl)hydroquinone by $FeCl_3$ in alcoholic HCl solutions [6]. It was purified by sublimation on gentle heating. It forms yellow needles of m. p. 151-152°.

* These determinations were performed under the guidance of E. V. Anufrieva.

Styrene was washed with 5% NaOH solution to remove hydroquinone, then with water to a neutral reaction, dried by $CaCl_2$, and distilled twice under vacuum in a current of nitrogen.

Vinyl acetate was purified by distillation in a high-efficiency column. The 72.5° fraction (at 760.5 mm) had $n^{20}D$ 1.3950.

The tubes were filled with monomer in a special apparatus under conditions such that traces of air could not get into the system [1, 2]. For polymerization in air, after the tubes had been filled with monomer by the usual technique the apparatus was filled with air and the tubes were sealed at normal pressure. The polymerization kinetics were studied dilatometrically.

SUMMARY

1. The inhibiting effects of di(tert-butyl)quinone and di(tert-butyl)hydroquinone on thermal and catalyzed polymerization of styrene and vinyl acetate were studied; the experimental results are considered in relation to the role of semiquinoid radicals in the inhibition process.

2. It is shown experimentally that the inhibiting effect of oxygen on polymerization in presence of di(tert-butyl)hydroquinone is due to formation of semiquinoid radicals by the consecutive reactions:

$$R\cdot + O_2 \longrightarrow RO_2\cdot$$

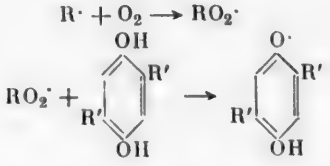

LITERATURE CITED

[1] B. A. Dolgoplosk and D. Sh. Korotkina, J. Gen. Chem. 27, 2226, 2546 (1957).*

[2] B. A. Dolgoplosk and G. A. Parfenova, J. Gen. Chem. 27, 2773, 3083 (1957).*

[3] M. S. Kharash, F. Kawahara, and W. Nudenberg, J. Org. Chem. 9, 12, 1977 (1954).

[4] A. F. Bickel and W. A. Waters, J. Chem. Soc. 1764 (1950).

[5] M. G. Evans, Trans. Faraday Soc. 45, No. 4, 312 (1949).

[6] F. J. L. Aparicio and W. A. Waters, J. Chem. Soc. 4666 (1952).

[7] B. A. Dolgoplosk, B. A. Erusalimskii, V. A. Krol', and L. M. Romanov, J.Gen. Chem. 24, 1774 (1954).

[8] A. A. Miller and F. R. Mayo, J.Am. Chem. Soc. 78, 1017 (1956).

[9] J. L. Bolland, P. Ten Have, Trans. Faraday Soc. 43, 201 (1947).

[10] Ch. E. Boozer and G. S. Hammond, J. Am. Chem. Soc. 76, 3861,(1954); 77, 3233, 3238 (1955).

Received July 17, 1958

*Original Russian pagination. See C.B. Translation.

FRACTIONAL DISTILLATION OF MIXTURES OF NITROETHYLBENZENES

O. S. Vladyrchik, P. M. Kochergin, K. E. Novikova,
L. L. Bespalova, R. M. Titkova, A. M. Tsyganova,
G. D. Krasnozhen, and A. M. Grigorovskii

Mononitration of ethylbenzene yields a mixture of approximately equal amounts of o- and p-nitroethylbenzenes and a small amount of m-nitroethylbenzene. According to Brown and Bonner [1], the different isomers are present in mononitroethylbenzene in the following proportions: o-isomer 45.0%, m-isomer 6.5%, and p-isomer 48.5%. Technical nitroethylbenzene (the common name for a mixture of isomeric mononitroethylbenzenes) may contain ethylbenzene, 2,4-dinitroethylbenzene, moisture, and resinuous products as impurities.

Separation of water and ethylbenzene presents no difficulties, as they boil considerably below the boiling point of any of the isomeric mononitroethylbenzenes. Some workers [2, 3] distilled nitroethylbenzene in steam in order to separate dinitroethylbenzene and resinous substances. This operation is essential in methods of ethylbenzene nitration which lead to formation of dinitroethylbenzene and resinous products. Otherwise, when nitroethylbenzene containing these impurities is distilled under vacuum the nitration products may explode or catch fire.

Great difficulties with regard to apparatus and technique arise in separation of nitroethylbenzenes into the individual components, as the boiling points of isomeric mononitroethylbenzenes are fairly close together [1, 4]. For example, Beilstein and Kuhlberg [5], who were the first to nitrate ethylbenzene, obtained o- and p-nitroethylbenzenes with constant boiling points after 20-fold distillation of the low-boiling and high-boiling nitroethylbenzene fractions at atmospheric pressure. Later Schultz and Flachslander [6] were able to separate nitroethylbenzene into constant-boiling substances only after 80-fold distillation under vacuum followed by 100-fold distillation under atmospheric pressure. Despite this tedious and meticulous work, they apparently did not obtain pure o- and p-nitroethylbenzenes. According to their data, the o-isomer melted at −23° and the p-isomer at −32°, whereas the individual o- and p-nitroethylbenzenes [4] solidify at −11 and −11.5° respectively.

Subsequently a number of workers [1,3,7,8] obtained o- and p-nitroethylbenzenes by fractional distillation of nitroethylbenzene under vacuum, with columns of different designs. However, it is difficult to judge the purity of the mononitroethylbenzenes isolated by them from the boiling points and refractive indices, especially as the values given by different authors are very contradictory.

Czech scientists [9] showed that nitroethylbenzene can be fractionated in steam. They found that the presence of water has no significant influence on the rectifying efficiency of the column. Distillation in presence of water, as in its absence, is effected under reduced pressure (6 mm), so that the role of water is merely to lower the boiling points of the mononitroethylbenzenes.

The purpose of the present investigation was to study fractional distillation, under laboratory conditions, of nitroethylbenzene for preparation of pure o- and p-nitroethylbenzenes. The latter are used as intermediates for synthesis of nitroacetophenones [10].

Fractionation of nitroethylbenzene was investigated in a laboratory unit consisting of a glass column 30 mm

in diameter and 1900 mm high, packed with porcelain Raschig rings 5 mm in diameter. To reduce heat loss to the surroundings the column was insulated by asbestos braid and equipped with an electrical heater regulated by means of LATR-1. The still was a two-necked round-bottomed flask 2 liters in capacity, fitted by a ground-glass joint to the lower end of the column and heated in a bath with Wood's alloy. The column had a complete condensation head. A bulb condenser was used as dephlegmator. A special adapter was used whereby distillate samples could be taken and receivers changed without disturbance of the operating conditions of the column. The unit was fitted with the requisite thermometers and vacuum gauges. The system was evacuated by means of an oil vacuum pump, and a water-jet pump was used to evacuate air from newly connected receivers.

Rectification was effected batchwise. The starting mixture was nitroethylbenzene prepared as described by Brown and Bonner [1] and distilled in steam. The composition of the distillate was determined from the boiling point, refractive index, and solidification temperature. The data of Vilim et al. [9] on vapor pressures of o- and p-nitroethylbenzenes proved useful for determinations of the distillate composition from the boiling point.

Having pure o-, p-, and m-nitroethylbenzenes [4] at our disposal, we determined their refractive indices (by means of a Pulfrich refractometer) at different temperatures (Table 1). These may be useful under plant conditions, when it is not always possible to determine rapidly the refractive indices of mononitroethylbenzenes at exactly 20°.

TABLE 1

Refractive Indices of Pure o-, m-, and p-Nitroethylbenzenes at Different Temperatures

Temperature (°C)	Refractive index n_D		
	o-isomer	m-isomer	p-isomer
16.5	—	—	1.54763
18	1.53638	—	1.54684
19	—	1.53929	—
20	1.53571	1.53904	1.54604
22	1.53512	1.53805	1.54523
24	1.53428	1.53721	1.54443
26	1.53335	1.53639	1.54378
28	—	1.53555	1.54297
30	—	1.53462	—

TABLE 2

Freezing Points and Refractive Indices of Mixtures of o- and p-Nitrobenzenes

o-Nitrobenzene (%)	p-Nitrobenzene (%)	Freezing point (°C)	n_D^{20}
100	—	—11	1.5357
98.27	1.73	—12	1.5358
97.04	2.96	—12.5	1.5359
95.96	4.04	—13	1.5360
94.66	5.34	—13.5	1.5362
89.36	10.94	—16	1.5368
8.40	91.60	—16	1.5443
5.18	94.82	—14	1.5449
2.88	97.12	—12.7	1.5450
2.34	97.66	—12.5	1.5452
1.04	98.96	—12	1.5457
—	100	—11.5	1.5460

Freezing points of the nitroethylbenzenes were determined in a test tube 15 mm in diameter and 120 mm long, inserted through a cork in another tube, 40 mm in diameter and 160 mm long. The latter tube was placed in a transparent Dewar flask 0.5 liter in capacity, filled with ethanol cooled by pieces of solid carbon dioxide.

The refractive indices and freezing points of binary mixtures of o- and p-nitrobenzenes are given in Table 2.

Nitroethylbenzene was fractionated under vacuum at a residual pressure of 11-16 mm. The column was allowed to run for one hour without collection of distillate. The experiments differed in the procedure used for collection of the distillate. When the necessary rate of vapor formation had been attained in the still, the following yields were obtained under the optimum collection conditions (in %): ethylbenzene 3.5-7; o-nitroethylbenzene (contents of other mononitroethylbenzenes did not exceed 3%) 42.7-43.5; p-nitroethylbenzene (with not more than 3% impurities) 44.7;46.2; intermediate fraction containing o-, m-, and p-nitroethylbenzenes 10.3-12.6; residue in still 1.8-3, which was redistilled to yield 2,4-dinitroethylbenzene of b. p. 149-153° (4.5 mm), $n^{20}D$ 1.5673, $n^{25}D$ 1.5653 (literature data [11] $n^{25}D$ 1.5655).

The intermediate fractions from several experiments were combined and redistilled under the same conditions. This yielded pure o- and p-nitroethylbenzenes in amounts of 20 and 40% respectively.

For synthesis of o- and p-nitroacetophenones [10] o- and p-nitroethylbenzenes containing not less than 95% of the main monomers are suitable.

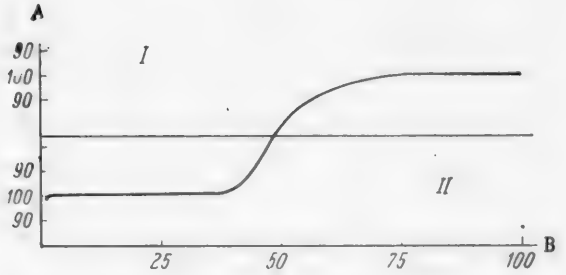

Rectification curve for mixture of mononitroethylbenzenes: A) distillate composition, B) fraction distilled off (%); I) p-nitroethylbenzene, II) o-nitroethylbenzene.

The figure shows the fractionation curve for nitroethylbenzene. Table 3 contains the data of a typical experiment on fractionation of nitroethylbenzene.

Nitroethylbenzenes were distilled at constant distillate composition. The reflux ratio rose from 10 to 20 in collection of o-nitroethylbenzene, remained at 20 in collection of the intermediate fraction, and varied in the 0.5-1 range in collection of p-nitroethylbenzene. The vapor velocity in the open section of the column was 5.93 m/ second in collection of o-nitroethylbenzene, and 5.63 m/ second in collection of the intermediate fraction.

Calculation of the number of theoretical plates required to give the degree of separation obtained was carried out for the binary mixture o-nitroethylbenzene–p-nitroethylbenzene (m-nitroethylbenzene is present in the mixture in very small amounts and was disregarded in the calculations). The binary mixture o-nitroethylbenzene–p-nitroethylbenzene was assumed to be ideal, i.e., conforming to Raoult's law. The vapor

TABLE 3

Results of a Fractionation Experiment on Nitroethylbenzene Mixture (1057 g of nitroethylbenzene taken for distillation; yield 964.3 g (91.23%) of total mononitroethylbenzenes)

Fraction No.	Boiling point (°C)	Residual pressure (mm)	Weight (g)	Yield, % of total mononitroethylbenzene	n_D^{20}	Freezing point (°C)	Substance	Contents of main component (%)
1	—	—	35.0	—	—	—	Ethylbenzene	—
2	112—115	16	8.4	0.8	1.5375	—17	o-Nitroethylbenzene	86
3	115	16	5.9	0.6	1.5354	—12		97.8
4	115	16	300.5	30.9	1.5357	—11		100
5	116	16	67.9	7.1	1.5360	—11.5		98.8
6	117—118	16	38.8	4.0	1.5364	—15		91
7	119—124	15—14	101.7	10.3	1.5432	—52	Intermediate fraction	—
8	123.5—124	13.5	42.7	4.4	1.5455	—20	p-Nitroethylbenzene	85
9	122—122.6	12.5	69.5	7.2	1.5460	—16.5		91
10	121	11.6	99.4	10.3	1.5463	—12.5		98
11	120	11	233.5	24.3	1.5463	—11.5		100
12	—	—	24.2	—	—	—	Still residue	—

pressure–temperature curves for the pure components were plotted from literature data [9], and the result was used to determine the relative volatility for the mixture, found to be 1.82. The number of theoretical plates was determined by the analytical method described in the literature [12, 13].

The calculations showed that the column efficiency should be equivalent to 12 theoretical plates to give the degree of separation achieved in our experiments. The packing height equivalent to one theoretical plate (HETP) was 158 mm.

We also studied fractional distillation of nitroethylbenzene free from ethylbenzene and dinitroethylbenzene. This mixture was fractionated in a laboratory unit. The column, 20 mm in diameter and 1500 mm high, was packedwith 5 mm rings of copper wire 1 mm thick . The still was a round-bottomed flask 1 liter in capacity. The rest of the apparatus was the same as described above. Nitroethylbenzene was again fractionated by the batch method under 8-11 mm residual pressure. The column ran for 1 hour without collection of distillate, and the reflux ratios during collection of the fractions varied in the range of 12 to 15. The following products were obtained (in %): o-nitroethylbenzene of 95-100% purity 40-42, p-nitroethylbenzene of 95-100% purity 38-40, intermediate fraction 18-22, residue in still 1.5-3.

The linear vapor velocity in the open section of the column was 4.76 m/ second during collection of o-nitroethylbenzene, and 3.86 m/ second during collection of the intermediate fraction. Calculations showed that the column efficiency should be 13 theoretical plates to give this degree of separation of the mixed nitroethylbenzenes. HETP was 112 mm.

SUMMARY

1. Procedure for fractional distillation of a technical mixture of nitroethylbenzenes was worked out by means of a laboratory column, and the column efficiency required to give o- and p-nitroethylbenzenes containing not more than 5% of other isomers was calculated.

2. Pure o- and p-nitroethylbenzenes, in yield of 30 and 24% respectively calculated on the total mononitroethylbenzenes, were obtained by fractionation of mixed nitroethylbenzenes, and the refractive indices and freezing points of their mixtures were determined.

3. The refractive indices of individual o-, p-, and m-nitroethylbenzenes were determined at various temperatures.

LITERATURE CITED

[1] H. C. Brown, and W. H. Bonner, J. Am. Chem. Soc. 76, 605 (1954).

[2] E. Schreiner, J. pr. Chem. (2), 81, 558 (1910).

[3] E. L. Cline and E. E. Reid, J. Am. Chem. Soc. 49, 3150 (1927).

[4] P. M. Kochergin, J. Gen. Chem. 27, 3204 (1957).*

[5] F. Beilstein and A. Kuhlberg, Lieb. Ann., 156, 206 (1870).

[6] G. Schultz and J. Flachslander, J. pr. Chem. (2), 66, 153 (1902).

[7] A. H. Ford-Moore and H. N. Rydon, J. Chem. Soc. 679 (1946).

[8] Kondo and S. Uyeo, Ber. 70, 1091 (1937).

[9] O. Vilim, E. Hala, V. Fried, and J. Pick, Chem. listy, 48, 1109 (1954).

[10] P. M. Kochergin, V. A. Zasosov, R. M. Titkova, and A. M. Grigorovskii, J. Appl. Chem.32, No. 8, 1806 (1959).*

[11] C. Hansch. and G. Helmkamp, J. Am. Chem. Soc. 73, 3080 (1951).

[12] N. I. Gel'perin, Distillation and Rectification [in Russian] (Goskhimizdat, Moscow–Leningrad, 1947) p. 151.

[13] N. I. Gel'perin and K. E. Novikova, Oxygen 5, 29 (1951).

Received February 25, 1959

* Original Russian pagination. See C.B. Translation.

METHODS FOR DETERMINATION OF THE DYEING COMPONENT IN DYES FOR ACETATE RAYON

L. M. Golomb

The K. E. Voroshilov Scientific Research Institute of Organic Intermediates and Dyes, Rubezhnoe Branch

Hydrophobic fibers (acetate rayon, capron, nitron, lavsan, and many others) are dyed from aqueous suspensions by special dyes known as dispersed dyes, which first appeared in the 1920's and were intended for dyeing of acetate fibers, the only ones of this type known at that time [1].

This class of dyes, known as acetate-rayon dyes, includes: 1) insoluble azo dyes and anthraquinone derivatives, 2) certain derivatives of nitrodiphenylamine, 3) some methine dyes, and 4) a few derivatives of naphthoquinoneimine [2].

The first group is the largest in this class. Dyes for acetate rayon are characterized by low solubility in water [3], and good solubility in acetone, acetate esters, and certain other organic solvents. These dyes are marketed in the form of fine powders containing from 15 to 40% of the pure dyes and several dispersing and wetting agents and fillers [3-5].

The photometric method is used for determinations of dye concentrations both in the commercial products and in dye baths. The determinations are usually performed in aqueous acetone (containing up to 75% acetone) or acetone solutions. The same method is used for determinations of dyes on bright acetate fibers [6].

A serious disadvantage of the acetone solutions used for this purpose is their volatility; evaporation of acetone cannot be prevented even by the use of firmly-closed photometric cells, and this leads to inaccuracies in the determinations. The preparation of standard solutions is difficult if commercial brands containing acetone-insoluble substances are used for this purpose. Moreover, relatively large volumes of a harmful and inflammable solvent have to be used.

We have developed a convenient photometric method for determinations of concentration of the dyeing component in acetate-rayon dyes in sol form.

In distinction from the known methods for preparation of hydrosols of insoluble dyes as described by Balen'kii [7] or hydrosulfosols (by Sokolov's method [8]), we used glacial acetic acid, in which most acetate dyes are easily soluble.

Stable acetic acid sols (which we term "hydroacetosols"), brightly colored and resembling true solutions, are formed when acid solutions of the dyes are poured into water at temperatures close to 0° in presence of the nonionic surface-active agent OP-10 (condensation product of ethylene oxide and an alkyl phenol). The formation of such sols is due to colloidal solubility as described by Rebinder [9] or to solubilization (McBain).

Hydrosulfosols were prepared and tested in parallel with the hydroacetosols. However, the former proved to be less universally applicable: some dyes (Table 1, No. 8) are decomposed in sulfuric acid, and the optical density is sometimes much lower than that of hydroacetosols of the same concentration (Dyes No. 2,5, and 6, Table 1); this effect is sometimes accompanied by shifts of the maximum-absorption bands into the

TABLE 1

Characteristics of the Investigated Dyes

Dye No.	Chemical structure	Color index No. [11]	Trade or chemical name	Form investigated	Migration rate on 'paper* k_f	Positions of maxima in absorption bands (m μ)		
						soln. in CH_3COOH	hydro-aceto-sols.	hydro-sulfo-sols.
1	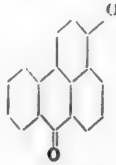	58900	3-Methoxybenzathrone	Pure, thrice re-crystallized from CH_3COOH, m.p. 173° [3]	a) 0.93 b) 0.53 d) 0.83	440	442	442
			Duranol bright-yellow 6G	C. F. **	a) 0.93 b) 0.53 d) 0.83	440	442	442
2	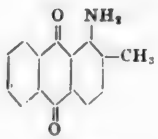	60700	Orange for acetate rayon	C. F.	c) 0.82 d) 0.97	476	482	482
			Celliton orange R	C. F.	a) 0.97	478	482	482
3	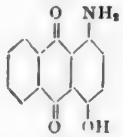	60710	1-Amino-4-hydroxy-anthraquinone	Pure, twice re-crystallized from acetone	a) 0.45	I 530 *** II 560	I 535 II 572	I 530 II 570
			Celliton fast pink B	C. F.	a) 0.45	I 530 II 560	I 535 II 572	I 530 II 572

* Eluents: a) ligroin (b. p. 73-83°) saturated with 98% methanol [10]; b) same, with addition of acetic acid to pH = 4; c) toluene saturated with water; d) 96% ethyl alcohol

** CF = commercial form.

*** In toluene.

Note. Duranols are made by I.C.I. Ltd; Cellitons are made by B.A.S.F.

(Continued)

Dye No.	Chemical structure	Color index No. [11]	Trade or chemical name	Form investigated	Migration rate on paper* k_f	Positions of maxima in absorption bands (mμ) soln in CH_3COOH	hydro-aceto-sols	hydro-sulfo-sols
4	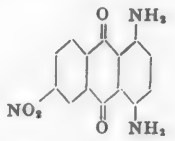	62030	1,4-Diamino-5-nitro-anthraquinone	C. F.	c) Sky-blue 0.98 Orange 0.95	I 563	I 570	I 570
					d) 0.80	II 605	II 610	II 610
			Celliton Fast Violet B	C. F.	c) Sky-blue 0.98 Orange 0.95	I 563 II 605	I 573 II 610	I 573 II 610
					d) 0.80			
5	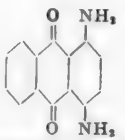 (partially methylated)	61105	1,4-Diaminoanthra-quinone (partially methylated)	C. F.	c) Greenish blue 0.98 Dark blue 0.95 Violet 0.00	591	591	580
			Celliton Fast Violet B	C. F.	a) Sky-blue 0.90 Violet 0.40 Reddish-violet 0.06 Violet 0.00	591	597	596
6	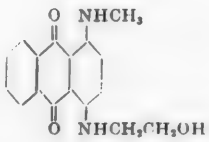	61505	Blue K for acetate	C. F.	a) Dark blue 0.99 Sky-blue 0.032	I 595 II 642	I 600 II 646	I 598 II 643
					c) Dark blue 0.99 Dark blue 0.68 Sky-blue 0.042			
			Celliton Fast Blue FFR	C. F.	a) Dark blue 0.99 Sky-blue 0.032	I 597 II 643	— —	— —
					c) Dark blue 0.99 Dark blue 0.68 Sky-blue 0.042			

(Continued)

Dye No.	Chemical structure	Color index No. [11]	Trade or chemical name	Form investigated	Migration rate on paper k_f	Positions of maxima in absorption bands (mμ)		
						soln. in CH_3COOH	hydro-aceto-sols	hydro sulfo-sols
7	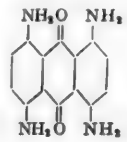	64500	1,4,5,8-Tetramino-anthraquinone	Pure, twice re-crystallized from CH_3COOH	a) 0.00	I 578 II 620	I 583 II 618	I 521 II 610
				Technical product, washed with water	d) 0.57	—	—	—
			Celliton Blue Extra	C. F.	a) 0.00 c) 0.15 d) 0.59	—	—	—
8	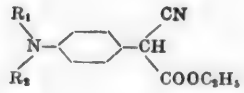	48000	Yellow methine dye of the type of Celliton Fast Yellow 7G	Pure, thrice re-crystallized from ethyl alcohol	—	428	430	Decom-posed
9	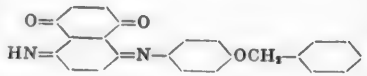	56060	Condensation product of napthoquinonediimine with p-aminophenyl benzyl ether	Technical product*	a) Blue-green 0.02 Gray 0.00 b) Blue-green 0.26 Gray 0.00	635	636	Decom-posed
			Celliton Fast Green 3B	C. F.	a) Blue-green 0.02 Gray 0.00 b) Blue-green 0.26 Gray 0.00	636	636	Decom-posed

*Resinifies when recrystallized from acetone and acetic acid.

short-wave region of the spectrum owing to possible formation of soluble dye sulfates (Table 1, Fig. 1, No. 6 and 7). Hydroacetosols, on the other hand, proved to be adequately stable and suitable for all the dyes studied.

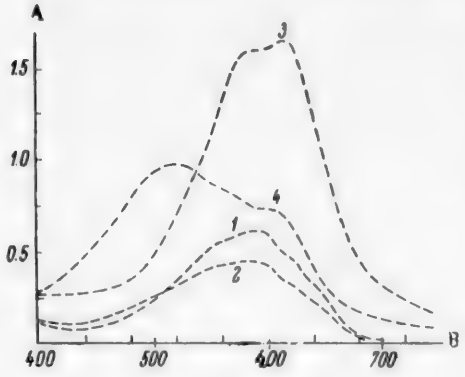

Fig. 1. Spectrograms for sols of partially methylated 1,4-diaminoanthraquinone (Table 1, No. 5) and 1,4,5,8-tetraminoanthraquinone (Table 1, No. 7): A) optical density, B) wave length (mμ); dye No. 5: 1) hydroacetosol, 2) hydrosulfosol; dye No. 7: 3) Hydroacetosol, 4) hydrosulfosol.

It should be noted that the commercial forms of certain dyes, containing large amounts of Glauber's salt and anion-active substances, yield unstable hydroacetosols because of the low solubility of sulfates in acetic acid, although hydroacetosols of these dyes in the pure or technical forms are fairly stable (Table 1, dyes No. 6 and 7). In such cases hydrosols of the commercials forms may be prepared in other solvents (acetone, alcohol), by the same general method.

EXPERIMENTAL

Dyes. Dyes of the anthraquinone series, methine yellow, and a green derivative of naphthoquinoneimine were studied in their commercial forms and as the pure dyes washed free of inorganic impurites (Table 1).

The pure substances were obtained by repeated recrystallization of the technical products from appropriate solvents. In some instances, when individual coloring components are removed by recrystallization, the treatment was confined to very thorough washing of the technical dyes with water followed by drying to constant weight (dye No. 7). Identity of dyes in the commercial forms produced by different manufacturers was confirmed by chromatographic separation on "rapid" grade paper in ascending streams of different eluents, and by comparison of their spectrograms.

TABLE 2

Determination of Stability of Sols of the Investigated Acetate Dyes

Dye No.	Hydroacetosols			Hydrosulfosols		
	conc. (mg/ liter)	stability (hours)	stabilization time (hours)	conc. (mg/ liter)	stability (hours)	stabilization time (hours)
1	20	120	2	20	—	—
2	10	5	2	10	—	5
		(D^* = 0.38)			(D = 0.33)	
3	20	19	2	20	24	3
4	20	24	4	20	24	4
5	10	28	4	10	6	1
		(D = 0.62)			(D = 0.450)	
6	20	24	4	20	—	—
		(D = 2.18)			(D = 1.34)	
7	20	24	3	20	—	—
		(D = 1.65)			(D = 1.0)	
8	10	24	3	—	—	—
9	10	22	4	10	5	1

*D is the optical density of the spectrograms.

*G. I. Krymskaya, V. V. Karpov, N. M. Kravchenko, N. D. Zheltukhina, and N. I. Maksimenko took part in the experimental work.

TABLE 3

Determinations of the Stability of Hydroacetosols of Dye No. 1 at Different Dilutions

Sol. No.	conc. (mg/ liter)	Optical density of sol		
		at instant of preparation	atfter 2 hrs.	after 15 hrs.
1	25.0	0.215	0.213	0.213
2	12.5	0.101	0.099	0.100
3	10.0	0.077	0.077	0.077
4	7.5	0.054	0.054	0.057

TABLE 4

Determinations of the Stability of Hydroacetosols of Dye No. 7

	Optical density of sol	
	sample No.1	sample No. 2
Pure dye recrystallized from acetic acid (20 mg/ liter)		
At instant of preparation	0.451	0.452
After 1 hour	0.450	0.450
After 2 hours	0.452	0.452
Technical product purified by washing with water (20 mg/ liter)		
After 1 hour	0.496	0.496
After 3 hours	0.497	0.496
After 24 hours	0.497	0.497

TABLE 5

Determinations of Dye Concentrations

Dye	Method 1, hydrosulfosols		Method 2, hydroacetosols		Relative discrepancy between methods 1 and 2 (%)
	conc.(%)	relative error (%)	conc.(%)	relative error (%)	
Blue K for acetate rayon	40.1 39.5	0.75	40.0 40.0	0	0.25
Celliton fast Blue FFR	46.5 46.1	0.45	46.8 46.2	0.65	0.22
Duranol Brilliant Blue BN	11.3 11.6	1.8	11.2 11.0	0.9	1.35
Celliton Fast Pink B	40.0 39.2	1.0	41.0 41.8	1.0	1.45
1-Amino-3-hydroxyanthraquinone C. F. No. 1	37.8 39.0	1.6	—	—	—
C. F. No. 2	33.2 34.5	0.9	—	—	—
C. F. No. 3	36.8 38.0	1.6	—	—	—

Instruments. The optical densities of the sols were determined by means of the FEK-M photoelectric colorimeter, and the spectrograms were obtained by means of the SFM-2 spectrophotometer.

Methods of sol preparation and construction of calibration curves. For preparation of a hydroacetosol or a hydrosulfosol a weighed sample of the pure or purified dye, or in some cases of the commercial form of accurately known concentration, weighing 0.010-0.20 g, was dissolved in a 30 ml beaker in 20 ml of glacial acetic or 10 ml of chemically pure sulfuric acid (sp. gr. 1.84) at 20-25°. The solution was poured out slowly dropwise into a liter beaker containing 800 ml of aqueous OP-10 solution (4 g/liter) previously cooled to about 0°. The OP-10 solution was stirred briskly during the addition. The resultant sol was left to stand until its temperature reached 20°, transferred to a liter measuring flask, made up to the mark with a solution of OP-10 of the same concentration, and its stability was determined (Table 2). The optical density of the sols was determined immediately after preparation and after storage at room temperature for definite time intervals – from half an hour to 24 hours and over.

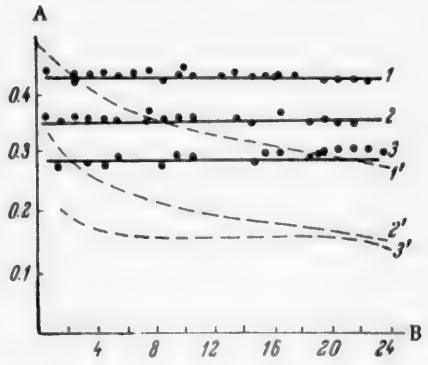

Fig. 2. Effect of OP-10 on the stability of sols and suspensions of dye No. 8: A) optical density, B) standing time (hours); concentrations: 1, 1') 10 mg dye/liter, 2, 2') 5 mg dye/liter, 3, 3') 20 mg TM powder per liter; 1, 2, 3) stability of sols in presence of OP-10; 1', 2', 3',) stability of suspensions without OP-10.

After the optimum holding time required for sol stabiliza- had been established, the calibration graph was plotted. Portions of 50, 25, 20, 15, 10 and 5 ml of the standard sols were transferred into 100 ml measuring flasks by means of pipets, the volume was made up to the mark with OP-10 solution, the optical densities of the diluted sols were determined, and plotted against the dye concentrations (in mg/liter). The reference liquid was distilled water containing 4 g/liter of OP-10 and the appropriate amount of acid.

Determinations of dye concentration in commercial bands. The method described above was used for preparation of sols containing about 10-100 mg of the commercial dye per liter, so that the measured optical density should correspond to values on the calibration curve.

The results of determinations of the stability of hydroacetosols of certain dyes on standing are given in Tables 5 and 4.

The effect of OP-10 on the stability of hydroacetosols of methine yellow dye (No. 3) is shown in Fig. 2.

It is clear from the specimen data (Table 5) that the reproducibility of the results obtained in determinations of dyes in sol form is quite satisfactory, and the error is less than in visual estimation (±5%) [12].

SUMMARY

1. In the course of work on a photometric method for determination of dyestuff concentration in acetate dyes in the form of hydroacetosols and hydrosulfosols, stable, intensely colored, and reproducible hydroacetosols have been prepared from all the investigated dyes – seven representatives of the anthraquinone series, one methine dye, and one naphthoquinoneimine derivative.

2. Hydrosulfosols suitable for photometric determinations are obtained only in some isolated instances (dyes No. 3 and 4); the hydrosulfosols formed (from dyes No. 2, 5, 6, and 7) have lower optical densities than hydroacetosols of the same concentrations, and the absorption-band maxima are shifted (for dyes No. 6 and 7).

3. Hydrosulfosols of dyes No. 8 and 9 cannot be prepared, as they are decomposed by sulfuric acid.

4. The reproducibility of the results varies in the range of up to 2%; the accuracy of the concentration determinations is higher than in the visual method; the relative discrepancy between the results obtained by the hydrosulfosol and the hydroacetosol methods does not exceed 1.5%.

5. It is shown that dyes which cannot be separated chromatographically with the use of ligroin (dyes No. 6 and 7) can be separated by paper chromatography with the aid of toluene and ethyl alcohol.

LITERATURE CITED

[1] J. Soc. Dyers and Colorists 69, 121 (1953).

[2] I. M. Kogan, Chemistry of Dyes [in Russian] (State Chem. Press, Moscow, 1956) p. 247, 530, 93, 420, 493.

[3] C. L. Bird, J. Soc. Dyers and Colorists 70, 71 (1954).

[4] FIAT No. 1040 (1947).

[5] R. K. Fourness, J. Soc. Dyers and Colorists 72, 513 (1956).

[6] T. Vickerstaff, Physical Chemistry of Dyeing (State Light Industry Press, Moscow, 1956) p. 59, 67 [Russian translation].

[7] L. I. Belen'kii, Proc. 3rd All-Union Conference on Colloid Chemistry [in Russian] (Izd. AN SSSR, 1956) p. 484.

[8] A. I. Sokolov, Proc. 4th Conference on Chemistry of Aniline Dyes [in Russian] (1939) p. 389; L. M. Golomb, J. Appl. Chem. 30, 329 (1957).*

[9] Z. N. Markina, K. A. Pospelova, and P. A. Rebinder, Proc. 3rd All-Union Conference on Colloid Chemistry [in Russian] (Izd. AN SSSR, 1956) p. 410; H. B. Klevens, Chem. Revs. 47, 1 (1950).

[10] K. Elliott and T. Telecz, J. Soc. Dyers and Colorists 73, 8 (1957).

[11] Color Index SDC (Bradford), AATCC (Lowell) 1, (1956).

[12] E. Stearns, Am. Dyest. Rep. 39, 358 (1950).

Received April 5, 1958

* Original Russian pagination. See C.B. Translation.

KINETICS OF SULFONATION OF XYLENE ISOMERS AND ETHYLBENZENE BY SULFURIC ACID

Ya. I. Leitman and M. S. Pevzner

The Lensoviet Technological Institute, Leningrad

The literature contains hardly any information on the kinetics of sulfonation of benzene isomers, although the preparation of m-xylene by selective sulfonation and hydrolysis of the sulfonic acid has been described [1-14]. The data available on the kinetics of sulfonation of xylene isomers [15] are mainly qualitative and do not give an idea of quantitative aspects of the process. We therefore undertook a more detailed study of the reactions of xylene isomers and ethylbenzene with sulfuric acid of different concentrations and at different temperatures.

EXPERIMENTAL*

Reagents, apparatus, and experimental procedure. The xylene isomers and ethylbenzene used in the experiments had the following characteristics:

	d^{20}_4	$n^{20}D$	Boiling point at 760 mm (°C)	Crystallization temperature (°C)
m-Xylene	0.8648	1.4972	139.03	–48.10
p-Xylene	0.8615	1.4960	138.31	+13.02
o-Xylene	0.8805	1.5047	144.31	–25.30
Ethylbenzene	0.8662	1.4960	136.10	–

The apparatus used for studies of sulfonation kinetics (Fig. 1) consisted of a sulfonation flask with a fitted reflux condenser, thermometer, and stirrer. The flask was immersed in a water or a glycerol thermostat (not shown in the diagram). A definite amount of sulfuric acid was put into the flask. The acid was heated to the required temperature, the hydrocarbon was added from a buret, and the time was noted. The reaction was allowed to continue at a definite stirrer speed, measured by means of a tachometer, for a definite time; the stirrer was then stopped, the contents of the flask cooled rapidly and transferred to a buret, where the amount of unconverted hydrocarbon was measured after the liquid had settled out. In some instances the reaction mixture was first diluted to avoid crystallization of the sulfonic acids. The solubility of xylenes and ethylbenzene in acid under these conditions is negligible, and therefore any error due to dissolution of hydrocarbons was disregarded.

Since in this case the sulfonation is a heterogeneous reaction (with hydrocarbon and acid phases), its rate greatly depends on the rate of agitation (stirrer speed). Therefore, comparable data on the kinetics of sulfonation of xylene isomers can be obtained only under such conditions of phase contact that the diffusion factors are reduced to a minimum (in the kinetic region).

Accordingly, we determined the stirrer speeds at which the transition from the diffusion to the kinetic

*L. S. Kabitova and G. B. Zhurunova took part in the experimental work.

region occurs in each case (Fig. 2), and based all the calculations and comparisons on measurements of the reaction rates in the kinetic region.

Effect of the ratio of the reactants on the sulfonation rate. Several series of experiments were carried out, with different molar ratios of hydrocarbon to acid. Sulfuric acid was taken in large excess, so that it was not diluted by more than 0.3-0.4% by the water and sulfonic acid formed in the reaction.

The experiments showed that the amount (in moles) of hydrocarbon which reacts under given conditions is independent of the amount of hydrocarbon and is directly proportional to the amount (in moles) of sulfuric acid (Table 1). This indicates that the reaction proceeds in the acid and not the hydrocarbon layer.

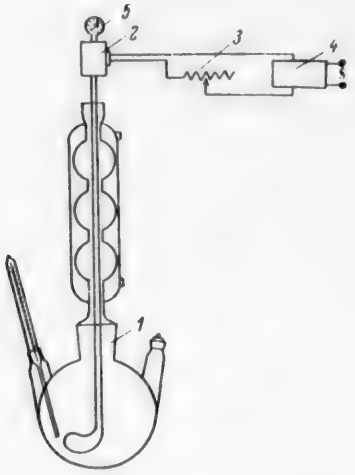

Fig. 1. Apparatus for studying sulfonation kinetics: 1) sulfonation flask, 2) electric motor, 3) rheostat, 4) voltage stabilizer, 5) tachometer.

TABLE 1

Sulfonation of m-Xylene at Different Ratios of Sulfuric Acid to Hydrocarbon (Temperature 60°, sulfuric acid concentration 85%, reaction time 5 minutes)

Amounts (in moles)		Amt. of m-xylene sulfonated (moles)
m-xylene	sulfuric acid	
0.049	1.710	0.027
0.049	2.570	0.0395
0.098	3.420	0.053
0.098	1.710	0.0262
0.147	1.710	0.027
0.196	1.710	0.0285
0.245	1.710	0.0277

Analogous results were obtained at other concentrations of sulfuric acid and with other xylene isomers.

In all the subsequent experiments the proportions were 0.049 mole (6.00 cc) of xylene to 1.710 moles (167.5 g) of sulfuric acid (calculated as the anhydrous acid), which is 1 : 35 ratio of xylene to acid.

Variation of the sulfonation rate with the concentration of sulfonic acid in the acid layer. It is known [16] that the rate of sulfonation falls as sulfonic acid accumulates in the reaction mass, owing to a decrease in the sulfuric acid concentration and to the reverse reaction – hydrolysis of the sulfonic acid. However, our experiments showed that if the sulfonation is performed under conditions such that hydrolysis of the sulfonic acid is suppressed the presence of the sulfonic acid raises the sulfonation rate.

The effect of concentrations of m- and p-xylenesulfonic acids on the rate of sulfonation of m- and p-xylene respectively by 85% sulfuric acid at 60° was studied. The results are presented in graphical form (Fig. 3).*

It is clear from Fig. 3 that the sulfonation rate increases appreciably with increase of sulfonic acid concentration. An explanation of the increase in the sulfonation rate is that the solubility of xylene in the acid increases in presence of the sulfonic acid. This shows once again that the reaction proceeds in the sulfuric acid layer.

Sulfonation of xylene isomers and ethylbenzene by sulfuric acid of different concentrations at various temperatures. Sulfonation experiments were carried out with sulfuric acid of the following concentrations (%):

* In this and all subsequent graphs 0.049 mole or 6 cc of xylene is taken as 100%.

70.0, 75.0, 80.0, 85.0, 90.6, in the temperature range between 0 and 115° at intervals of 10-20°.

Over one thousand experiments were performed. Several graphs are given here as examples; these represent only a small proportion of the experimental data (Fig. 4-7).

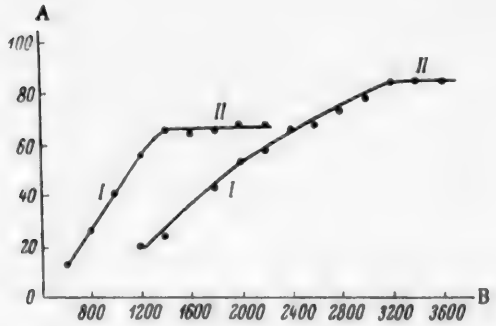

Fig. 2. Variation of sulfonation rate with stirrer speed: A) amount of m-xylene converted (% of initial), B) stirrer speed (r.p.m.); temperature (°C) and time of sulfonation (minutes) by 85% sulfuric acid respectively; 1) 40 and 25, 2) 60 and 3; region: I) diffusion; II) kinetic.

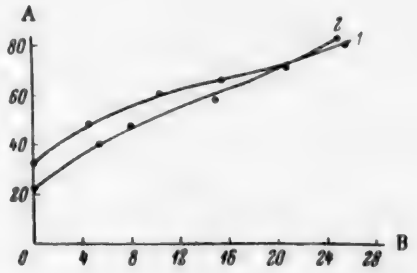

Fig. 3. Relationship between sulfonation rate and concentration of sulfonic acid (85% sulfuric acid, temperature 60°); A) concentration of sulfonic acid (wt. %), B) amount of xylene converted (%); duration of sulfonation (minutes): 1) p-xylene, 5; 2) m-xylene, 1.

The experiment showed that the course of sulfonation varies with the concentration of sulfuric acid. In sulfonation by 70% sulfuric acid the rate of sulfonation falls during the reaction, and eventually sulfonation ceases entirely, i.e., equilibrium is established (Fig. 4). When m-xylene is sulfonated by 75% sulfuric acid at 90-115° the reverse reaction (hydrolysis) still occurs, so that the sulfonation rate falls during the experiment.

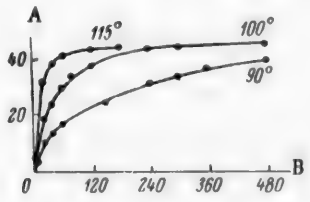

Fig. 4. Sulfonation of m-xylene by 70% sulfuric acid: A) amount of m-xylene converted (%), B) time (minutes).

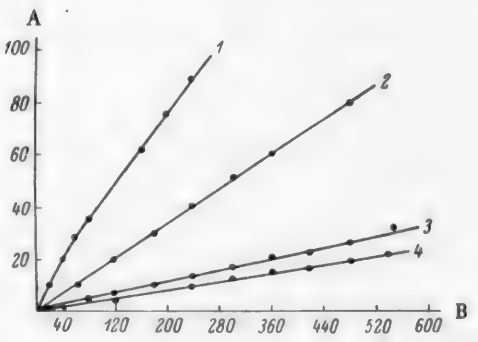

Fig. 5. Sulfonation of all xylene isomers and ethylbenzene by 75% sulfuric acid at 75°: A) amount of substance converted (%), B) time (minutes); 1) m-xylene, 2) o-xylene, 3) p-xylene, 4) ethylbenzene.

If m-xylene is sulfonated by 80-85% sulfuric acid and all the other isomers by 75-85% acid, hydrolysis of the sulfonic acids is completely suppresed and the reaction rates remain constant throughout. Sulfonation by 90.6% sulfuric acid takes a different course from sulfonation by more dilute acids. At first there is a sharp rise in the degree of sulfonation (25-30% within 1 minute); this is followed by a break, after which sulfonation proceeds at a lower but constant rate. The initial regions of the curves of m- and p-xylene coincide.

The situation with ethylbenzene is similar but less pronounced. An explanation of this course of sulfonation is that initially the hydrocarbon dissolves rapidly in sulfuric acid. The inflection point corresponds to

TABLE 2

Values of the Sulfonation Rate Constants $k \cdot 10^4$ $\left(\frac{\text{moles xylene}}{\text{moles sulfuric acid. min.}}\right)$

Temperature and activation energy	Rate constants for sulfonation by sulfuric acid of concentration (%):																
	70	75	80	85	90.6	70	75	80	85	90.6	75	80	85	75	80	85	90.6
	m-xylene					p-xylene					o-xylene			ethylbenzene			
Temperature (°C)																	
0	—	—	—	—	5.70 (+2°)	—	—		—	—	—	—	—	—	—	—	0.570
10	—	—	—	0.39	10.5	—	—		—	5.1 *	—	—	—	—	—	—	1.50
20	—	—	—	1.20	30.0	—	—		0.257	12.6	—	—	—	—	—	—	5.30
30	—	—	—	3.45	—	—	—		0.85	25.7	—	—	—	—	—	0.335	13.3
40	—	—	0.55	8.9	—	—	—		2.40	—	—	0.251	4.07	—	0.067	0.79	32.0
50	—	—	1.58	24.3	—	—	—	0.355	6.05	—	—	0.71	10.6	—	0.158	1.86	—
60	—	0.50	4.70	61.0	—	—	0.039	0.89	18.1	—	0.091	1.99	25.5	—	0.380	5.00	—
75	—	2.00	18.2	203 *	—	—	0.175	3.55	62.5	—	0.500	7.60	86.0	0.129	1.20	14.5	—
90	1.415	7.10	59.6	686 *	4200 *	—	0.96	13.3	204 *	4400 *	2.52	30.6	323 *	0.415	3.60	42.1	1660 *
100	2.37	15.5	—	—	—	0.38	—		—	—	—	—	—	—	—	—	—
115	4.73	47.0	—	—	—	0.86	—		—	—	—	—	—	—	—	—	—
Activation energy (kcal/ mole)	12.5	21.0	21.6	18.9	15.5	15.6	26.3	25.3	20.1	17.8	27.2	21.1	19.6	19.5	17.9	17.6	17.8

* Extrapolated from the Arrhenius equation.

saturation of sulfuric acid with the hydrocarbon. After saturation, equilibrium is established between the dissolving and reacting xylene, and sulfonation proceeds at a constant rate.

If the sulfuric-acid layer formed during 1 minute of reaction (corresponding to the portion of the curve before the inflection) is diluted with water, hydrocarbon which dissolved in the sulfuric acid but had not yet reacted separates out.

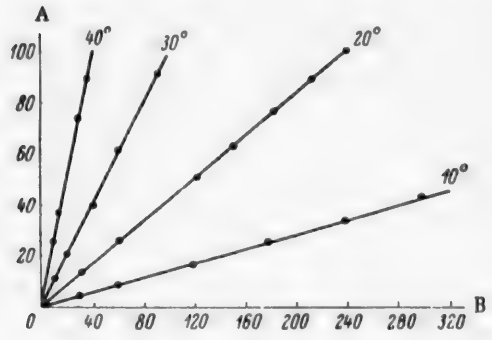

Fig. 6. Sulfonation of m-xylene by 85% sulfuric acid at various temperatures: A) amount of m-xylene converted, B) time (minutes).

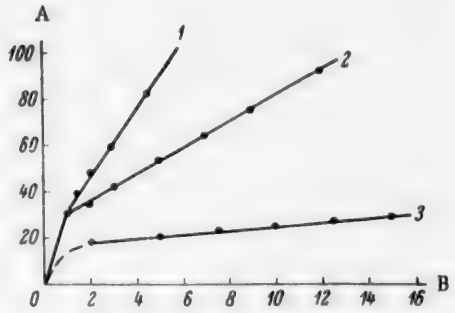

Fig. 7. Sulfonation of m-xylene (1), p-xylene (2), and ethylbenzene (3) by 90.6% sulfuric acid at 20°: A) amount of substance converted, B) time (minutes); 1) m-xylene, 2) p-xylene, 3) ethylbenzene.

Sulfonation experiments with 90.6% sulfuric acid indicate that the solubility of xylene isomers in sulfuric acid rises sharply at concentrations above 85%.

Calculation of the Rate Constants and Activation Energies of Sulfonation

For homogeneous sulfonation of xylene in accordance with the equation (in absence of hydrolysis)

$$C_8H_{10} + H_2SO_4 \rightarrow C_8H_9SO_3H + H_2O,$$

We can write the following general expression for the reaction rate:

$$\frac{dx}{dt} = k_2 [C_8H_{10}] [H_2SO_4], \qquad (I)$$

where $\frac{dx}{dt}$ is the amount of hydrocarbon sulfonated per unit time, k_2 is the rate constant for a second-order reaction, and $[C_8H_{10}]$ and $[H_2SO_4]$ are the molar amounts of xylene and sulfuric acid.

Since the system contains two phases (the acid and hydrocarbon layers) and the reaction proceeds in the acid layer, it follows that in Equation (I) the value of $[C_8H_{10}]$ must be equal to the solubility of xylene in sulfuric acid; i.e., $[C_8H_{10}]$ = const.

Equation (I) therefore becomes:

$$\frac{dx}{dt} = k [H_2SO_4], \qquad (II)$$

where $k = k_2 [C_8H_{10}]$.

Thus, in this case the reaction rate is proportional only to the amount of the sulfuric acid, as was found in our experiments.

With the large excesses of sulfuric acid such as were used in our experiments variations of its content during the reaction may be neglected, so that we may assume $[H_2SO_4]$ = const. In that case the sulfonation rate is constant (provided that the concentration of sulfuric acid is constant):

$$\frac{dx}{dt} = k [H_2SO_4] = \text{const}.$$

TABLE 3

Ratios of the Sulfonation Rates of Xylene Isomers

Sulfuric acid concentration (%)	Ratio of rates at temperature (°C)			
	90	60	40	20
	m-: o-: p-: ethylbenzene	m-: o-: p-: ethylbenzene	m-: o-: p-: ethylbenzene	m-: o-: p-: ethylbenzene
75	17 : 7 : 2.6 : 1	13.5 : 2.3 : 1 : 1	—	—
80	16 : 8 : 3.4 : 1	14 : 4.5 : 2.2 : 1	7 : 3.9 : 1.5 : 1	—
85	19 : 9 : 5.7 : 1	13 : 4.7 : 3.8 : 1	10 : 4.7 : 3.3 : 1	9 : 4.2 : 1.9 : 1
90.6	2.5 : . . .* : 2.6 : 1	—	—	11 : . . . : 4.2 : 1

* From extrapolated data.

Accordingly it was possible to use the following formula for calculating the sulfonation rate constants (k):

$$k = \frac{\frac{dx}{dt}}{[H_2SO_4]} \left(\frac{\text{moles xylene}}{\text{moles } H_2SO_4 \cdot \text{min.}}\right). \qquad \text{(III)}$$

In calculation of the rate constants for 70-75% sulfuric acid only the first few points on the sulfonation curves, where hydrolysis does not yet influence the reaction rate, were used.

Calculations of the constants for 90.6% sulfuric acid were based on points on the straight lines beyond the inflection, in the region of steady reaction with established equilibrium between the dissolving and reacting hydrocarbon.

Variations of the reaction rate constants with temperature conform to the Arrhenius equation.

The experimental data were used for calculating the coefficients A and B in the Arrhenius equation:

$$\log k = A - \frac{B}{T},$$

where k is the sulfonation rate constant and T is the absolute temperature.

The coefficients A and B are not given here; we give only the activation energies calculated from the coefficient B (Table 2).

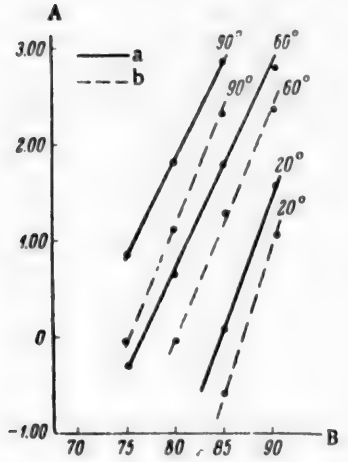

Fig. 8. Variations of the sulfonation rate constant and the sulfuric acid concentration for m- and p-xylene: A) log k · 10^4, B) H_2SO_4 concentration (%); a) m-xylene, b) p-xylene.

Values of the sulfonation rate constants calculated from the Arrhenius equation are also given in Table 2. They are in good agreement with the values obtained from experimental data and Equation (III).

It is seen that the activation energy changes with increase of the sulfuric acid concentration.

The activation energy for sulfonation of m-xylene is less in 70-75% sulfuric acid than in stronger sulfuric acid. Evidently in 70-75% sulfuric acid the rate of the reverse reaction – hydrolysis of m-xylene sulfonic acid – increases to a greater extent with increase of temperature than the sulfonation rate; this influences the values of the activation energy calculated from experimental data.

A similar effect is observed in sulfonation of p-xylene by 70% sulfuric acid.

The activation energy reaches a maximum with increase of the sulfuric acid concentration, and then diminishes.

These variations of the activation energy are not observed for ethylbenzene. The activation energy of sulfonation of ethylbenzene remains roughly constant in the 80-90% range of sulfuric acid concentrations. This may be due to differences between the structure of ethylbenzene and of xylene isomers.

The relationship between the reaction rate constant and the sulfuric acid concnetration in the 75-90% range was also determined from the experimental data (Fig. 8). Figure 8 shows that the logarithm of the sulfonation rate constant is a linear function of the sulfuric acid concentration.

Table 3 gives the ratios between the sulfonation rates of individual xylene isomers at different temperatures and sulfuric acid concentrations, calculated from the data in Table 2.

SUMMARY

1. The kinetics of sulfonation of xylene isomers and ethylbenzene was studied; the reaction rate constants and the ratios between the rates of sulfonation of individual isomers were found.

2. It was shown that the rate of sulfonation of xylenes and ethylbenzene is independent of the amount of hydrocarbon and is directly proportional to the amount of sulfuric acid (under otherwise constant conditions).

3. The rate of sulfonation increases with increase of the sulfonic acid content in the acid layer (under conditions which exclude the possibility of hydrolysis).

4. The sulfonation reaction proceeds mainly in the acid layers.

5. The relationship between sulfonation rate constants, reaction temperature, and sulfuric acid concentration has been determined.

6. The data obtained on the kinetics of sulfonation of xylene isomers and ethylbenzene can be used for selecting the optimum conditions of selective sulfonation for isolation of m-xylene from crude xylene.

LITERATURE CITED

[1] O. Jacobsen, Ber. Deut. Chem. Ges. 10, 1009 (1877).

[2] J. Levinstein, Ber., Deut. Chem. Ges. 17, 444 (1884).

[3] J. Crafts, Compt. rend. 114, 1110 (1892).

[4] H. Clarke and E. Taylor, J. Am. Chem. Soc. 45, 830 (1923).

[5] T. Patterson, A. McMillan, and K. Sommerville, J. Chem. Soc. 2488 (1924).

[6] N. M. Kizhner and G. Vendel'shtein, J. Russ. Phys.-Chem. Soc. 57, 1 (1925).

[7] N. Löftgren, Svensk. Kem. Tids., 60, 281 (1948).

[8] U. S. Patent 2,348,329; Ch. A. 39, 532 (1945).

[9] U. S. Patent 2,393,888; Ch. A. 40, 2468 (1946).

[10] U. S. Patent 2,511,711; Ch. A. 44, 8368 (1950).

[11] U. S. Patent 2,519,336; Ch. A. 44, 649 (1950).

[12] U. S. Patent 2,585,525; Ch. A. 46, 10200 (1952).

[13] U. S. Patent 2,688,644; Ch. A. 49, 11705 (1955).

[14] Federal German Patent 854,345; Zbl. 2521 (1953).

[15] K. I. Matkovskii, Candidate's Dissertation [in Russian] (Kiev, 1951).

[16] I. S. Ioffe, Sulfonation of Organic Compounds [in Russian] (Navy Medical Academy Press, Leningrad, 1944) p. 43.

Received May 15, 1958.

A STUDY OF THE KINETICS OF OXIDATION OF LIQUID PARAFFINS IN THE PRESENCE OF A K – Mn CATALYST*

B. G. Freidin

Scientific Research Institute of Petrochemical Processes

It is known that the simultaneous presence of transition-group and alkali metals in catalysts used for liquid-phase oxidation of paraffins has a favorable effect on the rate and selectivity of fatty acid formation. Potassium permanganate is an example of this type of catalyst. According to Prückner [1], its action can be regarded as catalysis by organic salts of manganese and potassium, formed by interaction of $KMnO_4$ with the oxidation products.

This hypothesis was consistent with the results which we obtained in comparing the catalytic effects of $KMnO_4$, manganese naphthenate, and a mixture of potassium and manganese naphthenates on the kinetics of acid formation in oxidation of Diesel fractions from synthine. The "potassium–manganese" catalysts proved to be very similar in properties. It was also shown that the joint effect of compounds of two metals cannot be attributed to simple addition of their catalytic properties.

The characteristics of reactions initiated by potassium–manganese catalysts have been studied little as yet. It was important to determine them in order to obtain information on conditions in which the oxidation reaction proceeds at a high rate. This prompted the present investigation of the kinetics of oxidation of liquid paraffins in presence of an equimolecular mixture of potassium and manganese naphthenate.

EXPERIMENTAL

Tsyskovskii' oxidation columns [2] provided with photoelectric devices for measurement of the light absorption of the oxidation products were used. The liquid paraffins oxidized were a technical fraction (250-350°) isolated from petroleum Diesel fuel by means of carbamide. The fraction contained 93% hydrocarbons of normal structure; the average molecular weight was 242, m. p. 20°. All the experiments were performed at 125°. The potassium–manganese catalyst was prepared from an equimolecular mixture of potassium and manganese naphthenates; the amount introduced corresponded to metal concentrations of 0.035% Mn and 0.025% K. The same concentrations were used in experiments with one-metal catalysts –0.035% Mn in experiments with manganese naphthenate, and 0.025% K in experiments with potassium naphthenate.

The kinetics of hydrocarbon conversion was studied by determinations of the contents of unchanged substance by chromatographic analysis on silica gel [3, 4].

Accumulation of oxygen-containing functional groups was determined by the usual analytical methods. Active oxygen was determined by iodometric titration, hydroxyl groups by acetylation by acetic anhydride in presence of pyridine, and carbonyl groups by titration with hydroxylamine hydrochloride; the acid and saponification numbers were determined by the standard methods. The duration of the induction period was 14.5 hours with the potassium–manganese catalyst, 4.5 hours with the manganese catalyst, and about 10 minutes with the potassium catalyst.

* Communication III in the series entitled "Certain characteristics of liquid-phase oxidation of hydrocarbons initiated by metal salts."

Valence transitions of manganese during the induction period of oxidation reactions catalyzed by manganese compounds have been repeatedly described in the literature [2, 5, 6]. The observed color changes from pale pink to intense red-brown, followed by disappearance of color, correspond to transition of manganese from bivalent to higher valence states and subsequent return to the initial bivalent state. Differences in the nature of these transitions caused by the presence of potassium salts have not been studied as yet.

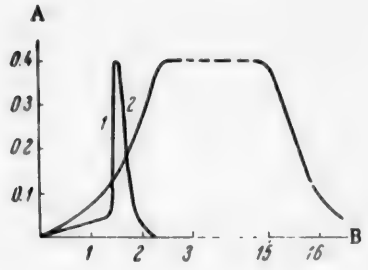

Fig. 1. Variation of light absorption during the induction period in oxidation of liquid paraffins: A) $\log \frac{I_0}{I}$, B) time (hours); 1) with Mn naphthenate, 2) with mixture of K and Mn naphthenates.

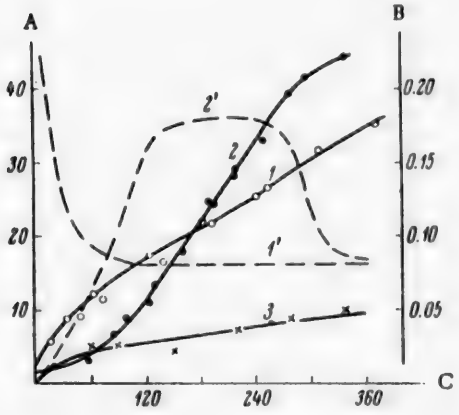

Fig. 2. Kinetics of hydrocarbon conversion in oxidation of liquid paraffins: A) contents of oxygen derivatives (wt. %), B) rate of hydrocarbon consumption (wt. %/minute), C) time (minutes) without the induction period (same in the other figures); conversion of hydrocarbons: 1) with Mn naphthenate, 2) with mixture of K and Mn naphthenates, 3) with K naphthenate; variations of the rate of hydrocarbon consumption with time: 1') with Mn naphthenate, 2') with mixture of K and Mn naphthenates (found by graphical differentiation of Curves 1 and 2).

Examination of the curves for variation of light absorption during the initial period (Fig. 1) and for conversion of hydrocarbons (Fig. 2) shows that the respective effects are interrelated. In oxidation in presence of the manganese catalyst the rapid transition of manganese to a lower valence state corresponds to such a sharp rise in the oxidation rate that the ascending branch of the rate curve could not be investigated experimentally. The oxidation rate then falls rapidly and soon becomes stabilized. Thus, a period of retardation of the reaction at the start of oxidation is characteristic for the manganse catalyst. In the experiment with K–Mn catalyst the increase of the oxidation rate is gradual, also because of peculiarities in conversion of the catalyst. The course of the kinetic curve is typical of chain reactions with degenerate branching [7], but in liquid phases it is usually observed in noncatalyzed reactions. The rate of hydrocarbon consumption slows down only after the oxidation has proceeded to about 30%.

The reaction in presence of potassium naphthenate began with a very short induction period (about 10 minutes), but the oxidation rate at the subsequent stages was the lowest. Errors of the analytical method ($\pm$1%) made it impossible in this case to investigate the character of the increase of the reaction rate during the initial period with sufficient accuracy.

The experimental data show that the level of the oxidation rate in presence of K–Mn catalyst cannot be attributed to simple addition of the effects of the catalyst components.

The nature of the curves for accumulation of functional groups (Fig. 3-5) is consistent with the kinetics of hydrocarbon consumption in the corresponding experiments. However, the peroxide concentration is higher in the experiment with the Mn catalyst, while the alcohol: ketone ratio is considerably higher with the potassium–manganese catalyst. The observed differences in the course of the reaction could be attributed both to the influence of the catalyst in the initiation stage, and to the continuing action of the catalyst remaining in the reaction zone in the form of a precipitate deposited after completion of the initial stages of the process. Accordingly, we present the results of experiments on introduction of potassium naphthenate into the reaction initiated by manganese naphthenate (Fig. 6).

In the experiment represented by Curve 2 in Fig. 6 the manganese was still present entirely in a state of homogeneous solution at the instant of addition, and the red-brown color present during the induction period

disappeared raipdly. Introduction of the potassium salt led to renewed darkening of the reaction mixture; evolution of reaction water ceased and conversion of the hydrocarbons was slowed down for some time. This was followed by a period in which the reaction proceeded at a higher rate.

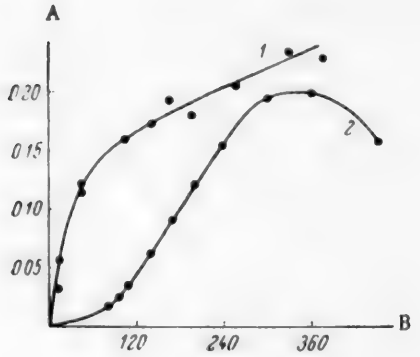

Fig. 3. Kinetics of peroxide accumulation in presence of Mn naphthenate (1) and of mixture of K and Mn naphthenates (2): A) content of active oxygen (wt. %), B) time (minutes).

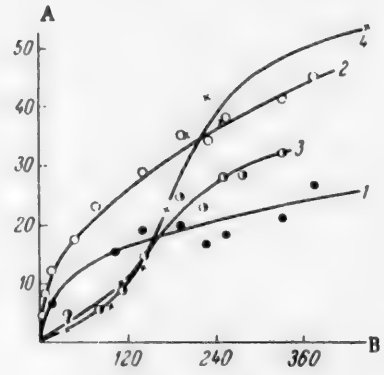

Fig. 4. Kinetics of accumulation of hydroxyl and carbonyl groups in presence of Mn naphthenate (1 and 2) and of mixture of K and Mn naphthenates (3 and 4): A) functional numbers, B) time (minutes); 1 and 4) hydroxyl numbers, 2 and 3) carbonyl numbers.

In other cases potassium naphthenate was introduced into the oxidation mixture when, according to the results of emission spectrum analysis, the content of dissolved manganese was $\leq 0.0001\%$.

Comparision of the experimental results of Fig. 2 and 6 shows that the greatest effect is obtained when the catalysts are introduced simultaneously. The effect produced by potassium naphthenate diminishes with increasing degree of reaction.

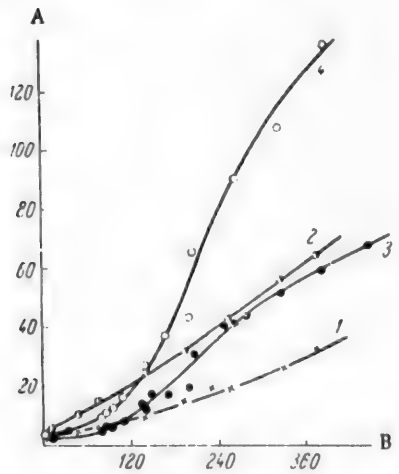

Fig. 5. Kinetics of accumulations of free and bound carboxyl groups in presence of Mn naphthenate [1 and 2) and of a mixture of K and Mn naphthenates (3 and 4): A) functional numbers, B) time (minutes); 1 and 3) acid numbers, 2 and 4) saponification numbers.

These results confirm that the initial stage of the reaction has a special role [2, 8] and are of interest in relation to elucidation of possible interactions in the course of subsequent oxidation stages.

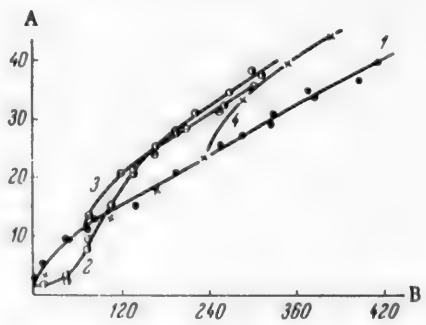

Fig. 6. Kinetics of hydrocarbon conversion on introduction of K naphthenate into a reaction initiated by Mn naphthenate: A) amount of hydrocarbons converted (wt. %), B) time (min.); 1) oxidation in presence of Mn naphthenate only; 2,3 and 4) K naphthenate added 5, 70, and 235 minutes respectively after the end of the induction period.

Émanuél' and his associates [9, 10] have postulated the following mechanism for initiation of liquid-phase oxidation of hydrocarbons by salts of the transition metals:

$$Me^{2+}Ac_2 + ROOH \rightarrow Me^{3+}(OH)Ac_2 + RO\cdot,$$
$$Me^{3+}(OH)Ac_2 + RCHO \rightarrow Me^{2+}Ac_2 + R\dot{C}O + H_2O\cdot$$

It is presumed that basic salts of the trivalent metal with organic acids are formed. According to literature data[11], such salts usually have the structure of multinucleate complexes of the $[Me_3^{III}(OH)_2(Ac)_6]Ac$. type. The formation of such compounds under oxidation conditions was demonstrated by us earlier [12]. Interaction between the metal and reducing agents in such cases occurs most probably after breakdown of coordination bonds as the result of hydroytic substitution of acidic residues in the inner sphere of the complex [12].

The presence of a relatively highly dissociated alkali metal salt probably causes a certain concentration of acidic ions to be set up in the reaction zone, hindering a shift of the hydrolysis equilibrium. This may explain why manganese remains in the highest valence state at the initial stage of oxidation in presence of the potassium salt.

It is known that fatty-acid salts of bivalent manganese and potassium interact readily, with formation of manganese-potassium coordination compounds [13]. The formation of such compounds may also possibly lead to stabilization of the valence states of manganese.

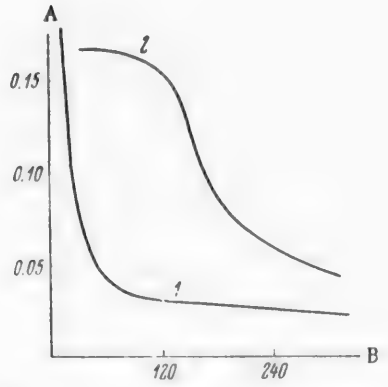

Fig. 7. Variation of the rate constant of hydroperoxide decomposition ($K_{(t)}$) with the oxidation time: A) decomposition rate constant $K_{(t)}$ (in min^{-1}), B) time (minutes); 1) with Mn naphthenate, 2) with mixture of K and Mn naphthenates.

The fact the reaction slows down soon after the end of the induction period, observed by us in oxidation in presence of manganese naphthenate only, was known earlier [14, 15] in relation to catalysis by other compounds of the transition-group metals. This effect is attributed to recombination of free radicals on interaction with the metal ions.

The hypothesis that manganese-potassium complexes are formed in presence of the K-Mn catalyst accounts for the absence of such retardation in this reaction. The transition metal present in the complex apparently takes part less readily both in reactions leading to formation of free radicals and in their recombination.

The mechanism of initiation by salts of univalent metals, and in particular by potassium naphthenate, is not well understood. Plisov [16] showed that such compounds catalyze decomposition of peroxides formed in oxidation of paraffins. The results obtained when potassium naphthenate was introduced into the progressing reaction indicate that the decomposition proceeds by a radical mechanism.

According to the accepted views, oxidation of hydrocarbons develops by way of the reactions:

$$R\cdot + O_2 \rightarrow RO_2\cdot, \quad (1)$$
$$RO_2\cdot + RH \rightarrow ROOH, \quad (2)$$

and hence the rate of hydroperoxide formation must be equal to the rate of hydrocarbon conversion.

When hydroperoxides decompose by a monomolecular mechanism

$$ROOH \rightarrow RO\cdot + \cdot OH \quad (3)$$

their change of concentration with time is given by the equation

$$\frac{d[ROOH]}{dt} = K_2[RO_2][RH] - K_3[ROOH]. \quad (4)$$

For analysis of the experimental results the active oxygen contents were calculated in terms of molar percentages of hydroperoxides, and data on consumption of hydrocarbons (in wt. %) were assumed to be approximately equal to the molar percentages of hydroperoxides formed. The curves for hydroperoxide accumulation were differentiated graphically to obtain curves for variations of their accumulation rates. Subtraction of the latter from the corresponding curves for variation of the rate of hydrocarbon consumption with time gave the rates of peroxide decomposition, $w_t = f(t) = K_t[ROOH]$. The values of K_t calculated from the results are given in Fig. 7.

The value of the rate constant of hydroperoxide decomposition with formation of free radicals determines the self-acceleration of the process. The influence of catalysts on it, clear from the data in Fig. 7, evidently accounts for the kinetic characteristics of the conversion of hydrocarbons in presence of different catalysts.

SUMMARY

1. In a study of differences in the kinetics of hydrocarbon conversion in the oxidation of liquid paraffins at 125° in presence of manganese naphthenate, potassium naphthenate, and an equimolecular mixture of manganese and potassium naphthenates as catalysts it was shown that the potassium salt stabilizes the valence states of manganese. This probably results in prolongation of the induction period in this case. However, subsequently the oxidation develops at a higher rate in presence of the K–Mn catalyst.

2. It is shown that variations of the reaction rate with time and the catalytic conditions are associated with changes in the rate constant of decomposition of peroxide compounds.

3. When the reaction proceeds at an increased rate (in presence of K-Mn catalyst), the relative content of alcohols in the oxidation products increases.

LITERATURE CITED

[1] H. Prückner, Chem. Techn. 4, 193 (1952).

[2] V. K. Tsyskovskii, Production of Synthetic Acids by Oxidation of Kerosene Fractions [in Russian] (State Fuel Tech. Press, 1954).

[3] L. I. Gulyaeva and N. I. Pyshkina, Trans. All-Union Sci. Res. Inst. of Shale Processing 2, 124 (1954).

[4] B. G. Freidin, J. Appl. Chem. 31, 881 (1958).*

[5] V. K. Tsyskovskii and N. A. Kiseleva, J. Appl. Chem. 23, 1001 (1950).*

[6] D. K. Knorre, Z. K. Maizus, and N. M. Émanuél', Proc. Acad. Sci. USSR 99, 415 (1954).

[7] N. N. Semenov, Chain Reactions [in Russian] (Goskhimizdat, 1934).

[8] N. M. Émanuél', Sci. Mem. MGU 174, 101 (1955).

[9] E. T. Denisov and N. M. Émanuél', J. Phys. Chem. 30, 2499 (1956) [USSR].

[10] I. Ya. Shlyapintokh and N. M. Émanuél', Bull. Acad. Sci. USSR, Div. Chem. Sci. 7, 782 (1957).*

[11] A. A. Grinberg, Introduction to the Chemistry of Complex Compounds [in Russian] (Leningrad-Moscow, (1951).

[12] B. G. Freidin, J. Appl. Chem. 30, 768 (1957).*

[13] S. Fisel, Akad, RPR, Fil. Jaci. 6, 3-4, 295 (1955).

[14] B. V. Erofeev and A. I. Chirko, Sci. Mem. Belorussian State Univ. 24, 3, 16, 24 (1955).

[15] E. T.Denisov and N. M. Émanuél', J. Phys. Chem. 30, 2327 (1956).

[16] A. K. Plisov, J. Gen. Chem. 9, 104 (1939).

Received May 24, 1958

* Original Russian pagination. See C.B. Translation.

BRIEF COMMUNICATIONS

A SIMPLE METHOD OF PREPARATION OF GASEOUS BORON TRIFLUORIDE

I. V. Andreeva

Institute of High-Molecular Compounds, Academy of Sciences USSR

The methods described in the literature [1-3] for preparation of gaseous boron trifluroide are inconvenient, as they either involve frothing and spattering the reaction medium (the acid methods), or require the use of high temperatures and in some instances special equipment, and the BF_3 formed is contaminated with reaction by-products.

We have prepared pure BF_3 fairly simply from phenyldiazonium fluoborate, the preparation of which has been described by Balz and Schiemann [4].

Preparation of Phenyldiazonium Fluoborate [4]

Into a wide-necked glass jar, 3 liters in capacity, there was put 200 g of cooled, aniline and 300 ml of distilled water, the mixture was cooled (to −10°), and 400 ml of hydrochloric acid (sp. gr. 1.19) was added with sitrring. Aniline hydrochloride was formed. An aqueous solution of sodium nitrite (150 g of $NaNO_2$ in 300 ml of distilled water) was added slowly dropwise to the mixture with stirring.

If sodium nitrite is added rapidly nitrogen oxides are formed. The reaction with aniline hydrochloride in an acid medium gives phenyldiazonium chloride.

During the preparation of phenyldiazonium chloride 400 ml of hydrofluoric acid was put in a cylindrical brass basin, and 144 g of boric acid was added to it by small portions with stirring.

The reaction of hydrofluroic acid with boric acid yields hydrofluoboric acid.

A cold solution of hydrofluoboric acid was added to the diazo solution with stirring and cooling. Phenyldiazonium fluoborate was precipitated; this was quickly filtered off on a Buchner funnel, washed with small portions (100-150 ml) of ice-cold water, methyl alcohol, and ether, pressed out thoroughly, and dried under vacuum. The precipitate darkened after prolonged exposure to air owing to decomposition of the diazo compound. It should be kept in a vacuum desiccator.

Preparation and Purification of Boron Trifluoride

Boron trifluoride was prepared by decomposition of phenyldiazonium fluoborate (30-50 g)

$$C_6H_5N_2BF_4 \rightarrow C_6H_5F + N_2 + BF_3.$$

The decomposition was effected in a weak current of pure dry nitrogen (Fig. 1).

The flask containing the diazo precipitate was heated on an open heater (cautiously at the start of the decomposition in order to avoid a very violent reaction, and more strongly toward the end).

At the end of the system, beyond a trap cooled to −180° and intended for collection of boron trifluoride (condensed in the solid state), there was another trap cooled to −180°. The buffer trap ensured that atmospheric oxygen did not enter the system. Before decomposition of the phenyldiazonium fluoborate the system was

evacuated three times and rinsed out by pure dry nitrogen. The apparatus used for purification of boron trifluoride is shown in Fig. 2.

The system containing solid boron trifluroide in trap 1 (-180°) was evacuated three times and then filled with pure nitrogen. Boron trifluoride was purified and distilled under 0.5-1.0 mm residual nitrogen pressure.

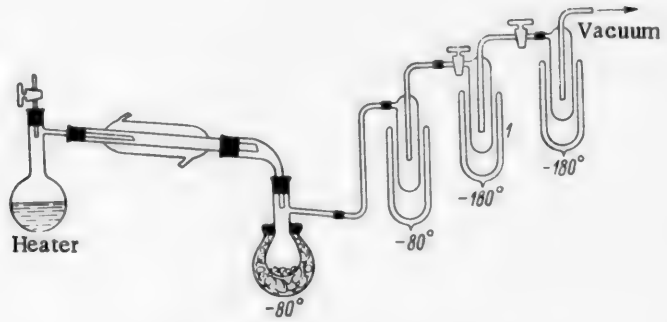

Fig. 1. Decomposition of the diazo compound for preparation of BF_3.

The substance was distilled from trap 1 into trap 3 through trap 2, which was cooled to -80°.

To effect the distillation, the temperature in trap 1 was changed from -180° to -80°, while trap 3 was cooled to -180°. A small amount of fluorobenzene, formed by decomposition of the diazo compound, remained in trap 1. If the temperature of the cooling system is changed from -180° to -80° (but not to room temperature) the distillation proceeds very smoothly.

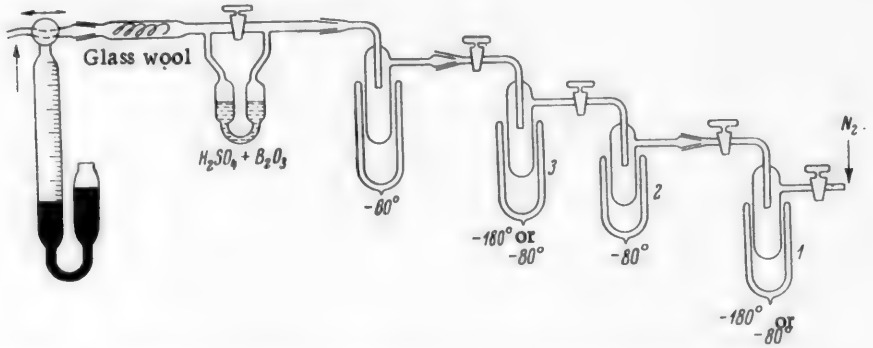

Fig. 2. Purification of BF_3 and preparation of the compound in the gaseous state.

Pure boron trifluoride collected in trap 3 in the form of a snowlike mass.

The temperature in trap 3 was raised from -180° to -80°, and the gaseous boron trifluoride was passed through a U-tube containing a solution of boron oxide in strong sulfuric acid to remove hydrogen fluoride, and then through a tube containing glass wool to remove droplets of sulfuric acid. The purified gas was collected and kept in a buret over mercury. Traces of moisture and air were previously removed carefully from the mercury.

LITERATURE CITED

[1] H. Booth and D. Martin, Boron Trifluoride and Its Derivatives (IL, Moscow, 1955) p. 19 [Russian translation].

[2] A. V. Topchiev, S. V. Zavgorodnii, and Ya. M. Paushkin, Boron Fluoride and Its Compounds as Catalyst in Organic Chemistry [in Russian] (Izd. AN SSSR, Moscow, 1956).

[3] Inorganic Syntheses, I [Russian translation edited by D. Ryabchikov] (IL, Mowcow, 1951), p. 26.

[4] G. Balz and G. Schiemann, Ber. Deut. Chem. Ges. 60, 1186 (1927); Manual of Preparative Inorganic Chemistry [Russian translation edited by Brauer] (IL, Moscow, 1956).

Received July 19, 1958

A STUDY OF THE SULFATION OF IRON, COPPER, AND COBALT BY SULFURIC ACID

V. V. Pechkovskii and N. L. Subocheva

The Perm' State University

In recent years sulfation of pulverized materials by sulfuric acid has become increasingly used in nonferrous metallurgy and chemical technology [1-5]. In this method the pulverized materials are granulated with sulfuric acid, with subsequent sulfating roasting of the granules in a fluidized bed. The roasting temperature in treatment of dusts from lead works is 300-350°. It was of interest to study the sulfation of various materials by sulfuric acid at higher temperatures. If the roasting is effected at a high temperature, selective extraction of different components of the sulfated material may be expected in some cases. The material chosen for the investigation was a cobalt concentrate containing (in %): Fe 36.0, S 38.5, Co 0.7, Cu 0.7, Zn 0.8 and other components. The calcine formed by oxidative roasting of the cobalt concentrate at 800-850° was used for sulfation. There was virtually no water-soluble cobalt in the calcine after oxidative roasting.

The aim of the investigation was to study the degree of sulfation of iron, copper, and cobalt by sulfuric acid in relation to the temperature, acid content and concentration of the original mixture, grain size of the roasted material, and duration of roasting. In addition, the volatility of sulfuric acid in roasting with the cobalt concentrate calcine was studied.

EXPERIMENTAL PROCEDURE

The cobalt concentrate calcine was granulated with sulfuric acid and the granules were fractionated by screening. The sulfuric acid contents of the granules were 18.0, 22.0, and 30.0% respectively. Acid of sp.gr. 1.84 and 1.30 was used. The granules were roasted for definite times at fixed temperatures in a laboratory muffle furnace. The samples weighed 2.0 g in all cases, 2-3 mm granules were used in most of the experiments, and the duration of each experiment was 60 minutes. Total and water-soluble iron, copper, and cobalt were

TABLE 1

Effects of Temperature and the Content of Sulfuric Acid in the Calcine on the Degree of Sulfation of Iron and Cobalt

H_2SO_4 in calcine (%)	Degree of sulfation of iron and cobalt (%)										
	18°		400°		500°		600°		700°		
	Fe	Co	Fe	Co	Fe	Co	Fe	Co	Fe	Co	
18.0	6.5	35.0	6.5	56.0	6.3	69.5	—	82.0	0.0	84.0	40.3
22.0	12.4	42.0	12.0	68.0	11.8	75.0	10.8	89.0	0.0	90.0	—
30.0	13.4	44.5	13.4	69.5	13.2	76.0	11.8	90.0	0.0	92.0	47.5

determined in the original granules and the products of roasting. Iron was determined by the bromate method, copper iodometrically, and cobalt colorimetrically (with α-nitroso-β-naphthol) [4]. Total sulfur in the calcine was determined by the Eschka method.

TABLE 2

Variation of the Degree of Sulfation of Cobalt with the Duration of the Experiment (18.0% acid in the calcine)

Temperature (°C)	Degree of sulfation of cobalt (%) after time (minutes)		
	15	30	45
400	46.5	50.0	54.0
500	59.0	60.5	67.5
600	76.5	76.5	82.0
700	84.0	81.0	80.1

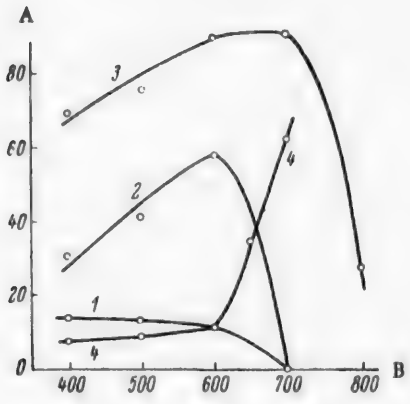

Effects of temperature on the degree of sulfation of iron, copper, and cobalt and on volatilization of sulfuric acid, with 30% of sulfuric acid in the calcine: A) degree of sulfation of metals and volatilization of sulfuric acid (%), B) temperature (°C); degree of sulfation (%): 1) iron, 2) copper, 3) cobalt, 4) volatilization of sulfuric acid (%).

The principal experimental results are given in Tables 1 and 2 and in the figure.

First, it must be pointed out that sulfates of iron, copper, and cobalt are formed when sulfuric acid is mixed with the calcine at room temperature. However, under such conditions the degree of sulfation of cobalt is relatively low, whereas the amount of iron which goes into solution is fairly considerable. The situation is different if the granules are roasted. The degree of extraction of cobalt and copper in the water-soluble form increases, and that of iron decreases, with increase of temperature. It is clear from Table 1 and the figure that sulfation of cobalt in the calcine by sulfuric acid proceeds rapidly at 500-600°, is at a maximum at 650-700°, and then diminishes on further increase of temperature. Under laboratory conditions the sulfation of copper was at a maximum at 600°. In the case of iron the degree of sulfation falls with increase of temperature above 500°, and cinder roasted at 700° contains only traces of water-soluble iron. It follows that if a calcine containing iron and cobalt in approximately 50: 1 ratio is sulfated by sulfuric acid it is possible under certain conditions to obtain a solution containing these components in approximately equal amounts. It follows from Table 1 that the degree of sulfation of iron and cobalt increases with the sulfuric acid content of the original mixture. However, at 500-700° increase of the acid content from 18.0 to 30.0% causes only a slight increase in the degree of sulfation of cobalt. It was found that decrease of the sulfuric acid concentration from 98.0 to 40.0% lowers the degree of sulfation of cobalt slightly. Thus, with 30.0% acid in the calcine, the degree of sulfation of cobalt at 500° at sulfuric acid concentrations of 98.0 and 40.0% was 76.0 and 73.5% respectively. It was also found that cobalt can be successfully sulfated by sulfuric acid in granules of different sizes. Nevertheless, the degree of sulfation of cobalt decreases somewhat when the granule size is increased above 3.00 mm.

Data on variation of the degree of sulfation of cobalt with the duration of the experiment are presented in Table 2. Examination of these data shows that sulfation of cobalt by sulfuric acid proceeds rapidly during the first 10-15 minutes, after which the rate of the process decreases considerably.

These experimental results indicate that by sulfation of the calcine by sulfuric acid under suitable conditions cobalt can be converted fairly fully into a water-soluble form while the sulfation of iron is at a minimum. Thus, at 650°, with 18-20% sulfuric acid in the original mixture, granule size 1-3 mm, and a roasting-time of 60 minutes it is possible under laboratory conditions to convert 82-84% of the cobalt into a water-soluble form, whereas the degree of sulfation of iron under these conditions does not exceed 1.5%. In the case of cobalt concentrate calcine this corresponds to formation of an aqueous solution containing iron and cobalt in approximately 1 : 1 ratio.

The figure shows data on volatilization of sulfuric acid when it is heated with cobalt concentrate calcine; it is seen that volatilization of sulfuric acid increases with temperature. Volatilization of sulfuric acid is especially rapid at temperatures above 600°. It was also found that volatilization of sulfuric acid decreases somewhat with increase of granule size and with decrease of the acid content in the original mixture. These results were obtained in sulfation of cobalt concentrate calcine by sulfuric acid.

LITERATURE CITED

[1] L. S. Getskin, A. G. Batyuk, and G. Ya. Leizerovich, Authors' Certif. No. 105,372; Inventions Bull. 2, 28 (1957).

[2] L. S. Getskin, A. G. Batyuk, and P. P. Tsyb, Nonferrous Metals 7, 23 (1957).

[3] R. M. Perel'man, A. Ya. Zvorykin, and N. V. Gudima, Cobalt [in Russian] (Izd. AN SSSR, 1949).

[4] S. Yu. Fainberg, Analysis of Nonferrous Metal Ores [in Russian] (Metallurgy Press, 1947).

[5] K. M. Malin, Suluric Acid Technology [in Russian] (Goskhimizdat, 1951).

Received May 26, 1958

NEW ETCHING AGENTS FOR SILICON*

B. I. Él'kin

At the present time very few substances, used either individually or in conjunction with each other, are available for dissolving silicon (even for analytical purposes) or for surface dissolution (etching). Only caustic alkali is used for dissolving elemental silicon, and alkali with HF for dissolving oxides; surface oxidation in acid etching agents is effected by HNO_3, and the oxides are subsequently dissolved in HF. Recently, several etching agents based on mixtures of HNO_3 and HF have been patented.

In some of these CH_3COOH and Br_2 are added to HNO_3 and HF (for example, SR-4 etching agent [1]); in others, salts of heavy metals such as copper, mercury [2], and silver [3] are added to mixtures of HNO_3 and HF. This completes the range of available etching agents for silicon without the use of electric current.

The literature contains no publications on investigations of the mechanism of dissolution of silicon, including data on the use of complex formers. The question of possible alteration of the composition of the surface layers, very important in a number of cases including semiconductor technology, therefore, remains obscure.

Brief data on the use of a number of substances for surface oxidation of silicon are presented below.

Oxygen-containing compounds of chlorine, bromine, and iodine in conjunction with HF solutions are good solvents for silicon. The silicon and solution become heated during the reaction and elemental halogens are liberated. Surface oxidation proceeds so vigorously that if a large amount of oxidizing agent is taken the process is inhibited, probably because HF cannot dissolve the thick oxide layer formed.

Potassium and sodium salts of $HBrO_3$, $HClO_3$, and HIO_3, added to the liquor in the form of small individual crystals, were used in the investigation. The effects of HIO_3 and its salts are exactly the same as was indicated by the weight loss, surface appearance, and determinations of physical properties. Silicon dissolves rapidly in the systems Br_2–H_2O_2–HF (1 : 5 : 5), HBr–H_2O_2–HF (1 : 10 : 10), HCl–H_2O_2–HF (1 : 10 : 10) and others. As the systems H_2O_2–HF, HBr–HF, HCl–HF do not dissolve silicon when taken separately, it is most likely that in the presence of three substances oxygen-containing compounds of bromine and chlorine, which oxidizes the silicon surface, are formed on the silicon surface and within the solution.

The diversity of the etched patterns formed by the action of the above-named solutions on silicon is indicative of the complexity of the process.

In the case of the system HBr–H_2O_2–HF the solution first turns brown owing to the liberated bromine, and the color then disappears or fades.

The amounts of silicon dissolved indicate that $KBrO_3$ or $NaBrO_3$ are utilized more completely than HNO_3 in the oxidation reaction.

Silicon is also dissolved on the surface in the system CrO_3–HF. The orange solution gradually turns green (as trivalent chromium is formed). At the same time the silicon loses weight; the weight loss may be as much as about 10%. Large amounts of silicon can be dissolved in the systems HBr–H_2O_2–HF, HCl–H_2O_2–HF, Br_2–H_2O_2–HF and $KBrO_3$–HF, $NaBrO_3$–HF.

*V. A. Vlasenko assisted in the work.

LITERATURE CITED

[1] Chem. Abs. 47, 7352 (1953).

[2] Chem. Abs. 49, 8084 (1955).

[3] Trans. AIME 197, 436 (1953).

Received September 9, 1958

A STUDY OF THE MECHANISM AND KINETICS OF OXIDATION OF TINE SULFIDE BY OXYGEN

D. N. Klushin and O. V. Nadinskaya

Our previous paper contained the main results of an investigation of the reaction between tin sulfide and atmospheric oxygen. The present paper deals with a study of the reaction between tin sulfide and pure oxygen. The apparatus described in the previous paper [1] was used for the investigation.

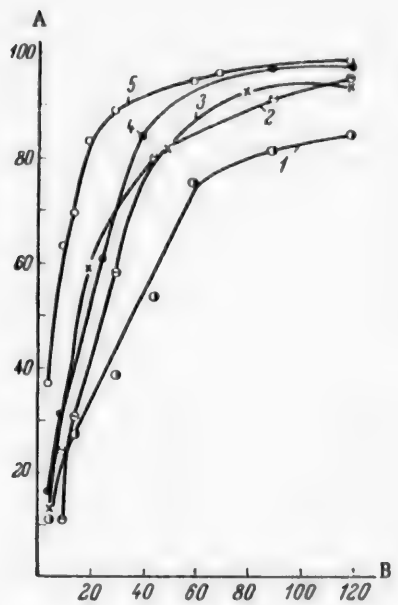

Fig. 1. Variation of the degree of oxidation of SnS by pure oxygen with the time of heating at different temperatures: A) degree of oxidation of SnS (%), B) heating time (minutes); temperature (°C): 1) 600, 2) 700, 3) 800, 4) 900, 5) 1000.

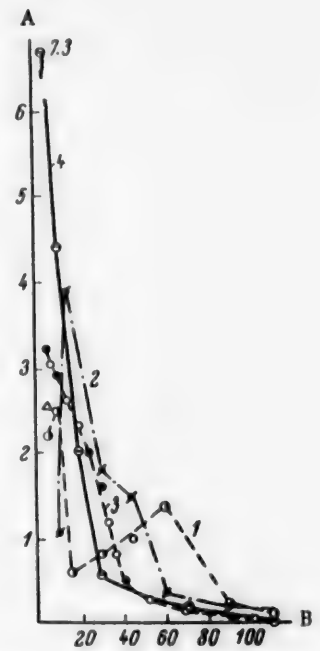

Fig. 2. Variation of the nominal rate of oxidation of SnS by oxygen with the time of heating at different temperatures: A) nominal oxidation rate (degree of oxidation/ minute), B) time (min.); temperature (°C): 1) 600, 2) 700, 3) 900, 4) 1000.

The experiments were performed at 600, 720, 800, 900, 1000° and were 15, 30, 60, and 120 minutes in duration; samples of 1.5 g of tin sulfide containing 1.173 g of tin and 0.327 g of sulfur were used.

The results of the experiments are presented in Table 1 and 2 and in Fig. 1-3.

TABLE 1

Change in Sample Weight and Phase Composition of Calcine in Oxidation of Tin Sulfide by Oxygen at Different Temperatures for Different Times

Temperature (°C)	Duration (min)	Wt. of calcine (g)	Change of sample weight		Composition of calcine								Discrepancy (%)
					Sn_{met}		$SnSO_4$		SnS, Sn_2S_3, SnS_2		SnO_2		
			g	%	g	%	g	%	g	%	g	%	
600	15	1.561	+0.061	+4.1	0.010	0.6	0.148	9.5	0.47	30.1	0.96	61.5	+1.7
	30	1.532	+0.032	+2.1	0.006	0.4	0.077	5.0	0.30	19.6	1.15	75.1	+0.1
	60	1.533	+0.033	+2.2	0.015	0.9	0.080	5.2	0.34	22.2	1.09	71.1	−0.6
	120	1.533	+0.033	+2.2	0.016	1.0	0.080	5.2	0.23	15.0	1.25	81.1	+2.3
700	15	1.548	+0.048	+3.2	0.014	0.9	0.116	7.5	0.81	52.3	0.68	43.9	+4.6
	30	1.557	+0.057	+3.8	0.008	0.5	0.138	8.9	0.84	53.9	0.60	38.5	−1.8
	60	1.502	+0.002	+0.1	0.020	1.3	0.005	0.3	0.06	5.9	1.39	92.5	0
	120	1.504	+0.004	+0.3	0.009	0.6	0.009	0.6	0.09	5.9	1.46	96.9	+4.0
800	15	1.537	+0.037	+2.5	0.006	0.4	0.089	5.8	0.84	54.6	0.60	39.0	−0.2
	30	1.540	+0.040	+2.7	0.015	0.9	0.097	6.3	0.42	27.3	0.01	65.6	+0.1
	60	1.545	+0.045	+3.0	0.007	0.4	0.109	7.0	0.22	14.0	1.22	78.9	+2.5
	120	1.506	+0.006	+0.4	0.007	0.5	0.010	0.7	0.41	27.0	1.01	67.1	−4.5
900	15	1.525	+0.025	+1.7	0.014	0.9	0.060	3.9	0.18	11.8	1.25	81.9	−1.5
	30	1.509	+0.009	+0.9	0.006	0.4	0.020	1.3	0.07	4.6	1.29	85.5	−8.2
	60	1.514	+0.014	+0.9	0.007	0.5	0.034	2.0	0.09	5.9	1.39	91.8	+0.4
	120	1.514	+0.014	+0.9	—	—	—	—	—	—	—	—	—
1000	15	1.492	−0.006	−0.4	0.014	0.9	—	—	0.11	7.4	1.23	82.3	−9.2
	30	1.496	−0.004	−0.3	0.009	0.6	—	—	0.11	7.3	1.32	88.2	−3.9
	60	1.494	−0.006	−0.4	0.007	0.5	—	—	0.09	6.0	1.41	94.4	+0.9
	120	1.493	−0.007	−0.5	0.022	1.5	—	—	0.09	6.0	1.42	95.1	+2.6

TABLE 2

Degree and Nominal Rate of Oxidation of Tin Sulfide by Pure Oxygen at Different Temperatures

Temperature (°C)	Time from start of expt. (min)	Degree of oxidation (%)		Nominal oxidation rate $\left(\frac{\text{deg. of oxidation}}{\text{minute}}\right)$	Temperature (°C)	Time from start of expt. (min)	Degree of oxidation (%)		Nominal oxidation rate $\left(\frac{\text{deg. of oxidation}}{\text{minute}}\right)$
		during measurements	from start of expt.				during measurements	from start of expt.	
600	5	11.4	11.4	2.2	800	20	36.5	59.3	3.65
	10	12.6	24	2.5		50	22.2	81.5	0.74
	15	3.2	27.2	0.6		80	11.7	93.2	0.39
	30	11.3	38.5	0.8		120	0.6	93.8	0.01
	45	15.1	53.6	1.0	900	5	16.4	16.4	3.2
	60	21.2	75.2	1.4		10	14.5	30.9	2.9
	90	6.6	81.8	0.22		25	29.9	60.8	2.0
	120	3.2	85.0	0.1		40	23.7	84.5	1.5
700	10	10.7	10.7	1.07		60	9.6	94.1	0.48
	15	19.4	30.1	3.89		90	2.7	96.8	0.09
	30	28.1	58.2	1.8		120	2.1	98.9	0.07
	45	22.3	80.5	1.48	1000	5	36.6	36.6	7.3
	60	5.4	85.9	0.36		10	22.2	62.9	4.4
	90	5.5	91.4	0.18		20	20.3	83.2	2.03
	120	4.4	95.8	0.15		30	5.8	89.0	0.58
800	5	12.1	12.1	2.4		70	7.3	96.3	0.18
	10	10.7	22.8	2.1		120	2.3	98.6	0.046

If follows from the data in Table 1 that the sample changes in weight during an experiment to approximately the same extent as in oxidation of tin sulfide by atmospheric oxygen, but whereas in the latter case there was a weight increase up to 700°, in this instance this effect continues up to 900°. Accordingly, as is clear from the data in Table 1, tin sulfate is present in the calcine formed at temperatures up to 900° inclusive. The explanation of this result lies in the higher degree of sulfate formation when tin sulfide is oxidized by pure oxygen.

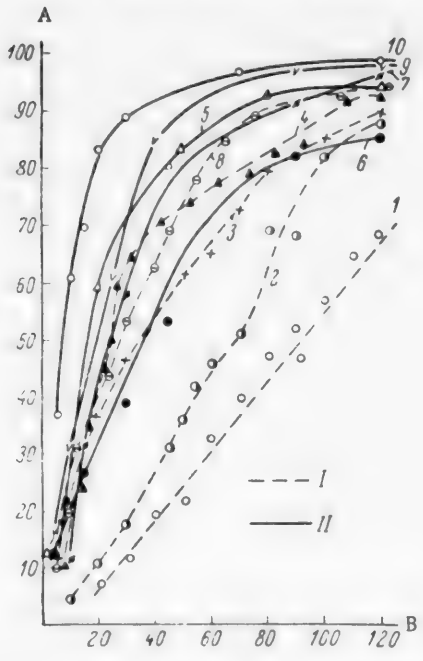

Fig. 3. Effect of heating time at different temperatures on the degree of oxidation of SnS by atmospheric oxygen and pure oxygen: A) degree of oxidation of SnS (%), B) duration of experiment (min.); temperature (°C); 1) 600, 2) 700, 3) 800, 4) 900, 5) 1000, 6) 600, 7) 700, 8) 800, 9) 900, 10) 1000. Oxidation of SnS: I) by atmospheric oxygen, II) by pure oxygen.

Fig. 4. Polished section of calcine obtained in experiment with pure O_2.

It follows from the data in Table 1 that the products formed by oxidation of tin sulfide by oxygen are metallic tin (the contents of which in the samples were almost the same at all temperatures), stannic oxide, and stannous sulfate. As in the experiments with air, oxidation of tin sulfide is almost complete after 60 minutes at 1000°. These results indicate that sublimation of tin sulfide and its oxidation to the dioxide in the upper zones of the same furnace probably cannot be achieved simultaneously under production conditions. The oxidation must be performed in a separate unit.

It is clear from the data in Fig. 3 that at low temperatures the oxidation rate is proportional to the concentration of oxygen in the gaseous phase, but the relationship is not linear even here. With increase of temperature increase of the oxygen concentration in the gaseous phase begins to have less influence in increasing the rate of oxidation.

It is also clear from Fig. 3 that the numerical values of the half life* of the tin sulfide in experiments with pure oxygen and air come closer together with increase of temperature (they become almost equal at 900°), and it follows that oxidation of tin sulfide by oxygen (pure or atmospheric) in the 600-900° range, in accordance with the van't Hoff rule, is of fractional order, such that $2 > n > 1$, where n is the reaction order.

At 900° the order of the reaction is virtually unity.

The photograph shown in Fig. 4 of a polished section of calcine obtained in oxidation by pure oxygen shows that, as was to be expected, the mechanism of oxidation of tin sulfide by pure oxygen is almost the same as that of oxidation by atmospheric oxygen. The same oxidation products as were formed in the oxidation of tin sulfide by air can be seen in Fig. 4.

SUMMARY

A study of the oxidation of tin sulfide by pure oxygen showed that the mechanism of this reaction is analogous to the oxidation of tin sulfide by atmospheric oxygen. At low temperatures the oxidation rate increases in proportion to the oxygen concentration in the gaseous phase, but even here there is no direct proportionality. At higher temperatures increase of the oxygen concentration in the gaseous phase has less effect on increase of the oxidation rate; in the 600-900° range the oxidation reaction is of fractional order (n) such that $2 > n > 1$; at 900° it is virtually a first- order reaction.

LITERATURE CITED

[1] D. N. Klushin and O.V. Nadinskaya, J. Appl. Chem. 32, No. 8, 1729 (1959) [USSR].**

Received March 1, 1958

* Time required for oxidation of 50% of the initial SnS.

** Original Russian pagination. See C.B. Translation.

EFFECTS OF AMMONIA CONCENTRATION AND DEGREE OF CARBONATION ON THE CARBONATION OF AMMONICAL BRINES IN GAS LIFT APPARATUS*

G. N. Gasyuk, A. G. Bol'shakov, and A. V. Kortnev

The preceding communications [1, 2] were concerned with the effects of carbon dioxide concentration in the incoming gas, temperature, and liquid and gas rates on the carbonation process.

This paper contains the results of a study of the effects of ammonia concentration and the degree of carbonation of an ammoniated brine on the carbonation process.

Effect of the Concentration of Ammonia in the Brine on the Carbonation Process

Four series of experiments were carried out for studying the effect of the initial ammonia concentration in the brine on carbonation. Brines with different ammonia contents were used in the different series. The ammonia concentrations were 115 normal divisions (n.d.) [1] in brine No. 1, 73 n. d. in No. 2, 42.9 n. d. in No. 3, and 13.9 n.d. in No. 4.

The over-all absorption coefficient is plotted against the ammonia content of the ammoniated brine in Fig. 1 in semilogarithmic coordinates. The concentration of ammonia in the brine has a considerable influence on the over-all coefficient of absorption of carbon dioxide by ammoniacal brines (if the ammonia concentration is increased 8-fold, the over-all absorption coefficient increases approximately 5.5-fold). This relationship can be represented analytically by the following equation:

$$K_G \cdot a = A \cdot e^{0.0168N},$$

where N is the concentration of ammonia in the brine.

The constant A depends on the hydrodynamic process conditions (immersion depth, gas and liquid rates) and the temperature.

It should be noted that at low ammonia concentrations the experimental points deviate considerably from the mean line. It is probable that at ammonia concentrations below those studied (13.9 n.d.) this expression for the over-all coefficient of absorption of carbon dioxide by ammoniacal chloride brines is not applicable. In such cases the process of chemical absorption approximates to simple physical absorption (absorption of a sparingly soluble gas).

Figure 2 shows variations of the conversion rate with the ammonia content of the brine. The conversion rate increases linearly with the ammonia content; this may be represented by the equation

$$U = B + 34.8N.$$

The constant B depends on the hydrodynamic conditions, the carbon dioxide concentration in the incoming gas, and the temperature.

The difference between the relationships for the over-all absorption coefficient and the conversion rate is due to the fact that the partial pressure of ammonia over the solution increases with its concentration, and

* Communication III in the series on carbonation of ammoniacal brines in gas lift equipment.

at constant carbon dioxide concentration in the carbonation gas the partial pressure of carbon dioxide accordingly decreases. Therefore, when the expression for the conversion rate as a function of the ammonia content in solution is used for calculations it is not necessary to know the state of ammonia equilibrium between the liquid and gas phases.

Effect of the Degree of Carbonation of the Solution on the Carbonation Process

The experimental data obtained in a study of the influence of gas liquid rate at constant immersion depth on carbonation in gas lift equipment [2] were used for investigation of the influence of the degree of carbonation on the over-all absorption coefficient and conversion rate. The degrees of carbonation of the ammoniated brines were 12.9% for brine No. 5, 27.6% for No. 6, 42.9% for No. 7, and 60% for No. 8; the initial ammonia content was 90 n.d. [1].

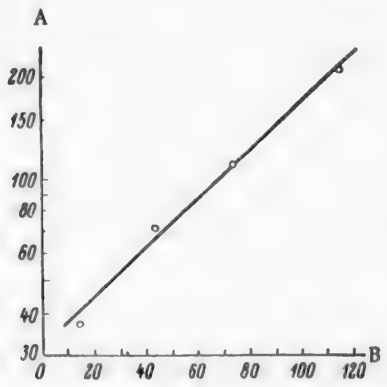

Fig. 1. Variation of the over-all coefficient of absorption of carbon dioxide by ammoniacal chloride brine with the ammonia content of the brine: A) over-all absorption coefficient $K_G \cdot a \cdot 10^{-2}$ (kg/ m^2 · atmos · hr), B) ammonia content (n.d.).

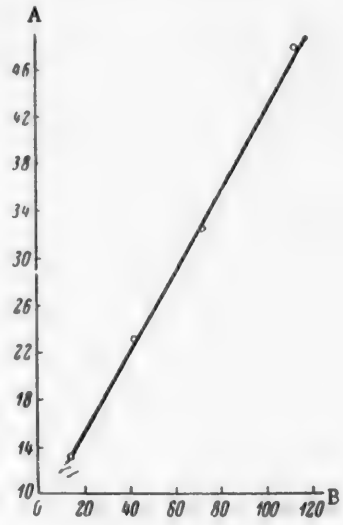

Fig. 2. Variation of the rate of conversion of carbon dioxide by ammoniacal chloride brine with the ammonia content of the brine: A) conversion rate $U \cdot 10^{-2}$ (kg/ / m^3 · hour), B) ammonia content (n.d.).

The relationship between the over-all absorption coefficient and the degree of carbonation is plotted in Fig. 3, and is represented by the following exponential equation:

$$K_G \cdot a = C \cdot e^{-0.014R}$$

where R is the degree of carbonation and C is a constant which depends on the hydrodynamic process conditions, temperature, and the initial ammonia content of the brine.

If the values of the absorption coefficient for different degrees of carbonation are plotted as a function of "free" ammonia (total ammonia less the amount of ammonia used for combining with carbon dioxide), the resultant points lie on a straight line analogous to the relationship between the over-all absorption coefficient and the initial ammonia content in the brine. This is consistent with the results of Belopol'skii [6], who noted that the decrease of the over-all absorption coefficient with increase of the degree of carbonation can be ascribed to decrease to the chemical factor β, and β primarily depends on the concentration of "free" ammonia, which decreases with increasing degree of carbonation.

The relationship between the conversion rate and the degree of carbonation is plotted in Fig. 4; it may be be represented by the following equation:

$$U = D \cdot e^{-0.0125R}.$$

The constant D depends on hydrodynamic factors, temperature, initial ammonia content, and gas concentration.

In calculations with the use of this relationship between the conversion rate and the degree of carbonation it is not necessary to know the parital pressures of ammonia and water over the carbonated liquors (the experiments were performed at constant carbon dioxide concentration in the incoming gas).

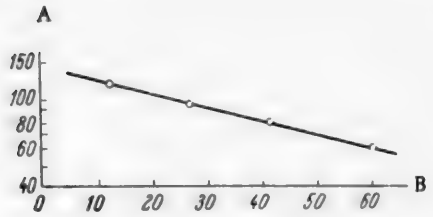

Fig. 3. Variation of the over-all coefficient of absorption of carbon dioxide by ammoniacal chloride brine with the degree of carbonation of the brine: A) over-all absorption coefficient $K_G \cdot a \cdot 10^{-2}$ (kg/ m³ · · atmos · hr), B) degree of carbonation (%).

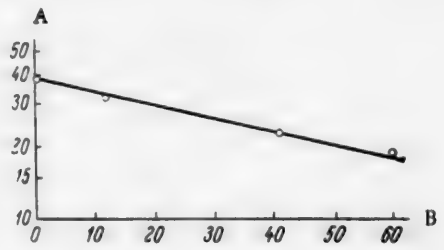

Fig. 4. Variation of the rate of conversion of carbon dioxide by ammoniacal chloride brine with the degree of carbonation of the brine: A) conversion rate U · · 10^{-2} (kg/ m³ · hr), B) degree of carbonation (%).

If the relationships between the carbonation process and the concentration of carbon dioxide [1], temperature [1], liquid and gas rates [2], initial ammonia content, and the degree of carbonation are used for determination of the over-all absorption coefficient, the following equations may be derived and used for calculations relating to absorption in gas lift equipment in the ammonia–soda process:

$$K_G \cdot a = 241 V^{0.33} \cdot L^{0.18} \cdot e^{0.0168N+0.0288t-0.014R-2.09},$$

where V is the gas rate (m³/ m² · hr); L is the liquid rate (m³/ m² · hr); N is the ammonia concentration (n.d.); t is the temperature of the process (°C); R is the degree of carbonation (%); $K_G a$ is the over-all absorption coefficient (kg/ m³ · hr · atmos) at 20% immersion: if the gas rate is known

$$K_G \cdot a = 160 V^{0.488} \cdot e^{0.0168N+0.0288t-0.014R-2.09},$$

and if the liquid rate is known

$$K_G \cdot a = 75 L^{0.93} \cdot e^{0.0168N+0.0288t-0.014R-2.09}.$$

SUMMARY

1. Expressions for the over-all absorption coefficient and the conversion rate as functions of the ammonia concentration and the degree of carbonation of ammoniacal chloride brines have been derived from experimental data.

2. General equations have been derived for calculations of the over-all coefficients of absorption of carbon dioxide by ammoniacal chloride brines in gas lift equipment for different concentrations of carbon dioxide in the gas, temperatures, liquid and gas rates, ammonia concentrations, and degrees of carbonation of the brines.

LITERATURE CITED

[1] G. N. Gasyuk, A. G. Bol'shakov, A. V. Kortnev, and P. Ya. Krainii, J. Appl. Chem. 32, 1787 (1958)* [USSR].

[2] G. N. Gasyuk, A. G. Bol'shakov, A. V. Kortnev, and P. Ya. Krainii, J. Appl. Chem. 32, No. 4, 770 (1959)* [USSR].

[3] A. P. Belopol'skii, J. Appl. Chem. No. 10-11 (1946); No. 11 (1947) [USSR].

Received May 13, 1958

* Original Russian pagination. See C.B. Translation.

COMPLEX FORMATION IN THE SYSTEM $NiSO_4-CS(NH_2)_2-H_2O$ ACCORDING TO DATA ON OPTICAL DENSITY, VISCOSITY, AND SURFACE TENSION

A. Ya. Deich

Additions of small amounts of thiourea to the main electrolyte have a stong influence on the structure of electrolytic deposits of nickel and copper; this fact has been explained in the literature on the basis of adsorption effects [1, 2].

It was of interest in this connection to study complex formation in the system $NiSO_3-CS(NH_2)_2-H_2O$ by physicochemical analysis based on data on optical density, viscosity, and surface tension.

We did not find any data in the literature on these properties of the system in question.

Chemically pure nickel sulfate and thiourea and redistilled water were used for the experiments. The solution mixtures were prepared by the addition method in such a manner that the $\frac{NiSO_4}{H_2O}$ ratio was the same in all mixtures, with variable values of the $\frac{CS(NH_2)_2}{NiSO_4}$ ratio. Weighed quantities of thiourea (from 0.2500 to 4.6722 g) were put in small flasks, and 50 ml of 0.9897 M $NiSo_4$ solution was then added to each flask. The concentration of this solution was checked by precipitation and weighing of Ni dimethylglyoxime. The optical density was determined by means of a photometer of the Pulfrich type. Investigations of the optical density of the system in relation to the wave length showed that the optical density increases sharply in the red region of the spectrum. Therefore, all the determinations were performed with light filters for wave lengths of 619, 665, and 726 mμ. The results obtained represent mean positions of the photometric equilibrium, and each is obtained from seven determinations. Viscosity and surface tension were determined at 20° by methods described previously [3].

The results obtained in the investigations are given in the table and plotted in the figure.

DISCUSSION OF RESULTS

Changes of the optical density of the system indicate that chemical reactions take place between the components; the curves for this property have two minima corresponding to values of 0.513 and 1.071 for the $\frac{CS(NH_2)_2}{NiSO_4}$ molar ratio; this suggests that two complex compounds are formed in the system. The curves obtained with all three light filters were very similar, and only the data determined at 726 mμ are given in the figure.

Complex formation evidently occurs as the result of two consecutive reactions. In presence of small amounts of thiourea one molecule combines with two molecules of nickel sulfate:

$$CS(NH_2)_2 + 2NiSO_4 \rightleftarrows CS(NH_2)_2 \cdot 2NiSO_4. \quad (1)$$

If the amount of thiourea is increased, it reacts with the compound formed previously:

$$CS(NH_2)_2 + CS(NH_2)_2 \cdot 2NiSO_4 \rightleftarrows 2CS(NH_2)_2 \cdot NiSO_4. \quad (2)$$

Increase of the optical density of the system and appearance of a maximum on the curve may be attributed to Reaction [2], as the result of which $CS(NH_2)_2 \cdot 2NiSo_4$ molecules are replaced by $CS(NH_2)_2 \cdot NiSO_4$ with different optical properties, and also to the fact that this reaction leads to an increased concentration of particles in the solution.

Optical Density, Viscosity, and Surface Tension in the System $NiSO_4$–$CS(NH_2)_2$–H_2O

$\frac{CS(NH_2)_2}{NiSO_4}$	η^{20} (poises)	σ^{20} (dynes cm^{-1})	D (scale divisions) at λ (in mμ)		
			726	665	619
0.066	1.519	73.75	1.47	1.44	0.90
0.266	1.591	74.30	1.37	1.34	0.80
0.409	1.608	74.72	1.31	1.28	0.75
0.451	1.645	75.36	1.29	1.23	0.71
0.513	1.670	76.01	1.28	1.19	0.67
0.637	1.662	75.16	1.31	1.23	0.65
0.672	1.660	75.16	1.33	1.25	0.66
0.740	1.625	75.41	1.39	1.31	0.76
0.785	1.598	75.61	1.42	1.32	0.78
0.876	1.600	75.61	1.38	1.30	0 76
0.980	1.620	75.76	1.30	1.28	0.75
1.031	1.650	76.16	1.28	1.24	0.74
1.071	1.683	76.56	1.27	1.20	0.70
1.101	1.672	76.50	1.27	1.22	0.68
1.132	1.662	76.20	1.26	1.22	0.69
1.240	1.618	75.76	1.37	1.31	0.79

The nature of the minima on the optical density curves indicates that the stability of the complex compounds formed is low. The composition of the compounds postulated here is somewhat unusual in the light of the generally accepted coordination numbers of nickel and of the coordination capacity of thiourea as an addend. Therefore, variations of viscosity and surface tension in the system were studied in order to verify these hypotheses.

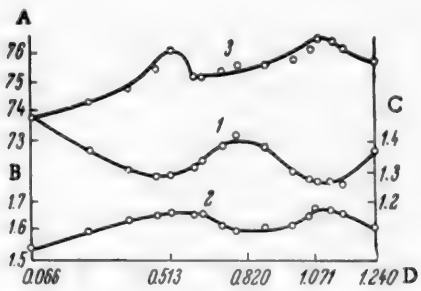

Optical density (1), viscosity (2), and surface tension (3) in the system $NiSo_4$–$CS(NH_2)_2$–H_2O. A) optical density (in scale divisions), B) viscosity (poises), C) surface tension (dynes · cm^{-1}), D) molar ratio $CS(NH_2)_2$: $NiSO_4$.

The viscosity curve confirms that chemical interaction occurs in the system, and is characterized by two maxima between which the curve is somewhat convex toward the composition axis. The maxima confirm the suggestion that two easily-dissociated compounds are formed in the system, while the concavity may be easily explained by Reaction (2).

The surface tension data are of particular interest. A plot of surface tension variations in the system basically resembles the viscosity curve; this can also be attributed to Reactions (1) and (2). In addition, a general tendency for the surface tension to increase with the thiourea content is noteworthy. The explanation may be that when nickel sulfate reacts chemically with thiourea, compounds of new properties are formed; these are surface-inactive substances with negative adsorption. The appearance of maxima on the surface-tension curve may be due to retarded diffusion and establishment of adsorption equilibrium because of the higher viscosity of the corresponding mixtures in the system.

The surface-tension data give some indication of the character of the adsorption effects, which may influence the structure of electrochemical deposits of nickel and copper [1, 2]. Moreover, these data also confirm that complex formation occurs in the system.

In connection with the hypothesis that complexes of the composition indicated above are present in the system it should be noted that no constant coordination number has been established for nickel thiourea compounds, as different nickel salts add on different numbers of thiourea molecules [4]. In a polarographic investigation no complex at all could be detected with ions of bivalent nickel and thiourea [5].

The fact that very unstable forms of thiourea compounds are formed when the complex former has a strong tendency to add on water [4] is also of interest in this connection. It follows that since nickel sulfate readily adds 6 molecules of water to form the blue and green crystalline hydrate forms, when it reacts with thiourea in aqueous solution the sulfur bond in thiourea and the oxygen bond in water probably compete with each other in combining with the central atom of the complex former; this may lead to formation of very unstable aquo complexes of different composition, containing definite amounts of water together with thiourea. However, this matter requires further investigation.

SUMMARY

Physicochemical analysis of the system $NiSO_4$–$CS(NH_2)_2$–H_2O, based on optical density, viscosity, and surface tension data has been carried out.

The results indicate that chemical intereaction between the components occurs in the system, with possible formation of two easily dissociated complex compounds corresponding to the molar ratios $CS(NH_2)_2$/ $NiSO_4$ = = 0.513 and 1.071.

It is suggested that definite numbers of water molecules may be present in these complexes.

LITERATURE CITED

[1] L. I. Antropov, S. Ya. Popov, and V.A. Smirnov, Trans. Novocherkassk Polytech. Inst. 25, 101 (1954).

[2] L. I. Antropov and S. Ya. Popov, J. Appl. Chem. 27, No. 1, 53 (1954)* [USSR].

[3] A. Ya. Deich, J. Inorg. Chem. 2, 903 (1957) [USSR].

[4] V. A. Golovnya and I. V. Prokof'eva, Bull. Sector Platinum and Other Noble Metals, Inst. Gen. Inorg. Chem. 27, 63 (1952).

[5] O. S. Fedorova, J. Gen. Chem. 24, 62 (1954).*

Received June 9, 1958

*Original Russian pagination. See C.B. Translation.

DENSITY AND REFRACTIVE INDEX OF AQUEOUS SOLUTIONS OF $K_2[HgI_4]$

É. A. Gyunner

The Frunze State Pedagogic Institute of the Crimea

Concentrated aqueous solutions of $K_2[HgI_4]$ are used in mineralogy for separation of solid mixtures into their components in accordance with density [1]. Our aim was to compile tables for determination of the density of aqueous $K_2[HgI_4]$ solutions from the refractive index at concentrations up to 65% (by weight). The solutions were prepared by the dissolving of exactly weighed amounts of potassium iodide and mercuric iodide (analytical grade) in weighed amounts of water. Density was determined by the pycnometric method [2] with a 50 ml pycnometer calibrated against triple-distilled water; this gave an accuracy of the order of ±0.0001 in the density determinations. Refractive indices were determined by means of an Abbe refractometer, type RPU. Table 1 contains the results of determinations of the refractive index n and density d_{exp} of $K_2[HgI_4]$ solutions. The concentrations of these solutions are given in weight fractions (p).

TABLE 1

Densities and Refractive Indices of $K_2[HgI_4]$ Solutions at 20°

p	n	d_{exp}	d_{calc}	$d_{exp}-d_{calc}$
0.0211	1.3360	1.0151	1.0151	0.0000
0.0468	1.3396	1.0365	1.0365	0.0000
0.0802	1.3446	1.0655	1.0656	—0.0001
0.1033	1.3482	1.0867	1.0867	0.0000
0.1303	1.3527	1.1125	1.1125	0.0000
0.1622	1.3582	1.1442	1.1444	—0.0002
0.1839	1.3619	1.1671	1.1671	0.0000
0.2120	1.3672	1.1979	1.1979	0.0000
0.2412	1.3732	1.2316	1.2315	0.0001
0.2710	1.3797	1.2679	1.2678	0.0001
0.3015	1.3865	1.3073	1.3071	0.0002
0.3213	1.3912	1.3339	1.3339	0.0000
0.3431	1.3967	1.3646	1.3646	0.0000
0.3739	1.4047	1.4105	1.4105	0.0000
0.4026	1.4130	1.4562	1.4562	0.0000
0.4318	1.4214	1.5058	1.5056	0.0002
0.4608	1.4308	1.5582	1.5582	0.0000
0.4901	1.4408	1.6151	1.6152	—0.0001
0.5104	1.4484	1.6573	1.6573	0.0000
0.5312	1.4569	1.7028	1.7030	—0.0002
0.5601	1.4688	1.7699	1.7699	0.0000
0.5714	1.4742	1.7971	1.7971	0.0000
0.5939	1.4854	1.8543	1.8542	0.0001
0.6145	1.4948	1.9100	1.9099	0.0001
0.6388	1.5063	1.9806	1.9806	0.0000
0.6500	1.5110	2.0152	2.0153	—0.0001

TABLE 2

Densities and Refractive Indices of $K_2[HgI_4]$ Solutions with Equal Concentration Increments (0.02) at 20°

p	d	n	p	d	n
0.00	0.9982	1.3330	0.34	1.3602	1.3959
0.02	1.0142	1.3358	0.36	1.3895	1.4011
0.04	1.0307	1.3386	0.38	1.4200	1.4066
0.06	1.0478	1.3415	0.40	1.4519	1.4123
0.08	1.0655	1.3446	0.42	1.4853	1.4180
0.10	1.0837	1.3478	0.44	1.5201	1.4241
0.12	1.1025	1.3510	0.46	1.5567	1.4305
0.14	1.1220	1.3544	0.48	1.5951	1.4372
0.16	1.1421	1.3578	0.50	1.6356	1.4445
0.18	1.1630	1.3612	0.52	1.6782	1.4520
0.20	1.1846	1.3649	0.54	1.7232	1.4600
0.22	1.2069	1.3688	0.56	1.7697	1.4688
0.24	1.2301	1.3729	0.58	1.8185	1.4783
0.26	1.2542	1.3772	0.60	1.8703	1.4882
0.28	1.2792	1.3816	0.62	1.9255	1.4973
0.30	1.3051	1.3861	0.64	1.9844	1.5064
0.32	1.3321	1.3909			

TABLE 3

Densities Calculated from Refractive Indices

p	n	d_{exp}	p_n	d_n	$d_{exp}-d_n$
0.1476	1.3556	1.1295	0.1470	1.1289	0.0006
0.2617	1.3776	1.2562	0.2618	1.2563	—0.0001
0.2842	1.3827	1.2848	0.2848	1.2858	—0.0010
0.3304	1.3935	1.3520	0.3304	1.3520	0.0000
0.4466	1.4263	1.5321	0.4469	1.5325	—0.0004
0.5225	1.4528	1.6836	0.5220	1.6829	0.0007

It was found that the density and refractive index isotherms for this system are curves convex toward the concentration axis.

The relationship between density and concentration of $K_2[HgI_4]$ solutions may be represented by the empirical equation

$$d = 0.9982 - \ln [1 - (B + \beta p)\, p], \qquad (1)$$

where 0.9982 is the density of water at 20°; B and β are empirical coefficients, equal to 0.7883 and 0.3084 respectively in the concentration range $0 < \underline{p} \leq 0.5.44$ and 0.8829 and 0.2448 in the range $0.544 < \underline{p} \leq 0.650$.

The densities d_{calc} given in Table 1 were calculated from Equation (1). It is seen in Table 1 that the difference $d_{exp}-d_{calc}$ does not exceed ± 0.0002, which is within the limits of experimental error.

Density variations in the system for constant concentration increments of 0.02 were taken calculated, and are given in Table 2.

The values of the density $\underline{d}$ in Table 2 were calculated from Equation (1), and the refractive indices were found by parabolic interpolation from the experimental data in Table 1. Table 2 can be used for determination of the concentration of $K_2[HgI_4]$ solutions of known density by interpolation, as determination of concentration by solution of Equation (1) for $\underline{p}$ is very laborious. In addition, Table 2 can be used to find the density of a solution if its refractive index is known. For this it is first necessary to find the concentration of the solution by interpolation from the refractive index, and the density is then found from Equation (1) after substitution of the value found for the concentration. To test this method, the densities of six $K_2[HgI_4]$ solutions were calculated from their refractive indices. The results are summarized in Table 3, where $\underline{p}$ is the true concentration; $\underline{n}$ is the refractive index; d_{exp} is the density found experimentally; p_n and d_n are the concentrations and densities found from the refractive index.

It follows from Table 3 that the differences $d_{exp}-d_n$ do not exceed ± 0.0010. It follows that densities can be determined from the refractive indices when errors of the order of ± 0.001-0.002 in the density determinations do not influence the result appreciably.

This method is convenient because the refractive index can be determined in 2-3 minutes and only a few drops of solution are required, whereas density determinations require at least several milliliters of solution and take considerable time.

SUMMARY

1. Densities and refractive indices of aqueous $K_2[HgI_4]$ solutions in the concentration range up to 65% (by weight) have been determined and tabulated.

2. It is shown that densities of $K_2[HgI_4]$ solutions can be calculated from their refractive indices.

3. The following equation is given for the density of $K_2[HgI_4]$ solutions:

$$d = 0.9982 - \ln [1 - (B + \beta p)\, p]$$

LITERATURE CITED

[1] E. V. Kopchenova, Mineralogical Composition of Ore Slimes [in Russian] (State Geological Press, 1940).

[2] I. K. Turubiner and M. D. Ippits, Techniques of Density Determination [in Russian] (Mashgiz, 1949).

Received June 2, 1958

DETERMINATION OF CARBON DIOXIDE IN MONOETHANOLAMINE SOLUTIONS, IN ACID SOLUTIONS OF SODIUM AND MONOETHANOLAMINE SULFATES

M. K. Shchennikova and I. A. Korshunov

Our preceding communications [1, 2] contained data on the solubility of carbon dioxide in aqueous solutions of sulfuric acid, sodium sulfate, and their mixtures at 20-75°; these results were obtained by the isotopic dilution method with the use of C^{14} radioactive isotope as tracer.

The present communication contains data on the contents of carbon dioxide in monoethanolamine solutions when they are boiled in acid solutions of sodium and monoethanolamine sulfates. Such data are of practical interest, as solutions of these substances are formed in the regeneration of carbon dioxide after absorption in alkaline solutions in removal of CO_2 from gases and in the industrial production of CO_2.

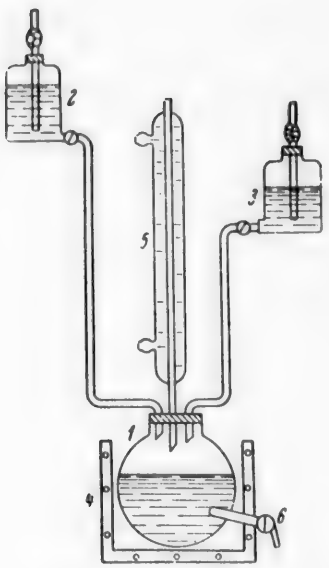

Apparatus for decomposition of monoethanolamine and sodium bicarbonates: 1) flask, 2) bottle with $NaHCO_3$, 3) bottle with H_2SO_4, 4) heater, 5) condenser, 6) tap.

EXPERIMENTAL

Commercial monoethanolamine and chemically pure sodium bicarbonate and sulfuric acid were used in the investigations. A solution of sodium bicarbonate containing C^{14} was prepared by addition of tagged bicarbonate to $NaHCO_3$ solution of the required concentration. For preparation of monoethanolamine bicarbonate containing C^{14} carbon dioxide with added $C^{14}O_2$ was passed at atmospheric pressure through an aqueous solution of monoethanolamine of the required concentration. When monoethanolamine solution is saturated with carbon dioxide at atmospheric pressure and at room temperature, monoethanolamine bicarbonate is formed [3, 4].

The method was as follows. A solution of sodium bicarbonate (or monoethanolamine) of known concentration was passed into the flask 1 from the bottle 2 (see diagram). If sulfuric acid was used for the decomposition, it was supplied into the same flask from the bottle 3. The contents of flask 1 were heated by the heater 4. Care was taken during each experiment to have the solutions boiling at the same rate (checked by the number of drops per unit time falling from the lower end of the condenser 5) and to have a uniform supply of solutions from the vessels 3 and 2. Samples of solution were then taken through the tap 6 into an evacuated flask which was then attached to the apparatus described previously [1], which was used for determinations of the CO_2 content.

Data are presented below on the contents of carbon dioxide in boiling aqueous solutions of 0.25-0.3 N sodium sulfate mixed with sulfuric acid of different concentrations at 100.3-103°.

Normality H_2SO_4	2.45	3.15	3.7	4.10	4.40	4.50	4.70	5.50
$\alpha \cdot 10^2$	3.4	2.9	2.7	2.3	2.3	2.4	2.0	1.7
Normality H_2SO_4	5.60	5.65	6.35	7.8	8.1	11.2	12.0	
$\alpha \cdot 10^2$	1.9	1.2	1.8	1.3	1.1	1.0	1.2	

These data correspond to established equilibrium between the gas and liquid phases. The time required for equilibrium to be reached was 40-70 minutes.

The carbon dioxide contents are represented by the coefficient α, calculated from the formula

$$\alpha = \frac{V_{CO_2} \cdot A_1 \cdot d}{a\,(A_0 - A_1)}, \qquad (1)$$

where V_{CO_2} is the volume of carbon dioxide (in ml reduced to standard conditions) taken for dilution of the sample; A_1 is the activity of the gas (in pulses per minute) in the liquid sample after dilution; A_0 is the initial activity of the gas; a is the weight of the sample in grams; d is the density of the solution.

In investigations with monoethanolamine solutions the solubility of carbon dioxide in mixtures of monoethanolamine and sulfuric acid was determined by the method described previsouly [1]. Results obtained in determinations of the solubility of CO_2 in a solution containing 0.5 N monoethanolamine and 2N H_2SO_4 are presented below.

Temperature (in °C)	α' (ml/ ml)
25	0.64
35	0.51
45	0.37
55	0.304
70	0.120

Here α' is the absorption coefficient, which is the solubility of carbon dioxide at 760 mm partial pressure of CO_2. The solution was saturated at 300 mm partial pressure of carbon dioxide. The absorption coefficient α' was calculated from the formula

$$\alpha' = \alpha \cdot \frac{760}{p - p_1}, \qquad (2)$$

Contents of Carbon Dioxide in Solutions of Monoethanolamine Bicarbonate at t = 100-101.5°

Expt. No.	Monoethanolamine concentration (N)	α (ml/ ml)	Expt. No.	Monoethanolamine concentration (N)	α (ml/ ml)
1	0.20	0.21	9	1.10	1.13
2	0.28	0.21	10	1.13	1.25
3	0.405	0.32	11	1.34	1.43
4	0.56	0.44	12	0.66	0.90
5	0.85	0.75	13	0.85	0.55
6	0.90	0.72	14	0.45	0.07
7	0.91	0.72	15	0.80	0.09
8	1.09	1.18	16	1.04	0.02

where p is the partial pressure of carbon dioxide used for saturation of the solution; p_1 is the vapor pressure of the solution.

When solutions of sodium and monoethanolamine bicarbonates are treated with sulfuric acid, considerable amounts of CO_2 remain unliberated from the solutions. This must be taken into account to volumetric determinations of CO_2 [5].

The amounts of carbon dioxide remaining in monoethanolamine bicarbonate solutions on boiling (at 100-101.5°) with continuous supply of solution into the reaction flask (see diagram) were determined. The results of these experiments are given in the Table. The carbon dioxide content α was calculated from Formula (1). In all the experiments the solution was fed into the still at the rate of 0.6 ml/ $cm^2 \cdot$ min. The rate of boiling was 2.1 ml/ minute in Experiments No. 1-11 and 14-15, 0.5 ml minute in Experiment No. 12, and 3.5 ml/ minute in Experiment No. 13. In Experiments No. 14 and 15 a column packed with glass coils (not shown in the diagram) was introduced between the flask 1 and the condenser 5 (Fig. 1). The efficiency of the column was 3.-4 theoretical plates. In Experiment No. 16 sulfuric acid was fed into the still to decompose the bicarbonate.

It is clear from the table that when aqueous solutions of monoethanolamine bicarbonate are boiled, with continuous supply of the solutions into the still, they liberate only small amounts of carbon dioxide. The amounts decrease appreciably if a column is introduced. The amount of carbon dioxide which remains unliberated decreases considerably when the column is introduced (Experiments No. 14 and 15), and especially in presence of sulfuric acid (Experiment No. 16).

LITERATURE CITED

[1] M. K. Shchennikova, G. G. Devyatykh, and I. A. Korshunov, J. Appl. Chem. 30, 833 (1957)* [USSR].

[2] M. K. Shchennikova, G. G. Devyatykh, and I. A. Korshunov, J. Appl. Chem. 30, 1080 (1957)* [USSR].

[3] M. A. Lyudkovskaya and A. G. Leibush, J. Appl. Chem. 22, 558 (1949) [USSR].

[4] J. Mason and B. Doge, Trans. Am. Inst. Chem. Eng. 32, 27 (1936).

[5] N. I. Stognii and F. P. Dorosh, Industrial Lab. 10, 1253 (1949).

Received July 3, 1958

*Original Russian pagination. See C.B. Translation.

TESTS OF THE PROTECTIVE PROPERTIES OF A FILM OF BF-2 ADHESIVE ON GALVANIC COATINGS

R. G. Genes

The protective properties of films of BF-2 adhesive were investigated in relation to their use for conferring higher corrosion resistance on galvanic coatings, especially in components of hydrometerological instruments for use under different climatic conditions. According to Berdinskikh [1], universal adhesives of the BF type protect metals against corrosion; they are resistant to fungi, water, frost, and vibrations, are neutral, and have good adhesion to metals. BF-2 adhesive has good heat resistance at elevated temperatures (60-80°) and in acid media; its elasticity on the scale of the Scientific Research Institute of Lacquers and Paints is 3 mm. The tests were carried out on BF-2 adhesive diluted with ethyl alcohol to a working viscosity of 23-25 seconds by the VZ-4 viscosimeter. The volume ratio was approximately 1 : 2.

The experiments were conducted with mass-produced zinc-plated and nickel-plated components and with unplated steel disks. At least five articles were tested in each case.

The basis metals from which the components for plating were made were: steel, brass, and "thermobimetal" (steel-Invar).

The components were subjected to the following treatment before the tests;

a) degreasing in ethyl alcohol, b) drying in air for 30 minutes, c) wetting in adhesive solution (this gives the components a yellowish color), d) drying in air for 1 hour, e) drying in a thermostat at 100 ± 5° for 2 hours, f) air cooling to room temperature.

The tests were performed in a glass exhaust chamber 1.25 m^3 in capacity. Water was evaporated at 2.5 liters/hour (on electric hot plates) to create a high relative humidity and temperature. The relative humidity and temperature were recorded throughout the tests by a recording hygrograph and thermograph. A 3% sodium chloride solution was used as the corrosive agent. The test pieces were suspended from glass rods; the chamber was in operation for 3 weeks intermittently – for 9 hours each day, during which time was fed in the pieces which were moistened in 3% sodium chloride solution at intervals of two hours (five times per day); during the rest of the time, on days off, and for an additional 20 days before the end of the test the pieces remained in the unheated chamber and were not moistened. The hygrograph and thermograph continued in operation during this period.

The relative humidity throughout the test period was maintained at 95-100%, but very rarely it fell to 75-70%. The temperature during the working day was in the 45-55° range, while during the nonworking periods it fell to 20-8°.

While the pieces were being moistened with 3% sodium chloride solution the relative humidity and temperature fell during 10-15 minutes (to 65-55% and 35-25° respectively).

The thickness of the coatings was determined by the streaming volumetric method. Zinc plating was effected in a sulfuric acid electrolyte, with subsequent passivation of some of the pieces in a colorless-passivation solution and some in an iridescent-passivation solution.

TEST RESULTS

The tests were performed on 20 hooks made by forging and coated with a zinc layer 20μ thick.

In absence of the adhesive film, attack of the zinc (appearance of white salts) on the coated surface (after colorless passivation) began after four days, and pinhole rusting began after 17 days. In analogous tests with the adhesive film, attack of the zinc began after 11 days, and pinhole rusting appeared after 30 days.

A zinc-plated surface (after iridescent passivation) without adhesive film showed similar attack of the zinc after 6 days, and pinhole rusting appeared after 17 days. In analogous tests with the adhesive film, attack of the zinc began after 11 days, and pinhole rusting after 40 days.

The time before corrosion sites appeared on zinc-plated hooks without the adhesive film was the same after both colorless and iridescent passivation, 17 days. However, after 46 days of testing the zinc-coated surface after iridescent passivation, despite its worse state (presence of projecting edges and flaws which favor the start of corrosion), was less corroded and the corrosion began 10 days later than in the case of surfaces after colorless passivation.

A screw coated with zinc 10 μ thick and covered with the adhesive film showed pinhole rusting and corrosion sites after 7 days; without the adhesive film the time in analogous tests was 5 days.

A nickel-plated surface (on steel) of a threaded ring, with a 3-layer coating (nickel–copper–nickel) 20 μ thick, withstood the test for 17 hours before corrosion appeared; the time in an analogous test with an adhesive film was 41 hours, and the surface was less attacked by corrosion. A nickel-plated screw (with steel as the basis metal) with a nickel layer 15 μ thick withstood the test before the appearance of corrosion for 17 hours without the adhesive film, and for 89 hours with the film, and the surface was less attacked. An unplated steel disk withstood the test for 17 hours before the appearance of corrosion when without the adhesive film, and for 41 hours with the adhesive film.

The tests on adhesive films under simulated tropical conditions were accompanied by tests conducted in psychrometric (meteorological) booths situated in the works, i.e., under the usual service conditions for hydrometeorological instruments. The articles were prepared for the tests as described above.

Tests were performed on 10 assemblies of pairs of mass-produced thermobimetal assemblies coated with a 20-24 μ layer of nickel deposited from a bright-plating bath. Five of these assemblies were without an adhesive film and five were coated with the adhesive by immersion before being put in the booths. After 24 days all 5 assemblies without the adhesive film showed corrosion points and sites in the nickel on steel; after 17 more days the nickel on Invar turned green. In analogous tests with the adhesive film one or two points of corrosion appeared on two assemblies out of 5 after 120 days; the relative humidity varied in the range of 40-96% and the temperature fluctuated between 19 and 0°.* After 228 days the five assemblies with the adhesive film each showed several points of corrosion; no traces of corrosion were detected in the nickel on Invar.

Tests were also carried out on 10 nickel-plated rings (with brass the basis metal) with nickel coatings 1.5 μ thick. The rings without adhesive film showed corrosion (turned green) after 53 days. The rings with the adhesive film were without any signs of corrosion after 228 days. The relative humidity was in the 40-92% range, and the temperature varied from −19 to +3°.

Pieces zinc-coated from a sulfate bath, without an adhesive film, showed signs of corrosion in a shielded region after 29 days; in an analogous test with an adhesive film there was no corrosion even after 228 days. The relative humidity was in the 49-90% range; the temperature varied from +14 to 28°.

German silver without adhesive film showed signs of corrosion (turned green) after 35 days; with an adhesive film, corrosion commenced after 200 days. The relative humidity was in the 32-98% range, and the temperature varied from 14 to 28°.

At the present time BF-2 adhesive is used in the works for coating some experimental batches of components, such as springs of icing recorders (2-layer coatings, each layer being heat-treated for 1 hour at 150-160° after gradual heating). The corrosion resistance of the spring coated (in 2 layers) by the adhesive was 8 times that of springs coated by alkaline surface oxidation, in steam corrosion tests.

* These and subsequent data on relative humidity and temperature apply to the test period before the start of corrosion.

The adhesive films are used with success as insulating layers of keys of the A-13 radiometeorograph.

After reconstruction of the heating equipment in the works the use of adhesive films for increasing the corrosion resistance of galvanic coatings will be extended.

SUMMARY

1. Films of BF-2 adhesive on zinc and nickel galvanic coatings and on uncoated steel increase the corrosion resistance from 2 to 5-fold and more under harsh test conditions at elevated temperatures and almost 100% relative humidity, and in tests in psychrometric booths. Therefore the use of BF-2 adhesive coatings is recommended for zinc-plated and nickel-plated parts and components destined for use under harsh conditions, and especially in tropical climates. Adhesive films should also be used on unplated metals.

2. Tests confirmed the suitability of iridescent passivation, which increases the corrosion resistance of zinc-plated surfaces.

LITERATURE CITED

[1] I. P. Berdinskikh, Adhesives and Adhesion [in Russian] (Mashgiz, 1952).

Received April 14, 1958

PHOTOSENSITIZED POLYMERIZATION OF METHYL METHACRYLATE

M. P. Tikhomolova, M. M. Koton, and A. N. Baburina

Polymerization of vinyl compounds under the influence of ultraviolet radiation in presence of sensitizers is of practical interest because of the possibility of effecting polymerization at approximately room temperature.

Many different densitizers have been described in the literature [1-5], but there have been no studies of polymerization under the influence of ultraviolet radiation to high degrees of conversion of monomer to polymer. We, therefore, studied the photopolymerization of methyl methacrylate in presence of various sensitizers: bromoacetophenone, benzoin methyl ether, azoisobutyric dinitrile, phenoxyisobutyrophenone, α-bromobutyrophenone, α-bromoisobutyrophenone, methyl ethyl ketone, acetone, chloral, and α-hydroxymethyl- and α-hydroxybutyl-p-tolyl sulfones. It follows from the results, given in Table 1, that the most active sensitizers of polymerization of of methyl methacrylate under the influence of ultraviolet radiation are bromoacetophenone and bromoisobutyrophenone, in presence of which the degree of conversion of monomer to polymer was 47% and 59% respectively.

TABLE 1

Photopolymerization of Methyl Methacrylate in Pyrex Glass Tubes at 20° during 2 Hours in Presence of Sensitizers (1%)

Sensitizer	Conversion (%)	Sensitizer	Conversion (%)
Without sensitizer	4	Bromoacetophenone	47
Azobisisobutyronitrile	21	Bromobutyrophenone	22
Methyl ethyl ketone	3	Bromoisobutyrophenone	59
Acetone	6	Chloral	4
Benzoin methyl ether	30	α-Hydroxymethyl-p-toyl sulfone	6
Phenoxyisobutyrophenone	11		

TABLE 2

Polymerization of Methyl Methacrylate in Presence of a Redox System (1% benzoyl peroxide + 1% α-hydroxymethylp-tolyl sulfone) and Different Sensitizers (1%) During 18 hours at 20°

Sensitizer	Conversion (%)	η	$M \cdot 10^{-5}$
Without sensitizer	7.5	4.3	10.5
Bromoacetophenone	7.9	3.3	7.7
Phenoxyisobutyrophenone	7.9	4.4	11
Azobisisobutyronitrile	10	8.7	25

Benzoin methyl ether is also an active sensitizer, but the polymer formed in its presence has a pale yellow color.

Polymerization of methyl methacrylate was studied in the greatest detail in presence of 1% of the following sensitizers: phenoxybutyrophenone and azobisisobutyronitrile (see figure). It is clear from the graph that the "conversion boundary" in polymerization of methyl methacrylate under the influence of ultraviolet radiation lies at 93% conversion of monomer to polymer. In polymerization of methyl methacrylate in presence of phenoxybutyrophenone it was shown that the temperature within the polymerizing mass rose very slightly (by 2-3°) at the instant of gelation, and was 22-23°. We showed previously [6] that in polymerization of methyl methacrylate at 20° in presence of oxidation–reduction systems the "conversion boundary" lies at about 86% conversion of monomer to polymer. We, therefore, attempted to increase the boundary of conversion of methyl methacrylate into the polymer by introducing a sensitizer into the polymerizing mass and subjecting the resultant solid polymer to additional ultraviolet irradiation. We accordingly studied the bulk polymerization of methyl methacrylate at 20° in presence of an oxidation–reduction system consisting of 2% benzoyl peroxide and 2% α-hydroxymethyl-p-tolylsulfone, with 1% of various sensitizers. In order to confirm that the sensitizers are not involved in the polymerization process, preliminary experiments were carried out on polymerization of methyl methacrylate with and without sensitizers, and the molecular weights of the resultant polymers were determined (Table 2). It follows from these results (Table 2) that the sensitizers used; phenoxyisobutyrophenone and azobisisobutyronitrile, do not take part in chain transfer and termination. Experiments showed (Table 3) that additional ultraviolet irradiation of methyl methacrylate polymers obtained at 20° in presence of oxidation–reduction systems and sensitizers increases the conversion of monomer to polymer somewhat, from 86-88% to 90-93%.

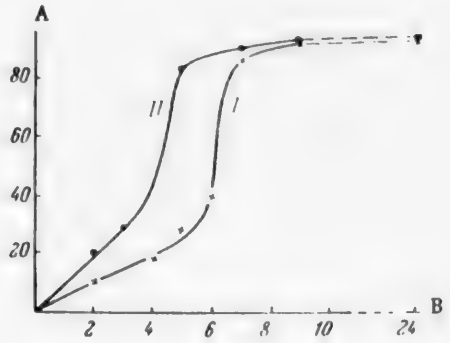

Photopolymerization of methyl methacrylate: A) conversion (%), B) time (hours); sensitizer (1%): I) phenoxyisobutyrophenone, II) azobisisobutyronitrile.

TABLE 3

Polymerization of Methyl Methacrylate in Presence of a Redox System (2% benzoyl peroxide + 2% α-hydroxymethyl-p-tolyl sulfone) and Different Sensitizers (1%), with Additional Ultraviolet Irradiation at 20°

Sensitizer (1%)	Irradiation time (hrs)	Conversion (%)	η	$M \cdot 10^{-5}$	Note
Without sensitizer	24	88	2.2	4.7	
Benzoin methyl ether	6	92	–	–	Yellow
Phenoxyisobutyrophenone	6	90	6.7	18.3	
Azobisisobutyronitrile	6	92	4.6	11.6	

SUMMARY

1. It is shown that if methyl methacrylate is subjected to the action of ultraviolet radiation in presence of sensitizers at 20° the conversion boundary is at 90-93% conversion of monomer to polymer.

2. If polymethyl methacrylate, formed at 20° in presence of redox systems and containing 1% sensitizer, s subjected to additional ultraviolet irradiation, the conversion boundary is raised from 86 to 90-93% conversion of monomer to polymer.

LITERATURE CITED

[1] L. Agre, U. S. Patent 2,367,660; Chem. Abs., 39, 3703 (1945).

[2] W. E. Mochel, I. E. Crandall, and L. H. Peterson, J. Am. Chem. Soc. 77, 494 (1955).

[3] L. M. Richards, U. S. Patent 2,460,105; Chem. Abs. 43, 2818 (1948).

[4] C. C. Sachs and I. Bond, U. S. Patent 2,579,095; Chem. Abs. 46, 3326 (1952).

[5] C. Mc Closkey and I. Bond, Ind. Eng. Ch. 47, 2125 (1955).

[6] M. P. Tikhomolova, M. M. Koton, and A. N. Baburina, J. Appl. Chem. 32, No. 8, 1794 (1959).*

Received April 16, 1958.

* Original Russian pagination. See C.B. Translation.

A STUDY OF THE REACTIONS OF ALKALI-METAL XANTHATES WITH COPPER SALTS

I. N. Plaksin, N. A. Suvorovskaya, and V. V. Shikhova

Alkali-metal xanthates may react with cupric salts with formation of dixanthogen and cuprous xanthate (1), or of cupric xanthate (2):

$$4KSSC{-}OC_4H_9 + CuSO_4 = (SSC{-}OC_4H_9)_2 + Cu_2(SSC{-}OC_4H_9)_2\downarrow + K_2SO_4, \quad (1)$$

$$2KSSC{-}OC_4H_9 + CuSO_4 = Cu(SSC{-}OC_4H_9)_2\downarrow + K_2SO_4. \quad (2)$$

An oxidation–reduction reaction takes place in the first case, and double decomposition in the second. Since alkali-metal xanthates are used as collecting agents in flotation, studies of their reaction with cupric ions are of interest. Some data on the course of Reaction (1) with formation of dixanthogen have been obtained by infrared spectroscopy [1].

In the present investigation the reaction between xanthates and copper ions was studied by analysis of the reaction products.

Method of investigation. A definite amount of 0.1 N solution of alkali-metal xanthate was put in a separating funnel, and 0.1 N copper sulfate solution was added to it from a buret in the stoichiometric proportions. The oily liquid which separated out – dixanthogen – was extracted in carbon tetrachloride or diethyl ether.

Separation of the organic and aqueous phases proceeded rather slowly owing to the high viscosity of the latter and the presence of precipitated copper xanthate. Accordingly, despite the high value of the coefficient of distribution of xanthogen between the extraction solvent and water, four-fold extraction of dixanthogen from the liquid and solid phases was carried out in order to avoid losses. After the extraction the organic solvent was distilled off on the water bath, and the oily liquid (dixanthogen) was analyzed. The residue was dried under vacuum and its copper and sulfur contents were determined.

The analytical results for the solid and liquid phases are given in the table.

Reaction products	Sulfur (%)		Copper (%)	
	theoretically calculated	found	theoretically calculated	found
Phase:				
liquid (dixanthogen)	42.98	41.87	—	—
solid (copper xanthate)	30.13	30.20	29.86	25.10

The analytical results and qualitative tests indicate that the product in the organic phases is dixanthogen, while the precipitate is probably a mixture of cupric and cuprous xanthates.

An attempt was made to determine the extent of the oxidation-reduction reaction with formation of dixanthogen and cuprous xanthate and to find how much cupric xanthate is formed at the same time. A series of experiments was accordingly carried out in which the weight ratio of the precipitate (a) to dixanthogen formed (b) was determined.

The average value of a/b found in the series of experiments is 3.6. If the reaction under consideration goes to completion, it may be assumed that the ratio a/b must be equal to the ratio of the molecular weights of cuprous xanthate and dixanthogen. In experiments with butyl xanthate this ratio was 1.42. It follows that the amount of dixanthogen obtained was less that the amount which should be formed if only cuprous xanthate is obtained, so that Reaction (1) must be accompanied by Reaction (2). This is due to the relatively weak oxidizing properties of the cupric salt.

The small solubility product of $Cu(SSC-OC_4H_9)_2$ also indicates that this compound may be formed under usual reaction conditions from cupric ions and xanthates.*

As the weight of dixanthogen formed in the experiment was 0.136 g, the weight of cuprous xanthate (c) must be:

$$c = \frac{0.136 \quad 425}{298}.$$

Since the total weight of precipitate in this experiment was 0.500 g, the percentate of cuprous xanthate formed is:

$$\frac{c \cdot 100}{d} = \frac{\frac{0.136 \quad 425}{298}}{0.500} 100 = 38.8.$$

It follows that about 40% of the precipitate is cuprous xanthate, and about 60% is cupric xanthate.

SUMMARY

1. In a study of the reactions between cupric ions and alkali-metal xanthates it was found that the oxidation-reduction reaction is accompanied by double decomposition.

2. In the former case the reaction products are dixanthogen and cuprous xanthate, and in the latter, cupric xanthate and an alkali-metal salt; under the conditions studied the cuprous and cupric xanthates are present in 2 : 3 ratio.

LITERATURE CITED

[1] L. Leya and I. N. Schulman, Trans. Am. Inst. Mining Metallurgical Eng. 9, 199, 221 (1954).

Received December 22, 1958

* According to Du-Rietz: $SP_{Cu(SSC-OC_4H_9)_2} = 5.5 \cdot 10^{-20}$, $SP_{Cu_2(SSC-OC_4H_9)_2} = 3.16 \cdot 10^{-14}$.

INVESTIGATION OF THE ESSENTIAL OIL OF ARTEMISIA RUFAEFOLIA

M. I. Goryaev and Zh. K. Gimaddinov

The essential oil of Artemisia rufaefolia P. Pol. has not been investigated previously. The plant was gathered at the flowering stage in the Pamir, 162 km from Osh in the direction of Murgab, near the Taldyk pass (Kirgizia). The upper parts of the plants were cut at branching level. The average moisture content of the plant mass was about 40%. The plants were distilled with steam under 3 atmos steam pressure as soon as gathered. 765 kg of raw material was treated for extraction of the essential oil. The oil yield was 0.3% on the fresh plant material. The essential oil is a transparent greenish-yellow mobile liquid with a bitter taste.

The oil distilled in the 172-197° range under atmospheric pressure. In distillation of 20 ml of the oil under atmospheric pressure, 5.2 ml distilled at 172-180°, 4.9 ml at 180-185°, and 9.0 ml at 185-197°; there was 0.9 ml of residue. The physicochemical constants of the oil are: d^{20}_{20} 0.917, $n^{20}D$ 1.4646. The solubility is 1 : 2.1 in 70% alcohol, 1 : 1.3 in 80% alcohol, and 1 : 0.8 in 90% alcohol. The acid number is 3.77, the ester number is 33.33, the ester number after acetylation is 74.66, and the saponification number is 37.10. The oil gave negative tests for sulfur, nitrogen, phenols ($FeCl_3$ test), and aldehydes (Schiff's test). The test of cineole with 50% aqueous resorcinol gave a crystalline addition product of cineole and resorcinol, which proved the presence of cineole. Action of 2,4-dinitrophenylhydrazine on the oil gave a 2,4-dinitrophenylhydrazone of m.p. 114-115°, showing the presence of carbonyl compounds in the oil.

Isolation and investigation of acids. For separation of the acids the oil was shaken repeatedly with 5% aqueous sodium carbonate in a separatory funnel. The aqueous soda extracts were combined, washed with ether to remove any mechanically-entrained droplets of the essential oil, and evaporated on the water bath to a syrupy state; the salts of the acids were decomposed by 10% sulfuric acid. The free acids were extracted in ether. The ether was evaporated off and the residual acids were distilled in steam. All the acids were volatile in steam; there was no nonvolatile residue. The acids were extracted from the aqueous distillate by means of ether. The ethereal extract was dried by freshly-calcined Na_2SO_4, filtered, and the ether was evaporated off. The resultant acid was a liquid with a sharp odor, readily soluble in water. The constants of the acid were: d^{20}_{20} 0.966, $n^{20}D$ 1.3990. According to the literature [1], these are close to the constants of n-butyric acid (d^{20}_4 0.9587, $n^{20}D$ 1.39906). The supposed butyric acid was converted into the ethyl ester for identification. The ester was a liquid with an odor of pineapple, b. p. 121°. According to the literature, the ethyl ester of n-butyric acid boils at 120-125° (760 mm) [2].

Isolation and identification of carbonyl compounds. For isolation of the carbonyl compounds 200 g of the original oil was treated with an aqueous solution of 125 g of semicarbazide hydrochloride and the equivalent amount of sodium acetate. The liquid was left to stand for one month and shaken periodically; at the end of this period the semicarbazones separated out, and were collected on a Buchner funnel, washed with ligroin and decomposed by phthalic anhydride in a current of steam.

A small quantity of the semicarbazones was recrystallized from alcohol; the melting point of the purified product was 170-172°, which corresponds to α- and β-thujone, according to the literature [3-5].

The carbonyl compounds isolated after decomposition of the semicarbazones were separated from the aqueous layer in a separating funnel and dried over freshly-calcined Na_2SO_4. The carbonyl compounds had the following constants: d^{20}_{20} = 0.914, $n^{20}D$ = 1.4530 and $\alpha^{20}D$ = + 7°.

These physical constants are close to those of α- and β-thujone, and probably correspond to a definite mixture of the two, as essential oils normally contain thujones in the form of a mixture:

α-Thujone: d^{20} 0.9120 [6], $n^{20}D$ 1.4530 [6], α −5° 12' [7];
β-Thujone; d 0.9160 [8], $n^{20}D$ 1.4507 [8], α +14.98° [3].

For identification, thujone was converted into the tribromide, which melted at 122-123°. According to the literature thujone tribromide melts at 121-122° [6]. The 2,4-dinitrophenylhydrazone of our thujone melted at 114-115°. Literature data on the melting point of the 2,4-dinitrophenylhydrazone show great variations (from 106-107.5° to 116-117°) [6], probably because these correspond to different mixtures of the α- and β-forms. The melting point of α-thujone is 106-107° [6] and of β-thujone, 116° [6].

From 200 g of oil we isolated 121.1 g of thujone, which corresponds to 60% in the oil.

Isolation and identification of cineole. The oil residue after separation of the carbonyl compounds was treated with 50% aqueous resorcinol solution. A complex cineole–resorcinol compound was instantly formed; this was collected on a Buchner funnel and washed with ligroin. The compound was decomposed by 10% aqueous NaOH on heating, and the liberated cineole was distilled in steam. A part of the crystals was recrystallized from benzene; the m. p. was 82-83° which, according to literature data, corresponds to the melting point of the cineole-resorcinol compound.

The cineole was distilled in steam, separated from the aqueous layer in the separating funnel, and dried over calcined Na_2SO_4. The constants of cineole were: d^{20}_{20} 0.926, $n^{20}D$ 1.4540; according to the literature $n^{20}D$ 1.4540 [6] and d^{20} 0.9267 [8]. A mixed sample with known cineole–resorcinol compound did not give a depression of melting point.

The yield of cineole was 36.4 g, so that the content in the oil was 18.2%.

Isolation of combined acids. The oil residue after separation of carbonyl compounds and cineole was saponified by 0.5 N alcoholic KOH solution and distilled in steam. The solution of salts of the acids was investigated as described above. The yield was 3.4 g of acid with the constants: d^{20}_{20} 0.966 and $n^{20}D$ 1.3990, so that the acid present in ester form was the same as that present free in the oil (n-butyric).

Isolation of alcohols. For isolation of alcohols the oil residue after extraction of the acids was dried over freshly-calcined Na_2SO_4 and treated with metallic sodium. The alcoholates which separated out were collected on a Buchner funnel, washed with ligroine, decomposed by distilled water, and distilled in steam. The alcohols were separated from the aqueous layer and dried over Na_2SO_4; their physical constants were: d^{20}_{20} 0.938, $n^{20}D$ 1.4808, $(\alpha)^{20}D$ +95°. The product was a liquid with an odor of lilac. The constants are in good agreement with literature data on D-α-terpineol; d^{20}_{20} 0.9380 [9], $n^{20}D$ 1.4808 [8] and (α)D + 95° 9' [6]. For additional identification, the alcohol was converted into the tetrabromide of m. p. 124°, which correspond to α-terpineol dibromide, identical with dipentene tetrabromide [4]. The amount of D-α-terpineol isolated and identified was 12.3 g, or 6% on the oil; it is present in the oil as the α-terpenyl ester of butyric acid, the content in the oil being 7.8%.

Fractionation of the oil residue. The oil residue after separation of thujone, cineole, and terpenyl butyrate (20.75 g) was fractionated under a residual pressure of 2 mm. The results are given below.

	Boiling point at 2 mm (°C)	Weight of fraction (g)
Fractions:		
I	37-37.5	9.25
II	62-63	10.4
Residue	–	0.8
Losses	–	0.3

Investigation of fractions. The physical constants of Fraction I were : d^{20}_{20} 0.854, $n^{20}D$ 1.4657 and $\alpha^{20}D$ +44°. The constants of Fraction I are close to those of α-pinene, which are, according to the literature: d^{25}_{4} 0.8542

[10], $n^{20}D$ 1.4658 [11], α_D +45.04° [12]. For identification of the presumed D-α-pinene, Fraction I was oxidized by potassium permanganate solution to pinonic acid. The resultant acid was syrupy and did not crystallize, and therefore we prepared the semicarbazone without attempting to obtain the acid in crystalline form. After recrystallization from alcohol the semicarbazone melted at 202-203°, which corresponds to the m. p. of pinonic acid semicarbazone as reported in the literature [3]. A mixed sample with known pinonic acid semicarbazone did not give a depression of melting point. It was thus shown that Fraction I consists of D-α-pinene; its content in the oil is about 5%.

Fraction II crystallized completely. After it had been purified by recrystallization from alcohol and sublimation the substance had m. p. 178-179° and $(\alpha)_D$ −44° (in 20% alcoholic solution). The constants coincide with those of camphor. For final confirmation of camphor the 2,4-dinitrophenylhydrazone of m. p. 174° and semicarbazone of m. p. 237-238° were prepared. It may therefore be regarded as proved that Fraction II consists of l-camphor, the content of which in the oil is about 5%.

SUMMARY

1. The essential oil of Artemisia rufaefolia was investigated; it is a greenish-yellow transparent liquid with a bitter taste.

2. The oil was shown to have the following constituents (in %): butyric acid 0.6, thujone 60, cineole 18.2, α-terpenyl butyrate 7.8, d-α-pinene 5, l-camphor 5.

3. The essential oil may provide a source of thujone and cineole.

LITERATURE CITED

[1] I. Heilbron and H. Bunbury (editors), Dictionary of Organic Compounds, I (1949) p. 372 [Russian translation].

[2] I. Heilbron and H. Bunbury (editors), Dictionary of Organic Compounds, II (1949) p. 23 [Russian translation].

[3] Ber. Schimmel, 8 (1924).

[4] M. I. Goryaev, Characteristics of Chemical Compounds Present in Essential Oils [in Russian] (Acad. Sci. Kazakh SSR Press, Alma-Ata, 1953).

[5] I. P. Shchukervanik and L. S. Grach, Trans. State Univ. Central Asia, Chem. Ser. 6, 36 (1937).

[6] E. Guenther, The Essential Oils II (1949).

[7] Ber. Schimmel. 175 (1938).

[8] N. Ya. Dem'yanov, V. I. Nilov, and V. V. Vil'yams, Essential Oils, Their Composition and Analysis [in Russian] (Goskhimizdat, 1930).

[9] J. Simonsen, The Terpenes, I (1947).

[10] J. Simonsen, The Terpenes, II (1949).

[11] I. I. Bardyshev, J. Appl. Chem. 21, 10 (1948) [USSR].

[12] A. Ginzberg, J. Russ. Phys.-Chem. Soc. 1-3 (1898).

Received May 23, 1958

DIRECT VINYLATION OF ADIPIC ACID

A. M. Shur and B. F. Filimonov

This paper contains the results of experiments on liquid-phase vinylation of adipic acid in monochloroacetic acid in presence of mercury catalysts and traces of oxidizing agents. The yields of divinyl adipate exceeded 80% calculated on the adipic acid converted, or 74% of the theoretical calculated on the acid taken. The effects of various catalyic additives on absorption of acetylene by the melted acid mixture were also studied.

EXPERIMENTAL

Starting materials. Acetylene was purified thoroughly to remove all air, washed in a solution in potassium dichromate in sulfuric acid, and collected in a graduated gas holder containing saturated sodium sulfate solution. Before the experiments the solution was kept for 3 days under moderate acetylene pressure.

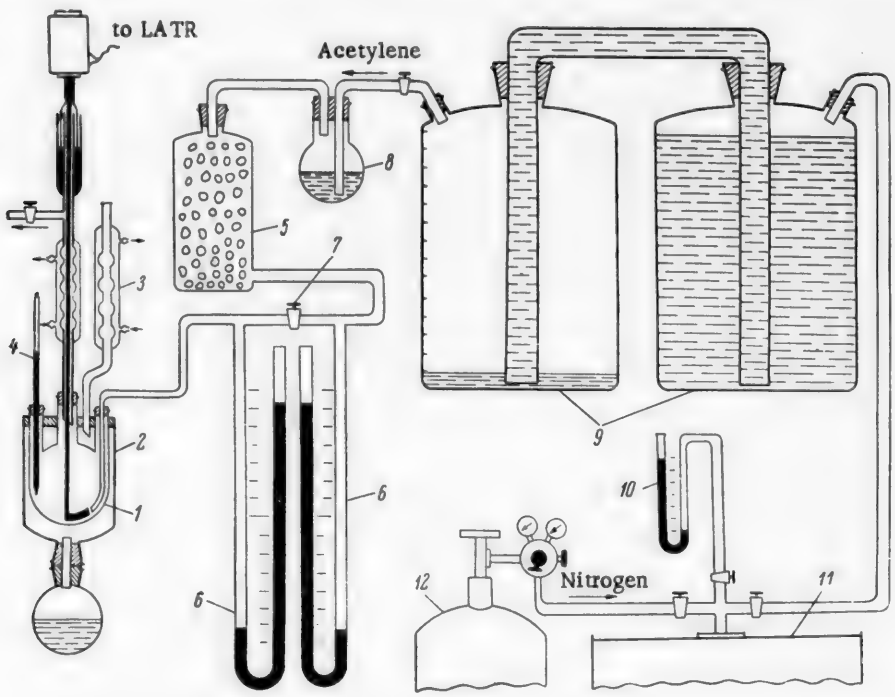

Fig. 1. Vinylation apparatus (schematic): 1) reaction flask, 2) steam jacket, 3) condenser, 4) thermometer, 5) drying column, 6) manometers with bromoform, 7) acetylene stopcock, 8) bubble counter, 9) gas holder, 10) mercury manometer, 11) buffer vessel, 12) nitrogen cylinder.

The original acids (with the exception of dichloroacetic), yellow mercury oxide, zinc chloride (which was remelted immediately before use), mercurous chloride, and the oxidizing agents were reagents of "pure"

grade and were not specially purified. Dichloroacetic acid was synthesized from chloral hydrate and potassium cyanide as described in the literature [1]. Ferric chloroacetate was prepared by dissolution of freshly-precipitated ferric hydroxide in melted monochloroacetic acid. Zinc oxide was prepared by calcination of the hydroxide or by combustion of zinc dust. Cuprous oxide was prepared from Fehling's solution.

Results of Fractionation of the Reaction Mixture (Mixture: 15 g adipic acid and 10 g monochloracetic acid; in each experiment 50 mg hydroquinone was added)

Expt. No.	Catalytic additives		Reaction time (hours)	Amount of C_2H_2 absorbed (%)	Yields of reaction products					Notes
					vinyl chloroacetate		divinyl adipate		monovinyl adipate	
	HgO (g)	Other substances (mg)			g	%	g	%	g	
1	2.5	—	4.25	68.6	7.0	55.2	11.0	55.4	1.2	After 4 hours 1.5 g more HgO added
5	2.5	Fe_2O_3 — 40	4	68.6	—	—	10.8	53	2	After 3 hours 1 g more HgO and 7 mg Fe_2O_3 added
11	2.5	0.5 g HgO added after one hr and then at half-hour intervals	7	90.5	9.2	72.5	10.0	49.2	—	3 g of fraction boiling at 131-133° at 5 mm Hg isolated
12	2.5	Anhydrous $FeCl_3$ — 50	3	68.5	5.5	43.3	14.2	69.8	2.5	—
13	2.5	$K_2Cr_2O_7$ — 50	3	68.5	5.1	40.2	15.0	73.7	0.5	Slight resinification during fractionation
18	2.5	$K_2Cr_2O_7$ — 70	0.5	53.9	3.2	25.2	6.0	29.6	—	15 g of adipic and 15 g of chloroacetic acid taken
20	2.5	Ferric chloroacetate	3	68.5	8.2	64.6	13.5	66.4	1.0	
25	2.5	Ferric chloroacetate	2	71.5	9.0	71.0	10.5	51.6	1.5	50 mg lots of K_2CrO_4 added after 0.5 and 1 hour
26	2.5	Anhydrous $FeCl_3$ — 60	3	73.0	8.0	63.0	12.5	61.5	2.3	50 mg $K_2Cr_2O_7$ added after 30 minutes, 50 mg $FeCl_3$ after 45 minutes, 50 mg HgO after 60 minutes
34	5	$K_2Cr_2O_7$ — 100	3	70.6	11.2	—	30.0	73.7	2	Double charge; adipate redistilled at 99-101° (1 mm Hg)

Method. The vinylation was performed under slight excess pressure (P = 330 mm bromoform column, which corresponds to an absolute pressure of 830 mm Hg) at 80° in the apparatus shown in Fig. 1. Before the start of an experiment acetylene was blown through the system in order to displace air.

The reaction flask was heated by means of a mixture of water and alcohol vapors. The pressure variations in the course of an experiment did not exceed ±3 mm $CHBr_3$; to achieve this, the gas holder was connected to a buffer vessel (100 liters) containing nitrogen. The drop of pressure in 15 seconds was taken as a measure of the reaction rate (the acetylene supply was cut off during the rate determinations). The absolute quantity of acetylene consumed was found from the volume change in the gas holder.

Approximately equimolecular amounts of adipic and monochloroacetic acids were used in the vinylation; with this component ratio a liquid reaction mixture could be obtained at 80°. In most experiments the amount of mercuric oxide was 10% on the acid mixture.

After absorption of acetylene had virtually ceased, the contents of the flask were cooled and separated from mercury and solid matter, mainly consisting of unconverted acids. In vacuum distillation vinyl chloroacetate was collected at 45-50° (20 mm Hg) and divinyl adipate at 118-125° (10 mm Hg), which is in agreement with literature data [2].

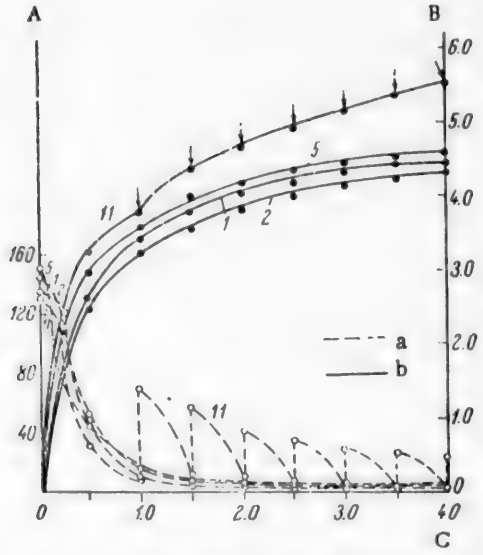

Fig. 2. Curves for acetylene absorption: A) pressure (mm $CHBr_3$), B) amount of acetylene (liters), C) reaction time (hours); the curve numbers correspond to experiment numbers in the table; a) absorption rate, b) acetylene consumption; vertical arrows represent the instants of fresh additions.

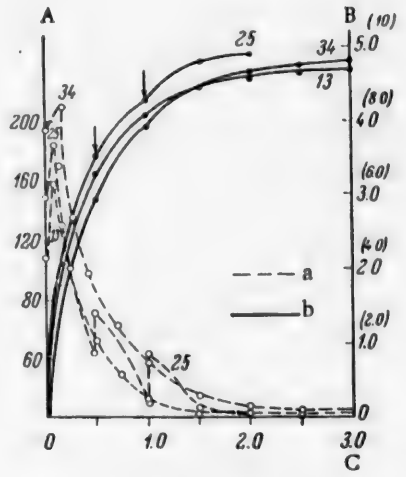

Fig. 3. Curves for acetylene absorption in presence of chromates: A) pressure (mm $CHBr_3$), B) amount of acetylene (liters), C) reaction time (hours); the curve numbers correspond to experiment numbers in the table; a) absorption rate, b) acetylene consumption; vertical arrows represent the instants of fresh additions; the values of (B) given in parentheses refer only to Experiment No. 34, where the charge was doubled.

The results of experiments on absorption of acetylene by the melted reaction mass are plotted in Fig. 2 and 3. The continuous lines represent the consumption of acetylene as a function of time, and the dash lines show variations of the absorption rate during the reaction. The fact that Curves 1 and 2 coincide almost completely indicates that the reproducibility of the experiments is satisfactory.

The presence of droplets of metallic mercury in the reaction mixture and the sharp retardation of the reaction soon after the start suggested that absorption of acetylene ceases owing to reduction of mercury compounds to the catalytically-inactive metal. An attempt was therefore made in subsequent experiments to prevent reduction of the catalyst by addition of small amounts of oxidizing agents to the reaction mixture (Fig. 2 and 3, table). The sharp initial jumps on the curves for the rate of acetylene absorption were accompanied by transitory rises of temperature (up to 107°).

The fractionation results of some of our experiments are presented in the table. It is seen that by addition of certain oxidizing agents the reaction time could be shortened appreciably and the yield of divinyl adipate increased, although the percentage of acetylene absorbed did not increase. The highest yield (about 74%) was obtained in Experiment No. 13 with the use of potassium dichromate; when the experiment was repeated with a doubled charge (No. 34), the same yield was obtained in 3 hours as before.

The yields given in the table were calculated on the amounts of acid taken; if calculated on the amounts of adipic acid converted, the yields of divinyl adipate are somewhat higher and reach 82% of the theoretical. At the same time, such oxidizing agents as potassium iodate, magnesium perchlorate, and lead dioxide have almost no effect on the course of vinylation. Although replacement of these substances by cuprous oxide produced very large jumps on the absorption-rate curves, it did not increase the percentage absorption or yield of adipate.

Attempts to replace mercuric acid partially or completely by zinc oxide, zinc chloride, or mercurous chloride were unsuccessful. The reaction either did not proceed at all or was much slower. Partial replacement of monochloroacetic acid by the dichloro- or trichloro- acids was of no advantage; if the amount of monochloroacetic acid was small, or in absence of this acid, the reaction did not proceed at all. Attempts to effect the reaction in vinyl chloroacetate in presence of the same catalysts and a small amount of monochloroacetic acid were also unsuccessful.

LITERATURE CITED

[1] Organic Syntheses, 2 (IL) p. 247 [Russian translation].

[2] M. F. Shostakovskii, A. M. Shur, and B. F. Filimonov, J. Appl. Chem. 30, 816 (1957)* [USSR].

Received May 14, 1958

*Original Russian pagination. See C.B. Translation.

REACTIONS OF N-(CARBOXYPHENYL)SUCCINAMIDES WITH ETHYLENE GLYCOL AND GLYCEROL

M. S. Dudkin

The Odessa Technological Institute

Studies of the synthesis of the relatively little-known compounds containing ester and amide groups in the principal chain of the macromolecule are of interest in relation to investigations of polyester resins.

This paper contains a description of reactions of N-(carboxyphenyl)-succinamides with ethylene glycol and glycerol at 160, 190, and 230°, leading to formation of macromolecules. The relative positions of the -COOH and $-NH_2$ groups in the aromatic nucleus of N-(carboxyphenyl)succinamides influences the condensation of these phenols with polyhydric alcohols. The activation energy for chain initiation and growth is less for the ortho derivative than the para derivative of N-(carboxyphenyl)succinamide. The ortho derivative reacts with ethylene glycol and glycerol at lower temperatures than the para derivative, forming polymers of higher molecular weight under the same conditions (see table).

Most of the compounds obtained were solid glassy light or dark brown resins, mostly soluble in pyridine and acetone, which soften on heating and form threads when stretched.

It follows from these results that when N-(carboxyphenyl)succinamides are heated with polyhydric alcohols polycondensation occurs; in the case of the ortho derivative and ethylene glycol this may be represented as follows:

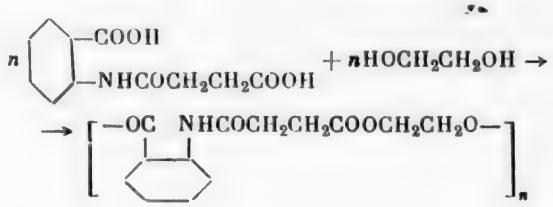

EXPERIMENTAL

Preparation of N-(2-carboxyphenyl)succinamide. To 10 g of 2-aminobenzoic acid suspended in 120 ml of water in a round-bottomed flask 5 g of potassium carbonate was added and the liquid was heated until the acid was completely dissolved. The 7.2 g of powdered succinic anhydride was added at − 1° and the liquid was shaken in a vibrator until precipitation of the potassium salt of N-(2-carboxyphenyl)succinamide ceased.

The flask was heated until the precipitate dissolved completely, cooled slightly, and hydrochloric acid was added to a strongly acid reaction. The precipitated N-(2-carboxyphenyl)succinamide was filtered off, washed with water to a negative reaction for hydrogen ions, and dried. The yield of acid was 35%.

Found %: N 5.90, 5.85; acid number 470, 472; m. p. 185°. $C_{11}H_{11}O_5N$. Calculated %: N 5.77; acid number 472; m. p. [1] 186°.

Reacting substances		Molar ratio reactants	Temperature (°C)	Heating time (hrs.)	Characteristics of reactions products						Appearance before purification
acid	alcohol				acid number	specific viscosity	molecular weight from acid number	molecular weight from viscosity	nitrogen content (%)	soluble in	
N-(2-carboxyphenyl)succinamide	Ethylene glycol	1 : 1	160	5	66.4	0.015	840	740	5.31	Pyridine, acetone, benzene	Solid, transparent, red-brown resinous substance
	Glycerol	1 : 1	160	5	90.1	0.019	620	630	4.90	Pyridine, acetone	Red-brown resinous solid
N-(4-carboxyphenyl)succinamide	Ethylene glycol	1 : 1	190	2	106.4	0.012	530	590	—	Pyridine, acetone, methyl alcohol	Pale yellow viscous liquid
		1 : 1	190	5	52	0.02	1080	1109	5.25	Pyridine, acetone	Pale red resinous solid
		1 : 1	190	10	25	0.04	2240	2800	—	Pyridine, acetone	Red resinous solid
		1 : 1	230	5	12.06	0.068	4640	4810	—	Pyridine, acetone	Brown resinous solid
	Glycerol	1 : 1	160	5	220	—	2545	—	—	Pyridine, acetone, methyl alcohol	Pale viscous liquid
		1 : 1	230	5	7.6	0.134	8000	7980	4.82	Pyridine, acetone	Pale brown solid

Preparation of N-(4-carboxyphenyl)succinamide. The method described above was used for the synthesis. 10 g of 4-aminobenzoic acid, 5 g of potassiur carbonate, and 7.2 g of succinic anhydride was taken for the amide preparation. The yield of N-(4-carboxyphenyl)succinamide was 70%.

Found %: N 6.85, 5.99; acid number 478, 476; m. p. 240-241°. $C_{11}C_{11}O_5N$. Calculated %: N 5.77; acid number 472.

Reaction of N-(carboxyphenyl)succinamides with ethylene glycol and glycerol. The reacting substances were put in 1 : 1 molar ratio in the reaction tube of the appratus described by Korshak and Rafikov [2]. The contents of the tube were heated for a definite time on a metal bath (Wood's alloy). The bath temperature was regulated by means of a contact thermometer and a system of relays. The reaction was conducted in an atmosphere of nitrogen, which was previously passed through a vessel filled with calcium chloride and soda lime and through a heated glass tube packed with reduced copper. The resins formed were purified by precipitation by alcohol or ligroin from solution in acetone or pyridine. The resins were filtered off and dried under vacuum at a temperature not higher than 50°. The substances, purified by twofold precipitation, were analyzed. The acid number and specific viscosity of the resins were determined in pyridine solutions. The molecular weights were found from the contents of carboxyl end groups and from the viscosity with the aid of the Staudinger equation with $K = 1.2 \cdot 10^{-4}$. Nitrogen was determined by the Kjeldahl method. The results are given in the table.

SUMMARY

1. When N-(carboxyphenyl)succinamides are heated with ethylene glycol or glycerol under various conditions polymers of molecular weight up to 8000 are formed.

2. Molecules containing amino and carboxyl groups in the ortho position in the benzene nucleus are more reactive than para derivatives.

LITERATURE CITED

[1] Y. Houben, Die Methoden der organischen Chemie, IV, 394 (1924).

[2] V. V. Korshak and S. R. Rafikov, J. Gen. Chem. 24, 976 (1944).

Received March 13, 1958

SEPARATION OF CHLOROANILINES BY PARTITION CHROMATOGRAPHY

D. F. Kutepov, A. A. Potashnik, and N. I. Karavanova

Chromatographic methods of analysis are being more and more widely used in recent years. In its original form the remarkable idea of the Russian scientist Tsvet (Tswett) consisted essentially of sorption and desorption of a mixture of substances in a column packed with a sorbent [1]. Subsequently the applicability range of this method was considerably extended [2].

Partition chromatography proved especially successful in analysis of amino acids [3-5], penicillin [6], and hexachlorocyclohexane [7, 8].

Practical aspects of the use of partition chromatography have been fully considered in the literature; for example, by Fuks [9]. Several theoretical papers have now been published; these are discussed most fully in the review article by Senyavin [10]. However, in any new attempt to use partition chromatography on the basis of existing experience and theory only tentative attempts can be made to predict the suitable moving and stationary solvents and the adsorbent for the column, and to determine the particle size of the adsorbent, the column dimensions, and certain other particulars. The final decisions can be made only after appropriate experimental trials.

We were faced with the task of separating and analyzing a mixture containing three components: 2,4,6-trichloroaniline, 2,4,5-trichloroaniline, and 2,4-dichloroaniline. Dichloroaniline, being a stronger base than trichloroaniline, can form a fairly stable water-soluble hydrochloride. Accordingly, if the three-component mixture is treated with 5-10% hydrochloric acid the dichloroaniline is dissolved. The residue contains a mixture of two isomeric trichloroanilines, separation of which by the usual methods involves considerable difficulties. We used partition chromatography for this purpose. The first pair of solvents to be tried was nitromethane and isooctane; both trichloroanilines dissolve fairly well in the former, while the solubility in isooctane is considerably lower. The distribution coefficient of our isomers in these solvents was determined; it was 2.5 for 2,4,6-trichloroaniline and 8 for 2,4,5-trichloroaniline. Therefore, nitromethane could be used as the stationary and isooctane as the moving solvent.

The comparative data on the distrobution coefficients of trichloroanilines in these solvents also suggested that the elution zones of the two isomers would not overlap, which indicates that sharp separation is possible.

At the same time we also studied the possibility of using this method for separation of mixtures of 2,4,6-trichloroaniline and 2,4-dichloroaniline, 2,4,5-trichloroaniline and 2,4-dichloroaniline, and a three-component mixture containing both trichloroaniline isomers and 2,4-dichloroaniline. It was found that only the first of these mixtures can be separated in the column, as because of the differences between the distribution coefficients in nitromethane and isooctane (the value for 2,4-dichloroaniline is 23) the zones are not superposed. The two other mixtures could not be separated into the individual components. However, 2,4,6-trichloroaniline can be separated fairly completely from the three-component mixture.

During the experiments each of the chloroanilines was first passed in the pure form through the column. It was found that 2,4,6-trichloroaniline moves in a fairly narrow fraction, and with a sample of 0.15-0.3 g the yield is 97-99.8%. Both 2,4,5-trichloroaniline and 2,4-dichloroaniline move in a broader fraction with somewhat lower yields, of about 92-95% and 87%. The following results were obtained in separation of an artificial mixture of pure trichloroaniline isomers: first a 25 ml fraction consisting of the pure solvent flows out; this is followed by a fraction 42 ml in volume containing 2,4,6-trichloroaniline, then 25 ml of pure solvent, and

finally the last fraction containing 2,4,5-trichloroaniline (60 ml). The boundaries between the fractions were determined by evaporation of drop samples on a glass slide. Appearance of residual crystals after evaporation of the solvent indicated the start of elution of a given compound from the column. Each of the components was qualitatively identified from the crystal form and melting point.

TABLE 1

Analysis of Chloroanilines and Their Artificial Mixtures in an Chromatographic Column

Expt. No.*	Name of isomer or composition of mixture	Weight taken	Fraction I, pure solvent (ml)	Fraction II, solvent with solvent (ml)	Fraction III, pure solvent (ml)	Fraction IV, solvent with substance (ml)	Substance isolated (g)	Yield (%)
	Chloroaniline solutions							
1	2,4,6-Trichloroaniline	0.2839	70—72	60—62	—	—	0.2835	99.8
2	2,4,6-Trichloroaniline	0.1816	32	50	—	—	0.1807	99.5
3	2,4,5-Trichloroaniline	0.0992	151	120	—	—	0.0918	92.5
4	2,4,5-Trichloroaniline	0.1632	91	85	—	—	0.1547	94.7
5	2,4-Dichloroaniline	0.1514	100	87	—	—	0.1324	87.4
	Solutions of artificial mixtures of chloroanilines							
6	2,4,6-Trichloroaniline (Fraction I)	0.1695	35	32	30	72	0.1668	98.4
	2,4-Dichloroaniline (II)	0.0822	—	—	—	—	0.075	91.2
7	2,4,6-Trichloroaniline (I)	0.1624	25	42	25	60	0.1624	100
	2,4,5-Trichloroaniline (II)	0.1097	—	—	—	—	0.1042	95
8	2,4,5-Trichloroaniline (I)	0.1022	30	25	35	156	0.1773	88
	2,4-Dichloroaniline** (II)	0.0992						
9	2,4,6-Trichloroaniline (I)	0.1004	20	28	25	92	0.0959	95.5
	2,4,5-Trichloroaniline (II)**	0.0960	—	—	—	—	0.1646	85.1
	2,4-Dichloroaniline (III)	0.0974	—	—	—	—	—	—

* In Experiments No. 1 and 3 the column contained 25 g of silica gel, with 15 g of nitromethane and 60 ml of isooctane; in the other experiments 12.5 g of silica gel, 7.5 g of nitromethane, and 30 ml of isooctane were used.

** No separation.

These data were used in subsequent practical work on separation and analysis of technical mixtures, which was successfully achieved. A technical mixture of 2,4,6-trichloroaniline and 2,4-dichloroaniline was analyzed. Separation by our method showed the mixture to contain 80% of 2,4,6-trichloroaniline and 12.5% of 2,4-dichloroaniline. Chemical analysis of the same mixture gave 12.8% of 2,4-dichloroaniline. Thus, the results were in agreement. Subsequent analyses of other technical mixtures of trichloroanilines showed absence of 2,4-dichloroaniline.

EXPERIMENTAL

Data on the column used, nature and particle size of the sorbent, and the experimental procedure were taken from the papers by Fuks [8]. The results are presented in Tables 1-3.

Method for chemical analysis of a mixture of trichloroaniline and dichloroaniline. A weighed sample of 1 g of the mixture was put into a flask. 5 ml of concentrated sulfuric acid was added; the mixture in the flask was slowly warmed up to 65-70° with stirring and held for 40 minutes. The hot contents of the flask were then poured out into water cooled to + 1° (70-100 ml). Trichloroanilines separated out; 15-20 minutes is needed

TABLE 2

Comparative Analyses of a Technical Mixture* of 2,4,6-Trichloroaniline

Chromatographic analysis, weight of mixture 0.2097 g				Evaporation of solvent gave		Chemical analysis, wt. of mixture 1 g	
vol. of Frac. I	vol. of Frac. II	vol. of Frac. III	vol. of Frac. IV	trichloroaniline from Frac. II	dichloroaniline from Frac. IV	trichloroaniline found	dichloroaniline found
32 ml of pure solvent	38 ml of 2,4,6-trichloroaniline solution	55 ml of of pure solvent	62 ml of 2,4-dichloroaniline solution	0.1678 g, 80%	0.0263 g, 12.5%	—	0.128 g, 12.8%

*The technical mixture contains certain amounts of other anilines.

TABLE 3

Chromatographic Determination of the Yield of 2,4,6-Trichloroaniline After Hydrolysis of Technical Hexachlorodiphenylurea

Expt. No.**	Technical mixture No.	Weight taken	Characteristics of fractions obtained		Yield of 2,4,6-trichloroaniline	
			fraction I, pure solvent (ml)	fraction II, with substance (ml)	(g)	(%)
1	1	0.2435	66	44	0.2368	97
2	3	0.2031	32	46	0.1929	95
3	4	0.2492	26	40	0.2358	94.6
4	5	0.1811	34	33	0.1749	96.5

**25 g of silica gel, 15 g of nitromethane, and 60 ml of isooctane were used in Experiment No. 1, and 12.5 g of silica gel, 7.5 g of nitromethane, and 30 ml of isooctane in Experiments No. 2, 3, and 4.

for complete precipitation. The precipitate was filtered off and washed with small portions of water, and the filtrate was made up to 200 ml. To 100 ml of the filtrate 2-3 ml of strong hydrochloric acid and 0.25 g of potassium bromide were added and the filtrate was titrated with 0.1 N sodium nitrite solution. The volume of of nitrite taken was 4.5 ml.

The dichloroaniline content was calculated from the formula $\frac{(4.5 \cdot K - 0.4) \cdot 0.0175}{1 \cdot 100} \times \frac{200 \cdot 100}{1 \cdot 100} =$ = 12.8%, where K = 0.902 and 0.4 is a correction for dissolved trichloroaniline.

LITERATURE CITED

[1] M. S. Tswett, Chromatographic Adsorption Analysis [in Russian] (Moscow, 1946).

[2] R. Synge, Biochem. J.,35, 1368 (1941).

[3] A. Gordon, A. Martin, and R. Synge, Biochem. J., 36, 21 (1942).

[4] G. Tustram, Biochem. J. 40, 720 (1946).

[5] S. Elsden, Biochem. J. 40, 252 (1946).

[6] R. Goodal and A. Lewi, Analyst, 72, 277 (1947).

[7] L. Ramsay and W. Patterson, J. Assoc. of Agr. Chem. 29, 337 (1946).

[8] N. A. Fuks and L. S. Chetverikova, J. Anal. Chem. 3, 213 (1948); 220 (1948) [USSR]; N. A. Fuks, Progr. Chem. 17, 45 (1948).

[9] Reactions and Methods of Investigation of Organic Compounds, I [in Russian] (Goskhimizdat, 1951) p. 179.

[10] M. M. Senyavin, J. Anal. Chem. 12, 637 (1957)* [USSR].

Received January 27, 1958

* Original Russian pagination. See C.B. Translation.